A study on impact of residual symmetries in some neutrino mass models

by

Rome Samanta

Enrolment No.: PHYS05201304004

Saha Institute of Nuclear Physics
Kolkata

A thesis submitted to the
Board of Studies in Physical Science Discipline
In partial fulfillment of requirements
For the Degree of

DOCTOR OF PHILOSOPHY

of

HOMI BHABHA NATIONAL INSTITUTE

August, 2017

Homi Bhabha National Institute

Recommendations of the Viva Voce Committee

As members of the Viva Voce Committee, we certify that we have read the dissertation prepared by Rome Samanta entitled "A study on impact of residual symmetries in some neutrino mass models " and recommend that it may be accepted as fulfilling the thesis requirement for the award of Degree of Doctor of Philosophy.

Debasish Majumdar Date : 02/12/2017

Chairman : DEBASISH MAJUMDAR

Ambar Ghosal Date : 2/12/2017

Guide & Convener : AMBAR GHOSAL

Arunansu Sil. Date : 02/12/2017.

Examiner : ARUNANSU SIL

Debades Bandyopadhyay Date : 2.12.2017

Member : DEBADES BANDYOPADHYAY

Pratik Majumdar Date : 2.12.2017

Member : PRATIK MAJUMDAR

Final approval and acceptance of this thesis is contingent upon the candidate's submission of the final copies of the thesis to HBNI.

I hereby certify that I have read this thesis prepared under my direction and recommend that it may be accepted as fulfilling the thesis requirement.

Date : 2/12/2017

Place : Kolkata

Ambar Ghosal

Guide

STATEMENT BY AUTHOR

This dissertation has been submitted in partial fulfillment of requirements for an advanced degree at Homi Bhabha National Institute (HBNI) and is deposited in the Library to be made available to borrowers under rules of the HBNI.

Brief quotations from this dissertation are allowable without special permission, provided that accurate acknowledgement of source is made. Requests for permission for extended quotation from or reproduction of this manuscript in whole or in part may be granted by the Competent Authority of HBNI when in his or her judgment the proposed use of the material is in the interests of scholarship. In all other instances, however, permission must be obtained from the author.

ROME SAMANTA

DECLARATION

I, hereby declare that the investigation presented in the thesis has been carried out by me. The work is original and has not been submitted earlier as a whole or in part for a degree / diploma at this or any other Institution / University.

ROME SAMANTA

List of Publications arising from the thesis

Journal

1. **"Probing texture zeros with scaling ansatz in inverse seesaw"**
   R. Samanta and A. Ghosal
   JHEP **1505**, 077 (2015).

2. **"Evaluation of the Majorana Phases of a General Majorana Neutrino Mass Matrix: Testability of hierarchical Flavour Models"**
   R. Samanta, M. Chakraborty and A. Ghosal
   Nucl. Phys. B **904**, 86 (2016).

3. **"Probing maximal zero textures with broken cyclic symmetry in inverse seesaw"**
   R. Samanta and A. Ghosal,
   Nucl. Phys. B **911**, 846 (2016).

4. **"Extended scaling and residual symmetry in the neutrino Majorana mass matrix "**
   R. Samanta, P. Roy and A. Ghosal
   Eur. Phys. J. C **76**, 662 (2016).

5. **"Baryon asymmetry via leptogenesis in a neutrino mass model with complex scaling"**
   R. Samanta,M. Chakraborty, P. Roy and A. Ghosal
   JCAP **1703**, 025 (2017).

ROME SAMANTA

DEDICATED TO

Ma, Baba, Family and Dalia

ACKNOWLEDGMENTS

Honestly, this is a surreal feeling to be at the end of a Ph.D journey for a person who well-nigh decided not to pursue physics few years back. Thanks to my parents and Prof. Rabindranath Sasmal. Certainly this period of four years was one of the best time I have ever spent. I have been blessed with so many wonderful people who can make life easier at any point of time. I'm sure that writing few lines will not suffice to pay gratitude towards them.

First of all I would like to thank my Ph.D advisor Prof. Ambar Ghosal for being so generous and helpful at every stage of my research work. He is such a good human being. Thanks to Prof. Palashbaran Pal, probably the best teacher I have learned from. Thanks to Prof. Probir Roy who taught me how precise physics can be. I would like to thank Prof. Debadesh Bandopadhyay, Prof. Debasish Majumdar and Prof. Pratik Majumder for helping me in various issues throughout.

A special thanks to Mainak Chakraborty who helped me a lot at the initial stages of my Ph.D time and the other seniors, Niluda, Dipankarda, Aminulda, Comrade, Goutamda, Prasantada, Anshuda, Amitda, Anirbanda, Debabratada, Kamakshyada, Apurbada, Aritrada, Chiruda, Kuntalda (theory), Kuntalda (CMS), Suvankarda, Naosadda, Sudipda, Koustavda, with whom I have spent plenty of good times.

I want to thank my college friends, Soumitra, Ramgopal, Biswajit, Spatshwa, Ayon, Somnath, Chima, Jiko, Dilipda, Devnil, Avilas, souma and M.Sc friends, Dalia, Sanjana, Krishanu, Abhoy, Amit, Kundu, Naba, Anamika, Soham for their cheerful presence and unconditional helping hands in various situations.

Now it's the turn for my SINP friends. Shamik and Sukannya should I thank you? Apart from my Ph.D work, what I have enjoyed, your company guys. I can't forget the endless addas with guitar, noodles and biriyani. How can I forget our song 'Brishti' which I hum countlessly in a day. Mugdha, Roopam, Sourav, Sudeshna, Shramana, Susmita, Maireyee, Arnab, Biswarup you guys are awesome.

I would also like to thank some of my lively juniors, Aritra, Zun tau, Madhurima, Avik, Sazad, Suman, Sanket, Sayan, Bankim, Debu, Prashant, Sridhar, Bibhuti, Samrat for their ebullient presence.

Finally, I acknowledge Saha Institute of Nuclear Physics for providing me adequate infrastructure to pursue my research work. I would like to thank Department of Atomic Energy (DAE), Government of India for financial support. I should acknowledge the cluster computational facility provided by the Astroparticle Physics and Cosmology (APC) division.

ROME SAMANTA

Contents

SYNOPSIS

Phenomenal success of experimental research in neutrino physics in the last two decades have led not only to unequivocally establishing that neutrinos have mass but also to an almost complete determination of flavor mixing between the different lepton generations. From theoretical perspective, their masses and mixing require physics beyond the Standard Model (SM), making them 'ghostly beacons of new physics'. Notwithstanding a sizable number of extensions of the SM, the leptonic flavor mixing is an aspect of a more general problem, the so called "flavor puzzle"; lepton mixing angles have apparently no relationship to the quark mixing angles, despite the fact that in Grand Unified Theories (GUT), where fermion quantum numbers find a natural justification, there is no fundamental distinction between leptons and quarks. Besides, there are open questions; the nature of the neutrinos – Dirac versus Majorana, the mass ordering, the absolute mass scale and the CP violating phases. Although, the measured nonvanishing value of reactor mixing angle θ_{13} opens up the prospect of measuring CP violation in leptonic sector which may have implications for the observed dominance of matter over antimatter in the universe, the theoretical significance of the reactor angle splits the model builders in three different communities. i) Models incorporating sequential dominance (SD), which predicts a normal neutrino mass hierarchy ($m_1 < m_2 < m_3$) and a large reactor angle θ_{13}. ii) The Anarchy approach, according to which the reactor angle is on the same footing as the atmospheric and solar angles, and hence was generally expected to be large. iii) Models with discrete family symmetries [1–3] which predict a vanishing value of θ_{13} in general. Equally attractive the first two models have a disadvantage that they are intrinsically untestable. By contrast, models with discrete family symmetries are highly testable as far as the mixing angles are concerned. In our work, we have focused on some neutrino mass models that belongs to the third category, i.e., the models motivated by discrete family symmetries.

After the breaking of a particular discrete symmetry, it is the mismatch between the residual symmetries of charged lepton and neutrino sector that generates mixing angles closed to their observed values. Beside predicting a zero value of the reactor angle, since the popular flavor symmetry groups such as A_4, $S_{3,4}$, D_4 etc. are unable to speculate the mass ordering of the light neutrinos, testable values of the CP phases and the absolute mass scale, they should be modified to perpetuate a phenomenologically viable theory. In our work, we have done that abatement in two different ways. First, we assume that the remnant (residual) symmetry in the low energy Lagrangian is broken with a small breaking parameter thus generates a nonzero θ_{13}, and along with that mildly broken remnant symmetry, there are also some vanishing elements in the neutrino mass matrix, commonly known as the texture zeros [4], predicting the mass ordering, constraint ranges of CP phases and the mass of the lightest neutrino. Without going into the detailed theoretical justification of the breaking which might be rationalized with several top-down approaches, such as the refinement of the model with an extended matter content which serves as a breaking of the remnant symmetry through a loop contribution [5] or adding soft breaking terms to the initially symmetric theory [6] at high energy etc., we zero in on the low energy predictions of the neutrino parameters such as CP phases, sum of the light neutrino masses $\Sigma_i m_i$ and neutrinoless double $(\beta\beta0\nu)$ decay parameter $|m_{ee}|$.

The second approach is to some extent different than the first one. Although the basic idea is the same, i.e., the residual symmetry in the Lagrangian determines the flavor mixing, it can be proved for the Majorana neutrinos, that whatever may be the high energy flavor symmetry group, the existing residual symmetry in the neutrino mass term is $\mathbb{Z}_2\times\mathbb{Z}_2$ [7–9]. Again due to the nonexistence of nonvanishing θ_{13} in such a model, we have supplemented the latter with a nonstandard CP transformation; CP-transformations followed by a flavor symmetry operation [10]. Unlike the canonical (standard) CP transformation, which is a CP conserving theory, this nonstandard CP transformation predicts maximally violating value $\pi/2$ or $3\pi/2$ for the Dirac CP phase δ and a CP conserving value for the Majorana phases α or β by restricting them to either 0 or π. High energy symmetry group for models of this kind may be constructed through the induced automorphism approach [11, 12].

In the simplest extension of the SM, popularly known as the Type-I seesaw, the light neutrino Majorana masses are generated through the incorporation of three extra right chiral (RH) singlet neutrino fields ν_{Ri} and a corresponding lepton number violating Majorana mass term with a new mass scale close to the GUT (10^{12} GeV). The CP violating and the out of equilibrium decays of the heavy Majorana neutrinos which also violate lepton number intrinsically by construction, creates a lepton asymmetry $Y_{\mathcal{L}}$. Further conversion of this $Y_{\mathcal{L}}$ through the sphaleron process leads to the observed baryon asymmetry $Y_B = (8.7 \pm 0.1) \times 10^{-11}$. The entire process is known as the baryogenesis through leptogenesis. The models with nonstandard CP transformation are also intriguing from the leptogenesis standpoint. Interesting upshots such as nonoccurrence of unflavored leptogenesis and nonvanishing baryon asymmetry preconditioned by a nonzero θ_{13} can be drawn by a suitable implementation of the symmetries under consideration, as explained briefly in an ephemeral description of my research works in the next few paragraphs.

Two of my research works [13, 14] are based on texture zeros along with the discrete residual symmetries; the Scaling Ansatz (SA) [15,16] and a cyclic permutation symmetry. The former is motivated by models with the high energy flavor symmetry groups such as a nonabelian $D_4 \times \mathbb{Z}_2$ and an abelian $U(1)_{L_e - L_\mu - L_\tau}$ while the latter is implemented by a discrete $A_4 \times \mathbb{Z}_3 \times \mathbb{Z}_2$ family symmetry. Some attractive variants of seesaw mechanism, namely, the inverse and the linear seesaw are also considered in both the cases here owing to the fact that the heavy neutrinos originated from these mechanisms are of masses of the order of TeV, thus accessible to the LHC. Due to the significant reduction of the number of parameters in the light neutrino mass matrices, absorbing conclusions regarding the low energy neutrino parameters are drawn for each of the cases. For example, the first case, i.e, the model with Scaling Ansatz, predicts almost a vanishing value of the Dirac CP phase δ thus confronting with testability since T2K's new data (2016) [17] continue to prefer a value of the Dirac CP phase near the maximally violating value $3\pi/2$. Along with an inverted ordering, both the models predict a constraint ranges of the light neutrino masses as well the $\beta\beta 0\nu$ parameter $|m_{ee}|$.

So far in the existing literature, CP-violating Majorana phases are calculated in a model dependent way. In one of my work [18] a general recipe for the evaluation of the Majorana phases is presented assuming the hierarchical mass spectrum of the light neutrinos. To evaluate the Majorana phases in Mohapatra-Rodejohann's phase convention [16], we use the rephasing invariant quantities [19] which remain unchanged even after the rotation of the light neutrino mass matrix in the phase space. In this prescription, the Majorana phases are calculable in a model independent way even for the vanishing values of the lightest neutrino masses m_1 and m_3, for normal and inverted hierarchy respectively. Furthermore, constraining the general methodology with the upper limits on $\Sigma_i m_i$ and $|m_{ee}|$ dictated by PLANCK [20] and GERDA-I [21] respectively, ranges of the Majorana phases are presented in a general context. Emphatic statement such as *given any hierarchical neutrino mass model, our prescription is able to compute the corresponding Majorana phases* is also made.

In the residual $\mathbb{Z}_2 \times \mathbb{Z}_2$ approach, as mentioned earlier, we have generalized the well known Simple Real Scaling ansatz (SRS) [15, 16] on the neutrino Majorana mass matrix to its complex extension and named the latter as Complex Extended Scaling (CES). In this case, the $\mathbb{Z}_2 \times \mathbb{Z}_2$ symmetry is complemented by a nonstandard CP-transformation on the neutrino fields as $\nu_{L\alpha} \rightarrow iG_{\alpha\beta}\gamma^0\nu^C_{L\beta}$ with $G_{\alpha\beta}$ being the generators of one of the $\mathbb{Z}_2$ symmetry and $\nu^C_{L\beta}$ represents the usual charged conjugated left chiral neutrino field. As a consequence, the usual horizontal symmetry $G^T M_\nu^{SRS} G = M_\nu^{SRS}$ is replaced with its complex version; $G^T M_\nu^{CES} G = (M_\nu^{CES})^*$. The entire work is divided into two parts, first one [22] of which focuses on the predictions of low energy neutrino parameters; specifically the robust prediction of $\cos\delta = 0$ and $\sin\alpha = \sin\beta = 0$ or π plus the $\beta\beta0\nu$ decay parameter $|m_{ee}|$ and the measurement of CP-asymmetry parameter $A_{\mu e}$ in the baseline oscillation experiments. In the other [23], we concentrate on the hierarchical flavored leptogenesis within the framework of Type-I seesaw mechanism. We assume strongly hierarchical mass eigenvalues for the RH Majorana neutrino mass matrix M_R. The leptonic CP asymmetry parameter ε_1^α with lepton flavor α, originating from the decays of the lightest of the heavy neutrinos N_1 (of mass M_1) at a temperature $T \sim M_1$, is what matters here with the lepton asymmetry originating from the decays of $N_{2,3}$, being washed out. Interesting feature is the structure of the Dirac mass matrix m_D, imaginary part of which generates the nonzero θ_{13}, maximal Dirac CP violation as well as a nonvanishing ε_1^α , thus serves as a common source of the said quantities. The light leptonic and heavy neutrino number densities (normalized to the entropy density) are evolved via Boltzmann equations down to electroweak temperatures to yield a baryon asymmetry through sphaleronic transitions. The effect of flavored vs. unflavored leptogenesis in the three mass regimes (1) $M_1 < 10^9$ GeV, (2) 10^9 GeV $< M_1 < 10^{12}$ GeV and (3) $M_1 > 10^{12}$ GeV are numerically worked out for both a normal and an inverted mass ordering of the light neutrinos. For best-fit values of the input neutrino mass and mixing parameters, obtained from neutrino oscillation experiments, successful baryogenesis is achieved for the mass regime (1) and a normal mass ordering of the light neutrinos with a nonzero θ_{13} playing a crucial role.

Although there have been significant developments in understanding the neutrino properties from an experimental as well as a theoretical perspective, there still exist some open questions to be answered as previously mentioned. With the construction of some highly predictive models we have tried to address on the those yet indecisive issues such as the CP violation in the neutrino sector, measurement of $\beta\beta0\nu$ decay parameter $|m_{ee}|$, masses of the lightest neutrinos etc. Regarding the predictions of our works, presently some efficacious experiments with greater sensitivity are going on and planned to draw credible conclusions on these issues in the near future.

The existence of leptonic CP violation would show up as the difference of oscillation probabilities between neutrino and anti-neutrinos. For the experiments like T2K, NOνA and DUNE, the relevant quantity is $A_{\mu e}$ in which δ will appear explicitly. Unlike the Dirac CP phase, the Majorana phases appear in neutrino $\rightarrow$ antineutrino oscillation experiments which are purely academic at this moment and practically difficult to design since the oscillation probability is highly suppressed by the factor m_i^2/E^2, where m_i being the mass of the light neutrino with E as the beam energy. Taking $E \sim$ MeV and m_i to be less than 1 eV, an estimation of m_i^2/E^2 might be done to be $\mathcal{O}(10^{-12})$. Although to improve m_i/E, a novel suggestion [24]is to lower the value of E, the size of the base line length as well as the detectors in that case are beyond the reach of the present experimental facilities. Nevertheless, search for the $\beta\beta0\nu$ decay might be a probe to yield one of the Majorana phases.

There are several experiments such as EXO [25], GERDA-I, KamLAND-Zen [26] are ongoing to measure $|m_{ee}|$. Among them GERDA-I puts a strong upper limits of 0.22 eV on $|m_{ee}|$. This limit is likely to be lowered by GERDA-II [27] to 0.098 eV. Thus predictions from our models on $|m_{ee}|$ will be tested in these experiments.

In summary, two very important physical issues of present day particle physics and cosmology – small but nonzero neutrino mass and baryon asymmetry of the universe are addressed from the symmetry point of view towards the quest of an ultimate elusive model.

List of Figures

List of Tables

Chapter 1

Introduction

"*A theory is a supposition which we hope to be true, a hypothesis is a supposition which we expect to be useful; fictions belong to the realm of art; if made to intrude elsewhere, they become either make-believes or mistakes*".

— *George Johnstone Stoney, 1826 to 1911*

Starting from the era of Greek philosopher Democritus (430 BC), when speculation about the fundamental invisible particles of the universe started, to the present time, it has been an exciting journey for the particle physicists. The ups and downs of the subject through this time line made people inquisitive towards the fundamental structure of nature. Gradual uncoiling of mystery of the universe still inspire us to hunt for the extreme elementary particles. It was the discovery of radio activity (1896) followed by the discovery of electron that had probably given a major breakthrough to the subatomic physics. Then came the 20th century, the golden era of particle physics, which started with Planck's blackbody radiation law and ended up with the discovery of neutrino oscillation at Super-Kamiokande [32]. In between, the actual revolution in particle physics happened, when envisioned by some fascinating theoretical frameworks, so many fundamental particles such as neutrinos, W, Z bosons, quarks etc. were discovered which then enforced physicists to knock the door of high energy colliders to search for the rest. Now we are celebrating two major recent time discoveries: 1. Neutrino Oscillation, which confirms the tiny masses of the light neutrinos and 2. The Higgs boson, a prediction of the Standard Model (SM) of particle physics.

The scope of this thesis is to discuss some of the aspects related to the former, i.e. the neutrinos. Speculated by Wolfgang Pauli in 1931 from the analysis of the continuous energy spectrum of β decay, the neutrinos are now one of the major subject area of research in modern particle physics. The mysterious nature of changing their flavor identities (neutrino oscillation) made people think about their tiny masses. The Nobel prize in physics, 2015, was given to Takaaki Kajita and Arthur B. McDonald for implementing those thoughts in experiments and showing those ideas a light of reality. In the following, we discuss a brief history of the neutrinos and some theoretical aspects related to them.

1.1 Neutrinos: The chameleons of space

1.1.1 A brief history of neutrino oscillation

Despite the elegant idea of Wolfgang Pauli of the spin-half and charge neutral particle to explain the 'missing energy' in $\beta-$decay of radioactive ions, actual discovery of the neutrinos happened in 1956 in Reines and Cowan's experiment [33]. They detected an electron anti-neutrino ($\bar{\nu}_e$) from a radioactive source. The idea of neutrino oscillation was first pioneered by B. Pontecorvo in 1957-58 [34, 35]. In his paper Pontecorvo proposed an oscillation between a right handed neutrino (ν_R) and its anti-particle analogous to the $K^0 - \bar{K}^0$ oscillation. Then a theory of virtual transformation of ν_μ to ν_e [36] was proposed by Maki, Nakagawa and Sakata (MNS) in the same year 1962, when the muon neutrino was discovered at Brookhaven National Laboratory, in an experiment led by Lederman, Schwartz and Steinberger [37]. In 1967 Pontecorvo formulated a theory of $\nu_\mu \to \nu_e$ oscillation. He also pointed out that the flux of the solar ν_e could be only the half of its expected flux in the solar neutrino experiment by Davis and collaborators. Davis's experiment was designed to detect the solar neutrinos produced by thermo-nuclear fusion at the core of the sun to study the stellar structure and evolution. However, the observed electron neutrino flux was only the one third of the expected flux from Standard Solar Model (SSM) Prediction. This was an anomaly commonly known at that time as the "Solar Neutrino Problem (SNP)". Apart from various alternative solutions [38–40] neutrino oscillation was one of the strong plausible one, since Pontecorvo already theoretically anticipated this deficit. Before discussing the absolute experimental confirmations of this deficit, let's recapitulate another strong evidence for neutrino oscillation. From the interactions of atomic nuclei and cosmic ray at the Earth's atmosphere, an unstable pion is created. Then through the following reactions

$$\begin{aligned} \pi^\pm(K^\pm) &\to \mu^\pm + \nu_\mu(\bar{\nu}_\mu), \\ \mu^\pm &\to e^\pm + \nu_e(\bar{\nu}_e) + \bar{\nu}_\mu(\nu_\mu) \end{aligned} \tag{1.1}$$

the atmospheric neutrinos are produced. It is obvious from the above reactions that, the approximate number of muon neutrinos should be twice the number of electron neutrinos. However, water Cerenkov detectors like Kamiokande [41], and iron calorimeter detector Soudan2 [42] reported results contrary to this expectation. Again, it was thought that the neutrinos might loose their flavor identities during their flight to the Earth and thus causing that flavor crisis. This convincingly strengthen the possibility of neutrino flavor oscillation further. Let's now come back to the SNP. In 1981-82, the neutrino-electron scattering experiment Kamiokande [43] confirmed the deficit observed in the Davis experiment along with the proof that the detected neutrinos actually came from the Sun. After few years, Gallium based experiments such as GALLEX [44] and SAGE [45] ratified the fact that the measured neutrino signal was indeed smaller than the SSM prediction. Then the Super-Kamiokande (SK), a modern version of the Kamiokande experiment [46] further established the solar neutrino deficit with significantly enhanced statistics. Now in the case of atmospheric neutrinos, oscillation of the neutrinos was established in a firm footing when the SK-detector showed a strong zenith angle dependence in the oscillation probabilities of upward going neutrinos. On the other hand, despite the confirmation of solar neutrino deficit from several experiments, there were no full-proof experimental evidence of neutrino oscillation as far as the results on the solar neutrinos were concerned. In 1975, the discovery of τ-lepton made people curious about the existence of the third neutrino, the τ-neutrino. Moreover existence of three light neutrinos was confirmed further by the LEP experiment [47] from the invisible decay width of the Z boson. However, the third species was not observed until 2000 by the DONUT experiment [48] in which the τ-neutrino was detected from the decay of charmed particle. Finally in 2002, Sudbery Neutrino Observatory (SNO) [49] convincingly confirmed the phenomenon of neutrino oscillation in solar neutrinos. Due to the sensitivity to both Charged Current (CC) and Neutral Current (NC) events, SNO measured contributions from all the three neutrinos. Measuring CC/NC < 1, SNO confirmed the ν_μ and ν_τ components in solar neutrino flux. Again the measurement of NC also confirmed that the total solar neutrino flux was in very good agreement with the SSM prediction. Thus neutrino oscillation served undoubtedly as the clear solution to the SNP. Presently some of the low energy neutrino parameters have been measured with significant confidence level while the rest are yet to be determined. Before going to a brief discussion about the determination of these parameters in different neutrino experiments, we should have an expeditious look at the mathematical formulation of neutrino oscillation both in vacuum as well as in matter and find out what are the oscillation parameters we are taking about.

In the next subsection, we first review the basic theoretical formulation of the oscillation probability within the three flavor scenario in vacuum and in a two flavor scenario in matter. We then discuss some recent experiments relevant to the measurement of these oscillation parameters and present the latest global-fit results in a tabular form.

1.1.2 Formulation of neutrino oscillation theory

The derivation of the oscillation probability is based on a simple quantum mechanical calculation that deals with the time evolution of a quantum mechanical state following the Schrodinger's Equation (SE). A neutrino with flavor eigenstate $|\nu_\alpha\rangle$ can be written as a coherent superposition of mass eigenstates $|\nu_i\rangle$:

$$|\nu_\alpha\rangle = \sum_i^n U^*_{\alpha i} |\nu_i\rangle \,, \tag{1.2}$$

where U is a unitary matrix, as we shall see, sometime it is also called as the U_{PMNS} after the name of the authors, Pontecorvo, Maki, Nakagawa and Sakata. The mass eigenstates are evolved according to SE as

$$i\frac{d}{dt} |\nu_i\rangle = H |\nu_i\rangle \,, \tag{1.3}$$

where $H = p_i + \frac{m_i^2}{2E}$ for extremely relativistic neutrinos ($p_i \gg m_i$). Now following SE, the time dependence of $|\nu_\alpha\rangle$ comes out as

$$|\nu_\alpha(t)\rangle = \sum_i U^*_{\alpha i} e^{-iHt} |\nu_i\rangle \equiv \sum_i U^*_{\alpha i} e^{-i(p_i + \frac{m_i^2}{2E})t} |\nu_i\rangle . \tag{1.4}$$

Further, assuming equal momentum for each mass state at the time of production, (1.4) can be simplified to

$$|\nu_\alpha(t)\rangle = e^{-ipt} \sum_i U^*_{\alpha i} e^{-i\frac{m_i^2}{2E}t} |\nu_i\rangle . \tag{1.5}$$

The amplitude of a flavor state $|\nu_\beta\rangle$ to be found in $|\nu_\alpha\rangle$ after a time t is given by

$$\langle \nu_\beta | \nu_\alpha(t)\rangle = \sum_i U_{\beta i} U^*_{\alpha i} e^{-i\frac{m_i^2}{2E}L}, \tag{1.6}$$

where we assume $L \sim t$ for extreme relativistic neutrinos. Therefore, in a neutrino beam of $|\nu_\alpha\rangle$ the probability of finding $|\nu_\beta\rangle$ state is

$$P_{\alpha\beta} \equiv P(\nu_\alpha \to \nu_\beta) = \left| \sum_i U_{\beta i} U^*_{\alpha i} e^{-i\frac{m_i^2}{2E}L} \right|^2 = \sum_{ij} U^*_{\alpha i} U_{\beta i} U_{\alpha j} U^*_{\beta j} e^{-i\frac{\Delta m_{ij}^2}{2E}L} \tag{1.7}$$

where $\Delta m_{ij}^2 = m_i^2 - m_j^2$ is the mass squared difference between the mass states. Eq. (1.7) can further be simplified to

$$P_{\alpha\beta} = \delta_{\alpha\beta} - 2\sum_{i\neq j} Re(U^*_{\alpha i} U_{\beta i} U_{\alpha j} U^*_{\beta j}) \sin^2 \Delta_{ij} + 2\sum_{i\neq j} Im(U^*_{\alpha i} U_{\beta i} U_{\alpha j} U^*_{\beta j}) \sin^2 \Delta_{ij} \tag{1.8}$$

with $\Delta_{ij} = \frac{\Delta m_{ij}^2 L}{4E}$.

Despite the hints of a light sterile neutrino in LSND [50] and Mini-Boone [51], let's stick to the three-flavor case (e, μ and τ) while deriving the oscillation probabilities. Now the U in (1.8) is a 3×3 mixing matrix that connects the flavored neutrino fields ν_e, ν_μ and ν_τ to the massive neutrino fields ν_1, ν_2 and ν_3. In a simplistic scenario, the mixing matrix U can be parametrized as a product of three orthogonal matrices:

$$U = \begin{pmatrix} 1 & 0 & 0 \\ 0 & c_{23} & s_{23} \\ 0 & -s_{23} & c_{23} \end{pmatrix} \begin{pmatrix} c_{13} & 0 & s_{13} \\ 0 & 1 & 0 \\ -s_{13} & 0 & c_{13} \end{pmatrix} \begin{pmatrix} c_{12} & s_{12} & 0 \\ -s_{12} & c_{12} & 0 \\ 0 & 0 & 1 \end{pmatrix} \tag{1.9}$$

where $s_{ij} \Rightarrow \sin\theta_{ij}$ and $c_{ij} \Rightarrow \cos\theta_{ij}$ with θ_{ij} as the mixing angles. Now, if U follows the parametrization of (1.9), one can conclude that the rate of the process in (1.8) and the rate of its complex conjugate, i.e. $P(\bar{\nu}_\alpha \to \bar{\nu}_\beta)$ are same, i.e. there is no CP violation in the leptonic sector. Therefore to include CP violation (presently T2K result is in favor of a CP violating theory [17]) in the theory of neutrino oscillation, we should consider atleast one unremovable phase in the mixing matrix. In the diagonal basis of charged leptons, the U matrix is parametrized (PDG convention [52]) as

$$U_{PMNS} \equiv \begin{pmatrix} c_{12}c_{13} & e^{i\frac{\alpha}{2}} s_{12}c_{13} & s_{13}e^{-i(\delta-\frac{\beta}{2})} \\ -s_{12}c_{23} - c_{12}s_{23}s_{13}e^{i\delta} & e^{i\frac{\alpha}{2}}(c_{12}c_{23} - s_{12}s_{13}s_{23}e^{i\delta}) & c_{13}s_{23}e^{i\frac{\beta}{2}} \\ s_{12}s_{23} - c_{12}s_{13}c_{23}e^{i\delta} & e^{i\frac{\alpha}{2}}(-c_{12}s_{23} - s_{12}s_{13}c_{23}e^{i\delta}) & c_{13}c_{23}e^{i\frac{\beta}{2}} \end{pmatrix}, \tag{1.10}$$

where the δ and α, β are commonly known as the Dirac (δ) and the Majorana phases (α, β). Appearance of these phases in the U_{PMNS} depends upon the nature of the neutrinos. In case of Dirac type neutrinos, α and β do not appear in (1.10).

For the time being let's leave an elaborate discussion about these phases for chapter 2 and have an emphatic look on the oscillation probabilities for this three-flavor case. In the experiments with small L/E, a vanishing value of $\sin^2(\Delta m^2_{12}\frac{L}{E})$ can be assumed. Then with a reasonable approximation $\Delta m^2_{23} \approx \Delta m^2_{13}$, the expressions for the oscillation probabilities are derived as

$$P(\nu_\mu \to \nu_\tau) = \cos^2\theta_{13}\sin^2\theta_{23}\sin^2\left(\frac{\Delta m^2_{23}L}{4E}\right), \tag{1.11}$$

$$P(\nu_e \to \nu_\mu) = \sin^2 2\theta_{13}\sin^2\theta_{23}\sin^2\left(\frac{\Delta m^2_{23}L}{4E}\right), \tag{1.12}$$

$$P(\nu_e \to \nu_\tau) = \sin^2 2\theta_{13}\cos^2\theta_{23}\sin^2\left(\frac{\Delta m^2_{23}L}{4E}\right). \tag{1.13}$$

For the experiments with large L/E, one can have

$$P(\nu_e \to \nu_{\mu+\tau}) = \cos^2\theta_{13}\sin^2 2\theta_{12}\sin^2\left(\frac{\Delta m^2_{12}L}{4E}\right) + \frac{1}{2}\sin^2 2\theta_{13}. \tag{1.14}$$

An intriguing point is to be noticed: For $\theta_{13} \to 0$, Eq. (1.11)-Eq. (1.13) reduce to

$$P(\nu_\mu \to \nu_\tau) = \sin^2\theta_{23}\sin^2\left(\frac{\Delta m^2_{23}L}{4E}\right), \tag{1.15}$$

$$P(\nu_e \to \nu_\mu) = 0, \tag{1.16}$$

$$P(\nu_e \to \nu_\tau) = 0 \tag{1.17}$$

for small L/E and

$$P(\nu_e \to \nu_{\mu+\tau}) = \sin^2 2\theta_{12}\sin^2\left(\frac{\Delta m^2_{12}L}{4E}\right) \tag{1.18}$$

for large L/E. These are the same equations one derives for a two flavor case [53]. Usually (1.15) and (1.18) are attributed to the atmospheric and solar neutrino oscillation respectively. In deriving the above expressions, the effect of CP violation has been neglected. However, in chapter 4, more compact expressions for the oscillation probabilities with nonvanishing CP violation effect are discussed. Now let's consider a more realistic scenario–propagation of the neutrinos through matter. For simplicity here we address only the two flavor case. The unitary mixing matrix

U having a form

$$U = \begin{pmatrix} \cos\theta & \sin\theta \\ -\sin\theta & \cos\theta \end{pmatrix} \tag{1.19}$$

connects the flavor and the massive neutrino fields through the equation

$$\begin{pmatrix} \nu_\alpha \\ \nu_\beta \end{pmatrix} = U \begin{pmatrix} \nu_1 \\ \nu_2 \end{pmatrix}. \tag{1.20}$$

Thus in terms of quantum fields (1.3) can be written as

$$i\frac{d}{dt}\begin{pmatrix} \nu_\alpha \\ \nu_\beta \end{pmatrix} = UHU^\dagger \begin{pmatrix} \nu_\alpha \\ \nu_\beta \end{pmatrix}. \tag{1.21}$$

This transformed Hamiltonian $H_f = UHU^\dagger$ has an expression

$$H_f = H_0 + \frac{\Delta m^2}{4E}\begin{pmatrix} -\cos 2\theta & \sin 2\theta \\ \sin 2\theta & \cos 2\theta \end{pmatrix} \tag{1.22}$$

with $H_0 = \frac{m_1^2+m_2^2}{4E}$ and $\Delta m^2 = m_2^2 - m_1^2$. Let's now add an interaction potential term $V = \text{diag}\,(V_\alpha, V_\beta)$ to the Hamiltonian H_f with the subtle assumption that the flavors α and β interact differently with matter. Eq.(1.21) can now be written as

$$i\frac{d}{dt}\begin{pmatrix} \nu_\alpha \\ \nu_\beta \end{pmatrix} = [H_0 + \begin{pmatrix} -\frac{\Delta m^2}{4E}\cos 2\theta + V_\alpha & \frac{\Delta m^2}{4E}\sin 2\theta \\ \frac{\Delta m^2}{4E}\sin 2\theta & \frac{\Delta m^2}{4E}\cos 2\theta + V_\beta \end{pmatrix}] \begin{pmatrix} \nu_\alpha \\ \nu_\beta \end{pmatrix}. \tag{1.23}$$

We can always add a constant to the effective Hamiltonian since that constant will ultimately appear as a overall phase with the neutrino fields and will vanish when one takes modulus square for calculating the probability. Thus through the addition of a constant term $-V_\beta$, (1.23) can be written as

$$i\frac{d}{dt}\begin{pmatrix}\nu_\alpha\\ \nu_\beta\end{pmatrix} = [H_0 + \begin{pmatrix}-\frac{\Delta m^2}{4E}\cos 2\theta + (V_\alpha - V_\beta) & \frac{\Delta m^2}{4E}\sin 2\theta \\ \frac{\Delta m^2}{4E}\sin 2\theta & \frac{\Delta m^2}{4E}\cos 2\theta\end{pmatrix}]\begin{pmatrix}\nu_\alpha\\ \nu_\beta\end{pmatrix}. \tag{1.24}$$

Now, transforming this flavor Hamiltonian into the vacuum mass basis we get

$$i\frac{d}{dt}\begin{pmatrix}\nu_1\\ \nu_2\end{pmatrix} = [\frac{1}{2E}\begin{pmatrix}m_1^2 + \Delta V\cos^2\theta & \Delta V\cos\theta\sin\theta \\ \Delta V\cos\theta\sin\theta & m_2^2 + \Delta V\sin^2\theta\end{pmatrix}]\begin{pmatrix}\nu_1\\ \nu_2\end{pmatrix} \tag{1.25}$$

where $\Delta V = V_\alpha - V_\beta$. From (1.25) we can see that the effective Hamiltonian is no longer diagonal. Thus the mass states in the vacuum are not the same mass states in matter [54, 55]. To obtain the mass eigenstates in matter, we need to diagonalize the Hamiltonian given in (1.25). After a short algebra one finds

$$\Delta m_m^2 = \Delta m^2\sqrt{(\Delta V/\Delta m^2 - \cos 2\theta)^2 + \sin^2 2\theta}, \tag{1.26}$$

$$\sin 2\theta_m = \frac{\sin 2\theta}{\sqrt{(\Delta V/\Delta m^2 - \cos 2\theta)^2 + \sin^2 2\theta}} \tag{1.27}$$

where Δm_m^2 is the mass splitting in the matter and θ_m is the mixing angles between the flavor states in vacuum and the mass states in matter. Therefore, the expression for the probability of $\nu_e \to \nu_\mu$ oscillation can be written as

$$P(\nu_e \to \nu_\mu) = \sin^2 2\theta_m \sin^2\left(\frac{\Delta m_m^2 L}{4E}\right). \tag{1.28}$$

Let's now have a quick look at some of the interesting points related this discussion:

- When $\Delta V = 0$, the mass splitting and the mixing angle in matter become $\Delta m_m^2 = \Delta m^2$ and $\sin^2 2\theta_m = \sin^2 2\theta$. That is, in absence of the interaction potential the matter parameters reduce to the vacuum parameters.

- If $\theta = 0$, then θ_m vanishes (cf. Eq.(1.27)). Therefore, oscillation to occur in matter, there should be a possibility for vacuum mixing.

- In the case of a very dense matter, i.e., $\Delta V \to \infty$, $\sin 2\theta_m \to 0$. Thus in a very dense matter there will be no oscillation.

- If $\Delta V = \Delta m^2 \cos 2\theta$, then the matter mixing angle is $\pi/4$–irrespective of vacuum mixing angle. Thus even if the vacuum mixing is tiny, the probability of oscillation in matter might be maximum for a certain value of matter potential. This is known as the MSW resonance. For a positive value of ΔV, and with the sign convention $\cos 2\theta > 1$, one finds Δm^2 to be positive. Thus from matter effect we can determine the sign of Δm^2.

This is the two flavor case of neutrino oscillation in matter. Similarly, a three flavor calculation can also be done with certain assumptions [56, 57] to simplify the long and complicated algebra. In realistic scenarios, the matter effect plays a crucial role for computation of the oscillation probabilities. As for example, for the calculation of solar neutrino flux, one has to consider the effect of matter in the Sun. Again, in the measurement of CP violation in the long baseline experiments such as T2K, NOνA, DUNE etc., matter of the Earth plays a significant role.

As we can see, basically there are eight relevant parameters (for Majorana type neutrinos) to deal with; three mixing angles $\{\theta_{12},\ \theta_{23},\ \theta_{13}\}$, two mass squared differences $\{\Delta m^2_{12},\ |\Delta m^2_{23}|\}$ and three CP violating phases $\{\delta,\ \alpha,\ \beta\}$. These are commonly known as the low energy neutrino parameters. Apart from the CP violating phases, all the parameters have been measured at a strong confidence level in Baseline, reactor and accelerator neutrino experiments. There have been a lot of efficient experiments devoted to the measurement of the neutrino parameters. Let's have a transitory look at some of the recent experiments, especially those that are relevant to the latest global fit data.

Solar neutrino experiments:

As mentioned earlier, solar neutrino experiment was first proposed by Davis and collaborators [58]. Thereafter several experiments have been developed. The Cl^{37} [59], SK [46], and SNO [49] experiments measured the neutrinos having high energy (~ 5 MeV), followed by Borexino [60] that measured intermediate energy solar neutrinos. Then there are SAGE [45], GALLEX [44] and GNO [61] experiments which dealt with low energy neutrinos. After the analysis of solar data it has been found that it can be explained with the parameters

$$\Delta m^2_{12} = (7.6 \pm 0.2) \times 10^{-5}\text{eV}^2, \quad \sin^2\theta_{12} = 0.8 \pm 0.1. \tag{1.29}$$

which is again verified by the long baseline KamLAND experiment [62].

Atmospheric neutrino experiments:

The SK was the first atmospheric neutrino experiment that provided the compelling evidence of neutrino oscillation in 1998. It is mentioned earlier that the atmospheric neutrinos are produced in the decays of $\pi^\pm$ and $K^\pm$. Now, since those particles are also produced in the accelerator when protons are thrown to a fixed target, there is a scope of verification of the atmospheric neutrino experimental results in the accelerator experiments. Different accelerator experiments such as K2K [63], T2K [17] and MINOS [64] confirmed those results at a high confidence level. A combined analysis of the above experiments leads to the best fit values for the parameters Δm^2_{23} and θ_{23} as:

$$|\Delta m_{23}|^2 = (2.41 \pm 0.1) \times 10^{-3}\text{eV}^2, \quad \sin^2\theta_{23} = 0.95 \pm 0.035. \tag{1.30}$$

Reactor neutrino experiments:

The mixing angle θ_{13} is measured from the $\bar{\nu}_e$ disappearance in the reactor experiments. An upper bound of $\sin^2\theta_{13} < 0.16$ has been set by CHOOZ at 90% C.L for a neutrino beam of energy $E \sim 3$ MeV. A nonzero value of the mixing angle has also been confirmed by the experiments such as T2K, MINOS, Double Chooz [65]. Recently, in the year 2012, two reactor experiments Daya Bay [66] and RENO [67] have confirmed the result with enhanced statistics. Particularly Daya Bay has confirmed a nonzero value of θ_{13} at the 5.2σ level. The best fit value of the Daya Bay data yields

$$\sin^2\theta_{13} = 0.090 \pm 0.009. \tag{1.31}$$

Beside the parameters mentioned above, there are experiments such as T2K, NOνA, DUNE that measure the Dirac CP phase δ. However, there is no scope for the measurement of the Majorana phases, since those do not appear in the usual neutrino$\rightarrow$neutrino ($\nu \rightarrow \nu$) oscillation experiments. In chapter 2 a brief discussion about neutrino$\rightarrow$anti-neutrino ($\nu \rightarrow \bar{\nu}$) oscillation has been presented with an emphasis on the Majorana phases that appear explicitly in the expression of $\nu \rightarrow \bar{\nu}$ oscillation probability. Although different experiments are devoted to the measurement of different parameters, a global fit analysis is needed to constrain the parameter space of a particular neutrino mass model.

Recent global-fit data and future prospects

In Table 1.1 the recent global-fit data [30] from various oscillation experiment are tabulated. Here we present only the 3σ data and the best fit points (Bfp). A subtle point in the global-fit analysis should be focused. As we found before, the sign of Δm^2_{12} is determined from the MSW effect. However, till now we do not have a firm statement about the sign of Δm^2_{13}. Thus the mass ordering of the light neutrinos has not been fixed yet. Again, since $|\Delta m_{13}|^2 \gg \Delta m^2_{12}$, the two masses m_1 and m_2 are taken to be nearly degenerate. In the global-fit analysis, $|\Delta m_{13}|^2$ is calculated as $|\Delta m_{13}|^2 \simeq |\Delta m_{23}|^2 \equiv |\Delta m|^2 = m_3^2 - \frac{(m_1^2+m_2^2)}{2}$. Thus for a normal (inverted) mass ordering, Δm^2 takes a positive (negative) value.

Table 1.1: Recent global-fit data [30] (Bfp: Best fit point, NO: Normal Ordering, IO: Inverted Ordering)

Parameters	θ_{12} (in deg.)	θ_{23} (in deg.)	θ_{13} (in deg.)	$\Delta m^2_{21}/10^{-5}$ (in eV^2)	$\lvert\Delta m^2_{31}\rvert/10^{-3}$ (in eV^2)
3σ	31.29 − 35.91	38.3−53.3	7.87−9.11	7.02 − 8.09	2.32 − 2.59
Bfp(NO)	33.48	42.3	8.50	7.50	2.46
Bfp(IO)	33.48	49.5	8.51	7.50	2.45

Some concluding remarks: As one finds, basically there are five parameters; $\{\theta_{12}, \theta_{23}, \theta_{13}, |\Delta m_{13}|^2, \Delta m_{12}\}$ that have been measured by several neutrino experiments. However, still there is no statistically significant result on δ. Nevertheless, it is worth mentioning that recently T2K has announced CP violation in the leptonic sector at 90% C.L.. In addition, there are some open problems; the nature of the neutrinos-Dirac or Majorana, the octant of θ_{23}, values of the Majorana phases-if neutrinos are Majorana, needed to be addressed to pin down our knowledge about leptonic sector of the SM and beyond.

1.2 Neutrino masses and a journey beyond the Standard Model

Neutrinos are massless in the standard $SU(2)_L \times U(1)_Y$ model (SM) which has been celebrated as the most successful model of particle physics. Before the discussion of neutrino masses in the SM and beyond, we would like to have a brief view on the fermionic mass terms in field theory. With ψ as a fermionic field, the Lagrangian for the mass term is written as

$$-\mathcal{L}_m = \overline{\psi} m \psi = m\overline{(\psi_L + \psi_R)}(\psi_L + \psi_R) = m\overline{\psi_L}\psi_R + m\overline{\psi_R}\psi_L, \tag{1.32}$$

where $\psi_L = P_L\psi$ and $\psi_R = P_R\psi$ with $P_{R,L} = \frac{1\pm\gamma_5}{2}$ as the right and left chirality projectors. From Eq. (1.32) it is clear that the mass of the fermion couples simultaneously to the both, left chiral as well as the right chiral components. Thus a massive fermionic field must possess both the components. Now if the right chiral component is completely independent from the left chiral one, then the corresponding mass term is a Dirac type mass term. Before, going to the other possibility, a subtle point should be addressed. The terms "left chiral" or "right chiral" imply the handedness of a relativistic particle. To be more precise, handedness or helicity of a particle is defined with the operator

$$\hat{H}_{\pm} = \frac{1}{2}(1 \pm \frac{\tau.\mathbf{p}}{|\mathbf{p}|}) \tag{1.33}$$

which is not Lorentz invariant but does not change with time. On the other hand, chirality is a Lorentz invariant quantity and not being a constant of motion. But in the limit $m \to 0$, both of them coincide. Thus for a relativistic particle chirality and the handedness or helicity is identical. Now let's come back again to the construction of the fermionic mass terms. This can be proved that upon charge conjugation chirality of a ferminon flips. For an example, with a charge conjugation operation 'C', the chiral fields transform as

$$C: \;\; \psi_L \to (\psi_L)^c = (\psi^c)_R, \;\; \psi_R \to (\psi_R)^c = (\psi^c)_L \tag{1.34}$$

with $C = i\gamma_0\gamma_2$. Thus unlike the Dirac composition of fermion field, i.e., $\psi = \psi_L + \psi_R$, now one can write ψ as

$$\psi = \psi_L + e^{i\alpha_1}(\psi_L)^C, \quad \psi = \psi_R + e^{i\alpha_2}(\psi_R)^C, \tag{1.35}$$

where $\alpha_{1,2}$ are some arbitrary phases. From the decomposition of ψ in (1.35), one can have

$$\psi^C = e^{-i\alpha_{1,2}}\psi \tag{1.36}$$

which means the particles described by the field ψ of (1.35) are basically their own anti-particles. These particles are commonly known as the Majorana fermions. Thus the Majorana mass term for a massive fermion can be written as

$$-\mathcal{L}_M = \frac{1}{2}\overline{\psi_L^C} m \psi_L + \text{h.c.}. \tag{1.37}$$

Note that unlike the Dirac mass term, this does not conserves any $U(1)$ quantum number. For n species of fermions (1.37) can easily be generalized to

$$-\mathcal{L}_M = \frac{1}{2}[\varphi_L^T C M \varphi_L + \text{h.c.}], \tag{1.38}$$

where $\varphi = (\psi_1, \psi_2 ... \psi_n)^T$ is a state vector in the flavor space and M is a complex, symmetric $n \times n$ mass matrix. Let's now come back to the discussion regarding the accommodation of neutrino masses in the SM. Unlike the charged leptons and the quarks there are no $SU(2)_L$-singlet right handed components for the neutrinos and thus they are massless in the SM. However, as discussed above, one can construct a Majorana mass term using left handed neutrino components as

$$-\mathcal{L}_M^\nu = \frac{1}{2}\overline{\nu_L^C} M_\nu \nu_L. \tag{1.39}$$

Now since a neutrino ν_{iL} is a part of the lepton doublet $\not{L} = (\nu_{iL} \;\; \ell_{iL})^T$, the operator $\overline{\nu_L^C}\nu_L$ is constructed by means of an isotriplet $\not{L}^T C i\tau_2\tau_a \not{L}$. Therefore in order to generate the Majorana mass term in a gauge invariant way, one should introduce an isotriplet Higgs field Δ_a which was not there in the SM. Obviously a gauge invariant and $d = 5$ term $(\not{L}^T C i\tau_2\tau_a \not{L})(\phi^T C i\tau_2\tau_a \phi)$ might also be constructed through the SM Higgs doublet $\phi = (\phi^+ \;\; \phi^0)^T$. However, this term is not allowed, since it violates the lepton number L which is conserved at perturbative level as well as the number $B - L$, a quantity that is conserved at nonperturbative level [68] in the SM. Thus convincingly, we should extend the SM to accommodate a nonzero neutrino mass. There have been quite a large number of extensions of the SM by enlarging the field contents. With the introduction of new RH singlets (N_{iR}), the simplest extension is done by writing a Dirac mass term

$$-\mathcal{L}_D = f_{ij}\overline{\not{L}_{iL}} i\tau_2\phi N_{jR} + \text{h.c.} = \overline{\not{L}_{iL}}(m_D)_{ij}N_{jR} + \text{h.c.} \tag{1.40}$$

for the neutrinos. However, given the same vacuum expectation value $\langle\phi^0\rangle$, unlike the charged leptons, an unnaturally smallness of the coupling f_{ij} is required to generate a neutrino mass of $\mathcal{O}$(eV). For this typical characteristic, despite being a theoretically correct model, this simplest extension of the SM fails to draw much attention. Although there are several neutrino mass models that deal with possible extensions of the SM, here we explore some simplistic scenarios which are also intriguing from various aspects, apart from generating the tiny neutrino masses.

Type-I seesaw: This is one of the most fundamental mechanisms to generate small Majorana neutrino masses. With the addition of extra RH singlets N_{Ri} to the SM, the pertinent Lagrangian can be written as

$$-\mathcal{L}_{T1} = \frac{1}{2}\overline{\nu}_L m_L \nu_L^C + \frac{1}{2}\overline{N_R^C} M_R N_R + \overline{\nu_L} m_D N_R + \text{h.c.}, \tag{1.41}$$

where we assume all the possible mass terms constructed by ν_L and N_R are present in the Lagrangian. Here we have omitted the generation indices that imply three generations of light neutrinos and for simplicity, three generations for the heavy neutrinos as well. Now using the properties of the charge conjugation matrix C, it can easily be shown that the concerned Lagrangian $\mathcal{L}_{T1}$ is of form

$$-\mathcal{L}_{T1} = \frac{1}{2}(\nu_L^C)^T C m_L \nu_L^C + \frac{1}{2}(N_R)^T C m_D^T \nu_L^C + \frac{1}{2}(\nu_L^C)^T C m_D N_R + \frac{1}{2} N_R^T C M_R N_R + \text{h.c.}. \tag{1.42}$$

In the basis $(\nu_L^c \;\; N_R)$, one can write the above Lagrangian in a more compact form with a 6×6 mass matrix $\mathcal{M}$ as

$$\begin{aligned} -\mathcal{L}_{T1} &= \frac{1}{2}\begin{pmatrix} \nu_L^C & N_R \end{pmatrix} C \begin{pmatrix} m_L & m_D \\ m_D^T & M_R \end{pmatrix} \begin{pmatrix} \nu_L^C \\ N_R \end{pmatrix} + \text{h.c.} &(1.43)\\ &= \frac{1}{2} n^T C \mathcal{M} n + \text{h.c.}, &(1.44)\end{aligned}$$

where $n = (\nu_L^C \;\; N_R)^T$. Now with the approximation $M_R \gg m_D \gg m_L$ the matrix $\mathcal{M}$ can be diagonalized by a unitary matrix U of form

$$U = \begin{pmatrix} 1 & \varrho \\ -\varrho^\dagger & 1 \end{pmatrix}, \tag{1.45}$$

where $U^\dagger U = 1 + \mathcal{O}(\varrho^2)$. With the diagonalization condition $U^T \mathcal{M} U = \text{diag}\,(M_1,\; M_2)$ and a reasonable approximation of ϱ being real, one evaluates

$$U^T \mathcal{M} U = \begin{pmatrix} m_L - \varrho m_d^T - m_D \varrho^T & m_L \varrho + m_D - \varrho M_R \\ \varrho^T m_L + m_D^T - M_R \varrho^T & m_D^T \varrho + \varrho^T m_D + M_R \end{pmatrix}. \tag{1.46}$$

Now recalling the assumption $M_R \gg m_D \gg m_L$, from '12' and '21' elements of the matrix in the RHS of (1.46), ϱ can be calculated as

$$\varrho \simeq m_D M_R^{-1}. \tag{1.47}$$

Thus from the '11' and '22' elements, M_1 and M_2 are calculated as

$$M_1 \simeq m_L - m_D M_R^{-1} m_D^T, \quad M_2 \simeq M_R. \tag{1.48}$$

Note that the matrix $\mathcal{M}$ is now block diagonalized and $M_{1,2}$ are 3×3 mass matrices. Eq. (1.44) can now be written as

$$\frac{1}{2} n^T C \mathcal{M} n + \text{h.c.}. = \frac{1}{2} \chi^T C \mathcal{M}_d \chi + \text{h.c.} = \frac{1}{2} \chi_1^T C M_1 \chi_1 + \frac{1}{2} \chi_2^T C M_2 \chi_2 + \text{h.c.}, \tag{1.49}$$

where

$$\chi = \begin{pmatrix} \chi_1 \\ \chi_2 \end{pmatrix} = U^\dagger n = U^\dagger \begin{pmatrix} \nu_L^C \\ N_R \end{pmatrix} = \begin{pmatrix} \nu_L^C - \varrho N_R \\ \varrho^T \nu_L^C + N_R \end{pmatrix} \simeq \begin{pmatrix} \nu_L^C - m_D M_R^{-1} N_R \\ M_R^{-1} m_D^T \nu_L^C + N_R \end{pmatrix}. \tag{1.50}$$

Finally, taking into account the hermitian conjugate term, Eq. (1.49) can be rewritten as

$$-\mathcal{L}_{T1} = \frac{1}{2} \varphi_1^T C M_1 \varphi_1 + \frac{1}{2} \varphi_2^T C M_2 \varphi_2 \tag{1.51}$$

with

$$\begin{aligned} \varphi_1 &\simeq (\nu_L + \nu_L^C) - m_D M_R^{-1} (N_R + N_R^C), \\ \varphi_2 &\simeq (N_R + N_R^C) + M_R^{-1} m_D^T (\nu_L + \nu_L^C). \end{aligned} \tag{1.52}$$

This is worth mentioning that the states in (1.52) are the Majorana states where the first one is predominantly made of ν_L while N_R dominates in the other. Thus starting from a general Lagrangian which contains all the mass terms constructed out of ν_L and N_R, we end up with two Majorana mass state φ_1 and φ_2 having masses $M_1 \simeq m_L - m_D M_R^{-1} m_D^T$ and $M_2 \simeq M_R$ respectively. Now with the values $m_L = 0$, $m_D \sim 10^2$ GeV and $M_R \sim 10^{14}$ GeV, the elements of the mass matrix M_1 become $\mathcal{O}(0.1)$ eV. Thus M_1 can be referred as the light neutrino mass matrix M_ν upon diagonalization of which, $\mathcal{O}$(eV) neutrinos are produced. Note that introduction of a new heavy scale ($\sim 10^{14}$) GeV is needed to have tiny neutrino masses in the theory. Philosophically, this may be compared to a seesaw, lowering of one end of which requires an upliftment of the other side. The whole procedure discussed here is known as the Type-I seesaw mechanism. Beside generating light neutrino masses, Type-I seesaw has an appealing implication on baryogenesis. From the decay of heavy RH Majorana neutrinos a lepton asymmetry is produced which is further converted into a baryon asymmetry by spheleronic transition. We have elaborately discussed this phenomena of baryogenesis via leptogenesis in the next section. There are some other variants of the seesaw model, a brief discussion regarding which is what follows.

Inverse seesaw: In addition to the field content of Type-I seesaw, if another species of fermionic singlets (S_L) are added for each generation to the Lagrangian as

$$-\mathcal{L}_{IS} = \mathcal{L}_{T1} + \bar{\nu_L} M_{DS} S_L^C + \overline{S_L} M_{RS} N_R + \frac{1}{2}\overline{S_L}\mu S_L^C + \text{h.c.}, \tag{1.53}$$

then in the basis $(\nu_L^C \;\; N_R \;\; S_L^C)$, the effective mass matrix $\mathcal{M}$ takes the form

$$\mathcal{M} = \begin{pmatrix} m_L & m_D & M_{DS} \\ m_D^T & M_R & M_{RS}^T \\ M_{DS}^T & M_{RS} & \mu \end{pmatrix}. \tag{1.54}$$

Note that now this $\mathcal{M}$ in (1.54) is a 9×9 mass matrix if all the three flavors are taken into account for each mass terms. Assuming 'zeros' (obviously dictated by some symmetry) in different positions in $\mathcal{M}$, varieties of seesaw mechanism might be explored [69]. Here we discuss only the Inverse seesaw mechanism in detail, due to its relevance to this thesis. A vanishing value in the '11', '13', '22' and '31' elements leads to the structure of $\mathcal{M}$ given by

$$\mathcal{M} = \begin{pmatrix} 0 & m_D & 0 \\ m_D^T & 0 & M_{RS}^T \\ 0 & M_{RS} & \mu \end{pmatrix}. \tag{1.55}$$

Now in this case also we follow the seesaw like diagonalization procedure with the hierarchical assumption $M_{RS} \gg m_D \gg \mu$. The matrix $\mathcal{M}$ in (1.55) can be block diagonalized as

$$\mathcal{M} = \left(\begin{array}{c|cc} 0 & m_D & 0 \\ \hline m_D^T & 0 & M_{RS}^T \\ 0 & M_{RS} & \mu \end{array}\right) = \left(\begin{array}{c|c} 0_{3\times3} & (\mathbb{M}_D)_{3\times6} \\ \hline (\mathbb{M}_D)^T_{6\times3} & (\mathbb{M}_{RS})_{6\times6} \end{array}\right),$$

where

$$\mathbb{M}_D = \begin{pmatrix} m_D & 0 \end{pmatrix}, \quad \mathbb{M}_{RS} = \begin{pmatrix} 0 & M_{RS}^T \\ M_{RS} & \mu \end{pmatrix}. \tag{1.56}$$

Now similar to Type-I seesaw, a diagonalizing matrix U can be taken as

$$U = \begin{pmatrix} 1_{3\times3} & \varrho_{3\times6} \\ -\varrho^\dagger_{6\times3} & 1_{6\times6} \end{pmatrix} \tag{1.57}$$

with $U^\dagger U = 1 + \mathcal{O}(\varrho^2)$. Thus the low energy effective light neutrino mass matrix M_ν

comes out as

$$M_\nu = -\varrho \mathbb{M}_D^T = -\mathbb{M}_D \mathbb{M}_{RS}^{-1} \mathbb{M}_D^T. \tag{1.58}$$

Writing explicitly the forms of $\mathbb{M}_D$ and $\mathbb{M}_{RS}$ from (1.56), one finds

$$\begin{aligned} M_\nu &= -\begin{pmatrix} m_D & 0 \end{pmatrix} \begin{pmatrix} M_{RS}^{-1}\mu(M_{RS}^T)^{-1} & M_{RS}^{-1} \\ (M_{RS}^T)^{-1} & 0 \end{pmatrix} \begin{pmatrix} m_D^T \\ 0 \end{pmatrix} \\ &= -m_D M_{RS}^{-1}\mu(M_{RS}^{-1})^T m_D^T, \end{aligned} \tag{1.59}$$

where we have used the block inversion formula for a 2×2 block matrix M_B as

$$M_B^{-1} = \begin{pmatrix} W & X \\ Y & Z \end{pmatrix}^{-1} = \begin{pmatrix} Y^{-1}ZX^{-1} & Y^{-1} \\ X^{-1} & W \end{pmatrix}. \tag{1.60}$$

Now taking $m_D \sim 100$ GeV, $M_{RS} \sim 10$ TeV and the lepton number breaking mass μ ~1 KeV one can generate neutrino mass $\mathcal{O}$(eV). Interesting point in this variant of seesaw is that only $\mathcal{O}$(TeV) heavy neutrinos are now required to realize the light neutrino masses. Thus unlike the conventional Type-I seesaw, inverse seesaw can be tested through collider experiments.

Neutrino mixing implies the generational lepton numbers such as electron number, muon number are not conserved. This gives rise to the flavor changing processes that involve the charged leptons. Amplitude of a lepton flavor violating (LFV) decay $\ell_i \to \ell_j\gamma$ is proportional to the mass square of the light neutrino propagators (cf. Fig 1.1) and hence the decay width is very much suppressed. However, in the models like seesaw and inverse seesaw that contain extra heavy neutral fermions, this LFV decay amplitude gets an additional contribution $\mathcal{O}(\varrho^2)$ [70]. Thus one expect an enhancement in the LFV decay width.

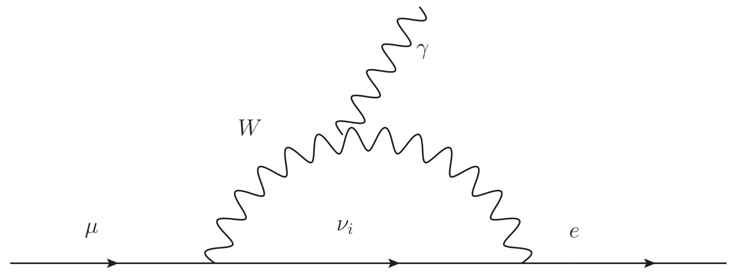

Figure 1.1: One loop diagram for $\mu \to e\gamma$ decay mediated by light neutrinos. Here W is a gauge boson.

In the case of Type-I seesaw, this additional contribution is much smaller since it is suppressed by the heavy neutrinos of masses $\mathcal{O}(10^{14})$ GeV. On the contrary, in the inverse seesaw mechanism $\varrho \sim \mathcal{O}(m_D/M_{RS})$ is much higher than that in the case of Type-I seesaw. Thus there are significant enhancements in the branching ratios (BR) for the LFV decays. Given the upper limits on the BRs of three LFV decays as $B(\mu \to e\gamma) < 2 \times 10^{-12}$, $B(\tau \to e\gamma) < 2.7 \times 10^{-6}$, $B(\tau \to \mu\gamma) < 2.7 \times 10^{-6}$, one can constrain a TeV scale seesaw model like inverse seesaw and check its viability. [71].

Type-II seesaw: In this extension of the SM, a triplet scalar field Δ having a form

$$\Delta = \begin{pmatrix} \delta^+/\sqrt{2} & \delta^{++} \\ \delta^0 & -\delta^+/\sqrt{2} \end{pmatrix} \tag{1.61}$$

is introduced in addition to the regular matter content of the SM. A $SU(2)_L \times U(1)_Y$ invariant Majorana mass term is then generated with Δ through the operator $\not{L}^T C i\tau_2 \tau_a \not{L}$ as

$$-\mathcal{L}_{T2} = (Y_\Delta)_{ij} \not{L}_i^T C i\tau_2 \Delta \not{L}_j + \text{h.c.}. \tag{1.62}$$

Thus a nonzero vacuum expectation value (VEV) of the neutral component of Δ

triggers nonvanishing neutrino masses. Note that although the triplet operator carries a lepton number 2, one can assign the same of value -2 to the triplet scalar. Thus the term in (1.62) is not necessarily a lepton number violating term–a requirement for the Majorana neutrinos. However when the neutral component δ^0 acquires VEV after spontaneous symmetry breaking (SSB) the lepton number symmetry is broken and thus nonvanishing neutrino masses are generated through a mass term with spontaneously broken lepton number. Now in Ref [72, 73] it has been shown that spontaneous breaking of a global $U(1)$ leads to a massless pseudo scalar particle (J) called 'Majoron'. In the present model, after SSB a 'triplet Majoron' will appear. However, this triplet Majoron model is now ruled out experimentally [74]. To avoid this Majoron problem a self-renormalized trilinear term $\frac{\Lambda_6}{\sqrt{2}}\phi^T i\tau_2\Delta^\dagger\phi$ + h.c which violates the lepton number explicitly is added to the interaction potential. Thus the scalar potential for Type-II seesaw can be written as

$$\begin{aligned}\mathcal{V}(\phi,\Delta) &= -\mu^2\phi^\dagger\phi + \frac{\lambda}{2}(\phi^\dagger\phi)^2 + M_\Delta^2\mathrm{Tr}(\Delta^\dagger\Delta) + \frac{\lambda_1}{2}[\mathrm{Tr}(\Delta^\dagger\Delta)]^2 \\ &+ \frac{\lambda_2}{2}\left([\mathrm{Tr}(\Delta^\dagger\Delta)]^2 - \mathrm{Tr}[(\Delta^\dagger\Delta)^2]\right) + \lambda_4(\phi^\dagger\phi)\mathrm{Tr}(\Delta^\dagger\Delta) + \lambda_5\phi^\dagger[\Delta^\dagger,\Delta]\phi \\ &+ \left(\frac{\Lambda_6}{\sqrt{2}}\phi^T i\tau_2\Delta^\dagger\phi + \mathrm{h.c.}\right). \end{aligned} \tag{1.63}$$

Now minimizing the scalar potential of (1.63) with respect to ϕ and Δ we get

$$m_\phi^2 = \frac{1}{2}\lambda v^2 - \Lambda_6 v_\Delta + \frac{1}{2}(\lambda_4-\lambda_5)v_\Delta^2, \tag{1.64}$$

$$M_\Delta^2 = \frac{1}{2}\frac{\Lambda_6 v^2}{v_\Delta} - \frac{1}{2}(\lambda_4-\lambda_5)v^2 - \frac{1}{2}\lambda_1 v_\Delta^2, \tag{1.65}$$

where $\langle\phi^0\rangle = v/\sqrt{2}$ and $\langle\delta^0\rangle = v_\Delta/\sqrt{2}$.

Note that the triplet VEV v_Δ also contributes to the W and Z masses, hence to the ρ parameter of the SM. Taking into account the electroweak (EW) precision data one can derive an upper limit $v_\Delta/v < 0.2$ which in turn implies v_Δ <5 GeV. Thus in the limit $v \gg v_\Delta$, Eq. (1.65) can be simplified to

$$v_\Delta = \frac{\Lambda_6 v^2}{2M_\Delta^2 + (\lambda_4 - \lambda_5)v^2}, \tag{1.66}$$

in the limit $M_\Delta \gg v^2$ or $\lambda_4 = \lambda_5$ which becomes

$$v_\Delta = \frac{\Lambda_6 v^2}{2M_\Delta^2}. \tag{1.67}$$

From (1.62), one can now write the neutrino mass matrix as

$$(M_\nu)_{ij} = \sqrt{2} v_\Delta (Y_\Delta)_{ij} \equiv \frac{\Lambda_6 v^2}{\sqrt{2} M_\Delta^2}(Y_\Delta)_{ij}. \tag{1.68}$$

Taking $v \sim 246$ GeV, $M_\nu \sim 0.05$ eV and $Y_\Delta \sim 1$, Λ_6 can be calculated as

$$\Lambda_6 \sim 0.8 \left(\frac{M_\Delta}{1\text{TeV}}\right)^2 \text{eV}. \tag{1.69}$$

Thus for $M_\Delta \sim 1$ TeV, Λ_6 is $\mathcal{O}$(eV) which is much smaller than m_ϕ and M_Δ. An interesting point is to be noted that since the trilinear term in $\mathcal{V}(\phi, \Delta)$ is lepton number violating, Λ_6 could be naturally small for a theory symmetric in lepton number. Due to the presence of $\mathcal{O}$(TeV) triplet scalar, Type-II seesaw has an enriched collider phenomenology [75]. This model is also intriguing from the leptogenesis perspective [76, 77].

Radiative neutrino masses: In the loop induced or radiative neutrino mass models, naturally small neutrino mass can be generated without an introduction of a much heavier scale that is beyond the collider reach. Here we discuss three economical loop induced neutrino mass models that are realized through minimal extensions of the SM field content.

Zee model:

Zee model [78] contains an extra singlet charged Higgs h^- and a Higgs doublet ϕ'. The source of lepton number violation is introduced through the dimension three trilinear term

$$-\mathcal{L}_{D3} = \mu\phi^T i\tau_2\phi' h^- + \text{h.c.}. \tag{1.70}$$

In principle both the Higgs fields ϕ and ϕ' might couple to the fermion fields. However, in that case the Higgs mediated flavor changing neutral current (FCNC) might appear. In order to restrict FCNC, a more simplified version of the Zee model (Zee-Wolfenstein (ZW) model) where only one Higgs field, say ϕ, couples to the fermions, was proposed in Ref. [79]. In the left panel of Fig.1.2, an one loop flavor diagram of the simplified Zee model has been presented. Despite the predictive structure of the effective light neutrino mass matrix, current experimental data excludes this simplistic Zee model at 3σ level. Nevertheless, there are lot of extensions of the model that have been proposed to accommodate the oscillation data.

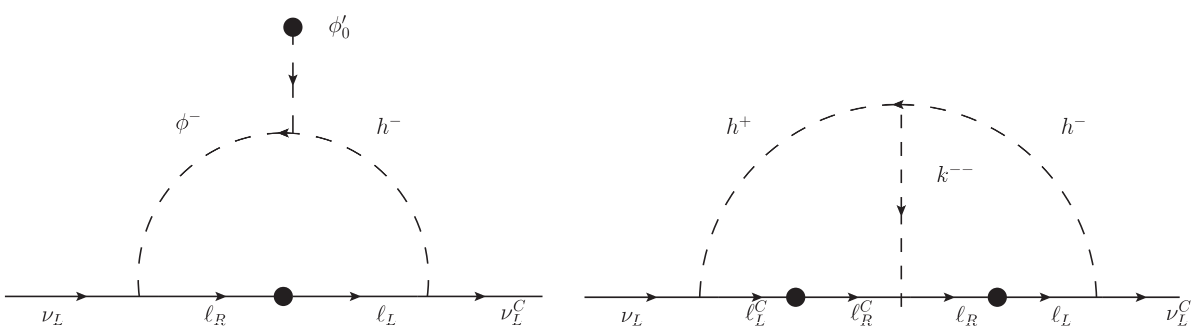

Figure 1.2: Left side: One loop flavor diagram for neutrino masses (Zee-Wolfenstein model). Right side: Two loop flavor diagram for neutrino masses (Zee-Babu) model. In both the figures we omit the flavor indices for simplicity.

Zee-Babu (ZB) model:

In this model [80] in addition to the SM field content, two $SU(2)_L$-singlets, a singly charged scalar $h-$ and a doubly charged scalar k^{++} are introduced. The doubly charged singlet can have interaction like

$$-\mathcal{L}' = \sum_{\ell\ell'} \bar{\ell_R^C} \ell'_R k^{++} + \text{h.c.}. \tag{1.71}$$

The violation of lepton number in this model is then ensured by the dimension three trilinear coupling

$$-\mathcal{L}_{D3} = \mu h^- h^- k^{++} + \text{h.c.}. \tag{1.72}$$

Thus small neutrino mass is generated at the two loop level as shown in the right panel of Fig.1.2. One of the interesting feature of this model is a vanishing eigenvalue which leads a particular mass ordering of the light neutrinos. In both the models, ZW and ZB, due to the presence of the charged singlets there a is great scope of collider phenomenology.

Ma model:

In the Ma model [81], three RH handed singlet fields N_{Ri} and an inert (vanishing VEV) scalar doublet $\eta = (\eta^{\pm} \ \eta^0_R + i\eta^0_I)^T$ are introduced to generate tiny neutrino masses at one loop level, as shown in Fig.1.3. In addition to the $SU(2)_L \times U(1)_Y$

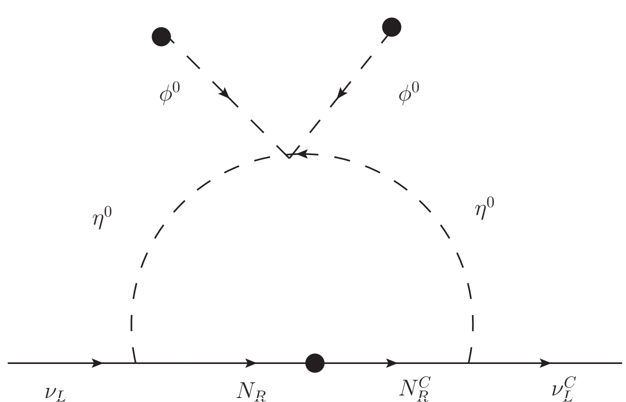

Figure 1.3: One loop diagram for light neutrino masses in Ma model.

symmetry an additional $\mathbb{Z}_2$ symmetry is imposed on the field contents. Two newly added fields N_{Ri} and η transform under $\mathbb{Z}_2$ operation while the other remain singlets. One of the motivation for this model is to introduce the Dark Matter (DM) candidate in a model of neutrino mass. Due the presence of an exact $\mathbb{Z}_2$ symmetry, it is easy to find out the stable DM particle between the freshers; N_{Ri} and $\eta_{I,R}$, depending upon their masses. One realizes this upon a percipient look at the interaction terms. The scalar potential under the $SU(2)_L \times U(1)_Y \times \mathbb{Z}_2$ symmetry can be written as

$$\begin{aligned} V_{\text{scalar}} &= m_1^2\phi^\dagger\phi + m_2^2\eta^\dagger\eta + \frac{1}{2}\lambda_1(\phi^\dagger\phi)^2 + \frac{1}{2}\lambda_2(\eta^\dagger\eta)^2 \\ &+ \lambda_3(\phi^\dagger\phi)(\eta^\dagger\eta) + \lambda_4(\phi^\dagger\eta)(\eta^\dagger\phi) + \frac{1}{2}\lambda_5\left[(\phi^\dagger\eta)^2 + \text{h.c.}\right]. \end{aligned} \tag{1.73}$$

Note that due to the assumed $\mathbb{Z}_2$ and the vanishing VEV for η, there will be no term in the potential that contains a single η–the decay term for η. Thus, apparently η is a stable particle in this model. However, the Dirac type term

$$-\mathcal{L}_{Yuk} = (Y_\nu)_{ij}\bar{L}_i i\tau_2\eta N_{Rj} \tag{1.74}$$

might also act as a decay term for the both, either N_{Ri} or η. Therefore the lightest among them will serve as a suitable candidate for the DM in this model.

Before closing this section we would like to emphasize on the following. In the entire thesis, only Type-I and the inverse seesaw have been taken under consideration as the basic mechanisms for the generation of light neutrino mass. Nevertheless, apart from the said mechanisms, the discussion about the other, e.g., Type-II seesaw, radiative mass generation etc. makes sense, since, we see later in this thesis that we have assumed some arbitrary perturbation to the effective light neutrino matrices without addressing the source for the former. Thus those mechanisms might give rise to the perturbation terms [5] if suitably implemented.

Other absorbing theories such as double seesaw [69], Type-III seesaw [82], Left-Right symmetric model [83,84], GUT models such as $SU(5)$ [85] and $SO(10)$ [86,87], super symmetric theories [88] are also the subject of research for the generation of light neutrino masses. These are beyond the scope of this thesis.

1.3 Neutrino masses and matter anti-matter asymmetry via leptogenesis

1.3.1 Introduction and a general setup

Our cardinal principles of the corpuscular world are encapsulated in the SM of particle physics that contains twelve types of matter particles: six quarks and six leptons. They all have animatter partners those which are identical with the matters in every aspects exceptthe electric charge. Particle physics has taught us that matter and anti matter behave essentially identically. On the other hand the standard cosmological theory are based on the assumption that the early universe was hot and energetic; an environment in which one would expect equal number of baryon and antibaryon to be copiously produced. This early state of the universe stands in stark contrast to what we observe in the universe today; the universe contains mostly matter but hardly antimatter. The theory of primordial nucleosynthesis allows the accurate prediction of the cosmological abundances of all the light elements requiring [20]

$$\begin{aligned} \eta_B &= \frac{n_B - n_{\bar{B}}}{n_\gamma} = (5.94 - 6.17) \times 10^{-10}, \\ Y_B &= \frac{n_B - n_{\bar{B}}}{s} = (8.43 - 8.76) \times 10^{-11} \end{aligned} \tag{1.75}$$

with $n_{B(\bar{B})}$, n_γ and s as the number densities of baryon (anti), photon and entropy respectively. Precise temperature measurement of the CMB observation constrain the total baryon content of the universe. As shown in the left panel of Fig. 1.4, the first acoustic peak of the CMB is especially sensitive to the amount of baryons in the

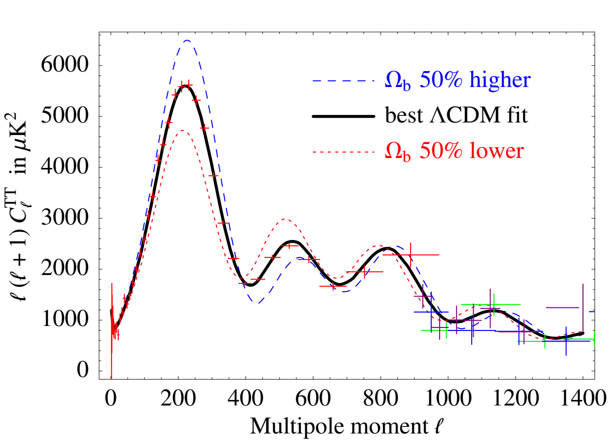

Figure 1.4: Sensitivity of the first acoustic peak in the CMB to the average baryon density of the universe (left). Concordance between the cosmic abundance of the lightest elements and η as required by BBN. Taken from [28] and [29].

universe. The latest CMB measurement by the PLANCK experiment constrains the average energy density of the baryons to

$$\Omega_B = 0.0490 \pm 0.0007. \tag{1.76}$$

This result is consitent with the amount of baryons required by the observed abundances of the lightest elements and the predictions of BBN.

As pointed out by Sakharov, a small baryon asymmetry might have been produced dynamically in the early universe if the following three conditions are satisfied [89]. i) Baryon number (B) violation, ii) violation of C and CP and iii) departure from thermal equilibrium. The first point is trivial, since starting from an initially symmetric universe, baryon number violation should take place for the universe to evolve in a state where baryon number is nonvanishing. Violation of the second condition implies the rate of the process in which an excess amount of baryon is created should be equal to the rate of the complementary process that creates an excess of antibaryons and thus no net baryon number is produced. Finally for the third condition one calculates an equilibrium average of B as

$$\begin{aligned}\langle B\rangle &= \mathrm{Tr}(e^{-\beta H}B) = \mathrm{Tr}[\hat{O}\hat{O}^{-1}e^{-\beta H}B] \\ &= \mathrm{Tr}[e^{-\beta H}\hat{O}^{-1}B\hat{O}] = -\mathrm{Tr}(e^{-\beta H}B)\end{aligned} \tag{1.77}$$

with $\hat{O}$ as a CPT operator and $[\hat{O}, H] = 0$. Thus thermal average of B in equilibrium vanishes and consequently no net baryon number is produced. A large amount of theoretical and experimental works suggest that within the framework of the SM the Sakharov conditions can not be fulfilled. At a glance, if we look up to the amount of CP violation provided by the CKM phase, we see that it is too small to generate Y_B in the observed range. Many extensions of the SM generate the observed Y_B by addressing this issue. However we focus on the '*baryogenesis via leptogenesis'* [90] due to its direct connection to the neutrino physics, especially with the Type-I seesaw scenario. In this mechanism, newly introduced heavy RH Majorana neutrinos decay out of equilibrium in a lepton number and CP violating way. The produced lepton number is then converted to baryon number by the nonperturbative sphalerons [91]. Before the construction of an explicit theoretical framework let's first construct a general setup that acts as a prerequisite.

CP violation in $\mathcal{L}$: For a simplified picture let's take one lepton doublet $\not{L}$ and three RH neutrinos $N_{1,2,3}$. The relevant part of the Lagrangian responsible for leptogenesis is then written as

$$\begin{aligned}\mathcal{L} &\subset \lambda_1 N_1 \phi \not{L} + \frac{M_1}{2} N_1^2 \\ &+ v\lambda_{2,3} N_{2,3} \phi \not{L} + \frac{M_{2,3}}{2} N_{2,3}^2 + \text{h.c.}. \end{aligned} \tag{1.78}$$

Here we also assume that N_1 is the lightest among the three heavy RH neutrinos and essentially asymmetry produced only by the decays of N_1 contributes to the final Y_B. Now by redefining the phases of the $N_{1,2,3}$ and $\not{L}$ fields one sets M_1, $M_{2,3}$ and λ_1 real leaving an unremovable CP violating phase in $\lambda_{2,3}$. The expression for CP asymmetry parameter ε_1 is then given by

$$\varepsilon_1 = \frac{\Gamma(N_1 \to \not{L}\phi) - \Gamma(N_1 \to \bar{\not{L}}\bar{\phi})}{\Gamma(N_1 \to \not{L}\phi) + \Gamma(N_1 \to \bar{\not{L}}\bar{\phi})} \sim \frac{M_1}{4\pi M_{2,3}} \text{Im}\lambda_{2,3}^2. \tag{1.79}$$

Thus in this scenario, in order to achieve CP violation, introduction of more than one heavy RH neutrinos are required.

Out of equilibrium condition and efficiency: If the $N_1 \to \not{L}\phi$ decays are slow enough ($\Gamma < H$), the abunndancy of N_1 does not decrease according to the Boltzmann equilibrium statistics $n_{N1} \sim e^{-M_1/T}$ demanded by thermal equilibrium. So late out of equilibrium decays of N_1 generate a lepton asymmetry Y_L. At $T \sim M_1$ one has

$$K = \frac{\Gamma}{H(M_1)} \sim \frac{\tilde{m}_1}{m^*}, \tag{1.80}$$

where Γ is the decay width, H is the Hubble parameter, $m^* = 2.3 \times 10^{-3}$ eV fixed by cosmology and $\tilde{m}_1 \equiv \lambda_1^2 v^2 / M_1$ is the effective mass which is related to the solar and atmospheric mass splitting in a model dependent way. Thus when $K << 1$, the N_1 decays are strongly out of equilibrium thus the production efficiency for the Y_L is close to one. This is known as the 'weak washout scenario'. On the other hand

$K \gg 1$ leads to a suppression of Y_L due to the fact that the inverse decays that try to maintain the thermal equilibrium by regenerating N_1, have rates suppressed by a Boltzmann factor at $T < M_1$: $\Gamma_{ID} \sim \Gamma_{ID} e^{-M_1/T}$. The N_1 quanta that decay when $K < 1$ leads to an unwashed asymmetry. This regime is named as the 'strong washout scenario'. This is worth mentioning that the current neutrino oscillation data favors the latter.

Boltzmann equation for leptogenesis: In absence of interaction the number of particles in a comoving volume remains constant. However, the change in the number of particles due to different types of interactions can be estimated through Boltzmann Equation (BE). As an example, for the process $1 \leftrightarrow 2{+}3$, the rate of change of number density n_1 of the particle '1' is given by

$$\begin{aligned} \frac{d}{dt}(n_1 V) &= V \int_p d\vec{p_1} d\vec{p_2} d\vec{p_3} (2\pi^4) \delta^4(p_1 - p_2 - p_3) \\ &\times [-|A_f|^2 f_1 (1 \pm f_2)(1 \pm f_3) + |A_b|^2 f_1 f_3 (1 \pm f_1)], \end{aligned} \tag{1.81}$$

where $d\vec{p_i} = \frac{d^3 p_i}{2E_i (2\pi)^3}$ is the phase space factor, $|A_{f,b}|$ is the amplitudes of the forward and backward processes with summed over initial and final state spins and f_i is the energy distribution function. Now assuming $f(p)$ as $f(p) \simeq f_{eq} n/n^{eq}$ (kinetic equilibrium), $|A_f| = |A_b|$, $f_{eq} \sim e^{-E/T}$ and $1 \pm f \simeq 1$, (1.81) is simplified as

$$\begin{aligned} \frac{1}{V}\frac{d}{dt}(n_1 V) &= \int_p d\vec{p_1} d\vec{p_2} d\vec{p_3} (2\pi^4) \delta^4(p_1 - p_2 - p_3) \\ &\times |A|^2 [-\frac{n_1}{n_1^{eq}} e^{-E_1/T} + \frac{n_2 n_3}{n_2^{eq} n_3^{eq}} e^{-(E_2+E_3)/T}] \\ &= \Gamma_1 n_1^{eq} [\frac{n_2 n_3}{n_2^{eq} n_3^{eq}} - \frac{n_1}{n_1^{eq}}], \end{aligned} \tag{1.82}$$

where Γ_1 is the Lorntz dilated decay width and is given by

$$\Gamma_1 = \frac{1}{2E_1} \int d\vec{p_1} d\vec{p_2} d\vec{p_3} (2\pi^4) \delta^4(p_1 - p_2 - p_3) |A|^2. \tag{1.83}$$

In the case of leptogenesis the final state particles i.e., $\not{L}$ and ϕ have fast gauge interactions and thus they are kept in equilibrium. Therefore, (1.82) can be written in this case as

$$\frac{1}{V}\frac{d}{dt}(n_1 V) = -\Gamma_1(n_1 - n_1^{eq}). \tag{1.84}$$

It is convenient to recast the above equation in terms of $N_1 = n_1/n_\gamma(T)$–number density normalized by photon density as

$$\frac{dN_1}{dz} = -D[N_1 - N_1^{eq}] \tag{1.85}$$

with $z = M_1/T$, $D = \frac{\Gamma_1}{Hz}$ and $Hdt = d\ln z$. In principle D should be written as $D = (\Gamma_1 + \bar{\Gamma}_1)/Hz$, since the the process $N_1 \to \bar{\not{L}}\bar{\phi}$ is also involved. Now one can derive the Boltzmann equation for the produced lepton asymmetry $N_L = Y_L s/n_\gamma$ as

$$\begin{aligned} \frac{dN_L}{dz} &= \frac{dN_{\bar{\not{L}}}}{dz} - \frac{dN_{\not{L}}}{dz} \\ &= -\varepsilon_1 D(N_1 - N_1^{eq}) - WN_L \end{aligned} \tag{1.86}$$

with $W = \frac{1}{2}\frac{\Gamma_1^{ID}+\bar{\Gamma}_1^{ID}}{Hz}$ and $Y_L = \frac{n_{\not{L}} - n_{\bar{\not{L}}}}{s}$. Here the evolutions of the normalized lepton number densities are controlled by the production due to the decay and dilution due to the inverse decay (ID). Thus they can be written as

$$\frac{dN_{\not{L}}}{dz} = \frac{\Gamma_1}{Hz}N_1 - \frac{\Gamma_1^{ID}}{Hz}N_{\not{L}}, \;\; s\frac{dN_{\bar{\not{L}}}}{dz} = \frac{\bar{\Gamma}_1}{Hz}N_1 - \frac{\bar{\Gamma}_1^{ID}}{Hz}N_{\bar{\not{L}}}. \tag{1.87}$$

We also assume

$$N_{\bar{\not{L}}} = \frac{1}{2}(N_{\bar{\not{L}}} + N_{\not{L}}) + \frac{1}{2}N_L, \;\; N_{\not{L}} = \frac{1}{2}(N_{\bar{\not{L}}} + N_{\not{L}}) - \frac{1}{2}N_L. \tag{1.88}$$

In a realistic leptogenesis scenario there will be additional contributions from $\Delta L =$

1, 2 terms which leads the complete set of BE for leptogenesis as

$$\frac{dN_1}{dz} = -(D + S_{\Delta L=1})[N_1 - N_1^{eq}], \tag{1.89}$$

$$\frac{dN_L}{dz} = -\varepsilon_1 D(N_1 - N_1^{eq}) - (W + S_{\Delta L=1,2})N_L. \tag{1.90}$$

Flavor effect: So far we have focused on the single flavor leptogenesis. Inclusion of flavor dependence needs more careful formalism which we discuss below. To start with, let's denote the quantum states produced from N_1 by $|1\rangle$ and $|\bar{1}\rangle$ which are state vectors in the flavor space as shown in Fig.1.5. They can now be expressed a linear combination of flavor eigenstate e, μ, τ as

$$|1\rangle = c_1 |\alpha\rangle , \quad |\bar{1}\rangle = c_2 |\bar{\alpha}\rangle \tag{1.91}$$

with $c_1 = \langle\alpha|1\rangle$, $c_2 = \langle\bar{\alpha}|\bar{1}\rangle$ are the normalization constants.

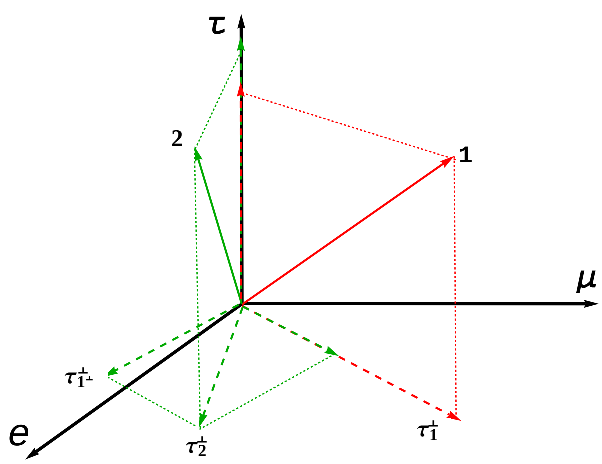

Figure 1.5: Geometric representaion of convenient bases in the flavor space for a two flavor scenario.

The regime where the interactions mediated by the charged lepton Yukawas are neglected, i.e., flavor plays no role in the process of leptogenesis is called the unflavored regime which is characterized by the scale $M_1 > 10^{12}$ GeV. In this regime the quantum states $|1, \bar{1}\rangle$ propagate coherently between the production from decays and absorption by inverse decays, since the gauge interactions are flavor blind. Now in the regime 10^9 GeV $< M_1 < 10^{12}$ GeV, the coherent evolution of the quantum states break down prior to inverse decay with ϕ, due to the collision with fast RH tau particles ($\Gamma_\tau > H$). At the inverse decays the lepton states then can be described as an incoherent mixture of tauon eigenstates $|\tau\rangle$ and $|\tau^\perp\rangle$. The second state ($\tau^\perp$) is now a coherent mixture of e and μ eigenstates and can be regarded as a projection of $|1\rangle$ on the plane orthogonal to $|\tau\rangle$ (c.f Fig.1.5). The produced lepton asymmetry is now no longer flavor blind, rather it is shared along τ and $\tau^\perp$ direction in the charged lepton flavor space. In the literature, this regime is denoted as the $\tau-$flavor regime. Therefore in this regime the evolution of the produced lepton asymmetry has to be tracked by writing BE for each flavor as

$$\frac{dN_1}{dz} = -D(N_1 - N_1^{eq}), \tag{1.92}$$
$$\frac{dN_L^{\tau\perp}}{dz} = -\varepsilon_1^{\tau\perp} D(N_1 - N_1^{eq}) - W^\tau N_L^\tau, \tag{1.93}$$
$$\frac{dN_L^{\tau\perp}}{dz} = -\varepsilon_1^{\tau\perp} D(N_1 - N_1^{eq}) - W^{\tau\perp} N_L^{\tau\perp}. \tag{1.94}$$

Similarly in the regime $M_1 < 10^9$ GeV, the coherence of the $|\tau^\perp\rangle$ is lost due to the fast interactions mediated by μ flavor in the thermal bath, consequently, $|\tau^\perp\rangle$ loses its flavor identity and become an incoherent mixture of e and μ flavors. Thus all the charged lepton flavors are distinguishable separately–fully flavored leptogenesis occur in this regime. Similar to the two flavor case, the evolution of the produced lepton asymmetry can be described through the BE for each flavor.

Baryon number violation and inclusion of sphalerons and Yukawas: As previously mentioned, starting from a baryon symmetric universe, to evolve to $B \neq 0$, violation of baryon number is necessary. In the SM, L or B are not violated due to an accidental symmetry in the model. However, in Ref. [68] it is shown that the non-perturbative instanton effects can give rise to the processes that violates $B+L$, but conserve $B-L$. Even though B and L are individually conserved at the tree level, Adler-Bell-Jackiw (ABJ) triangular anomalies [92] nevertheless do not vanish and thus B and L are anomalous at the quantum level through the intaractions with EW gauge field in the triangle diagrams. In other words, the divergences associated with B and L do not vanish at the quantum level, and they are given by

$$\partial_\mu J^\mu_B = \partial_\mu J^\mu_L = \frac{N_f}{32\pi^2}(g^2 W^\lambda_{\mu\nu}\tilde{W}^{\lambda\mu\nu} - g'^2 B_{\mu\nu}\tilde{B}^{\mu\nu}), \tag{1.95}$$

where $W_{\mu\nu}$ and $B_{\mu\nu}$ are the SM gauge field strengths with the forms

$$\begin{aligned} W^\lambda_{\mu\nu} &= \partial_\mu W^\lambda_\nu - \partial_\nu W^\lambda_\mu, \\ B^\lambda_{\mu\nu} &= \partial_\mu B_\nu - \partial_\nu B_\mu \end{aligned} \tag{1.96}$$

respectively and g, g', N_f are the gauge coupling constants and number of fermion generations. Since, $\partial^\mu(J^B_\mu - J^L_\mu) = 0$, $B-L$ is conserved. However, the $B+L$ term is violated with the divergence of the current given by

$$\partial^\mu(J^B_\mu + J^L_\mu) = 2N_f \partial_\mu K^\mu, \tag{1.97}$$

where

$$\begin{aligned} K^\mu \;\; &= \;\; -\frac{g^2}{32\pi^2} 2\epsilon^{\mu\nu\rho\sigma} W^\lambda_\nu(\partial_\rho W^\lambda_\sigma + \frac{g}{3}\epsilon^{\lambda qr} W^q_\rho W^r_\sigma \\ &+ \;\; \frac{g'^2}{32\pi^2}\epsilon^{\mu\nu\rho\sigma} B_\nu B_{\rho\sigma}. \end{aligned} \tag{1.98}$$

This violation is due to the vacuum structure of the non-abelian gauge theories. Changes in B and L are related to the change in topological charges (Chern-Simons number),

$$B(t_f) - B(t_i) = N_f[N_{cs}(t_f) - N_{cs}(t_i)], \tag{1.99}$$

where the topological charge of the gauge field is given by

$$N_{cs}(t) = \frac{g^3}{96\pi^2}\int d^3x \epsilon_{\alpha\beta\gamma}\epsilon^{ijk}W^{i\alpha}W^{j\beta}W^{k\gamma}. \tag{1.100}$$

Therefore there are infinitely many degenerate ground states with $\Delta N_{cs} = \pm 1$, ± 2 ..., separated by a potential barrier. The instanton configuration that determines the tunneling between one vacua to the other, gives rise to the effective operator at the leading order

$$\mathcal{O}_{B+L} = \Pi_i(Q_{Li}Q_{Li}Q_{Li}\not{L}_i). \tag{1.101}$$

At zero temperature, the transition rate is given by $\Gamma \sim e^{4\pi/\alpha} \approx \mathcal{O}(10^{-160})$ [68]. However, in thermal bath, the transition between different gauge vacua can be made not by tunneling [93] but through thermal fluctuations over the barrier. When the temperature is higher than the barrier hight $B + L$ violating interactions may occur at a significant rate and they can be in equilibrium in the expanding universe as well. The transition rate at finite temperature in EW theory is determined by sphelaron configurations [94], which are static configurations that correspond to the unstable solution of the equation of motion. Below the EW phase transition ($T < T_{EW}$) the transition rate [95] is given by

$$\frac{\Gamma_{B+L}}{V} \sim e^{-\frac{M_W}{\alpha k T}}, \tag{1.102}$$

which is still very suppressed. However, above the EW phase transition ($T > T_{EW}$), the rate [96,97] is

$$\frac{\Gamma_{B+L}}{V} \sim \alpha^5 \ln\alpha^{-1} T^4. \tag{1.103}$$

Thus baryon number violating processes is not suppressed in the $T > T_{EW}$ phase and give rise to the required baryon asymmetry of the universe.

As we have already seen for a realistic computation of BE one should also include the scattering terms (cf. Eq. 1.90) in addition with the decay terms. However, for a more accurate scenario, the sphaleronic scattering and the processes that contain the SM Yukawa couplings, should also be included. At a certain temperature when these processes are fast enough, the following chemical equilibrium conditions are satisfied:

$$\begin{aligned}
e_R \not{L} \phi \text{ Yukawa} &: \quad \mu_{e_R} + \mu_{\not{L}} + \mu_\phi = 0; \\
d_R Q \phi \text{ Yukawa} &: \quad \mu_{d_R} + \mu_Q + \mu_\phi = 0; \\
u_R Q \tilde{\phi} \text{ Yukawa} &: \quad \mu_{u_R} + \mu_Q - \mu_\phi = 0; \\
QQQ\not{L} \text{ sphalerons} &: \quad 3\mu_Q + \mu_{\not{L}} = 0.
\end{aligned} \tag{1.104}$$

In addition to these relations, irrespective of the temperature regime, there will be another condition due the hypercharge neutrality and is given by

$$N_f(\mu_Q - 2\mu_{u_R} + \mu d_R - \mu_{\not{L}} + \mu_{e_R}) - 2N_\phi \mu_\phi = 0, \tag{1.105}$$

where N_ϕ is the number of Higgs doublets. Now the expressions for Y_B and Y_L can be written as

$$Y_B = \frac{T^3}{6s}(2\mu_Q - \mu_{u_R} - \mu_{d_R}), \;\; Y_L = \frac{T^3}{6s}(2\mu_{\not{L}} - \mu_{e_R}). \tag{1.106}$$

It is convenient to express the final baryon asymmetry Y_B in terms of the asymmetry in the conserved quantum number $Y_B - Y_L \equiv Y_\Delta$ since the latter is not affected by the processes as discussed above. For $N_f = 3$ and $N_\phi = 1$ one can solve the above equations given in (1.104) and (1.105) and can have a relation between Y_B and Y_Δ as

$$Y_B = \frac{28}{79} Y_\Delta. \tag{1.107}$$

Note that all the chemical potential equations have been written assuming only a single generation. A discussion including all the generations and their relevance to the produced asymmetry is presented in the next section where we discussed leptogenesis in more detail including all the active flavor indices. In this thesis we use all the relevant equations related to leptogenesis from the next section.

1.3.2 Explicit calculation of CP asymmetry parameter and BE with active flavor indices

The part of our Lagrangian relevant to the generation of a CP asymmetry is

$$-\mathcal{L}_D = f^N_{i\alpha} \overline{N}_{Ri} \tilde{\phi}^\dagger \not{L}_\alpha + \text{h.c.}, \tag{1.108}$$

where $\not{L}_\alpha = (\nu_{L_\alpha} \;\; \ell^-_{L\alpha})^T$ is the left-chiral SM lepton doublet of flavor α, while $\tilde{\phi} = (\phi^{0*} \;\; -\phi^-)^T$ is the charge conjugated Higgs scaler doublet. It is evident from (1.108) that the decay products of N_i can be $\ell^-_\alpha \phi^+, \nu_\alpha \phi^0, \ell^+_\alpha \phi^-$ and $\nu^C_\alpha \phi^{0*}$. We are interested in the flavor dependent CP asymmetry parameter ε^α_i which is given by

$$\varepsilon^\alpha_i \;\; = \;\; \frac{\Gamma(N_i \to \not{L}_\alpha \phi) - \Gamma(N_i \to \not{L}^C_\alpha \phi^\dagger)}{\Gamma(N_i \to \not{L}_\alpha \phi) + \Gamma(N_i \to \not{L}^C_\alpha \phi^\dagger)}, \tag{1.109}$$

Γ being the corresponding partial decay width. A nonzero value of ε_i^α needs to arise out of the interference between the tree level and one loop contributions [90]. This is since at the tree level we have

$$\Gamma^{tree}(N_i \to \not{L}_\alpha \phi) = \Gamma^{tree}(N_i \to \not{L}_\alpha^C \phi^\dagger) = (16\pi)^{-1}(f_{i\alpha}^{N\dagger} f_{i\alpha}^N) M_i, \text{ (no sum over i)} \quad (1.110)$$

One loop contributions come both from vertex correction and self-energy terms (cf. Fig.1.6). For leptogenesis with hierarchical heavy RH neutrinos, (1.109) can be evaluated to be

$$\begin{aligned} \varepsilon_i^\alpha &= \frac{1}{4\pi v^2 \mathcal{H}_{ii}} \sum_{j\neq i} g(x_{ij}) \,\mathrm{Im}\, \mathcal{H}_{ij} (m_D)_{i\alpha} (m_D^*)_{j\alpha} \\ &+ \frac{1}{4\pi v^2 \mathcal{H}_{ii}} \sum_{j\neq i} \frac{\mathrm{Im}\, \mathcal{H}_{ji} (m_D)_{i\alpha} ({m_D}^*)_{j\alpha}}{(1-x_{ij})}. \end{aligned} \quad (1.111)$$

In (1.111), $\langle \phi^0 \rangle = v/\sqrt{2}$ so that $m_D = v f^N/\sqrt{2}$, $\mathcal{H} \equiv m_D {m_D}^\dagger$ and $x_{ij} = M_j/M_i$. Furthermore, $g(x_{ij})$ is given by

$$g(x_{ij}) = \frac{\sqrt{x_{ij}}}{1-x_{ij}} + f(x_{ij}), \quad (1.112)$$

where the first RHS term arises from the one loop self energy term interfering with the tree level contribution. The second RHS term in (1.112), originating from the interference of the contribution from the one loop vertex correction diagram with the tree level term, is given by

$$f(x_{ij}) = \sqrt{x_{ij}} \left[1 - (1+x_{ij}) \ln \left(\frac{1+x_{ij}}{x_{ij}} \right) \right]. \quad (1.113)$$

We would like to stress once again that the expression for ε_i^α in (1.111) is valid only for the hierarchical RH neutrino masses. For a quasi-degenerate scenario one should follow the formalism given in Ref. [98].

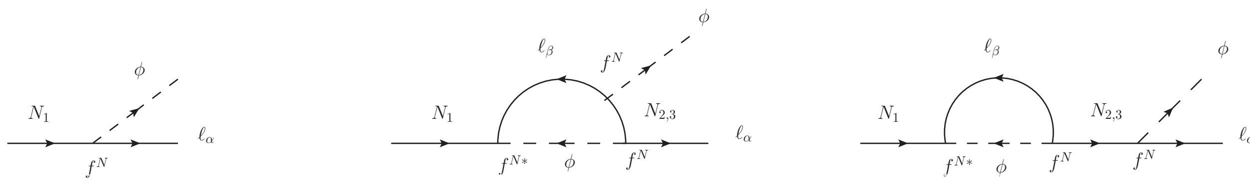

Figure 1.6: Tree level as well as one loop vertex correction and self energy diagrams that contribute to the CP asymmetry parameter ε_1^α. The flavor of the internal charged lepton ℓ_β is summed and the Yukawa coupling f^N is supplied with appropriate flavor indices in the interference amplitude.

Let us discuss some physics aspects of (1.111). As already mentioned, depending upon the temperature regime in which leptogenesis occurs, lepton flavors may be fully distinguishable, partly distinguishable or indistinguishable. It is reasonable to assume that leptogenesis takes place at $T \sim M_1$. It is known [99] that lepton flavors cannot be treated separately if the concerned process occurs above a temperature $T \sim M_1 > 10^{12}$ GeV. In case the said temperature is lower, two possibilities arise. When $T \sim M_1 < 10^9$ GeV all three (e, μ, τ) flavors are individually active and we need three CP asymmetry parameters $\varepsilon_i^e, \varepsilon_i^\mu, \varepsilon_i^\tau$ for each generation of RH neutrinos. On the other hand when we have 10^9 GeV $< T \sim M_1 < 10^{12}$ GeV, only the τ-flavor can be identified separately while the e and μ act indistinguishably. Here we need two CP asymmetry parameters $\varepsilon_i^{(2)} = \varepsilon_i^e + \varepsilon_i^\mu$ and ε_i^τ for each of the RH neutrinos. As an aside, let us point out a simplification of the CP asymmetry parameter for unflavored leptogenesis which is relevant for the high temperature regime. Summing over all α,

$$\sum_\alpha \mathrm{Im}\ \mathcal{H}_{ji}(m_D)_{i\alpha}(m_D{}^*)_{j\alpha} = \mathrm{Im}\ H_{ji}\mathcal{H}_{ij} = \mathrm{Im}\ H_{ji}\mathcal{H}^*_{ji} = \mathrm{Im}\ |\mathcal{H}_{ji}|^2 = 0, \qquad (1.114)$$

i.e. the second term in the RHS of (1.111) vanishes. The flavor-summed CP asymmetry parameter is therefore given by the simplified expression

$$\begin{aligned}\varepsilon_i &= \sum_\alpha \varepsilon_i^\alpha \\ &= \frac{1}{4\pi v^2 \mathcal{H}_{ii}} \sum_{j\neq i} \left[f(x_{ij}) + \frac{\sqrt{x_{ij}}}{(1-x_{ij})} \right] \mathrm{Im}\, \mathcal{H}_{ij}\mathcal{H}_{ij}. \end{aligned} \tag{1.115}$$

The Boltzmann equations of concern to us govern the evolution of the number densities of the hierarchical heavy neutrinos N_i and the left chiral lepton doublets $\not{L}_\alpha$. The equations involve decay transitions between N_i and $\not{L}_\alpha \phi$ as well as $\not{L}_\alpha^C \phi^\dagger$ plus scattering transitions $Qu^C \leftrightarrow N_i \not{L}_\alpha, \not{L}_\alpha Q^C \leftrightarrow N_i u^C, \not{L}_\alpha u \leftrightarrow N_i Q, \not{L}_\alpha \phi \leftrightarrow N_i V_\mu, \phi^\dagger V_\mu \leftrightarrow N_i \not{L}_\alpha, \not{L}_\alpha V_\mu \leftrightarrow N_i \phi^\dagger$. Here Q represents the left-chiral quark doublet with $Q^T = (u_L \;\, d_L)$ and V_μ can stand for either B or $W_{1,2,3}$. Now we are using the parametric function $\eta_a(z)$ instead of $N_L(z)$. When in thermal equilibrium, the former is denoted by $\eta_a^{eq}(z)$. The number density of a particle of species a and mass m_a with g_a internal degrees of freedom is given by [100]

$$n_a(T) = \frac{g_a\, m_a^2\, T\; e^{\mu_a(T)/T}}{2\pi^2}\; K_2\!\left(\frac{m_a}{T}\right), \tag{1.116}$$

K_2 being the modified Bessel function of the second kind with order 2. The corresponding equilibrium density, as given by setting the chemical potential $\mu_a(T)$ equal to zero, is

$$n_a^{\rm eq}(T) = \frac{g_a\, m_a^2\, T}{2\pi^2}\; K_2\!\left(\frac{m_a}{T}\right). \tag{1.117}$$

We are now in a position to make use of the Boltzmann evolution equations given in Ref. [98] – generalized with flavor [101]. In making this generalization, one comes across a subtlety: the active flavor in the mass regime (given by the value of M_1) under consideration may not be individually e, μ or τ but some combination thereof. So we use a general flavor index λ for the lepton asymmetry. Now we write

$$\begin{aligned}
\frac{d\eta_{N_i}}{dz} &= \frac{z}{H(z=1)}\Bigg[\left(1-\frac{\eta_{N_i}}{\eta^{\rm eq}_{N_i}}\right)\sum_{\beta=e,\mu,\tau}\left(\Gamma^{\beta Di}+\Gamma^{\beta Si}_{\rm Yukawa}+\Gamma^{\beta Si}_{\rm Gauge}\right)\\
&\quad -\frac{1}{4}\sum_{\beta=e,\mu,\tau}\eta^{\beta}_{L}\varepsilon^{\beta}_{i}\left(\Gamma^{\beta Di}+\tilde{\Gamma}^{\beta Si}_{\rm Yukawa}+\tilde{\Gamma}^{\beta Si}_{\rm Gauge}\right)\Bigg],\\
\frac{d\eta^{\lambda}_{L}}{dz} &= -\frac{z}{H(z=1)}\Bigg[\sum_{i=1}^{3}\varepsilon^{\lambda}_{i}\left(1-\frac{\eta_{N_i}}{\eta^{\rm eq}_{N_i}}\right)\sum_{\beta=e,\mu,\tau}\left(\Gamma^{\beta Di}+\Gamma^{\beta Si}_{\rm Yukawa}+\Gamma^{\beta Si}_{\rm Gauge}\right)\\
&\quad +\frac{1}{4}\eta^{\lambda}_{L}\left\{\sum_{i=1}^{3}\left(\Gamma^{\lambda Di}+\Gamma^{\lambda Wi}_{\rm Yukawa}+\Gamma^{\lambda Wi}_{\rm Gauge}\right)+\Gamma^{\lambda\Delta L=2}_{\rm Yukawa}\right\}\Bigg]. \qquad (1.118)
\end{aligned}$$

In each RHS of (1.118), apart from the Hubble rate of expansion H at the decay temperature, we have various transition widths Γ originally introduced in Ref. [98] which are linear combinations (normalized to the photon density) of different CP conserving collision terms γ^{X}_{Y} for the transitions $X\to Y$ and $\bar{X}\to\bar{Y}$. Here γ^{X}_{Y} is defined as

$$\gamma^{X}_{Y} \;\equiv\; \gamma(X\to Y)\,+\,\gamma(\overline{X}\to\overline{Y})\,, \qquad (1.119)$$

with

$$\gamma(X\to Y) \;=\; \int d\pi_X\, d\pi_Y\,(2\pi)^4\,\delta^{(4)}(p_X-p_Y)\,e^{-p^0_X/T}\,|\mathcal{M}(X\to Y)|^2\,. \qquad (1.120)$$

In (1.120) one has used a short hand notation for the phase space

$$d\pi_x=\frac{1}{S_x}\prod_{i=1}^{n_x}\frac{d^4p_i}{(2\pi)^3}\delta(p_i^2-m_i^2)\theta(p_i^0) \qquad (1.121)$$

with $S_X=n_{id}!$ being a symmetry factor in case the initial state X contains a number n_{id} of identical particles. Moreover, the squared matrix element in (1.120) is summed (not averaged) over the internal degrees of freedom of the initial and final states.

The transition widths Γ in (1.118) are given as follows:

$$\Gamma^{\lambda Di} = \frac{1}{n_\gamma}\,\gamma^{N_i}_{\not{L}_\lambda \phi^\dagger}\ , \tag{1.122}$$

$$\Gamma^{\lambda Si}_{\text{Yukawa}} = \frac{1}{n_\gamma}\left(\gamma^{N_i \not{L}_\lambda}_{Q u^C} + \gamma^{N_i u^C}_{\not{L}_\lambda Q^C} + \gamma^{N_i Q}_{\not{L}_\lambda u}\right), \tag{1.123}$$

$$\widetilde{\Gamma}^{\lambda Si}_{\text{Yukawa}} = \frac{1}{n_\gamma}\left(\frac{\eta_{N_i}}{\eta^{\text{eq}}_{N_i}}\,\gamma^{N_i \not{L}_\lambda}_{Q u^C} + \gamma^{N_i u^C}_{\not{L}_\lambda Q^C} + \gamma^{N_i Q}_{\not{L}_\lambda u}\right), \tag{1.124}$$

$$\Gamma^{\lambda Si}_{\text{Gauge}} = \frac{1}{n_\gamma}\left(\gamma^{N_i V_\mu}_{\not{L}_\lambda\ \phi} + \gamma^{N_i \not{L}_\lambda}_{\phi^\dagger V_\mu} + \gamma^{N_i \phi^\dagger}_{\not{L}_\lambda V_\mu}\right), \tag{1.125}$$

$$\widetilde{\Gamma}^{\lambda Si}_{\text{Gauge}} = \frac{1}{n_\gamma}\left(\gamma^{N_i V_\mu}_{\not{L}_\lambda \phi} + \frac{\eta_{N_i}}{\eta^{\text{eq}}_{N_i}}\,\gamma^{N_i \not{L}_\lambda}_{\phi^\dagger V_\mu} + \gamma^{N_i \phi^\dagger}_{\not{L}_\lambda V_\mu}\right), \tag{1.126}$$

$$\Gamma^{\lambda Wi}_{\text{Yukawa}} = \frac{2}{n_\gamma}\left(\gamma^{N_i \not{L}_\lambda}_{Q u^C} + \gamma^{N_i u^C}_{\not{L}_\lambda Q^C} + \gamma^{N_i Q}_{\not{L}_\lambda u} + \frac{\eta_{N_i}}{2\eta^{\text{eq}}_{N_i}}\,\gamma^{N_i \not{L}_\lambda}_{Q u^C}\right), \tag{1.127}$$

$$\Gamma^{\lambda Wi}_{\text{Gauge}} = \frac{2}{n_\gamma}\left(\gamma^{N_i V_\mu}_{\not{L}_\lambda \phi} + \gamma^{N_i \not{L}_\lambda}_{\phi^\dagger V_\mu} + \gamma^{N_i \phi^\dagger}_{\not{L}_\lambda V_\mu} + \frac{\eta_{N_i}}{2\eta^{\text{eq}}_{N_i}}\,\gamma^{N_i \not{L}_\lambda}_{\phi^\dagger V_\mu}\right), \tag{1.128}$$

$$\Gamma^{\lambda \Delta L=2}_{\text{Yukawa}} = \frac{2}{n_\gamma}\sum_{\beta=e,\mu\tau}\left(\gamma'^{\not{L}_\lambda \phi}_{L^C_\beta \phi^\dagger} + 2\gamma^{\not{L}_\lambda \not{L}_\beta}_{\phi^\dagger \phi^\dagger}\right). \tag{1.129}$$

The explicit expressions for γ and γ' are given in Appendix B of Ref. [98]. The subscripts D, S and W stand for decay, scattering and washout respectively. We rewrite the Boltzmann equations in terms of $Y_{N_i}(z) = \eta_{N_i} n_\gamma(z) s^{-1}$ and certain D-functions of z that are defined below.

Consider the first equation in (1.118) to start with. Its second RHS term has been neglected for an assumed hierarchical leptogenesis since both η^β_L and ε^β_i are each quite small and their product much smaller[1]. Using some shorthand notation, as explained in Eqs. (1.131) - (1.133) below, we can now write

$$\frac{dY_{N_i(z)}}{dz} = \{D_i(z) + D^{\text{SY}}_i(z) + D^{\text{SG}}_i(z)\}\{(Y^{\text{eq}}_{N_i}(z) - Y_{N_i}(z)\}, \tag{1.130}$$

[1]In order of magnitude this product is $10^{-6} \times 10^{-5} \sim 10^{-11}$, as compared with the first term which is $\mathcal{O}(1)$.

where

$$D_i(z) = \sum_{\beta=e,\mu,\tau} D_i^\beta(z) = \sum_{\beta=e,\mu,\tau} \frac{z}{H(z=1)} \frac{\Gamma^{\beta Di}}{\eta_{N_i}^{\rm eq}(z)}, \tag{1.131}$$

$$D_i^{\rm SY}(z) = \sum_{\beta=e,\mu,\tau} \frac{z}{H(z=1)} \frac{\Gamma^{\beta Si}_{\rm Yukawa}}{\eta_{N_i}^{\rm eq}(z)}, \tag{1.132}$$

$$D_i^{\rm SG}(z) = \sum_{\beta=e,\mu,\tau} \frac{z}{H(z=1)} \frac{\Gamma^{\beta Si}_{\rm Gauge}}{\eta_{N_i}^{\rm eq}(z)}. \tag{1.133}$$

Turning to the second equation in (1.118) and neglecting the $\Delta L = 2$ scattering terms, we rewrite it as

$$\begin{aligned} \frac{d\eta_L^\lambda(z)}{dz} = & - \sum_{i=1}^{3} \varepsilon_i^\lambda \{D_i(z) + D_i^{\rm SY}(z) + D_i^{\rm SG}(z))(\eta_{N_i}^{\rm eq}(z) - \eta_{N_i}(z)\} \\ & - \frac{1}{4}\eta_L^\lambda \sum_{i=1}^{3} \{\frac{1}{2} D_i^\lambda(z) z^2 K_2(z) + D_i^{\lambda \rm YW}(z) + D_i^{\lambda \rm GW}(z))\} \end{aligned} \tag{1.134}$$

with

$$D_i^{\rm YW}(z) = \sum_{\beta=e,\mu,\tau} \frac{z}{H(z=1)} \Gamma^{\beta Wi}_{\rm Yukawa}, \tag{1.135}$$

$$D_i^{\rm GW}(z) = \sum_{\beta=e,\mu,\tau} \frac{z}{H(z=1)} \Gamma^{\beta Wi}_{\rm Gauge}. \tag{1.136}$$

We are now ready to calculate the baryon asymmetry from the lepton asymmetry. To this end, it is first convenient to define the variable

$$Y_\lambda = \frac{n_L^\lambda - n_{\bar L}^\lambda}{s} = \frac{n_\gamma}{s}\eta_L^\lambda, \tag{1.137}$$

i.e. the leptonic minus the antileptonic number density of the active flavor λ normalized to the entropy density. The factor s/η_γ is known to equal $1.8 g_{*s}$ with g^* being the relativistic degrees of freedom. For $T > 10^2$ GeV, g_{*s} is known to remain nearly constant with temperature at a value (with three right chiral neutrinos) of about 112 [102]. Sphaleronic processes convert the lepton asymmetry created by the decay of the right chiral heavy neutrinos into a baryon asymmetry by keeping $\Delta_\lambda = \frac{1}{3}B - L^\lambda$ conserved. Y_{Δ_λ}, defined as $s^{-1}\{1/3(n_B - n_{\bar{B}}) - (n_L - n_{\bar{L}})\}$, and Y_λ are linearly related, as under

$$Y_\lambda = \sum_\rho A_{\lambda\rho} Y_{\Delta_\rho}, \tag{1.138}$$

where $A_{\lambda\rho}$ is a set of numbers which are obtained by the chemical equilibrium conditions of the redistributor processes as explained in the previous section and depends on which of the three mass regimes M_1 lies in. These are discussed in detail later in this section. Meanwhile, we can rewrite (1.134) as

$$\begin{aligned}\frac{dY_{\Delta_\lambda}}{dz} &= \sum_{i=1}^{3}[\varepsilon_i^\lambda\{D_i(z) + D_i^{\rm SY}(z) + D_i^{\rm SG}(z)\}\{Y_{N_i}^{\rm eq}(z) - Y_{N_i}(z)\}] \\ &+ \frac{1}{4}\sum_\rho A_{\lambda\rho}Y_{\Delta_\rho}\sum_{i=1}^{3}\{\frac{1}{2}D_i^\lambda(z)z^2K_2(z) + D_i^{\lambda\ \rm YW}(z) + D_i^{\lambda\ \rm GW}(z)\}\end{aligned} \tag{1.139}$$

We need to solve (1.130) and (1.139) and evolve Y_{N_i} as well as Y_{Δ_λ} upto a value of z where the quantities Y_{Δ_λ} become constant with z, i.e. do not change with z. The final baryon asymmetry Y_B which varies linearly with Y_{Δ_λ} [103] can be obtained depending upon the mass regime in which M_1 is located. We discuss this in detail in the following.

$\mathbf{M_1 < 10^9}$ GeV: Here all the three lepton flavors are separately distinguishable. Therefore the flavor index λ can just be $\lambda = e$ or μ or τ. In this regime, the QCD sphalerons, EW sphalerons, top, bottom, charm, tau, strange and muon Yukawa interactions are taken to be in chemical equilibrium. Solving these equations along with the hypercharge neutrality condition in (1.105), one obtains the 3×3 A matrix

as

$$A = \begin{pmatrix} -151/179 & 20/179 & 20/179 \\ 25/358 & -344/537 & 14/537 \\ 25/358 & 14/537 & -344/537 \end{pmatrix}. \tag{1.140}$$

Now the final baryon asymmetry normalized to the entropy density, is given by [103]

$$Y_B = \frac{28}{79}(Y_{\Delta_e} + Y_{\Delta_\mu} + Y_{\Delta_\tau}). \tag{1.141}$$

Another important parameter, namely the baryon asymmetry normalized to the photon density, obtains as

$$\eta_B = \left(\frac{s}{n_\gamma}\right)_0 Y_B = 7.0394 Y_B, \tag{1.142}$$

the subscript zero denoting the present epoch.

$\mathbf{10^9}$ GeV $< \mathbf{M_1} < \mathbf{10^{12}}$ GeV: In this regime, the QCD sphalerons, EW sphalerons, top, bottom, charm and tau Yukawas are taken to be in chemical equilibrium. Among the charged lepton flavors, τ is distinguishable but one cannot differentiate between the e and μ flavors. It is therefore convenient to define two sets of CP asymmetry parameters ε^τ and $\varepsilon^{(2)} = \varepsilon^e + \varepsilon^\mu$. Therefore the index λ takes the values τ and 2. The Boltzmann equations lead to the two asymmetries Y_{Δ_τ} and Y_{Δ_2}. These are related to Y_τ and $Y_2 = Y_e + Y_\mu$ by a 2×2 A-matrix derived from the relevant chemical equilibrium conditions as

$$A = \begin{pmatrix} -417/589 & 120/589 \\ 30/589 & -390/589 \end{pmatrix}. \tag{1.143}$$

The final baryon asymmetry Y_B is then calculated as

$$Y_B = \frac{28}{79}(Y_{\Delta_2} + Y_{\Delta_\tau}). \tag{1.144}$$

$\mathbf{M_1} > \mathbf{10^{12}}$ GeV: In this case all the lepton flavors act indistinguishably leading to a single CP asymmetry parameter $\varepsilon_i = \sum\limits_{\lambda} \varepsilon_i^\lambda$. Thus it is similar to a single flavor leptogenesis scenario. However, since in this temperature regime EW sphaleron interactions are out of equilibrium, no net baryon asymmetry is produced in the leptogenesis phase and thus Y_Δ and Y_L are related as

$$Y_\Delta = -Y_L. \tag{1.145}$$

Thus one can have an expression for the final baryon asymmetry as

$$Y_B = -\frac{28}{79} Y_L. \tag{1.146}$$

Given the general setup to realize neutrino masses in the extended SM, the main aim of this thesis is to construct viable neutrino mass models that are testable in the forthcoming experiments. The next section is devoted to the prerequisites, some new discrete symmetries which are needed to construct such models in addition to the standard $SU(2)_L \times U(1)_Y$ gauge symmetry. Although in general a symmetry should be implemented at the Lagrangian level, we will see, however, it is the residual symmetry at the end that dictates the texture of the effective light neutrino mass matrix M_ν and hence the mixing matrix U_ν that diagonalizes M_ν. The entire work of this thesis is based on few predictive residual symmetries which can generate the neutrino mass and mixing at least at the leading order. A brief insight of the strategy is given in what follows.

1.4 Discrete residual symmetries in the neutrino mass matrix

1.4.1 Importance of residual symmetries

The nature of the neutrinos–whether they are Dirac or Majorana type is yet to be established. Furthermore, there are some low energy neutrino parameters such as the leptonic CP violating phases δ, α, β which are not determined till date. In addition one has to establish the mass ordering of the light neutrinos. For a given low energy neutrino mass matrix, presumably originates from the mechanism as discussed earlier, one cannot predict those undetermined parameters, since a general M_ν contains eighteen (twelve) independent parameters for a Dirac (Majorana) type neutrinos. Thus to construct a viable model one has to invoke some symmetry/ansatz that reduces the number of parameters. There have been a lot of approaches [104–109] in the Beyond Standard Model (BSM) framework to establish relation between the parameters of M_ν. Inclusion of discrete symmetries [1–3, 110] in addition to the SM gauge group turns out to be the most attractive one to uncover the flavor structure of the neutrino mass matrix. Impact of these symmetries are mostly intriguing from the mixing perspective. A closer look to the the oscillation data given in Table 1.1 reveals that one can parametrize the mixing matrix U at leading order as

$$U = \begin{pmatrix} \sqrt{1-\lambda^2} & \lambda & 0 \\ -\frac{\lambda}{\sqrt{2}} & \frac{1}{\sqrt{2}}\sqrt{1-\lambda^2} & \frac{1}{\sqrt{2}} \\ \frac{\lambda}{\sqrt{2}} & -\frac{1}{\sqrt{2}}\sqrt{1-\lambda^2} & \frac{1}{\sqrt{2}} \end{pmatrix}, \tag{1.147}$$

where $\lambda = \sin\theta_{12}$. Note that here we assume a vanishing value of θ_{13} and a maximal value of θ_{23}. Although a nonzero value of θ_{13} is well established presently, the mixing matrix in (1.147) can be derived from an well motivated low energy symmetry, namely, the $\mu\tau-$interchange symmetry. To be precise, given a neutrino Majorana mass term (for example)

$$-\mathcal{L} = \frac{1}{2}\overline{\nu_{L\alpha}^{C}} M_{\nu\alpha\beta}\nu_{L\beta} + \text{h.c.} \tag{1.148}$$

if one demands an invariance of the mass term under the exchange of two flavor fields as $\nu_\mu \leftrightarrow \nu_\tau$, the following structure of M_ν is obtained:

$$M_\nu^{\mu\tau} = \begin{pmatrix} a & b & -b \\ b & c & d \\ -b & d & c \end{pmatrix}, \tag{1.149}$$

where all the parameters are complex in general and the minus sign is considered to be in conformity with the PDG convention of U_{PMNS}. Now the matrix $M_\nu^{\mu\tau}$ can be diagonalized by the matrix U given in (1.147) with $\lambda \to \lambda(a,b,c,d)$. One can also fix the solar mixing angle for λ being $1/\sqrt{3}$ as a consequence of a TBM [1] symmetry. Besides, there are other interesting residual symmetries such as scaling ansatz in neutrino mass matrix that predicts vanishing values for θ_{13} and m_3 along with a nonmaximal θ_{23} in general. All these effective symmetries are well motivated from the larger symmetry group such as A_4, S_3, D_4 etc. However, to comply with the present data, these effective residual symmetries should be broken. As a consequence, apart from generating a nonzero value of θ_{13} one can have predictions on the CP violating phases as well. A part of this thesis deals with such broken effective symmetries and their impact on low energy neutrino observables.

There is another way to realize the residual symmetries in the low energy neutrino mass matrix. In Ref [7, 8] C.S Lam has proved that whatever be the structure of M_ν, if it is Majorana type, the existing residual symmetry should always be a $\mathbb{Z}_2 \times \mathbb{Z}_2$. Unlike the previous case, these symmetries may not have a deep flavor meaning at the effective Lagrangian. Nevertheless, it possesses highly constraint relations among the mixing parameters. Due to its immense testability in the forthcoming experiments, a high attention is being paid to this scheme now a days. In chapter 4 where we elaborate this scheme, one finds the key equation that implements a couple of $\mathbb{Z}_2$ invariance in the neutrino mass term is given by

$$G_{2,3}^T M_\nu G_{2,3} = M_\nu, \tag{1.150}$$

where $G_{2,3}$ are the $\mathbb{Z}_2$ generators and the neutrino fields transform as $\nu_\alpha \to G_{\alpha\beta}\nu_\beta$. This real invariance may also be extended to its complex counter part by means of a nonstandard CP transformation $\nu_\alpha \to iG_{\alpha\beta}\gamma^0\nu_\beta^C$ [111–113] that leads to the invariance

$$G_{2,3}^T M_\nu G_{2,3} = M_\nu^*. \tag{1.151}$$

Note that the R.H.S of (1.150) is now replaced with its complex conjugate in (1.151). Thus one can implement a nonstandard $\mathbb{Z}_2^{CP}$ transformation in the low energy effective Lagrangian.

It is highly nontrivial to combine a flavor group with a CP symmetry. However, it has been shown in Ref. [114] that this can be done if they satisfy certain consistency conditions. In a top-down approach, a flavor group combined with a CP symmetry $G_f \times G_{CP}$ at high energy spontaneously breaks down to two different symmetries; $G_f^\ell \times G_{CP}^\ell$ in the charged lepton sector and $G_f^\nu \times G_{CP}^\nu$ neutrino sector [111]. A testable neutrino mixing scenario is obtained due to this mismatch between the residual symmetries of the two sectors. A bottom-up approach has also been proposed [12] to construct a minimal flavor group with the residual symmetries of the charged lepton and the neutrino sector.

1.4.2 Relevant residual symmetries connected to this thesis: A presummary of the present work

After the breaking of a particular discrete symmetry, it is the mismatch between the residual symmetries of charged lepton and neutrino sector that generates mixing angles closed to their observed values. Beside predicting a zero value of the reactor angle, since the popular flavor symmetry groups such as A_4, $S_{3,4}$, D_4 etc. are unable to speculate the mass ordering of the light neutrinos, testable values of the CP phases and the absolute mass scale, they should be modified in a certain way to produce a phenomenologically viable theory. In our work, we have done the modification in two different ways. First, we assume that the remnant (residual) symmetry in the low energy Lagrangian is broken with a small breaking parameter and thus generates a nonzero θ_{13}. Along with that mildly broken remnant symmetry, we also consider some vanishing elements in the neutrino mass matrix, commonly known as the texture zeros [4]. Due to the presence of the zeros in the neutrino mass matrix, constraint ranges for the CP violating phases are determined along with a definite mass ordering. Theoretical justification of the breaking might be rationalized with several top-down approaches, such as the refinement of the model with an extended matter content which serves as a breaking of the remnant symmetry through a loop contribution [5] or adding soft breaking terms to the initially symmetric theory [6] at high energy etc.. Without going into the explicit model building, we rather zero in on the low energy predictions of the neutrino parameters such as CP phases, sum of the light neutrino masses $\Sigma_i m_i$ and neutrinoless double ($\beta\beta0\nu$) decay parameter $|M_{ee}|$.

We also explore the other approach, i.e., invariance of M_ν under a $\mathbb{Z}_2 \times \mathbb{Z}_2$

symmetry. Again due to the nonexistence of a nonvanishing θ_{13} in the model under consideration, we have supplemented it with a nonstandard CP transformation; CP-transformations followed by a flavor symmetry operation [10]. Unlike the canonical (standard) CP transformation, which is a CP conserving theory, this nonstandard CP transformation predicts maximally violating value $\pi/2$ or $3\pi/2$ for the Dirac CP phase δ and a CP conserving value for the Majorana phases α or β by restricting them to either 0 or π. High energy symmetry group for models of this kind may be constructed through the induced automorphism approach [11, 12].

Two of my research works [13, 14] are based on texture zeros along with the discrete residual symmetries; the Scaling Ansatz (SA) [15,16] and a cyclic permutation symmetry. The former is motivated by the models with the high energy flavor symmetry groups such as a nonabelian $D_4 \times \mathbb{Z}_2$ and an abelian $U(1)_{L_e - L_\mu - L_\tau}$ while the latter is implemented by a discrete $A_4 \times \mathbb{Z}_3 \times \mathbb{Z}_2$ family symmetry. Some attractive variants of seesaw mechanism, namely, the inverse and the linear seesaw are also considered in both the cases here owing to the fact that the heavy neutrinos originated from these mechanisms are of masses of the order of TeV, thus accessible to the LHC. Due to the significant reduction of the number of parameters in the light neutrino mass matrices, interesting conclusions regarding the low energy neutrino parameters are drawn for each of the cases. For example, the first case, i.e, the model with Scaling Ansatz, predicts almost a vanishing value of the Dirac CP phase δ and thus confronting with testability since T2K's new data (2016) [17] continue to prefer a value of the Dirac CP phase near the maximally violating value $3\pi/2$. Along with an inverted ordering, both the models predict a constraint ranges of the light neutrino masses as well the $\beta\beta0\nu$ parameter $|M_{ee}|$. On the other hand a cyclic permutation symmetry invariant theory at the leading order has been modified with soft breaking terms. To constrain the number of parameters we also assume here the existence of texture zeros. This model is quite interesting from the neutrinoless double beta

($\beta\beta 0\nu$) decay perspective.

In the residual $\mathbb{Z}_2 \times \mathbb{Z}_2$ approach, as mentioned earlier, we have generalized the well known Simple Real Scaling ansatz (SRS) [15,16] on the neutrino Majorana mass matrix to its complex extension and named it as Complex Extended Scaling (CES). In this case, the $\mathbb{Z}_2 \times \mathbb{Z}_2$ symmetry is complemented by a nonstandard CP-transformation on the neutrino fields as $\nu_{L\alpha} \rightarrow iG_{\alpha\beta}\gamma^0\nu^C_{L\beta}$ with $G_{\alpha\beta}$ being the generators of one of the $\mathbb{Z}_2$ symmetry and $\nu^C_{L\beta}$ represents the usual charged conjugated left chiral neutrino field. As a consequence, the usual horizontal symmetry $G^T M^{SRS}_\nu G = M^{SRS}_\nu$ is replaced with its complex version; $G^T M^{CES}_\nu G = (M^{CES}_\nu)^*$. The entire work is divided into two parts, first one [22] of which focuses on the predictions of low energy neutrino parameters; specifically the robust predictions of $\cos\delta = 0$ and $\sin\alpha = \sin\beta = 0$ or π thus $|M_{ee}|$ and the measurement of CP-asymmetry parameter $A_{\mu e}$ in the baseline oscillation experiments. In the other [23], we concentrate on the hierarchical flavored leptogenesis within the framework of Type-I seesaw mechanism. We assume strongly hierarchical mass eigenvalues for the RH Majorana neutrino mass matrix M_R. The leptonic CP asymmetry parameter ε^α_1 with lepton flavor α, originating from the decays of the lightest of the heavy neutrinos N_1 (of mass M_1) at a temperature $T \sim M_1$, is what matters here with the lepton asymmetry originating from the decays of $N_{2,3}$, being washed out. Due to the presence of the residual $\mathbb{Z}_2 \times \mathbb{Z}_2$ and a CP transformation, a typical structure of the Dirac mass matrix m_D emerges. Imaginary part of the latter generates a nonzero θ_{13}, maximal Dirac CP violation as well as a nonvanishing ε^α_1 , thus it serves as a common source of the said quantities. The entire thesis is based on a study of these models that deal with various aspects of residual symmetries.

Before going to the explicit details of these works, we would first like to include a general technique for calculating the Majorana phases. As discussed in the next chapter in detail, given any hierarchical neutrino mass model, our prescription is able to compute the corresponding Majorana phases and thus useful to evaluate the Majorana phases for some of the models under consideration. Leaving an explicit discussion for the next chapter, let us present a brief introduction of the methodology adapted.

So far in the existing literature, CP-violating Majorana phases are calculated in a model dependent way. We present a general recipe for the evaluation of the Majorana phases assuming the hierarchical mass spectrum of the light neutrinos. To evaluate the Majorana phases in Mohapatra-Rodejohann's phase convention [16], we use the rephasing invariant quantities [19] which remain unchanged even after the rotation of the light neutrino mass matrix in the phase space (low energy phases of the effective M_ν). In this prescription, the Majorana phases are calculable in a model independent way even for a vanishing value of the lightest neutrino mass m_1 (m_3), for normal (inverted) hierarchy. Furthermore, constraining the general methodology with the upper limits on $\Sigma_i m_i$ and $|M_{ee}|$ dictated by PLANCK [20] and GERDA-I [21] respectively, ranges of the Majorana phases are presented in a general context.

The next chapters are based on following publications:

Chapter 2: Nucl. Phys. B **904**, 86 (2016).

Chapter 3: JHEP **1505**, 077 (2015) & Nucl. Phys. B **911**, 846 (2016).

Chapter 4: Eur. Phys. J. C **76**, 662 (2016).

Chapter 5: JCAP **1703**, 025 (2017).

Coauthors: Ambar Ghosal, Probir Roy and Mainak Chakraborty.

Chapter 2

Evaluation of the Majorana phases

2.1 Introduction

Apart from hierarchical structure of massive neutrinos a fundamental qualitative nature of these elusive particles whether they are Dirac or Majorana type is yet unknown. Neutrinoless double beta decay ($\beta\beta_{0\nu}$) mode [21, 27, 115–122] is able to discriminate between the two different types. Positive evidence of the above experimental search will be able to determine the Majorana nature of neutrinos. Several $\beta\beta_{0\nu}$ experiments are ongoing and planned. In Ref. [123] a brief discussion about some of the important experiments is presented. Among those experiments, EXO-200 [25] experiment puts an upper limit on the relevant neutrino mass matrix element[1] $|m_{11}|$ within a range as $|m_{11}| < (0.14\text{-}0.35 \text{ eV})$. Further, experiments like GERDA-II [27], NEXT-100 [124] will be able to bring down the above value of the order of 0.1 eV. Thus in an optimistic point of view such a property of neutrinos could be testified by the next generation experiments. However, even if it is possible to pin down the value of $|m_{11}|$, it is still difficult to predict the values of the Majorana phases

[1]In this chapter we refer $|M_{ee}|$ as $|m_{11}|$ throughout.

until we can fix the absolute neutrino mass scale. It is shown in Ref. [125] that in addition to the $\beta\beta_{0\nu}$ decay experiments, lepton number violating processes in which the Majorana phases show up, are also corroborative to determine the individual Majorana phases. Another interesting physical aspect, such as contribution of the Majorana phases to generate a nonvanishing θ_{13} within the present 3σ range of neutrino oscillation global fit data is also studied in the literature [126]. Ref. [127] discusses how to constrain the Majorana phases using the results from cosmology and double beta decay. Thus it is worthwhile to study the calculability of the Majorana phases in terms of a general neutrino mass matrix (M_ν) parameters.

In the present work we evaluate individual Majorana phases in terms of the parameters of a general M_ν using three rephasing invariants I_{12}, I_{13} and I_{23} presented in Ref. [19] on the basis of Mohapatra-Rodejohann's phase convention [16]. Although there are several papers which discusses the general procedure for calculating the Majorana phases, motivation behind taking the rephasing invariants is that the methodology we present here is capable of calculating the Majorana phase in a model independent way even if one of the eigenvalue is zero which is still allowed as far as the present neutrino oscillation global fit data is concerned. Moreover, as one of the rephasing invariant (I_{23}) is directly proportional to m_3, therefore it vanishes if $m_3 = 0$ and hence shows a strong dependency of the Majorana phases with the light neutrino masses. In the present work we evaluate the Majorana phases for a general complex symmetric neutrino mass matrix (M_ν) taking into account the global fit oscillation data and the upper bound on the sum of the three light neutrino masses ($\Sigma_i m_i$) along with the $\beta\beta_{0\nu}$ decay parameter for both the hierarchical cases. Except the case of quasi degeneracy[2], it is then concluded that the methodology presented in this work is able to calculate the Majorana phases, given any model of neutrino masses. For

[2]For the quasi-degenerate case the procedures of calculating the Majorana phases are stated in Sec.2.4

convenience, we further numerically estimate the ranges of each Majorana phase for both types of hierarchies, in the context of a cyclic symmetric model as well as a model with scaling ansatz property. Let us now have a brief look at the contents of this chapter.

In Section 2.2 we briefly discuss the basic formalism to set the convention of the Majorana phase representation within the framework of neutrino oscillation phenomena. CP violating rephasing invariants are presented in Section 2.3. Section 2.4 contains explicit calculation of the Majorana phases for both types of neutrino mass hierarchies along with phenomenologically viable different sub cases. Numerical estimation of the Majorana phases, their connection to the physical observables and their testability for the general case are presented in Section 2.5. In Section 2.6 application of the above methodology in the context of cyclic symmetric and scaling ansatz invariant models is presented. Section 2.7 contains summary of the present chapter.

2.2 Basic formalism

Experimental observation of neutrino flavor oscillation constitutes a robust evidence in favor of nonzero neutrino masses. The flavor transition process is basically a quantum mechanical interference phenomena with the explicit relationship between the quantum fields ($\nu_{\alpha L}$) in the flavor basis and the mass basis (ν_{iL}) as

$$\nu_{\alpha L} \quad = \quad \Sigma_i U^*_{\nu\alpha i} \nu_{iL}, \tag{2.1}$$

where α $(= 1, 2, ..., m)$ corresponds to the flavor and i $(= 1, 2, ..., n)$ implies the mass index. The matrix U_ν is the corresponding neutrino mixing matrix. For three generation of fermions, i.e, for $n = m = 3$, the weak Lagrangian containing the charged lepton fields and the neutrino fields can be written in the mass basis as

$$-\mathcal{L}^{cc} = \frac{g}{\sqrt{2}} \quad \bar{l}_{\alpha L}\gamma^{\mu}(U_l^{\dagger}U_{\nu}^{*})_{\alpha i}\nu_{iL}W_{\mu}^{-} + \text{h.c.}, \tag{2.2}$$

where U_l is the unitary mixing matrix in the charged lepton sector. The matrix $U_l^{\dagger}U_{\nu}$ is the leptonic mixing matrix and is known as the $Pontecorvo-Maki-Nakagawa-Sakata$ mixing matrix (U_{PMNS}) which contains 3 mixing angles and 6 phases in general. It is useful to redefine the mixing matrix by absorbing the unphysical phases into the charged lepton fields and the neutrino fields (Dirac type). If the neutrinos are Majorana type, they break the global $U(1)$ symmetry and hence, redefinition of the neutrino fields is not possible. Therefore, out of 6 phases 3 unphysical phases can be absorbed by redefining only the charged lepton fields and thus the U_{PMNS} matrix is parametrized as

$$U_{PMNS} = U_{CKM}P_M. \tag{2.3}$$

U_{CKM} is the usual CKM type matrix as defined in the previous section:

$$U_{CKM} = \begin{pmatrix} c_{12}c_{13} & s_{12}c_{13} & s_{13}e^{-i\delta} \\ -s_{12}c_{23} - c_{12}s_{23}s_{13}e^{i\delta} & c_{12}c_{23} - s_{12}s_{13}s_{23}e^{i\delta} & c_{13}s_{23} \\ s_{12}s_{23} - c_{12}s_{13}c_{23}e^{i\delta} & -c_{12}s_{23} - s_{12}s_{13}c_{23}e^{i\delta} & c_{13}c_{23} \end{pmatrix}. \tag{2.4}$$

P_M is a 3×3 diagonal phase matrix and following Mohapatra-Rodejohann's phase convention [16] it is given by

$$P_M = (1, e^{i\alpha}, e^{i(\beta+\delta)}), \tag{2.5}$$

where α and $\beta + \delta$ are the Majorana phases which do not appear in the *neutrino* $\rightarrow$ *neutrino* oscillation experiments [128, 129]. Regarding the structure of P_M matrix, we would like to mention the following: The advantage of using the above Majorana phase convention is that for $m_3 = 0$ it is possible to calculate the single existing Majorana phase α while, for $m_1 = 0$, only the phase difference $\alpha - (\beta + \delta)$ is calculable. The result will be reversed if we utilize the convention of Ref. [130]. Explicitly, with this convention, a vanishing value of m_3 implies, only the phase difference is calculable, however if m_1 is vanishing it is possible to calculate the existing Majorana phase. A detailed calculation to evaluate both the Majorana phases in the context of a general M_ν is presented in Ref. [130]. However, if one of the eigenvalue is zero which is still allowed by the present neutrino experimental data, it is not possible to calculate individual phases in that case. The above mentioned problem is successfully resolved in the present work. CP violating effect of Majorana phases in *neutrino* $\rightarrow$ *antineutrino* oscillation [24, 131, 132] and some lepton number violating (LNV) processes are studied in detail in Ref. [125]. In this work, using the rephasing invariants constructed out of the neutrino mass matrix elements [19] we determine the Majorana phases for two different hierarchical cases.

2.3 CP violating phase invariants

Considering the neutrinos as the Majorana fermions in an extended standard model one can parametrize the U_{PMNS} with the CP violating phases following (2.3) where we redefine the charged lepton fields by absorbing the unphysical phases of total mixing matrix U. Hence, in principle the mixing matrix U can be defined as

$$U \equiv P_\phi U_{PMNS}, \tag{2.6}$$

where P_ϕ is a 3×3 diagonal phase (unphysical) matrix and is given by

$$P_\phi \;=\; diag(e^{i\phi_1}, e^{i\phi_2}, e^{i\phi_3}). \tag{2.7}$$

Now, as the low energy neutrino mass matrix is complex symmetric it can be put into a diagonal form through the equation

$$U^\dagger M_\nu U^* \;=\; d_\nu, \tag{2.8}$$

where

$$d_\nu \;=\; diag(m_1, m_2, m_3). \tag{2.9}$$

Substituting (2.6) in (2.8) we get

$$U^\dagger_{PMNS} P^\dagger_\phi M_\nu P^*_\phi U^*_{PMNS} \;=\; d_\nu. \tag{2.10}$$

Thus P_ϕ rotates the mass matrix M_ν in phase space. Therefore, the rephasing invariants (remain invariant under phase rotation) of M_ν contain the informations about the CP violating phases. It has been shown explicitly in Ref. [19] that for three generations of neutrinos, there are three independent rephasing invariants which are given by

$$\begin{aligned} I_{12} &= Im[m_{11} m_{22} m^*_{12} m^*_{21}]; \\ I_{23} &= Im[m_{22} m_{33} m^*_{23} m^*_{32}]; \\ I_{13} &= Im[m_{11} m_{33} m^*_{13} m^*_{31}]; \end{aligned} \tag{2.11}$$

where $m_{\alpha\beta}$ is the element of M_ν at $\alpha\beta$ position with $\alpha, \beta = 1, 2, 3$. Now, since the invariants of (2.11) are independent of phase rotation of M_ν, therefore to evaluate them in terms of mixing angles, CP violating phases and the eigenvalues we can rewrite (2.10) as

$$M_\nu \;=\; U_{PMNS} d_\nu U^T_{PMNS}, \tag{2.12}$$

where without any loss of generality we assume $\phi_i = 0$ which corresponds to the structure of P_ϕ given by

$$P_\phi = diag(1,1,1). \tag{2.13}$$

Now writing down (2.12) explicitly one can find the mass matrix elements as

$$m_{11} \;=\; c_{12}^2 c_{13}^2 m_1 + s_{12}^2 c_{13}^2 m_2 e^{2i\alpha} + m_3 s_{13}^2 e^{-2i\delta+2i(\beta+\delta)}, \tag{2.14}$$

$$\begin{aligned} m_{12} \;=\; & c_{13}\{-m_1(c_{12}s_{12}c_{23} + c_{12}^2 s_{13}s_{23}e^{i\delta}) \\ & + m_2 e^{2i\alpha}(c_{12}s_{12}c_{23} - s_{12}^2 s_{13}s_{23}e^{i\delta})\} + m_3 c_{13}s_{13}s_{23}e^{-i\delta+2i(\beta+\delta)}, \end{aligned} \tag{2.15}$$

$$\begin{aligned} m_{13} \;=\; & c_{13}\{m_1(c_{12}s_{12}s_{23} - c_{12}^2 s_{13}c_{23}e^{i\delta}) \\ & - m_2 e^{2i\alpha}(c_{12}s_{12}s_{23} + s_{12}^2 s_{13}c_{23}e^{i\delta})\} + m_3 c_{13}s_{13}c_{23}e^{-i\delta+2i(\beta+\delta)}, \end{aligned} \tag{2.16}$$

$$\begin{aligned} m_{22} \;=\; & m_1(s_{12}c_{23} + c_{12}s_{23}s_{13}e^{i\delta})^2 \\ & + m_2 e^{2i\alpha}(c_{12}c_{23} - s_{12}s_{23}s_{13}e^{i\delta})^2 + m_3 c_{13}^2 s_{23}^2 e^{2i(\beta+\delta)}, \end{aligned} \tag{2.17}$$

$$\begin{aligned} m_{23} \;=\; & m_1\{c_{12}s_{12}s_{13}(c_{23}^2 - s_{23}^2)e^{i\delta} + c_{12}^2 c_{23}s_{23}s_{13}^2 e^{2i\delta} - s_{12}^2 s_{23}c_{23}\} \\ & - m_2 e^{2i\alpha}\{c_{12}s_{12}s_{13}(c_{23}^2 - s_{23}^2)e^{i\delta} - s_{12}^2 c_{23}s_{23}s_{13}^2 e^{2i\delta} + c_{12}^2 s_{23}c_{23}\} \\ & + m_3 c_{23}s_{23}c_{13}^2 e^{2i(\beta+\delta)}, \end{aligned} \tag{2.18}$$

$$\begin{aligned} m_{33} \;=\; & m_1(c_{12}c_{23}s_{13}e^{i\delta} - s_{12}s_{23})^2 \\ & + m_2 e^{2i\alpha}(s_{12}c_{23}s_{13}e^{i\delta} + c_{12}s_{23})^2 + m_3 c_{23}^2 c_{13}^2 e^{2i(\beta+\delta)}. \end{aligned} \tag{2.19}$$

It is now straightforward to calculate I_{12} and I_{13} using (2.14) to (2.19). Neglecting terms $O(s_{13}^2)$ and higher order we obtain I_{12} and I_{13} as

$$\begin{aligned} I_{12} &= Ac_{23}^3[Bc_{23} - 2s_{23}s_{13}\{c_{12}^2 m_1\Phi_1 + s_{12}^2 m_2\Phi_2\}] \\ &\quad + m_3^2 c_{12}c_{13}^4 s_{12}c_{23}[-2c_{12}^2 s_{23}^3 c_{13}^2 m_1 s_{13}A_1 + 2s_{23}^3 c_{13}^2 s_{12}^2 m_2 s_{13}A_2] \\ &\quad + m_3 c_{12}c_{13}^4 s_{12}c_{23}[s_{12}s_{23}^2 c_{13}^2 m_1 c_{12}^3 c_{23}A_3 + s_{12}^3 s_{23}^2 c_{13}^2 m_2 c_{12}c_{23}A_4 \\ &\quad - 2c_{12}^4 s_{23}m_1 m_2 c_{23}^2 s_{13}A_5 - 2s_{23}m_1 m_2 s_{12}^4 c_{23}^2 s_{13}A_5 + 2c_{12}^2 s_{23}s_{12}^2 s_{13}c_{23}^2 A_6 \\ &\quad + 2c_{12}^4 s_{23}^3 c_{13}^2 m_1^2 s_{13}A_7 + 4\cos(2\alpha)c_{12}^2 s_{23}^2 c_{13}^2 m_1 m_2 s_{12}^2 s_{13}A_7 \\ &\quad + 2s_{23}^3 c_{13}^2 m_2^2 s_{12}^4 s_{13}A_7], \end{aligned} \tag{2.20}$$

$$\begin{aligned} I_{13} &= As_{23}^3[Bs_{23} + 2c_{23}s_{13}\{c_{12}^2 m_1\Phi_1 + s_{12}^2 m_2\Phi_2\}] \\ &\quad - m_3^2 c_{12}c_{13}^4 s_{12}s_{23}[-2c_{12}^2 c_{23}^3 c_{13}^2 m_1 s_{13}A_1 + 2c_{23}^3 c_{13}^2 m_2 s_{12}^2 s_{13}A_2] \\ &\quad + m_3 c_{12}c_{13}^4 s_{12}s_{23}[c_{12}^3 c_{23}^2 c_{13}^2 m_1 s_{12}s_{23}A_3 + c_{12}c_{23}^2 c_{13}^2 m_2 s_{12}^3 s_{23}A_4 \\ &\quad + 2c_{12}^4 c_{23}m_1 m_2 s_{23}^2 s_{13}A_5 + 2c_{23}m_1 m_2 s_{12}^4 s_{23}^2 s_{13}A_5 - 2c_{12}^2 c_{23}s_{12}^2 s_{13}s_{23}^2 A_6 \\ &\quad - 2c_{12}^4 c_{23}^3 c_{13}^2 m_1^2 s_{13}A_7 - 4\cos(2\alpha)c_{12}^2 c_{23}^3 c_{13}^2 m_1 m_2 s_{12}^2 s_{13}A_7 \\ &\quad - 2c_{23}^3 c_{13}^2 m_2^2 s_{12}^4 s_{13}A_7], \end{aligned} \tag{2.21}$$

where

$$A = -c_{12}s_{12}m_1 m_2 c_{13}^4, \tag{2.22}$$

$$B = \sin(2\alpha)c_{12}s_{12}(m_2^2 - m_1^2), \tag{2.23}$$

$$\Phi_1 = \{\sin(2\alpha - \delta)m_1 + \sin[\delta]m_2\}, \tag{2.24}$$

$$\Phi_2 = \{\sin(2\alpha + \delta)m_2 - \sin[\delta]m_1\} \tag{2.25}$$

and

$$
\begin{aligned}
A_1 &= \sin(\delta)m_1 + \sin(2\alpha - \delta)m_2, \\
A_2 &= \sin(\delta)m_2 - \sin(2\alpha + \delta)m_1, \\
A_3 &= \sin 2(\beta + \delta)m_1^2 + 2\sin(2\alpha - 2\beta - 2\delta)m_1 m_2 - \sin(4\alpha - 2\beta - 2\delta)m_2^2, \\
A_4 &= \sin 2(\alpha + \beta + \delta)m_1^2 - 2\sin 2(\beta + \delta)m_1 m_2 - \sin(2\alpha - 2\beta - 2\delta)m_2^2, \\
A_5 &= \sin(2\alpha - 2\beta - \delta)m_1 + \sin(2\beta + \delta)m_2, \\
A_6 &= \sin(2\beta + \delta)m_1^3 - \sin(2\alpha + 2\beta + \delta)m_1^2 m_2 - \sin(4\alpha - 2\beta - \delta)m_1 m_2^2 + \sin(2\alpha - 2\beta - \delta), \\
A_7 &= \sin(2\beta + \delta)m_1 + \sin(2\alpha - 2\beta - \delta)m_2.
\end{aligned} \tag{2.26}
$$

A careful inspection reveals that the invariants are expressed in a tricky way. To be more precise, they are written as

$$
I_{ij} = \zeta_1 + s_{13}\zeta_2 + m_3^2\zeta_3 + m_3\zeta_4, \tag{2.27}
$$

where 'ζ_i' is some combination of parameter dictated by (2.20) and (2.21). The reason behind such a way to write down the invariants are the following: the popular paradigm in the neutrino mass models is to generate vanishing θ_{13} at the leading order and thereafter nonzero value of the same is generated by means of some perturbation to the mass matrix and finally since the oscillation data dictates the mass squared differences only, there is also a possibility of a vanishing neutrino mass (e.g, models with scaling ansatz, Zee-Babu model etc.). Therefore one can see the direct impact of their presence or absence in the measures of CP violation.

The remaining invariant (I_{23}) has a special character; that it vanishes for $m_3 = 0$. The expression for I_{23} can be written as

$$
\begin{aligned}
I_{23} &= m_3^3 c_{23} s_{23} c_{13}^2 B_1 + m_3^2 c_{23} s_{23} c_{13}^2 [2 c_{12}^3 c_{13}^2 m_2 s_{12} s_{13} (c_{23}^2 - s_{23}^2) B_2 \\
&\quad -2 c_{12} c_{13}^2 m_1 s_{12}^3 s_{13} (c_{23}^2 - s_{23}^2) B_3] + m_3 c_{23} s_{23} c_{13}^2 [c_{12}^6 c_{23} m_2^3 s_{23} B_4 \\
&\quad + c_{12}^4 c_{23} m_1 m_2^2 s_{12}^2 s_{23} B_5 + c_{12}^2 c_{23}^2 m_1^2 m_2 s_{12}^4 s_{23} B_6 + c_{23} m_1^3 s_{12}^6 s_{23} B_7 \\
&\quad -2 c_{12}^5 m_2^2 s_{12} s_{13} (c_{23}^2 - s_{23}^2) B_8 - 4\cos(2\alpha) c_{12}^3 m_1 m_2 s_{12}^3 s_{13} (c_{23}^2 - s_{23}^2) B_8] \\
&\quad -2 c_{12} m_1^2 s_{12}^5 s_{13} (c_{23}^2 - s_{23}^2) B_8],
\end{aligned} \tag{2.28}
$$

where

$$
\begin{aligned}
B_1 &= \sin 2(\alpha - \beta - \delta) c_{12}^2 c_{23}^2 c_{13}^4 m_2 s_2 - \sin 2(\beta + \delta) c_{23} c_{13}^4 m_1 s_{12}^2 s_{23} \\
&= \Phi_1, \\
B_2 &= \sin(2\alpha - \delta) m_1 + \sin(\delta) m_2 \\
&= -\Phi_2, \\
B_3 &= \sin(\delta) m_1 - \sin(2\alpha + \delta) m_2, \\
B_4 &= -\sin(2\alpha - 2\beta - 2\delta), \\
B_5 &= 2\sin 2(\beta + \delta) - \sin(4\alpha - 2\beta - 2\delta), \\
B_6 &= -2\sin(2\alpha - \beta - \delta) + \sin 2(2\alpha + \beta + \delta), \\
B_7 &= \sin 2(\beta + \delta), \\
B_8 &= \sin(2\beta + \delta) m_1 + \sin(2\alpha - 2\beta - \delta) m_2.
\end{aligned} \tag{2.29}
$$

2.4 The Majorana phases

At the outset, first we would like to mention that the three independent invariants I_{12}, I_{13} and I_{23} stand for the three CP violating phases α, $\beta+\delta$ and δ, however, in this section we solve the invariants only for the Majorana phases $(\alpha, \beta+\delta)$ while the Dirac CP phase δ is calculable from the usual Jarlskog measure of CP violation. Next, for a general M_ν where all the parameters are present and all the eigenvalues and mixing angles are nonzero, all the invariants are independent and in principle one can extract the α and $\beta+\delta$ phases without any specific hierarchical assumption which is also useful for the quasi-degenerate case. However, the calculation is too cumbersome in this general situation. In the present work we consider a simplified approach assuming hierarchical structure of neutrino masses and calculate the Majorana phases utilizing the invariants I_{12}, I_{13} and I_{23} for both the hierarchical cases.

- **Inverted hierarchy** $(m_2 > m_1 >> m_3)$

  Case I: $m_1, m_2, m_3 \neq 0$, $\theta_{13} \neq 0$: *Three independent invariants.*

  In this case utilizing (2.20) and (2.21) the Majorana phase α comes out as

$$\alpha = \frac{1}{2}\sin^{-1}\left\{-\frac{I_{12}s_{23}^2 + I_{13}c_{23}^2}{c_{23}^2 s_{23}^2 c_{13}^4 c_{12}^2 s_{12}^2 m_1 m_2 \Delta m_\odot^2}\right\} \tag{2.30}$$

  where $\Delta m_\odot^2 = m_2^2 - m_1^2$ and we neglect the terms containing $m_3(m_{min})$ in both the invariants (I_{12} and I_{13}). Another equivalent expression of α can also be obtained from (2.14) (neglecting the term containing $m_3 s_{13}^2$) showing explicit relationship with $\beta\beta_{0\nu}$ decay parameter $|m_{11}|$ as

$$\alpha = \frac{1}{2}\cos^{-1}\left\{\frac{|m_{11}|^2}{2c_{12}^2 s_{12}^2 c_{13}^4 m_1 m_2} - \frac{(c_{12}^4 m_1^2 + s_{12}^4 m_2^2)}{2c_{12}^2 s_{12}^2 m_1 m_2}\right\}. \tag{2.31}$$

  In principle we can use any of the equations, (2.30) or (2.31), to find α. The first one depends upon the explicit construction of I_{12} and I_{13} in terms of the neutrino mass matrix (M_ν) elements while the second one requires the knowledge of $\beta\beta_{0\nu}$ decay parameter $|m_{11}|$.

  In order to calculate $\beta+\delta$ from (2.28) the terms involving $s_{13}(c_{23}^2 - s_{23}^2)$ can be neglected. Therefore, assuming inverted hierarchy I_{23} can be approximated with dominant term as

$$\begin{aligned} I_{23} &= m_2^3 m_3 c_{23} s_{23} c_{13}^2 c_{12}^6 c_{23} s_{23} B_4 \\ &= -m_2^3 m_3 c_{23}^2 s_{23}^2 c_{13}^2 c_{12}^6 \sin(2\alpha - 2[\beta+\delta]). \end{aligned} \tag{2.32}$$

Reverting the above equation the Majorana phase $\beta + \delta$ is expressed as

$$\beta + \delta = -\frac{1}{2} \sin^{-1} \left\{ -\frac{I_{23}}{m_2^3 m_3 c_{23}^2 s_{23}^2 c_{13}^2 c_{12}^6} \right\} + \alpha. \tag{2.33}$$

Case II: $m_1, m_2, \theta_{13} \neq 0$, $m_3 = 0$: *Two independent invariants.*

In this case utilizing (2.20), (2.21) and (2.28) the three rephasing invariants I_{12}, I_{13} and I_{23} come out as

$$I_{12} = A c_{23}^3 [B c_{23} - 2 s_{23} s_{13} \{ c_{12}^2 m_1 \Phi_1 + s_{12}^2 m_2 \Phi_2 \}] \tag{2.34}$$

$$= I_{12}^0 - 2 A c_{23}^3 s_{23} s_{13} \{ c_{12}^2 m_1 \Phi_1 + s_{12}^2 m_2 \Phi_2 \}, \tag{2.35}$$

$$I_{13} = A s_{23}^3 [B s_{23} + 2 c_{23} s_{13} \{ c_{12}^2 m_1 \Phi_1 + s_{12}^2 m_2 \Phi_2 \}] \tag{2.36}$$

$$= I_{13}^0 + 2 A s_{23}^3 c_{23} s_{13} \{ c_{12}^2 m_1 \Phi_1 + s_{12}^2 m_2 \Phi_2 \}, \tag{2.37}$$

$$I_{23} = 0, \tag{2.38}$$

where

$$I_{12}^0 = A B c_{23}^4, \tag{2.39}$$

$$I_{13}^0 = A B s_{23}^4 \tag{2.40}$$

with A, B already defined in (2.22) and (2.23) respectively. As one of the invariant vanishes due to the condition $m_3 = 0$, therefore, the three independent CP phases can not be solved from the above invariants and thus the two nonzero invariants corresponds to one Majorana phase (α) and the Dirac CP phase (δ) as $\beta + \delta$ vanishes for $m_3 = 0$. Proceeding as previous we get the same expression for the Majorana phase α as given in (2.31). Furthermore, solving (2.34) to (2.36) an equivalent expression of α, same as (2.30) is also obtained.

Case III: $m_1, m_2 \neq 0$, $m_3, \theta_{13} = 0$: *One independent invariant.*

In this case the invariants given in (2.34), (2.36) and (2.38) become

$$I_{12} = I_{12}^0, \tag{2.41}$$

$$I_{13} = I_{13}^0 \tag{2.42}$$

and

$$I_{23} = 0. \tag{2.43}$$

It is amply clear that the first two invariants I_{12} and I_{13} are not independent of each other and their correlated relationship leads to the estimation of only one Majorana phase α while the information about the Dirac CP phase is lost. Similarly one can calculate the invariants for a normal mass hierarchy in the following way as demonstrated below.

- **Normal hierarchy** ($m_3 >> m_2 > m_1$)

  Case I: $m_1, m_2, m_3 \neq 0$, $\theta_{13} \neq 0$: *Three independent invariants.*

  In this case since $m_1 = m_{min}$ and $m_3 >> m_2 > m_1$, we simplify I_{12} and I_{13} as

$$\begin{aligned} I_{12} &= \kappa \sin(2\alpha - 2[\beta + \delta]) + \eta s_{13} s_{23}^2 \sin[\delta], \\ I_{13} &= \kappa \sin(2\alpha - 2[\beta + \delta]) - \eta s_{13} c_{23}^2 \sin[\delta], \end{aligned} \tag{2.44}$$

where the parameters κ and η are defined through the equations

$$\kappa = -c_{12}^2 c_{23}^2 c_{13}^6 m_2^3 m_3 s_{12}^4 s_{23}^2, \tag{2.45}$$

$$\eta = 2c_{12}c_{23}c_{13}^6 m_2^2 m_3^2 s_{12}^3 s_{23}. \tag{2.46}$$

Now from (2.44) we get

$$\begin{aligned} \sin(2\alpha - 2[\beta+\delta]) &= \left\{ \frac{c_{23}^2 I_{12} + s_{23}^2 I_{13}}{\kappa} \right\} \\ &= \Gamma. \end{aligned} \tag{2.47}$$

Again due to the hierarchical condition $m_3 >> m_2 > m_1$, I_{23} can be approximated as

$$\begin{aligned} I_{23} &\simeq m_3^3 c_{23} s_{23} B_1 \\ &= m_3^3 c_{23} s_{23} [\sin(2\alpha - 2[\beta+\delta]) c_{12}^2 c_{23} c_{13}^4 m_2 s_2 \\ &\quad - \sin 2(\beta+\delta) c_{23} c_{13}^4 m_1 s_{12}^2 s_{23}]. \end{aligned} \tag{2.48}$$

Inserting (2.47) in (2.48) we get

$$\beta + \delta = \frac{1}{2}\sin^{-1}\left\{ \frac{m_2}{m_1} ct_{12}^2 \Gamma - \frac{I_{23}}{m_3^3 m_1 c_{23}^2 s_{23}^2 s_{12}^2 c_{13}^6} \right\}, \tag{2.49}$$

where $ct_{12} \Rightarrow \cot\theta_{12}$.

It is now straight forward to calculate the other Majorana phase α from (2.47) and it comes out as

$$\alpha = \frac{\sin^{-1}\Gamma + 2(\beta+\delta)}{2}. \tag{2.50}$$

Case II: $m_2, m_3, \theta_{13} \neq 0$, $m_1 = 0$: *Two independent invariants.*

In this case neglecting terms like s_{13}^2 and $s_{13}(c_{23}^2 - s_{23}^2)$ in I_{23} only the Majorana phase difference $(\alpha - [\beta + \delta])$ is calculable and is given by

$$\alpha - [\beta + \delta] \ = \ \frac{1}{2} \sin^{-1} \left\{ \frac{I_{23} m_2^2 s_{12}^4}{-\kappa m_3^2} \right\} \tag{2.51}$$

along with an explicit relationship between the three invariants as

$$\frac{I_{23}}{c_{23}^2 I_{12} + s_{23}^2 I_{13}} \simeq -\frac{m_3^2}{m_2^2 \sin^4 \theta_{12}}. \tag{2.52}$$

Therefore, essentially we get two independent invariants corresponding to the Majorana phase difference and the Dirac CP phase.

Case III: $m_2, m_3 \neq 0$, m_1, $\theta_{13} = 0$: *One independent invariant.*

In such a condition the three invariants come out in a correlated manner as

$$\begin{aligned}
I_{12} &= \kappa \sin 2(\alpha - [\beta + \delta]) \\
&= -\sin 2(\alpha - [\beta + \delta]) c_{12}^2 c_{23}^2 s_{23}^2 c_{13}^6 s_{12}^4 m_2^3 m_3 \\
&= I_{13}, \\
I_{23} &= \sin 2(\alpha - [\beta + \delta]) c_{12}^2 c_{23}^2 s_{23}^2 c_{13}^6 m_2 m_3^3 \\
&= \left(-\frac{m_3^2}{m_2^2} s_{12}^{-4} \right) I_{12} \\
&= \left(-\frac{m_3^2}{m_2^2} s_{12}^{-4} \right) I_{13}.
\end{aligned} \tag{2.53}$$

In this case only independent invariant I_{12} is connected to the Majorana phase difference $(\alpha - [\beta + \delta])$.

- **Quasi-degenerate case**

Although in the present work we are not discussing the quasi-degenerate case which is relevant in the cosmological context [133], however, one can calculate the Majorana phases in a model independent way by directly solving the invariants as mentioned at the beginning of Sec.2.4. To be precise, using (2.20), (2.21) and (2.28) one can extract all the CP violating phases without any hierarchical assumption. However, the calculation is tedious and will be studied elsewhere. Another alternative way is to follow the calculations presented in Ref. [130] in which the phase convention is different. However, utilizing the phase convention presented in this work one can also calculate all the phases following the method presented in Ref. [130].

2.5 Numerical estimation

This section is devoted to the discussion on a numerical estimation of our methodology in a general context, taking all the available constraints from the oscillation data, sum of the the light neutrino masses and neutrino-less double beta decay and a proposed technique (within textbook yet) for the measurement of the Majorana phase.

- **Parametrization, diagonalization and the ranges of the Majorana phases**

  A general solution for a three generation complex symmetric Majorana mass matrix is given in Ref. [130]. In order to estimate the Majorana phases obtained in the present work we utilize the expressions of the three eigenvalues and the three mixing angles. Unlike the oscillation data presented in Chapter.1, here we use a data set, older a bit than the said one [31] and the upper limits on the sum of the neutrino masses ($\Sigma_i m_i (= m_1 + m_2 + m_3) < 0.23$ eV) [20] and the $\beta\beta_{0\nu}$ parameter ($|m_{11}| < 0.35$ eV) [25] to obtain model independent ranges of the Majorana phases. We consider a most general 3×3 complex symmetric neutrino mass matrix M_ν as

$$M_\nu = \begin{pmatrix} P & Q & R \\ Q & S & T \\ R & T & V \end{pmatrix} \tag{2.54}$$

with all parameter complex. M_ν can further be parametrized as

$$M_\nu = m_0 e^{i\alpha_m} \begin{pmatrix} 1 & xe^{i\alpha_x} & ye^{i\alpha_y} \\ xe^{i\alpha_x} & ze^{i\alpha_z} & we^{i\alpha_w} \\ ye^{i\alpha_y} & we^{i\alpha_w} & ve^{i\alpha_v} \end{pmatrix}, \tag{2.55}$$

where $P = m_0 e^{i\alpha_m}, Q/P = xe^{i\alpha_x}, R/P = ye^{i\alpha_y}, S/P = ze^{i\alpha_z}, T/P = we^{i\alpha_w}, V/P = ve^{i\alpha_v}$. We can now give a phase rotation to the matrix of (2.55) by a diagonal phase matrix $K = \text{diag}\,(e^{i\phi_1}, e^{i\phi_2}, e^{i\phi_3})$ as

$$M'_\nu = K^T M_\nu K \tag{2.56}$$

and consequently the rotated matrix comes out with 9 parameters as

$$M'_\nu = m_0 \begin{pmatrix} 1 & x & y \\ x & ze^{i\Omega_1} & we^{\Omega_2} \\ y & we^{i\Omega_2} & ve^{i\Omega_3} \end{pmatrix} \tag{2.57}$$

where $x,\ y,\ z,\ w$ are the real parameters and the other parameters are defined as

$$\Omega_1 = \alpha_z - 2\alpha_x, \Omega_2 = \alpha_w - \alpha_x - \alpha_y, \Omega_3 = \alpha_v - 2\alpha_y \tag{2.58}$$

and

$$\phi_1 = -\frac{\alpha_m}{2}, \phi_2 = -(\alpha_x - \frac{\alpha_m}{2}), \phi_3 = -(\alpha_y - \frac{\alpha_m}{2}). \tag{2.59}$$

Now using (2.11) we can explicitly calculate the rephasing invariants in terms of the elements of M'_ν. It is to be noted, that in the general case the number of parameters are 9 and we have only 7 experimental inputs. However, among the 9 parameters there are three angle parameters (Ω_1, Ω_2 and Ω_3). We set the values of these angle parameters in an arbitrary manner within the range $0-2\pi$ and vary the other parameters in a wide range to estimate the overall ranges of the Majorana phases which are depicted in Fig.2.1. We first constrain the rephasing invariants which in turn generate the correlated plot of the Majorana phases. The correlation between the phases are the consequences of (2.50) and (2.33) respectively.

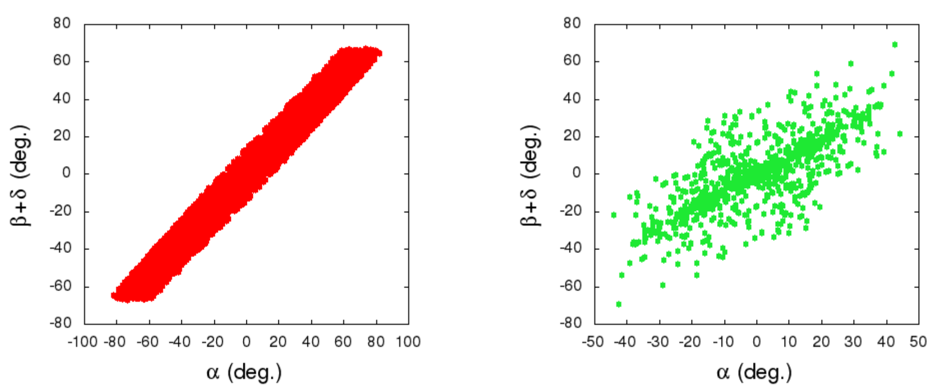

Figure 2.1: *Plots of the Majorana phases (α vs $\beta+\delta$) for normal (left) and inverted (right) hierarchies .*

Upon numerical estimation, the model independent ranges for α and $\beta+\delta$ come out as $-90^o < \alpha < 90^o$ and $-71^o < \beta+\delta < 71^o$ for normal hierarchy ($m_1 \neq 0$, $\theta_{13} \neq 0$) and $-45^o < \alpha < 45^o$, $-70^o < \beta+\delta < 70^0$ for inverted hierarchy

($m_3 \neq 0$, $\theta_{13} \neq 0$) and are shown explicitly in Fig.2.1. For $m_3 = 0$ case, the range of α is obtained as $-45^o < \alpha < 45^o$ and for the case $m_1 = 0$, the phase difference is constrained as $-82^o < \alpha - [\beta + \delta] < 82^o$. We also present the parameter ranges in Table 2.1.

Table 2.1: Parameter ranges for a phenomenologically viable M_ν.

Hierarchies ↓	$m_0 \times 10^3$	x	y	z	w	v
NH : $m_1 \neq 0$	$0.24 - 1.7$	$0.15 - 3.7$	$0.15 - 4.6$	$0.14 - 9.5$	$0.1 - 8.6$	$0.13 - 8.4$
NH : $m_1 = 0$	$0.2 - 1.2$	$0.1 - 3.2$	$0.14 - 4.7$	$0.09 - 7.5$	$0.09 - 8$	$0.11 - 8.1$
IH : $m_3 \neq 0$	$0.12 - 1.8$	$0.5 - 3.5$	$0.5 - 3.47$	$0.1 - 2.6$	$0 - 1.8$	$0 - .4$
IH : $m_3 = 0$	$0.11 - 1.4$	$0.1 - 3$	$0.2 - 3.4$	$0 - 2.4$	$0 - 1.7$	$0 - 2.4$

- **Connection to the physical observables and future of the Majorana phases**

  As previously mentioned, unlike the Dirac CP phase δ, the Majorana phases do not appear in the neutrino→neutrino oscillation. Therefore, a natural question arises how and where these phases can be measured. As a direct detection, in Ref. [24] Xing has suggested a thought experiment (neutrino→ antineutrino oscillation) in which it has been pointed out that these phases may appear in the probability expression of the favour oscillation and thus also in the expression of the CP asymmetry parameter $\mathcal{A}_{\alpha\beta}$ which is the measure of CP violation. However, this kind of experiment is purely academic at this moment and practically difficult to design as the oscillation probability is highly suppressed by the factor m_i^2/E^2, where m_i is the mass of the light neutrino and E is the beam energy. Now considering $E \sim$ MeV and the masses of the neutrinos to be less than 1 eV, one can calculate m_i^2/E^2 to be $\mathcal{O}(10^{-12})$. To improve m_i/E, a novel suggestion [24, 125] is to lower the value of E, however, in that case the estimated size of the base line length and the detector are beyond the reach of the present experimental facilities.

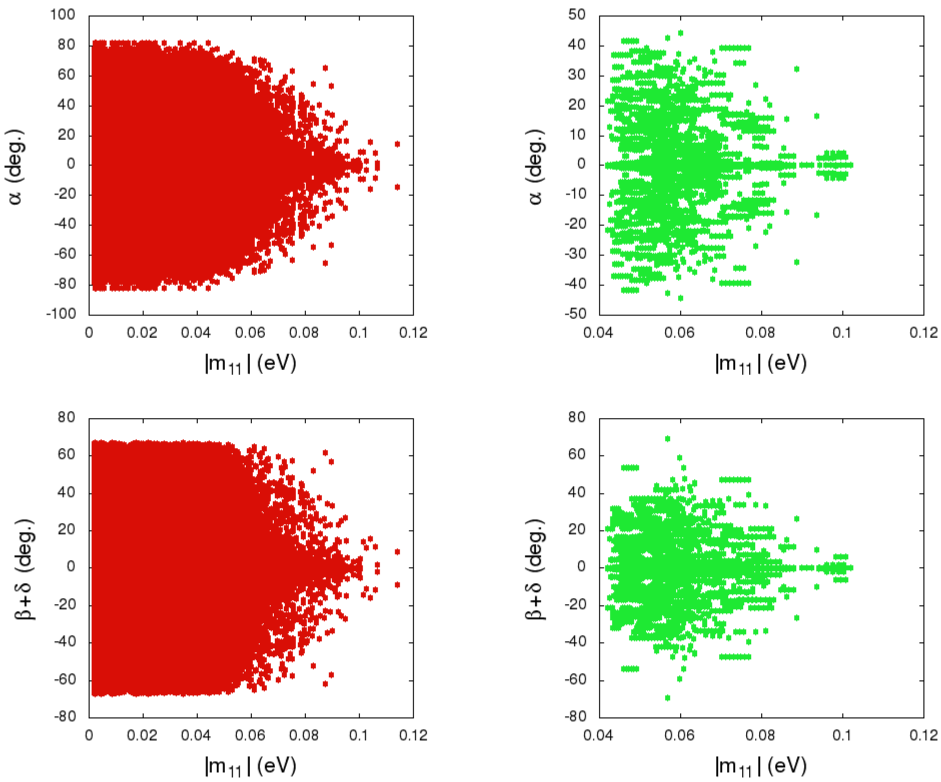

Figure 2.2: *Plots of the Majorana phases (α, $\beta+\delta$) vs $|m_{11}|$ for normal (left) and inverted (right) hierarchies for best fit values of Δm^2_{21}.*

But from an optimistic point of view we expect these kind of experiments will be designed in future and thus the prediction of the Majorana phases will be tested. Beside neutrino $\rightarrow$ antineutrino oscillation there are several LNV processes like $\beta\beta_{0\nu}$ decay, $\Delta^{++} \rightarrow l^+_\alpha l^+_\beta$ (in Type II seesaw model) [125] etc., which play a crucial role for the indirect measurement of the Majorana phases.

Now coming into our work, we present a table in the appendix which shows the ranges of the obtained Majorana phases for some typical values of $|m_{11}|$ and for convenience, in Fig.2.2 we present variation of the Majorana phases with $|m_{11}|$

for the best fit value of Δm_{21}^2 and taking all the other constraints in their 3σ ranges for both the hierarchies. We would like to mention that even if we take the 3σ range of Δm_{21}^2, over all ranges of the Majorana phases do not differ much, however, unlike the plots of Fig.2.2, the plots in that case become more wide for the larger values of $|m_{11}|$ (> 0.08 eV). Although, the present experimental upper bound on $|m_{11}|$ is 0.35 eV, NEXT will be able to bring down the value to 0.1 eV and thus the approximate ranges of the Majorana phases can be predicted.

Thus far we have estimated the Majorana phases in a general context. Latter, we apply the expressions obtained for α and $\beta + \delta$ for few testable flavor models (models with lesser number of parameters) as an application of the general result although our analysis is true for any hierarchical model of neutrino masses.

2.6 Some testable flavor models

The reason we discuss this section is to make certain whether the results obtained in the general case are consistent with the other models or not. Moreover, the models with certain flavor symmetries are highly predictive in nature. Therefore, precise measurement of the CP violating phases might act as an important tool to verify the testability of the flavor models [134]. In inverted hierarchy section we present a model with scaling ansatz and texture zeros within the framework of inverse seesaw through which all the sub cases presented in Sec.2.4 can be realized while in the normal hierarchy section we present a model with cyclic symmetry within the framework of Type-I seesaw. Obviously the choices are for illustration. One can also consider inverse or linear seesaw for normal hierarchy [135,136] and Type I seesaw for inverted hierarchy [137]. In principle one can use the technique in any hierarchical flavor models.

The above numerical results are obtained for the general M_ν where all the 9 independent parameters are present. However, as previously said, one can reduce the number of parameters by invoking some symmetry or ansatz in the Lagrangian which is more predictive in nature and thus testable in the experiments. In this section we provide applications of the general results in few typical cases for both the hierarchies, normal and inverted.

2.6.1 Normal hierarchy

In this case we explore a model that corresponds to **Case I** of the normal hierarchical scenario mentioned in Sec.(2.4). The model is based on cyclic symmetry on the left-chiral neutrino fields within the framework of Type-I seesaw mechanism. Inspired by the models of Harrison et. al. [138] and later Wolfenstein et. al. [139], we have taken advantage of this symmetry to reduce the number of parameters in the effective light neutrino mass matrix. In the fundamental level the symmetry exists in the neutrino sector of the Lagrangian and due to this symmetry a degeneracy in masses occurs removal of which therefore requires breaking of the symmetry. It is shown that a minimal breaking in the Majorana mass matrix is sufficient to fit the extant data. In this model the low energy broken symmetric Majorana type mass matrix $M_\nu(= -m_D M_R^{-1} m_D^T)$ originated from Type-I seesaw mechanism is given by $M_\nu =$

$$m_0 \begin{pmatrix} p^2e^{2i\alpha} + \frac{q^2e^{2i\beta}}{1+\frac{\epsilon_1}{m}} + \frac{1}{1+\frac{\epsilon_2}{m}} & pe^{i\alpha} + \frac{pqe^{i(\alpha+\beta)}}{1+\frac{\epsilon_1}{m}} + \frac{qe^{i\beta}}{1+\frac{\epsilon_2}{m}} & \frac{pe^{i\alpha}}{1+\frac{\epsilon_2}{m}} + pqe^{i(\alpha+\beta)} + \frac{qe^{i\beta}}{1+\frac{\epsilon_1}{m}} \\ pe^{i\alpha} + \frac{pqe^{i(\alpha+\beta)}}{1+\frac{\epsilon_1}{m}} + \frac{qe^{i\beta}}{1+\frac{\epsilon_2}{m}} & 1 + \frac{p^2e^{2i\alpha}}{1+\frac{\epsilon_1}{m}} + \frac{q^2e^{2i\beta}}{1+\frac{\epsilon_2}{m}} & \frac{pe^{i\alpha}}{1+\frac{\epsilon_1}{m}} + \frac{pqe^{i(\alpha+\beta)}}{1+\frac{\epsilon_2}{m}} + qe^{i\beta} \\ \frac{pe^{i\alpha}}{1+\frac{\epsilon_2}{m}} + pqe^{i(\alpha+\beta)} + \frac{qe^{i\beta}}{1+\frac{\epsilon_1}{m}} & \frac{pe^{i\alpha}}{1+\frac{\epsilon_1}{m}} + \frac{pqe^{i(\alpha+\beta)}}{1+\frac{\epsilon_2}{m}} + qe^{i\beta} & \frac{p^2e^{2i\alpha}}{1+\frac{\epsilon_2}{m}} + q^2e^{2i\beta} + \frac{1}{1+\frac{\epsilon_1}{m}} \end{pmatrix} \tag{2.60}$$

where

$$M_R = diag(m+\epsilon_1, m+\epsilon_2, m), \tag{2.61}$$

$$m_D = \begin{pmatrix} y_1 & y_2 & y_3 \\ y_3 & y_1 & y_2 \\ y_2 & y_3 & y_1 \end{pmatrix}. \tag{2.62}$$

Here ϵ_1 and ϵ_2 are the breaking parameters while the other parameters are defined as

$$m_0 = -\frac{y_3^2}{m}, pe^{i\alpha} = \frac{y_1}{y_3}, qe^{i\beta} = \frac{y_2}{y_3}. \tag{2.63}$$

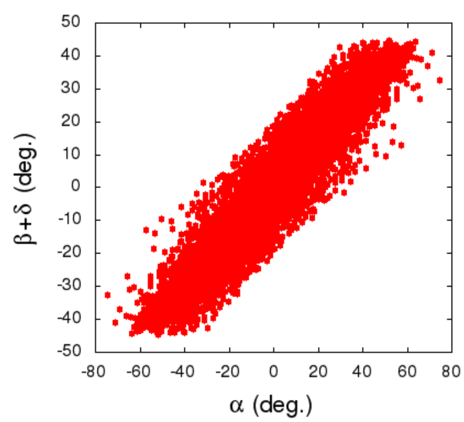

Figure 2.3: *Correlation of α vs $\beta + \delta$.*

For numerical analysis we choose the mass scale of M_R to be of the order of 10^{15} GeV and m_D to be at electroweak scale. Further redefining the breaking parameters as $\epsilon_1' = \frac{\epsilon_1}{m}$ and $\epsilon_2' = \frac{\epsilon_2}{m}$ we allow them to vary in between $-0.1 < \epsilon_1', \epsilon_2' < 0.1$ to keep the effect of symmetry breaking small. We then constrain the parameter space by taking into account the 3σ ranges of neutrino oscillation global fit data and explicitly

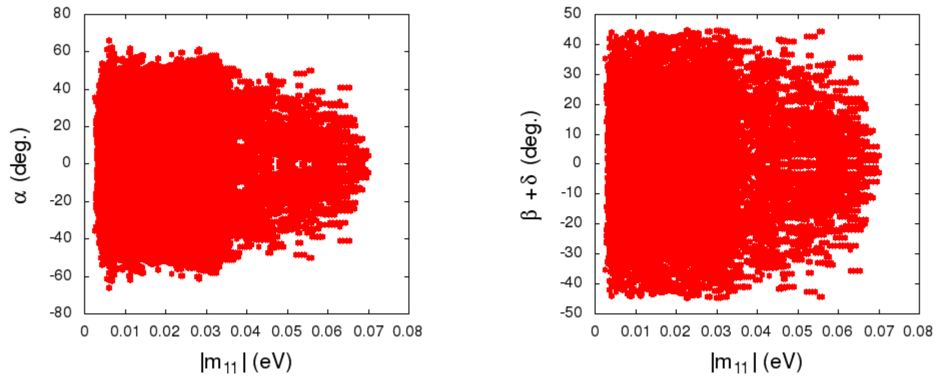

Figure 2.4: *Variation of α and $\beta+\delta$ with $|m_{11}|$ for cyclic symmetric case (normal hierarchy).*

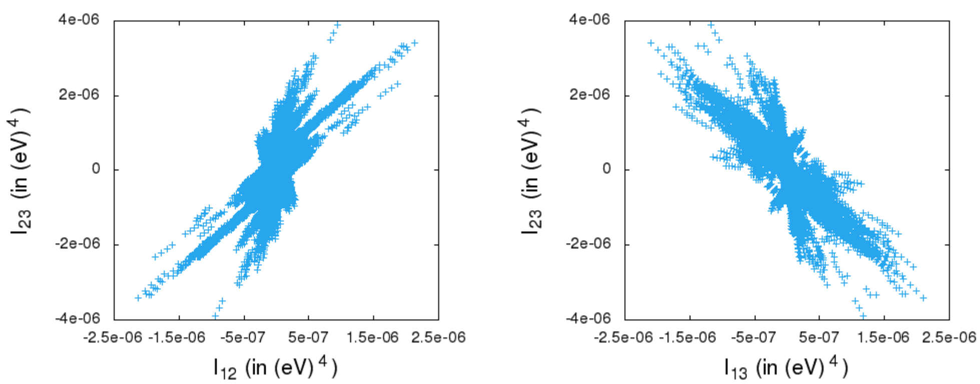

Figure 2.5: *Correlated plots of the rephasing invariants, I_{12} vs I_{23} (left) and I_{13} vs I_{23} (right).*

evaluate both the Majorana phases. From Fig.2.3 the ranges read as $-77.2^o < \alpha < 76.7^o$ and $-45.3^o < \beta+\delta < 45.5^o$. Note that the ranges of both the phases are embedded within the values obtained for the general case. Similar to the general case, in Fig.2.4 we also present the variation of the Majorana phases with the $\beta\beta_{0\nu}$ parameter. One can see the upper limit of $|m_{11}|$ is ~ 0.07 eV which is well within the reach of the future planned experiments.

Although the rephasing invariants are not physically measurable quantity, they are crucial for the computation of the CP violating phases. Since the model consists of lesser number of parameters, we also expect a significant correlation between the phase invariants which are depicted in Fig.2.5.

2.6.2 Inverted hierarchy

In this case, we explore a model based on scaling ansatz with inverse seesaw mechanism [69, 140–150] . In the next chapter we explore this model with much more detailed descriptions. In this mechanism M_ν is given by

$$M_\nu = m_D M_{RS}^{-1} \mu (m_D M_{RS}^{-1})^T, \tag{2.64}$$

where m_D is the usual Dirac type matrix and the other two matrices μ (Majorana type) and M_{RS} (Dirac type) arise due to the interaction between the additional singlet fermion and right handed neutrino considered in this type of seesaw mechanism. To further reduce the number of parameters texture zeros [136,137,151–176] are assumed in the constituent m_D and μ matrices. Scaling ansatz invariance dictates $m_3 = 0$ and $\theta_{13} = 0$ and this case corresponds to **Case III** of Sec.2.4. Thus to generate non zero θ_{13} breaking of the ansatz is necessary. Incorporating breaking in m_D through a small parameter ϵ, there are two different phenomenologically survived textures which are given by

$$M_\nu^1 = m_0 \begin{pmatrix} 1 & k_1 p & p \\ k_1 p & k_1^2(q^2 e^{i\theta} + p^2) & k_1(q^2 e^{i\theta} + p^2) \\ p & k_1(q^2 e^{i\theta} + p^2) & (q^2 e^{i\theta} + p^2) \end{pmatrix} + m_0 \epsilon \begin{pmatrix} 0 & 0 & 0 \\ 0 & 2k_1^2 q^2 e^{i\theta} & k_1 q^2 e^{i\theta} \\ 0 & k_1 q^2 e^{i\theta} & 0 \end{pmatrix} \tag{2.65}$$

and

$$M_\nu^2 = m_0 \begin{pmatrix} 1 & k_1(p+qe^{i\theta}) & p+qe^{i\theta} \\ k_1(p+qe^{i\theta}) & k_1^2(2pqe^{i\theta}+p^2) & k_1(2pqe^{i\theta}+p^2) \\ p+qe^{i\theta} & k_1(2pqe^{i\theta}+p^2) & (2pqe^{i\theta}+p^2) \end{pmatrix} + m_0\epsilon \begin{pmatrix} 0 & k_1qe^{i\theta} & 0 \\ k_1qe^{i\theta} & 2k_1^2pqe^{i\theta} & k_1pqe^{i\theta} \\ 0 & k_1pqe^{i\theta} & 0 \end{pmatrix}, \tag{2.66}$$

where all the parameters are complex [13]. In both the cases $\theta_{13} \neq 0$ however, $m_3 = 0$ due to singular nature of μ matrix and this case corresponds to **Case II** in the inverted hierarchy part of Sec.2.4. We further consider the most general version of the above case through the breaking of the ansatz in both m_D and μ matrices through two small parameters ϵ and ϵ' respectively and the neutrino mass matrix m_ν^3 comes out as

$$m_\nu^3 = m_0 \begin{pmatrix} 1 & k_1p & p \\ k_1p & k_1^2(q^2e^{i\theta}+p^2) & k_1(q^2e^{i\theta}+p^2) \\ p & k_1(q^2e^{i\theta}+p^2) & (q^2e^{i\theta}+p^2) \end{pmatrix} + m_0\epsilon \begin{pmatrix} 0 & 0 & 0 \\ 0 & 2k_1^2q^2e^{i\theta} & k_1q^2e^{i\theta} \\ 0 & k_1q^2e^{i\theta} & 0 \end{pmatrix} + m_0\epsilon' \begin{pmatrix} 0 & k_1p & p \\ k_1p & 0 & 0 \\ p & 0 & 0 \end{pmatrix} \tag{2.67}$$

In this case both θ_{13} and m_3 are nonzero and that corresponds to **Case I** (inverted) of Sec.2.4. Thus the whole inverted hierarchical sector is generated through the choice of the above model. Now, with explicit construction of the rephasing invariants we calculate the Majorana phases in each case. Interestingly, for all the cases, the value of J_{CP} comes out very small due to smallness of the Dirac CP phase δ, or more precisely, due to almost real nature of the mass matrices. Therefore, such typical nature of the mass matrices also constrain the Majorana phases approximately as $-1.2^o < \alpha < 0.8^o$ for the first two matrices (M_ν^1 and M_ν^2) and $-0.17^o < \alpha < 0.17^o$,$-1.5^o < \beta+\delta < 1.5^o$ for the matrix M_ν^3 along with an approximate range of $\beta\beta_{0\nu}$ decay parameter $|m_{11}|$ as 0.01 eV $< |m_{11}| <$ 0.0148 eV and 0.01 eV $< |m_{11}| <$ 0.0152 eV respectively.

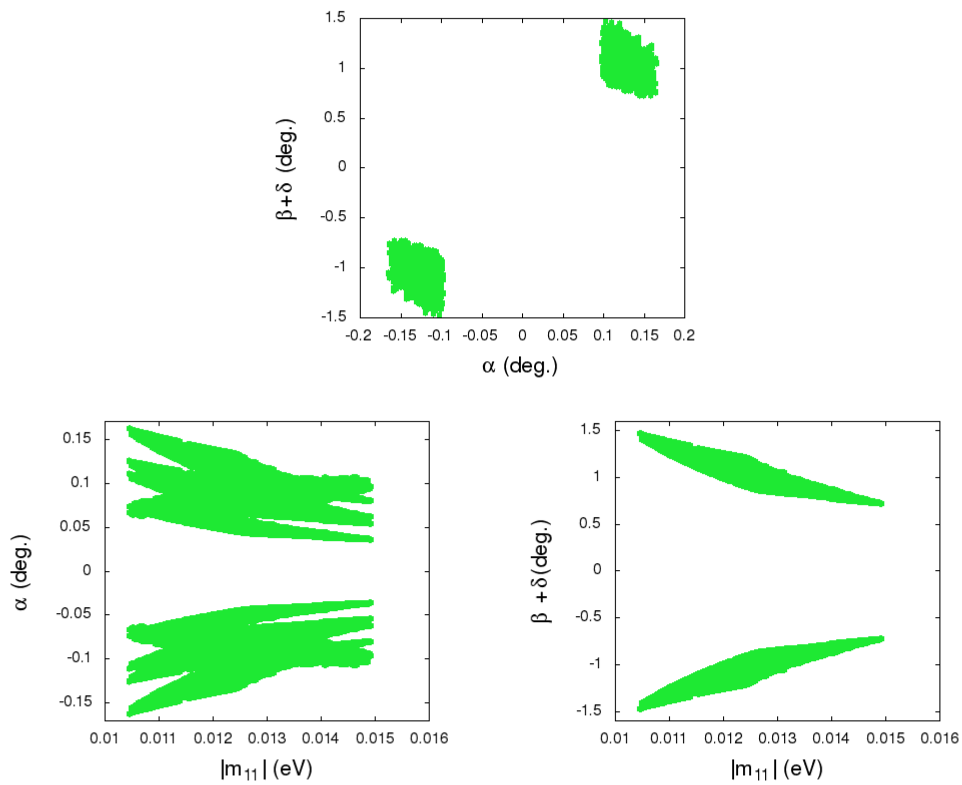

Figure 2.6: *Correlation plot of α vs $\beta+\delta$ (upper panel) and variation of α and $\beta+\delta$ with $|m_{11}|$ for inverted hierarchy : scaling ansatz case (lower panel).*

As an illustration, in Fig.2.6 we plot α and $\beta+\delta$ with $|m_{11}|$ for M_ν^3. For other two matrices (M_ν^1 and M_ν^2) the variation of α with $|m_{11}|$ is almost same as that of the extreme left plot of the lower panel of Fig.2.6. The model is highly predictive and hence, if significant CP violation is observed, the model will be ruled out. We plot the correlation between the invariants in Fig.2.7.

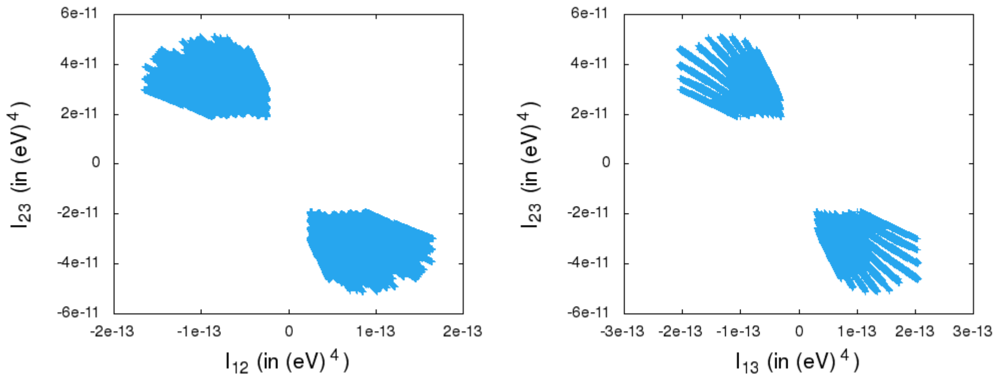

Figure 2.7: *Correlated plots of the rephasing invariants, I_{12} vs I_{23} (left) and I_{13} vs I_{23} (right).*

Table 2.2: *Summary of the numerical results.*

	General case		**Cyclic symmetry**	**Scaling ansatz**	
Hierarchies →	NH	IH	NH	IH	IH
Cases →	$m_1 \neq 0$ $\theta_{13} \neq 0$	$m_3 \neq 0$ $\theta_{13} \neq 0$	$m_1 \neq 0$ $\theta_{13} \neq 0$	$m_3 \neq 0$ $\theta_{13} \neq 0$	$m_3 = 0$ $\theta_{13} \neq 0$
α (deg.)	$-90 - 90$	$-45 - 45$	$-77.2 - 76.7$	$-0.17 - 0.17$	$-1.2 - 0.8$
$\beta + \delta$ (deg.)	$-71 - 71$	$-70 - 70$	$-45.3 - 45.5$	$-1.5 - 1.5$	*absent*

Finally, we summarize our results in Table 2.2 that shows the ranges of the Majorana phases for all the cases.

2.7 Summary

In this chapter we have presented a methodology for the evaluation of the Majorana phases of a general complex symmetric 3×3 neutrino mass matrix utilizing the three rephasing invariant quantities I_{12}, I_{13} and I_{23} proposed by Sarkar and Singh. Using Mohapatra-Rodejohann's phase convention, we explore both the hierarchical structures of the light neutrinos. Motivation behind the usage of the invariants to calculate the Majorana phases is that such a methodology enables us to evaluate the existing Majorana phase even if one of the eigenvalue (m_3) is zero in a model independent way. However, if $m_1 = 0$, this methodology only enables us to calculate the difference between the Majorana phases. Following the presentation of the generalized prescription, we have further estimated the maximal allowed ranges of the Majorana phases in a general context for both the hierarchical structures of the light neutrinos and have shown that our methodology is applicable for any model except the case of quasi degeneracy in light neutrino masses. We have also studied the connection of the Majorana phases with physical observables like $\beta\beta_{0\nu}$ decay parameter $|m_{11}|$ and the branching ratios of charged Higgs (Δ^{++}) decay where these phases appear. As a direct measurement of the Majorana phases we have given the example of neutrino$\rightarrow$ antineutrino oscillation which is a thought experiment right now, however, well studied in the literature. After discussing the general case we have further exemplified our methodology in two testable models (models with lesser number of parameters) leading to a normal and an inverted hierarchy respectively. For a normal hierarchical case, we have given an example of a model based on cyclic symmetry with Type-I seesaw mechanism. We have then estimated the Majorana phases for the broken symmetric case, since cyclic symmetry dictates a degeneracy in the mass eigenvalues. As an example of inverted hierarchy, we have cited a model comprised of scaling ansatz, texture zeros and inverse seesaw mechanism. It has been observed that all the sub cases belonging to inverted hierarchy (Sec.2.4) can be tested depending upon the scheme of incorporation of ansatz breaking mechanism while a phenomenologically viable sub case ($m_1 = 0$) of the normal hierarchy is yet to be established through the choice of a suitable model.

Chapter 3

Scaling ansatz, Cyclic symmetry and texture zeros in inverse seesaw

3.1 Introduction

Among the variants of the seesaw mechanism, inverse seesaw [69, 71, 135, 140–143, 147–150, 177, 178] stands out as an attractive one due to its characteristic feature of generation of small neutrino mass without invoking high energy scale in the theory. Although to realize such feature one has to pay the price in terms of incorporation of additional singlet fermions, nevertheless, in different GUT models accommodation of such type of neutral fermions are natural. Furthermore, such mechanism appeals to the foreseeable collider experiments to be testified due to its unique signature. The 9×9 neutrino mass matrix in this mechanism is written as

$$M_\nu = \begin{pmatrix} 0 & m_D & 0 \\ m_D^T & 0 & M_{RS} \\ 0 & M_{RS}^T & \mu \end{pmatrix} \tag{3.1}$$

with the choice of basis (ν_L, ν_R^c, S_L). The three matrices appear in M_ν are m_D, M_{RS} and μ among them m_D and M_{RS} are Dirac type whereas μ is Majorana type mass matrix. After diagonalization, the low energy effective neutrino mass comes out as

$$\begin{aligned} M_\nu &= m_D M_{RS}^{-1} \mu (m_D M_{RS}^{-1})^T \\ &= F \mu F^T \end{aligned} \tag{3.2}$$

where $F = m_D M_{RS}^{-1}$. Such definition resembles the above formula as a conventional type-I seesaw expression of M_ν. However, this general m_ν contains large number of parameters and it is possible to fit them with neutrino oscillation experimental data [31,179,180] (but the predictability is less). Our goal in this work is to find out a phenomenologically viable texture of m_D and μ with minimum number of parameters or equivalently maximum number of zeros. We bring together two theoretical ideas to find out a minimal texture and they are

i) Scaling ansatz [137,151–155,181,182],

ii) Texture Zeros [4,156,157,159,164–171,173].

At the outset of the analysis, we choose a basis where the charged lepton mass matrix (m_E) and M_{RS} are diagonal along with texture zeros in m_D and μ matrices. We also start by assuming the scaling property in the elements of m_D and μ to reduce the number of relevant matrices. Although, we are not addressing the explicit origin of such choice of matrices, however, qualitatively we can assume that this can be achieved due to some flavour symmetry [183] which is required to make certain that the texture zeros appear in m_D and μ are in the same basis in which m_E and M_{RS} are diagonal. We restrict ourselves within the frame work of $SU(2)_L \times U(1)_Y$ gauge group however, explicit realization of such scheme obviously more elusive which will be studied elsewhere.

3.2 Scaling property and texture zeros

We consider scaling property between the second and third row of m_D matrix and the same for μ matrix also. Explicitly the relationships are written as

$$\frac{(m_D)_{2i}}{(m_D)_{3i}} = k_1, \tag{3.3}$$

$$\frac{(\mu)_{2i}}{(\mu)_{3i}} = k_2, \tag{3.4}$$

where $i = 1, 2, 3$ is the column index. We would like to mention that although we have considered different scale factors for m_D and μ matrices, however, the effective M_ν is still scale invariant and leads to $\theta_{13} = 0$. Thus, it is obvious to further break the scaling ansatz. In order to generate nonzero θ_{13} it is necessary to break the ansatz in m_D since, breaking in μ does not affect the generation of nonzero θ_{13} although in some cases it provides $m_3 \neq 0$. In our scheme texture zero format is robust and it remains intact while the scaling ansatz is explicitly broken. Such a scenario can be realized by considering the scaling ansatz and texture zeros to have a different origin.

Another point is to be noted that, since the μ matrix is complex symmetric whereas m_D is asymmetric, the scale factor considered in μ matrix is different from that of m_D to keep the row wise invariance as dictated by (3.3) (for m_D), and (3.4) (for μ). Finally, since the texture of M_{RS} matrix is diagonal it is not possible to accommodate row wise scaling ansatz.

Let us further constrain the matrices assuming texture zeros in different entries. Since, in our present scheme the matrix M_{RS} is diagonal, we constrain the other two matrices. We start with the maximal zero textures with scaling ansatz of general 3×3 matrices and list different cases systematically in Table 3.1.

Table 3.1: Texture zeros with scaling ansatz of a general 3×3 matrix

7 zero texture		
$m_1^7 = \begin{pmatrix} 0 & 0 & 0 \\ k_1c_1 & 0 & 0 \\ c_1 & 0 & 0 \end{pmatrix}$	$m_2^7 = \begin{pmatrix} 0 & 0 & 0 \\ 0 & k_1c_2 & 0 \\ 0 & c_2 & 0 \end{pmatrix}$	$m_3^7 = \begin{pmatrix} 0 & 0 & 0 \\ 0 & 0 & k_1c_3 \\ 0 & 0 & c_3 \end{pmatrix}$
6 zero texture		
$m_1^6 = \begin{pmatrix} d_1 & 0 & 0 \\ k_1c_1 & 0 & 0 \\ c_1 & 0 & 0 \end{pmatrix}$	$m_2^6 = \begin{pmatrix} 0 & d_2 & 0 \\ k_1c_1 & 0 & 0 \\ c_1 & 0 & 0 \end{pmatrix}$	$m_3^6 = \begin{pmatrix} 0 & 0 & d_3 \\ k_1c_1 & 0 & 0 \\ c_1 & 0 & 0 \end{pmatrix}$
$m_4^6 = \begin{pmatrix} d_1 & 0 & 0 \\ 0 & k_1c_2 & 0 \\ 0 & c_2 & 0 \end{pmatrix}$	$m_5^6 = \begin{pmatrix} 0 & d_2 & 0 \\ 0 & k_1c_2 & 0 \\ 0 & c_2 & 0 \end{pmatrix}$	$m_6^6 = \begin{pmatrix} 0 & 0 & d_3 \\ 0 & k_1c_2 & 0 \\ 0 & c_2 & 0 \end{pmatrix}$
$m_7^6 = \begin{pmatrix} d_1 & 0 & 0 \\ 0 & 0 & k_1c_3 \\ 0 & 0 & c_3 \end{pmatrix}$	$m_8^6 = \begin{pmatrix} 0 & d_2 & 0 \\ 0 & 0 & k_1c_3 \\ 0 & 0 & c_3 \end{pmatrix}$	$m_9^6 = \begin{pmatrix} 0 & 0 & d_3 \\ 0 & 0 & k_1c_3 \\ 0 & 0 & c_3 \end{pmatrix}$
5 zero texture		
$m_1^5 = \begin{pmatrix} 0 & 0 & 0 \\ k_1c_1 & k_1c_2 & 0 \\ c_1 & c_2 & 0 \end{pmatrix}$	$m_2^5 = \begin{pmatrix} 0 & 0 & 0 \\ k_1c_1 & 0 & k_1c_3 \\ c_1 & 0 & c_3 \end{pmatrix}$	$m_3^5 = \begin{pmatrix} 0 & 0 & 0 \\ 0 & k_1c_1 & k_1c_3 \\ 0 & c_1 & c_3 \end{pmatrix}$
$m_4^5 = \begin{pmatrix} d_1 & d_2 & 0 \\ k_1c_1 & 0 & 0 \\ c_1 & 0 & 0 \end{pmatrix}$	$m_5^5 = \begin{pmatrix} 0 & d_2 & d_3 \\ k_1c_1 & 0 & 0 \\ c_1 & 0 & 0 \end{pmatrix}$	$m_6^5 = \begin{pmatrix} d_1 & 0 & d_3 \\ k_1c_1 & 0 & 0 \\ c_1 & 0 & 0 \end{pmatrix}$
$m_7^5 = \begin{pmatrix} d_1 & d_2 & 0 \\ 0 & k_1c_2 & 0 \\ 0 & c_2 & 0 \end{pmatrix}$	$m_8^5 = \begin{pmatrix} 0 & d_2 & d_3 \\ 0 & k_1c_2 & 0 \\ 0 & c_2 & 0 \end{pmatrix}$	$m_9^5 = \begin{pmatrix} d_1 & 0 & d_3 \\ 0 & k_1c_2 & 0 \\ 0 & c_2 & 0 \end{pmatrix}$

$m^5_{10} = \begin{pmatrix} d_1 & d_2 & 0 \\ 0 & 0 & k_1c_3 \\ 0 & 0 & c_3 \end{pmatrix}$	$m^5_{11} = \begin{pmatrix} 0 & d_2 & d_3 \\ 0 & 0 & k_1c_3 \\ 0 & 0 & c_3 \end{pmatrix}$	$m^5_{12} = \begin{pmatrix} d_1 & 0 & d_3 \\ 0 & 0 & k_1c_3 \\ 0 & 0 & c_3 \end{pmatrix}$
4 **zero texture**		
$m^4_1 = \begin{pmatrix} d_1 & 0 & 0 \\ 0 & k_1c_2 & k_1c_3 \\ 0 & c_2 & c_3 \end{pmatrix}$	$m^4_2 = \begin{pmatrix} 0 & d_2 & 0 \\ 0 & k_1c_2 & k_1c_3 \\ 0 & c_2 & c_3 \end{pmatrix}$	$m^4_3 = \begin{pmatrix} 0 & 0 & d_3 \\ 0 & k_1c_2 & k_1c_3 \\ 0 & c_2 & c_3 \end{pmatrix}$
$m^4_4 = \begin{pmatrix} d_1 & 0 & 0 \\ k_1c_1 & 0 & k_1c_3 \\ c_1 & 0 & c_3 \end{pmatrix}$	$m^4_5 = \begin{pmatrix} 0 & d_2 & 0 \\ k_1c_1 & 0 & k_1c_3 \\ c_1 & 0 & c_3 \end{pmatrix}$	$m^4_6 = \begin{pmatrix} 0 & 0 & d_3 \\ k_1c_1 & 0 & k_1c_3 \\ c_1 & 0 & c_3 \end{pmatrix}$
$m^4_7 = \begin{pmatrix} d_1 & 0 & 0 \\ k_1c_1 & k_1c_2 & 0 \\ c_1 & c_2 & 0 \end{pmatrix}$	$m^4_8 = \begin{pmatrix} 0 & d_2 & 0 \\ k_1c_1 & k_1c_2 & 0 \\ c_1 & c_2 & 0 \end{pmatrix}$	$m^4_9 = \begin{pmatrix} 0 & 0 & d_3 \\ k_1c_1 & k_1c_2 & 0 \\ c_1 & c_2 & 0 \end{pmatrix}$
$m^4_{10} = \begin{pmatrix} d_1 & d_2 & d_3 \\ k_1c_1 & 0 & 0 \\ c_1 & 0 & 0 \end{pmatrix}$	$m^4_{11} = \begin{pmatrix} d_1 & d_2 & d_3 \\ 0 & k_1c_2 & 0 \\ 0 & c_2 & 0 \end{pmatrix}$	$m^4_{12} = \begin{pmatrix} d_1 & d_2 & d_3 \\ 0 & 0 & k_1c_3 \\ 0 & 0 & c_3 \end{pmatrix}$

We consider all the matrices[1] listed in Table 3.1 as the Dirac type matrices(m_D). As the lepton number violating mass matrix μ is complex symmetric, therefore, the maximal number of zeros with scaling invariance is 5. Therefore, only m^5_3 and m^5_5 type matrices can be made complex symmetric with the scaling property and are shown in Table 3.2 where they are renamed as μ^5_1 and μ^5_2 with a different scale factor k_2. Now using (3.2) we can construct M_ν and it is found that all the mass matrices constructed out of these matrices are not suitable to satisfy the neutrino oscillation data. The reason goes as follows:

[1]From now on we use m^n as a mass matrix where $n(= 4, 5, 6, 7)$ is the number of zeros in that matrix.

Table 3.2: Maximal zero texture of μ matrix

$\mu_1^5 = \begin{pmatrix} 0 & 0 & 0 \\ 0 & k_2^2 s_3 & k_2 s_3 \\ 0 & k_2 s_3 & s_3 \end{pmatrix}$	$\mu_2^5 = \begin{pmatrix} 0 & k_2 s_3 & s_3 \\ k_2 s_3 & 0 & 0 \\ s_3 & 0 & 0 \end{pmatrix}$

Case A: m_D (7, 6 zero) + μ_1^5, μ_2^5 (5 zero):

We can not generate nonzero θ_{13} by breaking the scaling ansatz because in this case all the structures of m_D are scaling ansatz invariant. This can be understood in the following way: if we incorporate scaling ansatz breaking by $k_1' \to k_1(1+\epsilon)$ all the structures of m_D are still invariant and M_ν matrix will still give $\theta_{13} = 0$ as breaking of scaling in μ_1^5 and μ_2^5 plays no role for the generation of nonzero value of θ_{13}. To generate nonzero θ_{13} it is necessary to break scaling ansatz in the Dirac sector.

Case B: m_D (5 zero) + μ_1^5, μ_2^5 (5 zero):

The matrices in the last three rows (m_4^5 to m_{12}^5) of the '5 zero texture' part of Table 3.1 are ruled out due to the same reason as mentioned in **Case A** while, the matrices in the first row i.e. m_1^5, m_2^5 and m_3^5 give rise to the structure of M_ν as

$$A_1 = \begin{pmatrix} 0 & 0 & 0 \\ 0 & * & * \\ 0 & * & * \end{pmatrix} \tag{3.5}$$

where '$*$' represents some nonzero entries in M_ν. This structure leads to complete disappearance of one generation. Moreover it has been shown in Ref. [156] that if the number of independent zeros in an effective neutrino mass matrix (M_ν) is ≥ 3 it doesn't favour the oscillation data and hence, 'A_1' type mass matrix is ruled out.

Case C: m_D (4 zero) + μ_1^5 (5 zero):

There are 12 m_D matrices with 4 zero texture and they are designated as m_1^4,...m_{12}^4 in

Table 3.1. Due to the same reason as discussed in **Case A**, m^4_{10}, m^4_{11} and m^4_{12} are not considered. Furthermore, M_ν arises through m^4_1, m^4_4 and m^4_7 also correspond to the 'A_1' type matrix (shown in (3.5)) and hence are also discarded. Finally, remaining six m_D matrices m^4_2, m^4_3, m^4_5, m^4_6, m^4_8 and m^4_9 lead to the structure of M_ν with two zero eigenvalues.

Case D: m_D (4 zero) + μ^5_2 (5 zero):

In this case, for m^4_2 and m^4_3 the low energy mass matrix M_ν comes out as a null matrix while for m^4_1 the structure of M_ν is given by

$$A_2 = \begin{pmatrix} 0 & * & * \\ * & 0 & 0 \\ * & 0 & 0 \end{pmatrix} \tag{3.6}$$

which is also neglected since the number of independent zeros ≥ 3.

On the other hand rest of the m_D matrices (m^4_4 to m^4_9) correspond to the structure of M_ν as

$$A_3 = \begin{pmatrix} 0 & * & * \\ * & * & * \\ * & * & * \end{pmatrix}. \tag{3.7}$$

Interestingly, a priori we cannot rule out the matrices of type A_3, however it is observed that M_ν of this type fails to generate θ_{13} within the present experimental bound (details are mentioned in section (3.6.2)). It is also observed that in this scheme to generate viable neutrino oscillation data, four zero texture of both m_D and μ matrices are necessary. Therefore, let's now discuss extensively the 4 zero texture in both the matrices, m_D and μ.

3.3 4 zero texture

There are 126 ways to choose 4 zeros out of 9 elements of a general 3×3 matrix. Hence there are 126 textures. Incorporation of scaling ansatz leads to a drastic reduction to only 12 textures as given in the Table 3.1. In our chosen basis since M_{RS} is taken as diagonal, therefore, the structure of m_D leads to the same structure of F. On the other hand the lepton number violating mass matrix μ is complex symmetric and therefore from the matrices listed in Table 3.1, only m_1^4 and m_{10}^4 type matrices are acceptable. We renamed those matrices as μ_1^4 and μ_2^4 and explicit structures of them are presented in Table 3.3.

Table 3.3: Four zero texture of μ matrix

$\mu_1^4 = \begin{pmatrix} r_1 & 0 & 0 \\ 0 & k_2^2 s_3 & k_2 s_3 \\ 0 & k_2 s_3 & s_3 \end{pmatrix}$	$\mu_2^4 = \begin{pmatrix} r_1 & k_2 s_3 & s_3 \\ k_2 s_3 & 0 & 0 \\ s_3 & 0 & 0 \end{pmatrix}$

There are now $2 \times 12 = 24$ types of M_ν due to both the choices of μ matrices. We discriminate different types of m_D matrices in the following way:

i) First of all, the texture m_{10}^4, m_{11}^4 and m_{12}^4 are always scaling ansatz invariant due to the same reason mentioned earlier in **Case A** and hence are all discarded.

Next the matrices m_1^4, m_2^4 and m_3^4 are also ruled out due to the following:

a) When μ_1^4 matrix is taken to generate M_ν along with m_1^4, m_2^4 and m_3^4 as the Dirac matrices, then the structure of the effective M_ν appears such that, one generation is completely decoupled thus leading to two mixing angles zero for the matrix m_1^4 and two zero eigenvalues in addition, when we consider m_2^4 and m_3^4 matrices.

b) In case of μ_2^4 matrix, the form of M_ν for m_1^4 comes out as

$$A_4 = \begin{pmatrix} * & * & * \\ * & 0 & 0 \\ * & 0 & 0 \end{pmatrix} \tag{3.8}$$

which is phenomenologically ruled out. For other two matrices (m_2^4 and m_3^4), M_ν becomes a null matrix. For a compact view of the above analysis we present the ruled out and survived structures of M_ν symbolically in Table 3.4.

Table 3.4: Compositions of the discarded and survived structures of M_ν

	m_D											
μ	m_1^4	m_2^4	m_3^4	m_4^4	m_5^4	m_6^4	m_7^4	m_8^4	m_9^4	m_{10}^4	m_{11}^4	m_{12}^4
μ_1^4	×	×	×	✓	✓	✓	✓	✓	✓	×	×	×
μ_2^4	×	×	×	✓	✓	✓	✓	✓	✓	×	×	×

Thus we are left with same six textures of m_D for both the choices of μ and they are renamed in Table 3.5 as m_{D1}^4, m_{D2}^4, ... $m_{D_6}^4$. It is clear that the above analysis leads

Table 3.5: Four zero textures of the Dirac mass matrices

$m_{D1}^4 = \begin{pmatrix} d_1 & 0 & 0 \\ k_1c_1 & 0 & k_1c_3 \\ c_1 & 0 & c_3 \end{pmatrix}$	$m_{D2}^4 = \begin{pmatrix} 0 & d_2 & 0 \\ k_1c_1 & 0 & k_1c_3 \\ c_1 & 0 & c_3 \end{pmatrix}$	$m_{D3}^4 = \begin{pmatrix} 0 & 0 & d_3 \\ k_1c_1 & 0 & k_1c_3 \\ c_1 & 0 & c_3 \end{pmatrix}$
$m_{D4}^4 = \begin{pmatrix} d_1 & 0 & 0 \\ k_1c_1 & k_1c_2 & 0 \\ c_1 & c_2 & 0 \end{pmatrix}$	$m_{D5}^4 = \begin{pmatrix} 0 & d_2 & 0 \\ k_1c_1 & k_1c_2 & 0 \\ c_1 & c_2 & 0 \end{pmatrix}$	$m_{D6}^4 = \begin{pmatrix} 0 & 0 & d_3 \\ k_1c_1 & k_1c_2 & 0 \\ c_1 & c_2 & 0 \end{pmatrix}$

to altogether 12 effective M_ν matrices arising due to six m_D (m_{D1}^4 to m_{D6}^4) and two μ (μ_1^4 and μ_2^4) matrices.

3.4 Parametrization

Depending upon the composition of m_D and μ we subdivide those 12 M_ν matrices in four broad categories and each category is again separated in few cases and the decomposition is presented in Table 3.6 and Table 3.7.

Table 3.6: Different composition of m_D and μ_1 matrices to generate M_ν.

	Category A		**Category B**			
Matrices	I_A	II_A	I_B	II_B	III_B	IV_B
m_D	m_{D2}^4	m_{D6}^4	m_{D1}^4	m_{D3}^4	m_{D4}^4	m_{D5}^4
μ	μ_1^4	μ_1^4	μ_1^4	μ_1^4	μ_1^4	μ_1^4

Table 3.7: Different composition of m_D and μ_2 matrices to generate M_ν.

	Category C		**Category D**			
Matrices	I_C	II_C	I_D	II_D	III_D	IV_D
m_D	m_{D1}^4	m_{D4}^4	m_{D2}^4	m_{D3}^4	m_{D5}^4	m_{D6}^4
μ	μ_2^4	μ_2^4	μ_2^4	μ_2^4	μ_2^4	μ_2^4

Throughout our analysis we consider M_{RS} to be diagonal and is form $M_{RS} =$ diag (p_1, p_2, p_3). Following (3.2), the M_ν matrix arises in Category A and Category B can be written in a generic way as

$$M_\nu^{AB} = m_0 \begin{pmatrix} 1 & k_1 p & p \\ k_1 p & k_1^2(q^2+p^2) & k_1(q^2+p^2) \\ p & k_1(q^2+p^2) & (q^2+p^2) \end{pmatrix} \tag{3.9}$$

with the definition of parameters as following

$$\begin{aligned}
Set\ I_A : m_0' &= \frac{d_3^2 s_3}{p_3^2}, p' = \frac{p_3 c_2}{p_2 d_3}, q' = \frac{c_1 p_3}{d_3 p_1}\sqrt{\frac{r_1}{s_3}}, m_0 = m_0', p = k_2 p', q = q', \\
Set\ II_A : m_0' &= \frac{d_2^2 s_3}{p_2^2}, p' = \frac{p_2 c_2}{p_3 d_2}, q' = \frac{c_1 p_2}{d_2 p_1}\sqrt{\frac{r_1}{s_1}}, m_0 = m_0' k_2^2, p = \frac{p'}{k_2}, q = \frac{q'}{k_2}, \\
Set\ I_B : m_0' &= \frac{d_1^2 r_1}{p_1^2}, p' = \frac{c_1}{d_1}, q' = \frac{c_3 p_1}{d_1 p_3}\sqrt{\frac{s_3}{r_1}}, m_0 = m_0', p = p', q = q', \\
Set\ II_B : m_0' &= \frac{d_3^2 s_3}{p_3^2}, p' = \frac{c_3}{d_3}, q' = \frac{c_1 p_3}{d_3 p_1}\sqrt{\frac{r_1}{s_1}}, m_0 = m_0', p = p', q = q', \\
Set\ III_B : m_0' &= \frac{d_1^2 r_1}{p_1^2}, p' = \frac{c_1}{d_1}, q' = \frac{c_2 p_1}{d_1 p_2}\sqrt{\frac{s_3}{r_1}}, m_0 = m_0', p = p', q = k_2 q', \\
Set\ IV_B : m_0' &= \frac{d_2^2 s_3}{p_2^2}, p' = \frac{c_2}{d_2}, q' = \frac{c_1 p_2}{d_2 p_1}\sqrt{\frac{r_1}{s_1}}, m_0 = m_0' k_2^2, p = p', q = \frac{q'}{k_2}.
\end{aligned} \tag{3.10}$$

Similarly the M_ν matrix arises in Category C can be written as

$$M_\nu^C = m_0 \begin{pmatrix} 1 & k_1(p+q) & p+q \\ k_1(p+q) & k_1^2(2pq+p^2) & k_1(2pq+p^2) \\ p+q & k_1(2pq+p^2) & (2pq+p^2) \end{pmatrix} \tag{3.11}$$

with the following choice of parameters

$$\begin{aligned}
Set\ I_C : m_0' &= \frac{d_1^2 r_1}{p_1^2}, p' = \frac{c_1}{d_1}, q' = \frac{c_2 p_1}{d_1 p_2}\sqrt{\frac{s_3}{r_1}}, m_0 = m_0', p = p', q = k_2 q', \\
Set\ II_C : m_0' &= \frac{d_1^2 r_1}{p_1^2}, p' = \frac{c_1}{d_1}, q' = \frac{c_3 p_1}{d_1 p_3}\sqrt{\frac{s_3}{r_1}}, m_0 = m_0', p = p', q = q'.
\end{aligned} \tag{3.12}$$

For the Category D, the effective M_ν comes out as

$$M_\nu^D = m_0 \begin{pmatrix} 0 & k_1 p & p \\ k_1 p & k_1^2(q^2+2rp) & k_1(q^2+2rp) \\ p & k_1(q^2+2rp) & (q^2+2rp) \end{pmatrix} \tag{3.13}$$

with the definition of parameters as

$$
\begin{aligned}
Set\ I_D : m_0' &= \frac{d_2^2 r_1}{p_1^2}, p' = \frac{c_1 p_1 s_3}{d_2 p_2 r_1}, q' = \frac{c_1}{d_2}, r' = \frac{c_3}{d_2}, m_0 = m_0', p = k_2 p', q = q', r = r',\\
Set\ II_D : m_0' &= \frac{d_3^2 r_1}{p_1^2}, p' = \frac{c_1 p_1 s_3}{d_3 p_3 r_1}, q' = \frac{c_1}{d_3}, r' = \frac{c_2}{d_3}, m_0 = m_0', p = p', q = q' r = k_2 r',\\
Set\ III_D : m_0' &= \frac{c_1 p_1 s_3}{d_3 p_3 r_1}, p' = \frac{c_1}{d_1}, q' = \frac{c_1}{d_3}, r' = \frac{c_3}{d_3}, m_0 = m_0', p = p', q = k_2 q', r = r',\\
Set\ IV_D : m_0' &= \frac{d_2^2 r_1}{p_1^2}, p' = \frac{c_1 p_1 s_3}{d_2 p_2 r_1}, q' = \frac{c_1}{d_2}, r' = \frac{c_2}{d_2}, m_0 = m_0', p = k_2 p', q = q', r = r'.
\end{aligned}
\tag{3.14}
$$

Here we consider all the parameters m_0, k_1, p, r and q are complex.

3.5 Phase Rotation

As mentioned earlier, all the parameters of M_ν are complex and therefore we can rephase M_ν by a phase rotation to remove the redundant phases. Here, we systematically study the phase rotation for each category.

- **Category A,B**

  The Majorana type mass matrix M_ν can be rotated in phase space through

$$M_\nu'^{AB} = P^T M_\nu^{AB} P, \tag{3.15}$$

  where P is a diagonal phase matrix and is given by $P = diag(e^{i\Phi_1}, e^{i\Phi_2}, e^{i\Phi_3})$. Now redefining the parameters of M_ν as $m_0 \rightarrow m_0 e^{i\alpha_m}, p \rightarrow p e^{i\theta_p}, q \rightarrow q e^{i\theta_q}, k_1 \rightarrow k_1 e^{i\theta_1}$ and choosing the phases of P as $\Phi_1 = -\frac{\alpha_m}{2}, \Phi_2 = -(\theta_1 + \theta_p + \frac{\alpha_m}{2}), \Phi_3 = -(\theta_p + \frac{\alpha_m}{2})$ the phase rotated Effective neutrino mass matrix appears as

$$M_\nu'^{AB} = m_0 \begin{pmatrix} 1 & k_1 p & p \\ k_1 p & k_1^2(q^2 e^{i\theta} + p^2) & k_1(q^2 e^{i\theta} + p^2) \\ p & k_1(q^2 e^{i\theta} + p^2) & (q^2 e^{i\theta} + p^2) \end{pmatrix}, \tag{3.16}$$

where $\theta = 2(\theta_q - \theta_p)$ and all the parameters m_0, p, q and k_1 are real. Thus there is only a single phase parameter in $M_\nu'^{AB}$.

- **Category C**

  In a similar way, the mass matrix of Category C can be rephased as

$$M_\nu'^{C} = m_0 \begin{pmatrix} 1 & k_1(p + q e^{i\theta}) & p + q e^{i\theta} \\ k_1(p + q e^{i\theta}) & k_1^2(2pq e^{i\theta} + p^2) & k_1(2pq e^{i\theta} + p^2) \\ p + q e^{i\theta} & k_1(2pq e^{i\theta} + p^2) & (2pq e^{i\theta} + p^2) \end{pmatrix} \tag{3.17}$$

  with the same set of redefined parameters as mentioned earlier along with $\theta = \theta_q - \theta_p$.

- **Category D**

  For this category the rephased mass matrix comes out as

$$M_\nu'^{D} = m_0 \begin{pmatrix} 0 & k_1 p & p \\ k_1 p & k_1^2(q^2 e^{i\alpha} + 2rp e^{i\beta}) & k_1(q^2 e^{i\alpha} + 2rp e^{i\beta}) \\ p & k_1(q^2 e^{i\alpha} + 2rp e^{i\beta}) & (q^2 e^{i\alpha} + 2rp e^{i\beta}) \end{pmatrix} \tag{3.18}$$

  with $r \to r e^{i\theta_r}$, $\alpha = 2(\theta_q - \theta_p)$, $\beta = (\theta_r - \theta_p)$ and the rest of the parameters are defined identically similar to the previous case.

3.6 Breaking of the scaling ansatz

Since the neutrino mass matrix obtained in (3.16), (3.17) and (3.18) are all invariant under scaling ansatz and thereby give rise to $\theta_{13} = 0$ as well as $m_3 = 0$. Although vanishing value of m_3 is yet not ruled out however, the former, $\theta_{13} = 0$ is refuted by the reactor experimental results. Popular paradigm is to consider $\theta_{13} = 0$ at the leading order and by further perturbation nonzero value of θ_{13} is generated. We follow the same way to produce nonzero θ_{13} through small breaking of scaling ansatz. It is to be noted in our scheme that generation of nonzero θ_{13} always requires breaking in m_D. To generate nonzero m_3 breaking in μ matrix is also necessary along with m_D. However, in Category B since det $(m_D = 0)$, even after breaking in the μ matrix, M_ν still gives rise to a vanishing eigenvalue. On the other hand for Category C and D, μ_2^4 has always a zero determinant for being a scaling ansatz invariant matrix. Thus it leads to one zero eigenvalue similar to Category B. It is the Category A for which we get nonzero θ_{13} as well as nonzero m_3 after breaking the scaling ansatz in both the matrices (m_D and μ).

We invoke breaking of scaling ansatz in all four categories in two ways:

- breaking in the Dirac sector ($\theta_{13} \neq 0$, $m_3 = 0$),
- breaking in the Dirac sector as well as Majorana sector ($\theta_{13} \neq 0$, $m_3 \neq 0$). A systematic analysis with numerical discussion is demonstrated in the following way.

3.6.1 Breaking in the Dirac sector

- **Category A, B**

We consider minimal breaking of the scaling ansatz through a dimensionless real parameter ϵ in a single term of different m_D matrices of those categories as

$$m_{D2}^4 = \begin{pmatrix} 0 & d_2 & 0 \\ k_1(1+\epsilon)c_1 & 0 & k_1c_3 \\ c_1 & 0 & c_3 \end{pmatrix}, m_{D6}^4 = \begin{pmatrix} 0 & 0 & d_3 \\ k_1(1+\epsilon)c_1 & k_1c_2 & 0 \\ c_1 & c_2 & 0 \end{pmatrix} \tag{3.19}$$

for Category A and

$$m_{D1}^4 = \begin{pmatrix} d_1 & 0 & 0 \\ k_1c_1 & 0 & k_1(1+\epsilon)c_3 \\ c_1 & 0 & c_3 \end{pmatrix}, m_{D3}^4 = \begin{pmatrix} 0 & 0 & d_3 \\ k_1(1+\epsilon)c_1 & 0 & k_1c_3 \\ c_1 & 0 & c_3 \end{pmatrix},$$

$$m_{D4}^4 = \begin{pmatrix} d_1 & 0 & 0 \\ k_1c_1 & k_1(1+\epsilon)c_2 & 0 \\ c_1 & c_2 & 0 \end{pmatrix}, m_{D5}^4 = \begin{pmatrix} 0 & d_2 & 0 \\ k_1(1+\epsilon)c_1 & k_1c_2 & 0 \\ c_1 & c_2 & 0 \end{pmatrix} \tag{3.20}$$

for Category B. We further want to mention that breaking considered in any element of the second row are all equivalent. For example, if we consider breaking in the '23' element of m_{D2}^4 it is equivalent to as considered in (3.19). Neglecting the $\mathcal{O}(\epsilon^2)$ and higher order terms, the effective M_ν matrix comes out as

$$M_\nu^{\prime AB\epsilon} = m_0 \begin{pmatrix} 1 & k_1p & p \\ k_1p & k_1^2(q^2e^{i\theta}+p^2) & k_1(q^2e^{i\theta}+p^2) \\ p & k_1(q^2e^{i\theta}+p^2) & (q^2e^{i\theta}+p^2) \end{pmatrix} + m_0\epsilon \begin{pmatrix} 0 & 0 & 0 \\ 0 & 2k_1^2q^2e^{i\theta} & k_1q^2e^{i\theta} \\ 0 & k_1q^2e^{i\theta} & 0 \end{pmatrix}. \tag{3.21}$$

As mentioned earlier, that for Category B, det $(m_D) = 0$ and it is not possible to generate $m_3 \neq 0$ even if we consider breaking in the μ matrices. On the other hand , the matrices in Category A posses det $(m_D) \neq 0$ and thereby give rise to $m_3 \neq 0$. Now for the numerical computation of the eigenvalues, mixing angles, J_{CP}, the Dirac and Majorana phases we utilize the results obtained in ref. [130], for a general complex matrix. We should mention that the formula obtained in ref. [130], for Majorana phases is valid when all three eigenvalues are nonzero. However, when one of the eigenvalue is zero (in this case $m_3 = 0$) one has to utilize the methodology given in ref. [16]. We follow the same diagonalization procedure of the effective light neutrino mass matrix as defined in the previous section. Similar to the previous chapter here we parametrize U_{PMNS} as $U = U_{CKM}P_M$, where P_M is the Majorana phase matrix given as

$$P_M = diag(1, e^{\alpha_M}, e^{i(\beta_M+\delta_{CP})}). \tag{3.22}$$

Writing (2.12) explicitly with $m_3 = 0$ we can have expressions for six independent elements of M_ν in terms of the mixing angles, two eigenvalues and the Dirac CP phase, from which the m_{11} element can be expressed as

$$m_{11} = c_{12}^2 c_{13}^2 m_1 + s_{12}^2 c_{13}^2 m_2 e^{2i\alpha_M} \tag{3.23}$$

and therefore the Majorana phase α_M comes out as

$$\alpha_M = \frac{1}{2}\cos^{-1}\left\{\frac{|m_{11}|^2}{2c_{12}^2 s_{12}^2 c_{13}^4 m_1 m_2} - \frac{(c_{12}^4 m_1^2 + s_{12}^4 m_2^2)}{2c_{12}^2 s_{12}^2 m_1 m_2}\right\}. \tag{3.24}$$

The Jarlskog measure of CP violation J_{CP} is defined in usual way as

$$J_{CP} = \frac{Im(h_{12}h_{23}h_{31})}{(\Delta m_{21}^2)(\Delta m_{32}^2)(\Delta m_{31}^2)}, \tag{3.25}$$

where h is a hermitian matrix constructed out of M_ν as $h = M_\nu M_\nu^\dagger$. For all the categories, we follow the same numerical technique as done for this category (Category A).

- **Category C**

In this case breaking is considered in m_D as

$$m^4_{D1} = \begin{pmatrix} d_1 & 0 & 0 \\ k_1(1+\epsilon)c_1 & k_1c_2 & 0 \\ c_1 & c_2 & 0 \end{pmatrix}, m^4_{D4} = \begin{pmatrix} d_1 & 0 & 0 \\ k_1(1+\epsilon)c_1 & 0 & k_1c_3 \\ c_1 & 0 & c_3 \end{pmatrix} \tag{3.26}$$

and the scaling ansatz broken M_ν appears as

$$M_\nu'^{C\epsilon} = m_0 \begin{pmatrix} 1 & k_1(p+qe^{i\theta}) & p+qe^{i\theta} \\ k_1(p+qe^{i\theta}) & k_1^2(2pqe^{i\theta}+p^2) & k_1(2pqe^{i\theta}+p^2) \\ p+qe^{i\theta} & k_1(2pqe^{i\theta}+p^2) & (2pqe^{i\theta}+p^2) \end{pmatrix} + m_0\epsilon \begin{pmatrix} 0 & k_1qe^{i\theta} & 0 \\ k_1qe^{i\theta} & 2k_1^2pqe^{i\theta} & k_1pqe^{i\theta} \\ 0 & k_1pqe^{i\theta} & 0 \end{pmatrix}. \tag{3.27}$$

- **Category D**

Breaking in m_D in this case is incorporated through

$$m^4_{D2} = \begin{pmatrix} 0 & d_2 & 0 \\ k_1c_1 & 0 & k_1(1+\epsilon)c_3 \\ c_1 & 0 & c_3 \end{pmatrix}, m^4_{D3} = \begin{pmatrix} 0 & 0 & d_3 \\ k_1c_1 & 0 & k_1(1+\epsilon)c_3 \\ c_1 & 0 & c_3 \end{pmatrix} \tag{3.28}$$

$$m_{D5}^4 = \begin{pmatrix} 0 & d_2 & 0 \\ k_1 c_1 & k_1(1+\epsilon)c_2 & 0 \\ c_1 & c_2 & 0 \end{pmatrix}, m_{D6}^4 = \begin{pmatrix} 0 & 0 & d_3 \\ k_1 c_1 & k_1(1+\epsilon)c_2 & 0 \\ c_1 & c_2 & 0 \end{pmatrix} \tag{3.29}$$

and the corresponding M_ν comes out as

$$M_\nu'^{D\epsilon} = m_0 \begin{pmatrix} 0 & k_1 p & p \\ k_1 p & k_1^2(q^2 e^{i\alpha} + 2rpe^{i\beta}) & k_1(q^2 e^{i\alpha} + 2rpe^{i\beta}) \\ p & k_1(q^2 e^{i\alpha} + 2rpe^{i\beta}) & (q^2 e^{i\alpha} + 2rpe^{i\beta}) \end{pmatrix} + m_0\epsilon \begin{pmatrix} 0 & 0 & 0 \\ 0 & 2k_1^2 rpe^{i\beta} & k_1 rpe^{i\beta} \\ 0 & k_1 rpe^{i\beta} & 0 \end{pmatrix}. \tag{3.30}$$

3.6.2 Numerical Analysis

In order to perform the numerical analysis to obtain allowed parameter space we utilize the neutrino oscillation data obtained from global fit shown in Table 3.8.

Table 3.8: Input experimental values [31]

Quantity	3σ ranges
$\|\Delta m^2_{31}\|$ N	2.31$<\Delta m^2_{31}(10^3 eV^{-2}) < 2.74$
$\|\Delta m^2_{31}\|$ I	2.21$<\Delta m^2_{31}(10^3 eV^{-2}) < 2.64$
Δm^2_{21}	7.21$<\Delta m^2_{21}(10^5 eV^{-2}) < 8.20$
θ_{12}	$31.3^o < \theta_{12} < 37.46^o$
θ_{23}	$36.86^o < \theta_{23} < 55.55^o$
θ_{13}	$7.49^o < \theta_{13} < 10.46^o$

- **Category A, B**

  We first consider Category A,B for which the neutrino mass matrix is given in (3.21). The parameter ϵ is varied freely to fit the extant data and it is constrained as $0.04 < \epsilon < 0.7$. However, to keep the ansatz breaking effect small we restrict the value of ϵ only upto 0.1. For this range of ϵ $(0 < \epsilon < 0.1)$ under consideration the parameter spaces are obtained as $1.78 < p < 3.40$, $1.76 < q < 3.42$ and $0.66 < k_1 < 1.3$. It is interesting to note a typical feature of this category is that the Dirac CP phase δ_{CP} comes out too tiny and thereby generating almost vanishing value of J_{CP} $(\approx 10^{-6})$ while the range of the only Majorana phase in this category is obtained as $77^o < \alpha_M < 90^o$.

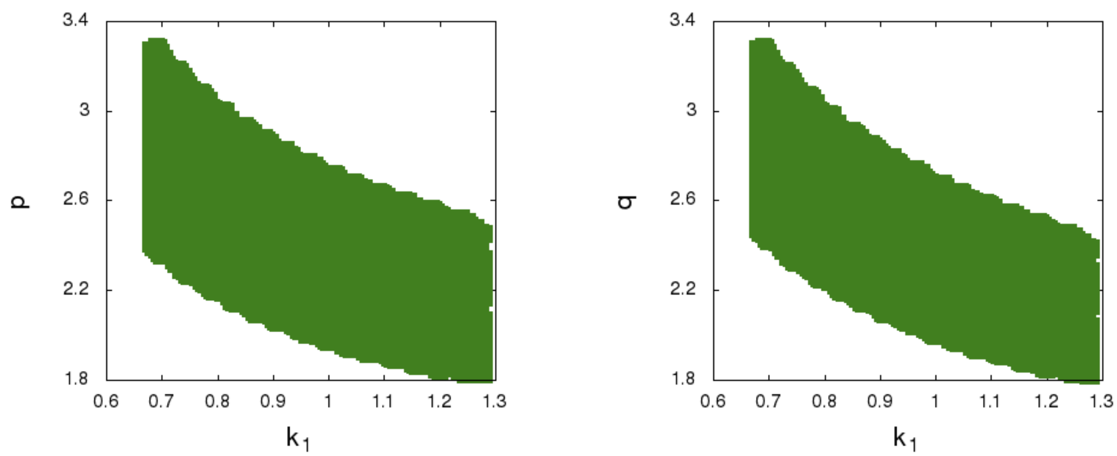

Figure 3.1: *Plot of p vs k_1 (left), q vs k_1 (right) for the Category A,B with $\epsilon = 0.1$.*

Since one of the eigenvalue $m_3 = 0$ therefore, the hierarchy of the masses is clearly inverted in this category. The sum of the three neutrino masses $\Sigma_i m_i (= m_1 + m_2 + m_3)$ and $|m_{11}|$ are obtained as 0.088 eV $< \Sigma_i m_i <$ 0.104 eV and 0.0102 eV $< |m_{11}| <$ 0.0181 eV which predict the value of the two quantities below the present experimental upper bounds. To illustrate the nature of variation, in Fig.3.1 we plot p vs k_1 and q vs k_1 while in Fig.3.2 a correlation plot of $\Sigma_i m_i$ with $|m_{11}|$ is shown for $\epsilon = 0.1$ and it is also seen from Fig.3.1 and 3.2 that the ranges of the parameters do not differ much compare to the values obtained for the whole range of ϵ parameter.

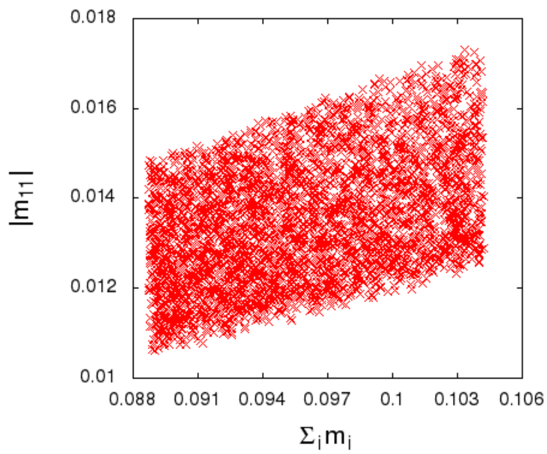

Figure 3.2: *Plot of $|m_{11}|$ vs $\Sigma_i m_i$ for Category A,B with $\epsilon = 0.1$.*

In brief, distinguishable characteristics of this category are i) tiny J_{CP} and δ_{CP} ii) inverted hierarchy of the neutrino masses. At the end of this section we will further discuss the experimental testability of these quantities for all the categories.

- **Category C**

  In this case it is found that a small breaking of ϵ ($0.02 < \epsilon < 0.09$) is sufficient to accommodate all the oscillation data. We explore the parameter space and the ranges obtained as $3.42 < p < 6.07$, $1.68 < q < 3.02$ and $0.7 < k_1 < 1.32$. The hierarchy obtained in this case is also inverted due to the vanishing value of m_3. The other two quantities $\Sigma_i m_i$ and $|m_{11}|$ come out as 0.0118 eV $< |m_{11}| <$ 0.019 eV and 0.088 eV $< \Sigma_i m_i <$ 0.105 eV. Similar to the previous category J_{CP} is vanishingly small due to low value of δ_{CP}. The range of the Majorana phase α_M is obtained as $81^o < \alpha_M < 89^o$. In Fig.3.3 we plot k_1 vs p and k_1 vs q for $\epsilon = 0.09$ that predicts almost the same ranges of the parameters (p, q and k_1) and all other quantities ($|m_{11}|$, $\Sigma_i m_i$, α_M and J_{CP}) as obtained from the whole range of ϵ. We present a correlation plot of $\Sigma_i m_i$ with $|m_{11}|$ in Fig.3.4.

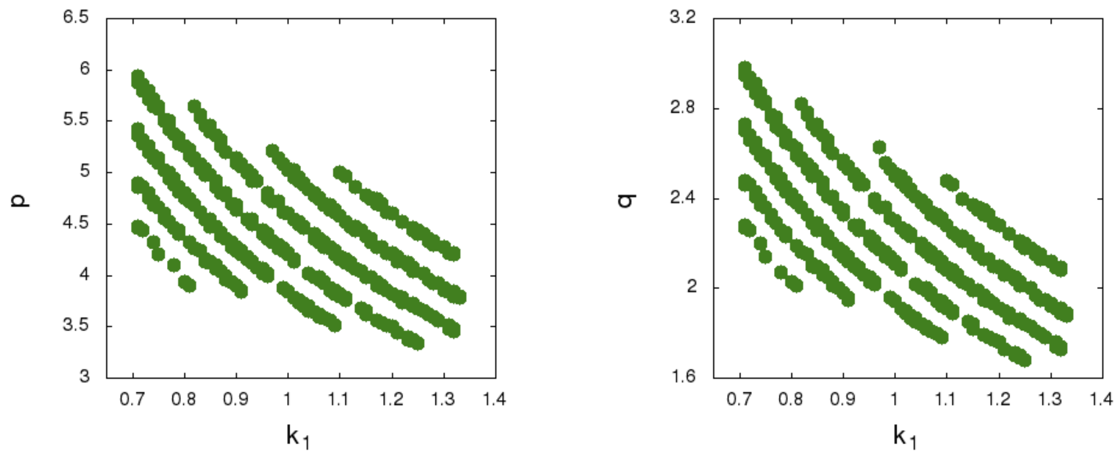

Figure 3.3: *Plot of p vs k_1 (left), q vs k_1 (right) for the Category C with* $\epsilon = 0.09$.

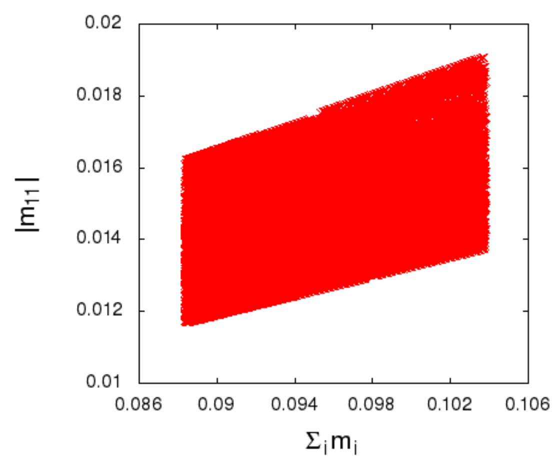

Figure 3.4: *Plot of $|m_{11}|$ vs $\Sigma_i m_i$ for Category C with* $\epsilon = 0.09$.

- **Category D**

  In case of Category D, although a priori it is not possible to rule out $M_\nu'^{D\epsilon}$ without going into the detailed numerical analysis, however in this case even if with $\epsilon = 1$ it is not possible to accommodate the neutrino oscillation data. Specifically, the value of θ_{13} is always beyond the reach of the parameter space. Exactly for the same reason the M_ν matrix of type A_3 in (3.7) is phenomenologically ruled out.

3.6.3 Breaking in Dirac+Majorana sector

In this section we focus on the phenomenology of the neutrino mass matrix where the scaling ansatz is broken in both the sectors. This type of breaking is only relevant for Category A since in this case m_D is nonsingular after breaking of the ansatz and the resultant M_ν gives rise to nonzero θ_{13} along with $m_3 \neq 0$. In all the other categories due to the singular nature of m_D, inclusion of symmetry breaking in the Majorana sector will not generate $m_3 \neq 0$. Thus we consider only Category A under this scheme. We consider the breaking in m_D as mentioned in (3.19) and the ansatz broken texture of μ_1^4 matrix is given by

$$\mu_1^4 = \begin{pmatrix} r_1 & 0 & 0 \\ 0 & k_2^2 s_3 & k_2(1+\epsilon')s_3 \\ 0 & k_2(1+\epsilon')s_3 & s_3 \end{pmatrix}, \tag{3.31}$$

where ϵ' is a dimensionless real parameter. The effective neutrino mass matrix M_ν comes out as

$$m_{\nu\epsilon'}^{\prime A\epsilon} = m_0 \begin{pmatrix} 1 & k_1 p & p \\ k_1 p & k_1^2(q^2e^{i\theta}+p^2) & k_1(q^2e^{i\theta}+p^2) \\ p & k_1(q^2e^{i\theta}+p^2) & (q^2e^{i\theta}+p^2) \end{pmatrix} + m_0\epsilon \begin{pmatrix} 0 & 0 & 0 \\ 0 & 2k_1^2q^2e^{i\theta} & k_1q^2e^{i\theta} \\ 0 & k_1q^2e^{i\theta} & 0 \end{pmatrix} + m_0\epsilon' \begin{pmatrix} 0 & k_1 p & p \\ k_1 p & 0 & 0 \\ p & 0 & 0 \end{pmatrix} \tag{3.32}$$

- **Numerical results**

  As mentioned above, $\epsilon' = 0$ leads to inverted hierarchy with $m_3 = 0$ and thus to generate nonzero m_3 a small value of ϵ' is needed. Similar to the previous cases two breaking parameters ϵ and ϵ' can be varied freely through the ranges that are sensitive to the oscillation data and are obtained as $0.06 < \epsilon < 0.68$ and $0 < \epsilon' < 1$. It is to be noted that although the ϵ parameter is restricted due to θ_{13} value, ϵ' is almost insensitive to θ_{13} and it can vary within a wide range as $0 < \epsilon' < 1$. A correlation plot of ϵ with ϵ' is shown in Fig.3.5. However, as mentioned earlier, the effect of the breaking term should be smaller than the unbroken one, therefore, to obtain the parameter space for this category we consider breaking of the scaling ansatz in both the sectors only upto 10 % and consequently for all combinatorial values of ϵ and ϵ' the parameters p, q and k_1 vary within the ranges as $1.07 < p < 3.10$, $1.03 < q < 3.12$ and $0.67 < k_1 < 1.31$. Interestingly, although all the eigenvalues are nonzero in this case, the hierarchy is still inverted. J_{CP} is found to be tiny ($\approx 10^{-6}$) again due to small value of δ_{CP}. The Majorana phases are obtained as $-96^o < \alpha_M < 74^o$ and $-100^0 < \beta_M + \delta_{CP} < 102^o$ followed by the bounds on $\Sigma_i m_i$ and $|m_{11}|$ as 0.088 eV $< \Sigma_i m_i < 0.11$ eV and 0.010 eV $< |m_{11}| < 0.022$ eV which are well below the present experimental upper bounds.

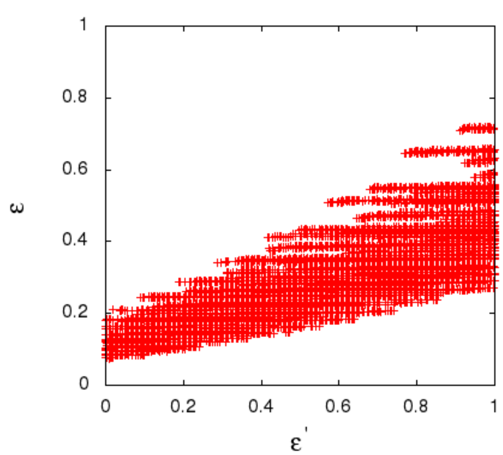

Figure 3.5: *Correlated plot of ϵ with ϵ'.*

In Fig.3.6 we demonstrate the above predictions for $\epsilon = \epsilon' = 0.1$. In the left panel of Fig.3.6 the inverted hierarchical nature is shown and in the right panel variation of the Majorana phases is demonstrated.

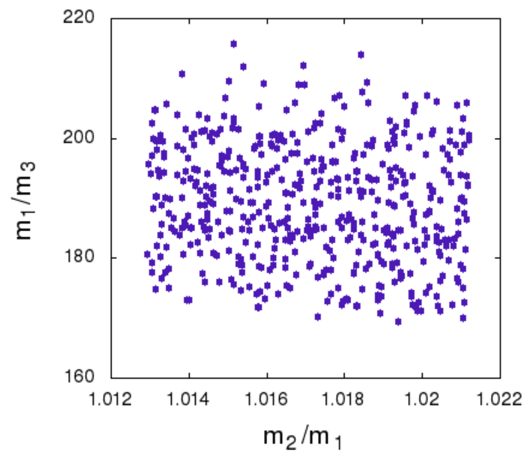

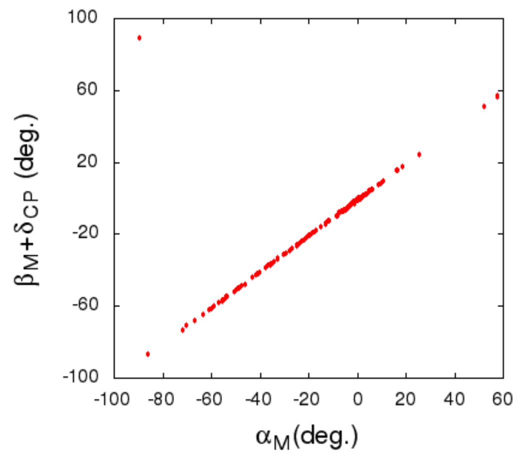

Figure 3.6: *Plot of* (m_1/m_3) *vs* (m_2/m_1) *(left) and* $\beta_M + \delta_{CP}$ *vs* α_M *(right) after breaking of the scaling ansatz in both the sectors of Category A for a representative value of* $\epsilon = \epsilon' = 0.1$.

Some comments are in order regarding predictions of the present scheme:

1. After precise determination of θ_{13} taking full account of reactor neutrino experimental data, it is shown that the hierarchy of the light neutrino masses can be probed through combined utilization of NOνA and T2K [184] neutrino oscillation experimental results in near future. Thus the speculation of hierarchy in the present scheme will be clearly verified. Moreover, taking the difference of probabilities between $P(\nu_\mu \rightarrow \nu_e)$ and $P(\bar{\nu_\mu} \rightarrow \bar{\nu_e})$ information on the value of J_{CP} can be obtained using neutrino and anti neutrino beams. This procedure elaborately clarified in chapter 4.

2. More precise estimation of the sum of the three light neutrino masses will be obtained utilizing a combined analysis with PLANCK data [185] and other cosmological and astrophysical experiments [186] such as, Baryon oscillation spectroscopic survey, The Dark energy survey, Large Synoptic Survey Telescope or the Euclid

satellite data etc. Such type of analysis will push $\Sigma_i m_i \sim 0.1$ eV (at the 4σ level for inverted ordering) and $\Sigma_i m_i \sim 0.05$ eV (at the 2σ level for normal ordering). Thus the prediction of the value of $\Sigma_i m_i$ in the different categories discussed in the present work will also be tested in the near future. Furthermore, GERDA-II [27] and NEXT-100 [124] will probe the value of $|m_{11}|$ up to 0.1 eV which is a more precise value than the EXO-200 [25] experimental range (0.14-0.38 eV).

3.7 Cyclic symmetry and texture zeros

So far in the above analysis we discuss the scaling ansatz as an effective residual symmetry in the low energy light neutrino mass matrix. In the following, within the framework of same mechanism, i.e. the inverse seesaw, we deal with the effect of cyclic permutation symmetry on the neutrino fields. It will be shown that this is a Z_3 type symmetry, that might arise from a larger symmetry group such as A_4. Explicit matrix representation of the former also replicates a group element of S_3 that leads to a rotation of a equilateral triangle by 120^0. As mention in the previous chapter, application of the permutation symmetry to the neutrino physics was primarily introduced by Harrison and co-authors [138], later this has been a topic of great interest [130, 139, 187, 188] in neutrino physics. In the following, some interesting effects of cyclic symmetry as well as texture zeros on neutrino mass matrix are discussed.

- **Explicit cyclic symmetry and texture zeros**

  We assume the following cyclic symmetry in ν_{iL}, ν_{iR} and S_{iL} fields as

$$\nu_{eL,R} \rightarrow \nu_{\mu L,R} \rightarrow \nu_{\tau L,R} \rightarrow \nu_{eL,R}, \tag{3.33}$$

$$S_{eL} \rightarrow S_{\mu L} \rightarrow S_{\tau L} \rightarrow S_{eL}. \tag{3.34}$$

After imposition of the above cyclic symmetry general Dirac and Majorana type mass matrices look like

$$m_D = \begin{pmatrix} y_1 & y_2 & y_3 \\ y_3 & y_1 & y_2 \\ y_2 & y_3 & y_1 \end{pmatrix}, M = \begin{pmatrix} x_1 & x_2 & x_2 \\ x_2 & x_1 & x_2 \\ x_2 & x_2 & x_1 \end{pmatrix}. \tag{3.35}$$

Now if we consider texture zeros along with the cyclic symmetry, clearly maximum number of zeros that can be accommodated within the above matrices are 6. In Table 3.9 all the 6 zero textures of m_D and M_{RS} are presented.

Table 3.9: Texture zeros with cyclic symmetry of m_D and M_{RS}

6 **zero textures of** m_D **and** M_{RS}
$m_D^1 = \begin{pmatrix} y_1 & 0 & 0 \\ 0 & y_1 & 0 \\ 0 & 0 & y_1 \end{pmatrix}, M_{RS}^1 = \begin{pmatrix} M_1 & 0 & 0 \\ 0 & M_1 & 0 \\ 0 & 0 & M_1 \end{pmatrix}$
$m_D^2 = \begin{pmatrix} 0 & y_2 & 0 \\ 0 & 0 & y_2 \\ y_2 & 0 & 0 \end{pmatrix}, M_{RS}^2 = \begin{pmatrix} 0 & M_2 & 0 \\ 0 & 0 & M_2 \\ M_2 & 0 & 0 \end{pmatrix}$
$m_D^3 = \begin{pmatrix} 0 & 0 & y_3 \\ y_3 & 0 & 0 \\ 0 & y_3 & 0 \end{pmatrix}, M_{RS}^3 = \begin{pmatrix} 0 & 0 & M_3 \\ M_3 & 0 & 0 \\ 0 & M_3 & 0 \end{pmatrix}$

Since the low energy lepton number violating mass matrix μ is Majorana type, only one texture with 6 zeros is possible and is given as

$$\mu^1 = \mathrm{diag}\,(\mu_1, \mu_1, \mu_1). \tag{3.36}$$

Now, utilizing (3.36) we construct M_ν and interestingly it is seen that along with diagonal μ any matrix presented in Table 3.9 can not generate phenomenologically viable M_ν, to be precise, all the emerged mass matrices (M_ν) are diagonal. We now consider the next maximal texture zero (3 zero) structure of μ, and is given by

$$\mu^2 = \begin{pmatrix} 0 & \mu_2 & \mu_2 \\ \mu_2 & 0 & \mu_2 \\ \mu_2 & \mu_2 & 0 \end{pmatrix}. \tag{3.37}$$

The above choice of μ matrix, along with the matrices presented in Table 3.9 enforces the M_ν to be nondiagonal. However, since the emerged M_ν is also cyclic symmetry invariant and hence leading to a degeneracy in the eigenvalues, therefore removal of the degeneracy requires a small breaking of the symmetry. Since our philosophy is to find out a viable texture with least number of parameters, we consider minimal symmetry breaking in the different elements of M_{RS} matrix only. For a compact view we present Table 3.10 which contains all the combinations and the corresponding neutrino mass matrices (M_ν) with

Table 3.10: Different Composition of m_D and μ matrices to generate M_ν.

m_D and μ		$M_{RS}^{1\epsilon}$	$M_{RS}^{2\epsilon}$	$M_{RS}^{3\epsilon}$
$\Updownarrow$		M_ν		
m_D^1	μ^2	N^1	N^3	N^2
m_D^2	μ^2	N^2	N^1	N^3
m_D^3	μ^2	N^3	N^2	N^1
$m_D^{1,2,3}$	μ^1	$d^{1,2,3}$	$d^{3,1,2}$	$d^{2,3,1}$

the definitions $M_{RS}^{1\epsilon} = \text{diag}\,(M_1 + \epsilon, M_1, M_1)$, $M_{RS}^{2\epsilon} = \text{diag}\,(M_1, M_1 + \epsilon, M_1)$, $M_{RS}^{3\epsilon} = \text{diag}\,(M_1, M_1, M_1 + \epsilon)$. The $d^{i(i=1,2,3)}$ matrices are diagonal and not our concern since those are obtained due to 6 zero texture of μ as discussed earlier. The matrices N^1, N^2 and N^3 arise due to 3 zero texture of μ matrix and explicitly their forms are given by

$$N^1 = \begin{pmatrix} 0 & A_1 & A_1 \\ A_1 & 0 & B_1 \\ A_1 & B_1 & 0 \end{pmatrix}, N^2 = \begin{pmatrix} 0 & B_2 & A_2 \\ B_2 & 0 & A_2 \\ A_2 & A_2 & 0 \end{pmatrix}, N^3 = \begin{pmatrix} 0 & A_3 & B_3 \\ A_3 & 0 & A_3 \\ B_3 & A_3 & 0 \end{pmatrix} \quad (3.38)$$

with the definition of the parameters as

$$A_i = \frac{\mu_2 y_i^2}{M_1(M_1+\epsilon)}, B_i = \frac{\mu_2 y_i^2}{M_1^2}. \quad (3.39)$$

Phenomenological consequences : As the left chiral neutrino fields obey cyclic symmetry, their charged lepton partners also follow the same. Hence, the charged lepton mass matrix (m_l) is diagonalized by trimaximal mixing matrix [189]. In the basis where the m_l is diagonal the effective neutrino mass matrix will be modified by the trimaximal mixing matrix. However, it is found that due to the lack of sufficient number of parameters, all the mixing angles cannot be obtained simultaneously in their 3σ range. We also consider the nondiagonal forms of M_{RS} matrices (i.e., all the possible cases given in Table 3.9) and find that the above conclusion is valid for all the cases. Now at this stage one could move one step ahead, i.e. one may consider three zero texture of m_D and M_{RS}. In that case all the constraints from the oscillation data can be accommodated undoubtedly. However, in such a scenario as the effective number of parameters in the M_ν itself (without considering the charged lepton correction) increase, thus, the predictions on the light neutrino masses (m_i), their sum ($\Sigma_i m_i$) and neutrinoless double beta decay parameter ($|m_{11}|$) are less significant (vary in a wide range). Thus, since the maximality of zeros is our concern, in the next section we present an alternative approach to preserve the maximal zero textures of the constituent neutrino mass matrices. In this approach the required texture zero mass matrices with cyclic symmetry in the neutrino sector and simple four zero textures with naturally broken Z_3 in the charged lepton sector are realized from an effective residual symmetry to reproduce the forms of M_ν matrices presented in Table 3.10.

- **Cyclic symmetry and texture zeros as an effective residual symmetry**

  In this section we present a toy model based on A_4 symmetry as a bigger symmetry group. Due to spontaneous breaking of A_4, cyclic symmetry (Z_3) is preserved only in the neutrino sector while the charged lepton mass matrix is obtained with four zero Yukawa texture with decoupled third generation. Thus charged lepton correction also plays a crucial role to fit the extant data. However, before going into the detailed discussion, we would like to mention that although there are several cases in the analysis, we present a toy model only for one case. Furthermore, the symmetry group A_4 is not the only group to realize the cyclic symmetry with the texture zeros. Other symmetry groups such as S_4, $U(1)_{B-L}$ etc. [187–190] can also lead to Z_3 invariance in the neutrino sector due to their spontaneous breaking. Now let us recall the problem we faced in the previous section. First, the maximal zero textures with cyclic symmetry in the neutrino sector do not entertain cyclic symmetry invariant form of the charged lepton mass matrix as far as the present experimental data is concerned. Apart from that one also needs to break cyclic symmetry in the neutrino sector since at the leading order it leads to a degeneracy in masses. Here, in the charged lepton sector, breaking of Z_3 is obtained due to spontaneous breaking of A_4 whereas in the neutrino sector the breaking scheme is similar to the previous section, i.e. the degeneracy is removed by due to a soft breaking term (ϵ) in the elements of M_{RS}. Thus we need the structure of M_{RS} due to minimal breaking

as

$$M_{RS} = \text{diag}\,(M_1, M_2, M_2) \tag{3.40}$$

with $M_1 = M_2 + \epsilon$, to generate $N^{1,2,3}$ type mas matrices shown in Table 3.10. Obviously such choice of M_{RS} matrices with all nondegenerate eigenvalues are also consistent with the oscillation data. Although there are several effective M_ν arises due to suitable combinations of m_D, μ and M_{RS}, of them N^1 type matrix is a two parameter $\mu\tau$ symmetric matrix with zero diagonal entries. Consequently, the matrix leads to vanishing θ_{13} which is discarded by the present oscillation data at $> 10\sigma$ level [191]. Thus to generate nonzero θ_{13} corrections from the charged lepton sector [155, 192–194] should be taken into account. As a simplistic scenario, in this section we consider corrections from all the three sectors of m_l. These simple structures of m_l are well motivated by popular discrete flavor groups which are used to explain neutrino mass and mixing. Here we consider A_4 as the flavor symmetry group. However, there are other groups, e.g. S_4 [134], Z_6 [155] etc. which can also lead to these structures of m_l. Interestingly, all the emerged M_ν which arises from $M_{RS} = \text{diag}\,(M_1, M_2, M_3)$ also require charged lepton correction which we discuss in the next section. Although there are several papers on A_4 symmetry we are motivated by Ref [71]. We discuss the required A_4 model in brief.

Table 3.11: Field content of the model with lepton and scalar assignment

	L	l_{lR}	N_{lR}	S_{lL}	ξ_{ch}, ϕ_{ch}	ξ_D	ξ_{RS}	ϕ_μ
$SU(2)_L$	2	1	1	1	2	2	1	1
Z_3	ω	1	ω	ω^2	ω	1	ω	ω^2
Z_2	$+$	$+$	$-$	$+$	$+$	$-$	$-$	$+$
A_4	3	3	3	3	1, 3	1	1	3

Fermionic part of the Lagrangian consists of four part as shown below

$$\mathcal{L}^{A_4}_{mass} = \mathcal{L}_{ch} + \mathcal{L}_{Dirac} + \mathcal{L}_{RS} + \mathcal{L}_{ss}. \tag{3.41}$$

Explicitly each term is written as

$$\begin{aligned}\mathcal{L}^{A_4}_{mass} &= Y_{ch}\bar{L}l_R(\phi_{ch} + \xi_{ch}) + Y_D\bar{L}N_R\xi_D \\ &+ Y_M\bar{S_L}N_R\xi_{RS} + Y_u\bar{S_L^C}S_L\phi_\mu + \text{h.c}\end{aligned} \tag{3.42}$$

with the following choice of the alignment $\xi_{ch} \sim < v^\xi_{ch} >$, $\phi_{ch} \sim < 0, 0, v^\phi_{ch} >$, $\xi_D \sim < v^\xi_D >$, $\xi_{RS} \sim < v^\xi_{RS} >$ and $\phi_\mu \sim < v^\phi_\mu, v^\phi_\mu, v^\phi_\mu >$. With such choice of VEV one can realize the charged lepton correction from $1-2$ sector and the structures of m^1_D and μ^2 along with M_{RS} as $M_{RS} = \text{diag}(M, M, M)$. Here we assume A_4 group is generated by two generators

$$S = \begin{pmatrix} 1 & 0 & 0 \\ 0 & -1 & 0 \\ 0 & 0 & -1 \end{pmatrix}, \quad T = \begin{pmatrix} 0 & 1 & 0 \\ 0 & 0 & 1 \\ 1 & 0 & 0 \end{pmatrix}. \tag{3.43}$$

The three dimensional representation satisfy the product rule

$$3 \times 3 = 1 + 1' + 1'' + 3_S + 3_A, \tag{3.44}$$

where

$$1 = a_1b_1 + a_2b_2 + a_3b_3, \tag{3.45}$$

$$1' = a_1b_1 + \omega^2 a_2b_2 + \omega a_3b_3, \tag{3.46}$$

$$1'' = a_1b_1 + \omega a_2b_2 + \omega^2 a_3b_3 \tag{3.47}$$

and

$$3_S = (\frac{a_2b_3 + a_3b_2}{2}, \frac{a_3b_1 + a_1b_3}{2}, \frac{a_1b_2 + a_2b_1}{2}), \tag{3.48}$$
$$3_A = (\frac{a_2b_3 - a_3b_2}{2}, \frac{a_3b_1 - a_1b_3}{2}, \frac{a_1b_2 - a_2b_1}{2}). \tag{3.49}$$

Thus, A_4 is spontaneously broken in the charged lepton sector such that there is no effective Z_3 symmetry, however, the neutrino sector enjoys an effective residual Z_3 symmetry. As previously mentioned, Z_3 in M_{RS} should be broken, we consider soft A_4 breaking term in the Lagrangian which is well studied earlier [5, 6, 195]. We consider $\mathcal{L}^{soft}$ as

$$\mathcal{L}^{soft} = \epsilon_{\alpha\beta}\bar{S}_{\alpha L}N_{\beta R}, \tag{3.50}$$

where $\epsilon_{\alpha\beta\ (\alpha,\beta=1,2,3)}$ is a coupling constant with mass dimension one and the double indices do not mean the summation over the indices. The term contributes to the (α, β) element of M_{RS} and breaks the residual Z_3 symmetry. Now if we choose $(\alpha, \beta = 1)$ then the soft term contributes to (1,1) element of M_{RS} which in turn generates N^1 type M_ν with m_D^1 and μ^2. In the following two sections we present detailed analysis of all the emerged M_ν.

Two degenerate eigenvalues of M_{RS}

The matrix of type $N^{1,2,3}$ can be realized by changing the nondegenerate value at three different diagonal entries of M_{RS} matrix given in (3.40) along with m_D^1 and μ^2. First we consider the N^1 matrix which is given by

$$N^1 = M_\nu = \begin{pmatrix} 0 & yp & yp \\ yp & 0 & y \\ yp & y & 0 \end{pmatrix} \tag{3.51}$$

with $y = \mu_2 y_1^2/M_2^2$, $p = M_2/M_1$. The matrix of (3.51) is diagonalized by the unitary mixing matrix U_ν given by

$$U_\nu = \begin{pmatrix} c_{12} & s_{12} & 0 \\ -\frac{1}{\sqrt{2}}s_{12} & \frac{1}{\sqrt{2}}c_{12} & -\frac{1}{\sqrt{2}} \\ -\frac{1}{\sqrt{2}}s_{12} & \frac{1}{\sqrt{2}}c_{12} & \frac{1}{\sqrt{2}} \end{pmatrix}, \tag{3.52}$$

where

$$c_{12} = \frac{\sqrt{1+\frac{1}{\sqrt{1+8p^2}}}}{\sqrt{2}},\; s_{12} = \sqrt{\frac{1}{2} - \frac{1}{2\sqrt{1+8p^2}}}. \tag{3.53}$$

Interestingly, if $p \to \infty$ ($M_2 >> M_1$) we can have the well known bi-maximal mixing of neutrino masses. The eigenvalues of M_ν are given by

$$\begin{aligned} -m_1 &= \frac{1}{2}(y - \sqrt{1+8p^2}y), \\ m_2 &= \frac{1}{2}(y + \sqrt{1+8p^2}y), \\ -m_3 &= -y, \end{aligned} \tag{3.54}$$

where $m_2 > m_1 > m_3$. Now defining $\Delta m^2_{sol} = m_2^2 - m_1^2$ and $\Delta m^2_{atm} = m_2^2 - m_3^2$ we get an explicit relationship between Δm^2_{sol} and Δm^2_{atm} as

$$\Delta m^2_{atm} = \frac{1}{2}\frac{\Delta m^2_{sol}}{\sqrt{1+8p^2}}(4p^2-1) + \frac{\Delta m^2_{sol}}{2} \tag{3.55}$$

from which we obtain an approximate range for p through the experimental inputs of 3σ ranges. In order to generate nonzero θ_{13} we invoke contribution from the charged lepton sector in the following way. We consider Altarelli-Ferugilo-Masina parametrization [196] for U_{PMNS} which is written as $U_{PMNS} = U_l^\dagger U_\nu = \tilde{U}_l^\dagger diag(-e^{i\phi_1}, e^{i\phi_2}, 1) U_\nu \times diag(1, e^{i\alpha}, e^{i(\beta+\delta_{CP})})$, where U_l diagonalizes the charged lepton mass matrix and $\tilde{U}_l$ follows usual CKM type parametrization and is given by

$$\tilde{U}_l = \tilde{R}(\theta_{23})\tilde{R}(\theta_{13},\delta)\tilde{R}(\theta_{12}), \tag{3.56}$$

where

$$\tilde{R}(\theta_{23}) = \begin{pmatrix} 1 & 0 & 0 \\ 0 & \sqrt{1-\lambda_{23}^2} & \lambda_{23} \\ 0 & -\lambda_{23} & \sqrt{1-\lambda_{23}^2} \end{pmatrix}, \tilde{R}(\theta_{13},\delta) = \begin{pmatrix} \sqrt{1-\lambda_{13}^2} & 0 & \lambda_{13}e^{i\delta} \\ 0 & 1 & 0 \\ -\lambda_{13}e^{-i\delta} & 0 & \sqrt{1-\lambda_{13}^2} \end{pmatrix} \tag{3.57}$$

and

$$\tilde{R}(\theta_{12}) = \begin{pmatrix} \sqrt{1-\lambda_{12}^2} & \lambda_{12} & 0 \\ -\lambda_{12} & \sqrt{1-\lambda_{12}^2} & 0 \\ 0 & 0 & 1 \end{pmatrix}, \tag{3.58}$$

where $\lambda_{ij} = \sin\theta_{ij}$. Since we are considering CKM type mixing matrix therefore, we expect small mixing in the charged lepton sector. Moreover the small value of reactor mixing angle also enforces the value of λ to be small. The textures of the charged lepton mass matrices are presented in Table 3.12

Table 3.12: Texturs of the charged lepton mass matrix (m_l)

4 zero textures of m_l		
$m_l^{12} = \begin{pmatrix} \times & \times & 0 \\ \times & \times & 0 \\ 0 & 0 & \times \end{pmatrix}$	$m_l^{13} = \begin{pmatrix} \times & 0 & \times \\ 0 & \times & 0 \\ \times & 0 & \times \end{pmatrix}$	$m_l^{23} = \begin{pmatrix} \times & 0 & 0 \\ 0 & \times & \times \\ 0 & \times & \times \end{pmatrix}$

where '$\times$' corresponds to some nonzero entries in m_l. Considering $|e_{\alpha=(e,\mu,\tau)} >$

to be the flavour eigenstate and $|e_i>$ the mass eigenstate of the charged leptons we address three possible cases corresponding to the three textures of m_l for modifications of U_ν.

Case I: $|e_\tau>^{flavour}=|e_i>^{mass}$, $m_l \Rightarrow m_l^{12}$

In this case U_ν is modified by the 1-2 sector ($\tilde{R}(\theta_{12})$) of U_l and the elements of U_{PMNS} can be written as

$$\begin{aligned}
U_{11} &= -e^{i\phi_1}\sqrt{1-\lambda_{12}^2}c_{12} - \frac{1}{\sqrt{2}}\lambda_{12}e^{i\phi_2}s_{12},\\
U_{12} &= -e^{i\phi_1}\sqrt{1-\lambda_{12}^2}s_{12} + \frac{1}{\sqrt{2}}\lambda_{12}e^{i\phi_2}c_{12},\\
U_{13} &= -\frac{1}{\sqrt{2}}\lambda_{12}e^{i\phi_2},\\
U_{22} &= -\lambda_{12}e^{i\phi_1}s_{12} + \frac{1}{\sqrt{2}}\sqrt{1-\lambda_{12}^2}e^{i\phi_2}c_{12},\\
U_{23} &= -\frac{1}{\sqrt{2}}\sqrt{1-\lambda_{12}^2}e^{i\phi_2}, U_{33} = \frac{1}{\sqrt{2}}.
\end{aligned} \tag{3.59}$$

and hence the three mixing angles come out as

$$\begin{aligned}
\sin\theta_{13} &= |U_{13}| = \frac{\lambda_{12}}{\sqrt{2}},\\
\tan\theta_{12} &= \frac{|U_{12}|}{|U_{11}|} = \frac{s_{12}(s_{12}-\sqrt{2}\cos[\phi_1-\phi_2]c_{12}\lambda_{12})}{c_{12}(c_{12}+\sqrt{2}\cos[\phi_1-\phi_2]s_{12}\lambda_{12})},\\
\tan\theta_{23} &= \frac{|U_{23}|}{|U_{33}|} = \sqrt{1-\lambda_{12}^2}.
\end{aligned} \tag{3.60}$$

The measure of CP violation J_{CP} can be written in terms of the mixing matrix elements as

$$J_{CP} = \frac{\sin(\phi_2-\phi_1)c_{12}s_{12}\lambda_{12}}{2\sqrt{2}} \tag{3.61}$$

and hence the Dirac CP phase δ_{CP} is obtained as

$$\sin\delta_{CP} = \frac{J_{CP}}{\Omega} \tag{3.62}$$

with the definition of Ω as

$$\Omega = c'_{12}c'^2_{13}c'_{23}s'_{12}s'_{13}s'_{23}, \tag{3.63}$$

where $s'_{ij} \Rightarrow \sin\theta_{ij}$ and $c'_{ij} \Rightarrow \cos\theta_{ij}$ are the usual mixing parameters in the CKM part of U_{PMNS} which is defined as

$$U_{PMNS} = P_\alpha U_{CKM} P_M, \tag{3.64}$$

where $P_\alpha = diag(e^{i\alpha_1}, e^{i\alpha_2}, e^{i\alpha_3})$ as the unphysical phase matrix, $U_{CKM} = \tilde{U}_l^\dagger diag(-e^{i\phi_1}, e^{i\phi_2}, 1)U_\nu$ and $P_M = diag(1, e^{i\alpha}, e^{i(\beta+\delta_{CP})})$ as the Majorana phsae matrix. We use other two rephasing invariant quantities to calculate the Majorana phases as [192]

$$\begin{aligned}\alpha &= arg(U^*_{11}U_{12}),\\ \beta &= arg(U_{13}U^*_{11}).\end{aligned} \tag{3.65}$$

Therefore the Majorana phases come out as

$$\tan\alpha = \frac{\sqrt{2}\sin(\phi_2-\phi_1)\lambda_{12}}{\sqrt{2}\cos(\phi_2-\phi_1)(c^2_{12}-s^2_{12})\lambda_{12}-2c_{12}s_{12}} \tag{3.66}$$

and

$$\tan\beta = \frac{\sin(\phi_2-\phi_1)c_{12}}{\sqrt{2}\cos(\phi_2-\phi_1)c_{12}+s_{12}\lambda_{12}}. \tag{3.67}$$

Case II: $|e_\mu>^{flavour}=|e_i>^{mass}$, $m_l \Rightarrow m_l^{13}$

In this case modification to U_ν originates from 1-3 sector ($\tilde{R}(\theta_{13},\delta)$) of U_l and the elements of U_{PMNS} can be written as

$$\begin{aligned}
U_{11} &= -e^{i\phi_1}\sqrt{1-\lambda_{13}^2}c_{12} - \frac{1}{\sqrt{2}}\lambda_{13}e^{i\delta}s_{12},\\
U_{12} &= -e^{i\phi_1}\sqrt{1-\lambda_{13}^2}s_{12} + \frac{1}{\sqrt{2}}\lambda_{13}e^{i\delta}c_{12},\\
U_{13} &= -\frac{1}{\sqrt{2}}\lambda_{13}e^{i\delta},\\
U_{22} = \frac{1}{\sqrt{2}}c_{12}, U_{23} &= -\frac{1}{\sqrt{2}}, U_{33} = \frac{1}{\sqrt{2}}\sqrt{1-\lambda_{13}^2}.
\end{aligned} \tag{3.68}$$

Thus the three mixing angles come out as

$$\begin{aligned}
\sin\theta_{13} &= |U_{13}| = \frac{\lambda_{13}}{\sqrt{2}}\\
\tan\theta_{12} = \frac{|U_{12}|}{|U_{11}|} &= \frac{s_{12}(s_{12}-\sqrt{2}\cos[\delta-\phi_1]c_{12}\lambda_{13})}{c_{12}(c_{12}+\sqrt{2}\cos[\delta-\phi_1]s_{12}\lambda_{13})}\\
\tan\theta_{23} = \frac{|U_{23}|}{|U_{33}|} &= \frac{1}{\sqrt{1-\lambda_{13}^2}}.
\end{aligned} \tag{3.69}$$

Proceeding in the same way as discussed in **Case I**, J_{CP} can be written in terms of the mass matrix elements as

$$J_{CP} = \frac{\sin(\phi_1-\delta)c_{12}s_{12}\lambda_{13}}{2\sqrt{2}} \tag{3.70}$$

and

$$\sin\delta_{CP} = \frac{J_{CP}}{\Omega}, \tag{3.71}$$

where Ω is already defined in (3.63). Finally the Majorana phases are calculated

as

$$\tan\alpha = \frac{\sqrt{2}\sin(\delta-\phi_1)\lambda_{13}}{\sqrt{2}\cos(\delta-\phi_1)(c_{12}^2-s_{12}^2)\lambda_{13}-2c_{12}s_{12}} \tag{3.72}$$

and

$$\tan\beta = \frac{\sin(\delta-\phi_1)c_{12}}{\sqrt{2}\cos(\delta-\phi_1)c_{12}+s_{12}\lambda_{13}}. \tag{3.73}$$

Case III: $|e_e>^{flavour}=|e_i>^{mass}$, $m_l \Rightarrow m_l^{23}$

For this texture of m_l (alternatively $\tilde{R}(\theta_{23})$ as the mixing matrix) it is not possible to generate θ_{13}, hence is not taken into account. We also consider the other two matrices N^2 and N^3 and obtained all the mixing angles and eigenvalues. However, from numerical estimation it is found that both the cases do not admit the present experimental data and hence discarded.

All nondegenerate eigenvalues of M_{RS}

Taking three different 6 zero textures of $m_D(m_D^{1,2,3})$ and one 3 zero texture of $\mu(\mu^2)$ with $M_{RS}=diag(M_1,M_2,M_3)$, we construct three different textures of M_ν using inverse seesaw formula and they lead to

$$M_\nu^1 = \begin{pmatrix} 0 & yp & ypq \\ yp & 0 & yq \\ ypq & yq & 0 \end{pmatrix}, M_\nu^2 = \begin{pmatrix} 0 & yq & yp \\ yq & 0 & ypq \\ yp & ypq & 0 \end{pmatrix}, M_\nu^3 = \begin{pmatrix} 0 & ypq & yq \\ ypq & 0 & yq \\ yq & yp & 0 \end{pmatrix} \tag{3.74}$$

where $p = M_2/M_1$ and $q = M_2/M_3$ and $y = \mu y_i^2/M_2^2$ for each M_ν^i. Now in the basis where the charged lepton mass matrix is diagonal one can easily construct the effective M_νs as $m_{\nu f} = U_l^\dagger M_\nu^i U_l^*$, where U_l is already defined earlier in Sec.3.7. Since we are considering three specific textures of the charged lepton mass matrices (Table 3.12), therefore, for a given M_ν we can construct three $m_{\nu f}$ taking contribution from each sectors of the charged leptons. Hence, we have altogether 9 effective $m_{\nu f}$. We consistently denote them as $m_{\nu f ij}$ after getting correction from the 'ij'th sector of U_l. We do not present explicit structures of all the mass matrices. However, numerical estimation for each viable matrix is presented in the next section.

3.8 Numerical analysis and phenomenological discussion

i) Two degenerate eigenvalues of M_{RS}

Before going into the details of the numerical analysis an important point is to be noted that except $\tan\theta_{23}$ the expressions for the physical parameters obtained in Case II are the same as that of the Case I if we replace λ_{13} by λ_{12} and δ by ϕ_2 and therefore the numerical estimation for one case can be automatically translated to the other. Therefore from now on in a generic way we rename λ_{12} and λ_{13} as λ.

We consider small mixing arises from the charged lepton sector and accordingly written down the expressions for the physical parameters with the terms dominant in λ. Moreover, the smallness of θ_{13} automatically implies that the order of λ should be of the order of Sine of the reactor mixing angle. Taking into account the neutrino oscillation global fit data presented in Table 3.8 we randomly vary λ and $\phi_2-\phi_1$ within the ranges as $0 < \lambda < 0.3$ and $-180^o < \phi_2 - \phi_1 < 180^o$ and scan the parameter space. It is seen that the matrices of type N^2 and N^3 are not phenomenologically viable (even after considering charged lepton contribution) as far as the present neutrino oscillation data is concerned.

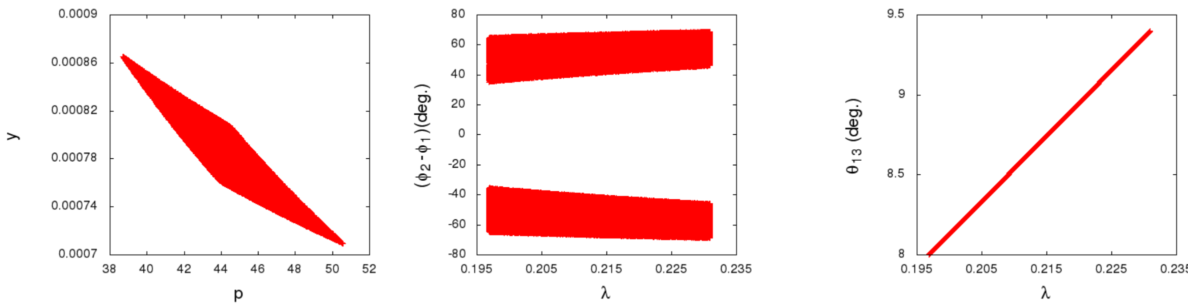

Figure 3.7: *(colour online) Correlation plots: Extreme left plot represents y Vs p while the middle one shows λ Vs $\phi_2 - \phi_1$ for Case I. For Case II we get the same plot just by replacing $\phi_2 - \phi_1$ with $\delta - \phi_1$ and finally the plot in the extreme right shows the variation of λ with θ_{13} for both the cases.*

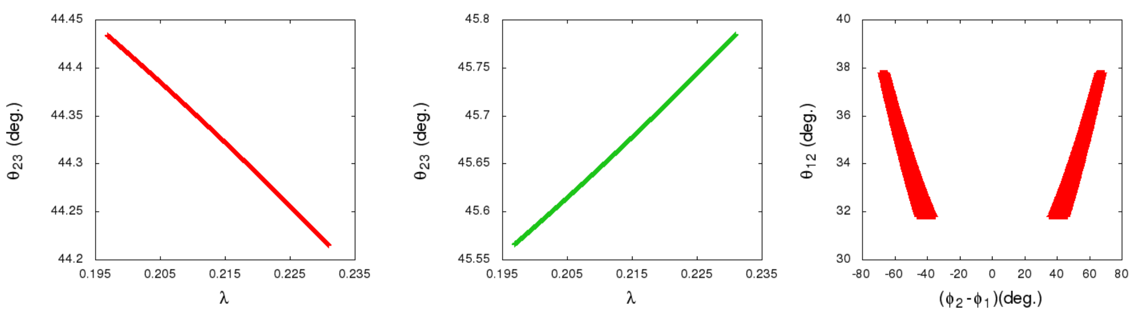

Figure 3.8: *(colour online) The first figure (the red line) shows the variation of the atmospheric mixing angle (θ_{23}) with λ for Case I while the second one (the green line) shows the same for Case II. The last one represents the correlation between θ_{12} and $\phi_2 - \phi_1$ for case I. We get the same plot for case II by replacing $\phi_2 - \phi_1$ with $\delta - \phi_1$.*

For N^1 type matrix we plot in Fig.3.7 the variation of p Vs y, λ Vs $\Phi_2 - \Phi_1$ and λ Vs θ_{13} and it is depicted from the plots that the parameters y and p vary within the ranges as $0.00071 < y < 0.00087$ and $38 < p < 51$ which is presented in the extreme left of Fig.3.7. The ranges of λ and $\phi_2 - \phi_1$ are obtained as $0.197 < \lambda < 0.231$ and $35.5^0 < \phi_2 - \phi_1 < 74^o$, $-35.5^0 < \phi_2 - \phi_1 < -74^o$ as one can read from the middle plot of Fig.3.7.

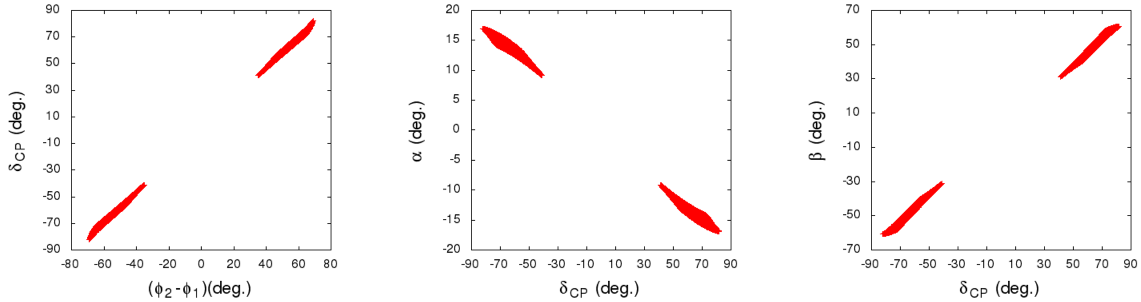

Figure 3.9: *(colour online) The plot in the extreme left side shows the variation of $\phi_2 - \phi_1$ with δ_{CP} for Case I and we get the same plot for Case II by replacing $\phi_2 - \phi_1$ with $\delta - \phi_1$ while the other two plots show the correlation between the Majorana phases with δ_{CP} and are same for both the cases.*

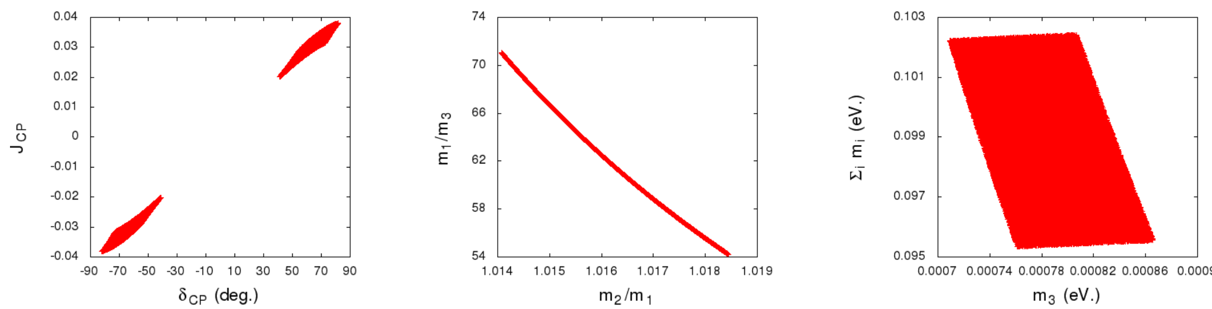

Figure 3.10: *(colour online) The first one shows the variation of J_{CP} with δ_{CP}, the second one stands for the inverted hierarchy of neutrino masses and last one shows a correlation between $\Sigma_i m_i$ with m_3 and all the plots presented in this figure are same for both the cases.*

Now since $|U_{e3}|$ is directly proportional to λ it is needless to say that there is a linear variation of $|U_{e3}|$ with λ and is depicted in the last plot of Fig.3.7. As $\tan\theta_{12}$ has a strong dependence on $\phi_2 - \phi_1$ we also present the variation of θ_{12} with $\phi_2 - \phi_1$ in the extreme right panel of Fig.3.8. The atmospheric mixing angle θ_{23} doesn't deviate much from 45^o. For Case I, θ_{23} is smaller than the bi-maximal value while for the Case II it is slightly enhanced and we plot them in the first two figures of Fig.3.8. This is a distinguishable characteristic between the two cases. Now as the CP violation in U_{PMNS} is solely controlled by the phases arising from the charged lepton sector therefore we expect a great dependency of δ_{CP} on $\phi_2 - \phi_1$ ($\delta - \phi_1$ for Case II) and a correlation between the CP phases. We plot δ_{CP} with $\phi_2 - \phi_1$ in the extreme left panel of Fig.3.9 while the correlation of the Majorana phases with δ_{CP} is shown in the other two figures of Fig.3.9. The ranges of the Dirac CP phase δ_{CP} is obtained as $38^o < |\delta_{CP}| < 85^o$ while the Majorana phases are constrained as $30^o < |\beta| < 65^0$ and $8^o < |\alpha| < 17^o$. The J_{CP} value is obtained within the range as $0.017 < |J_{CP}| < 0.04$ as one can read from the extreme left plot of Fig.3.10.

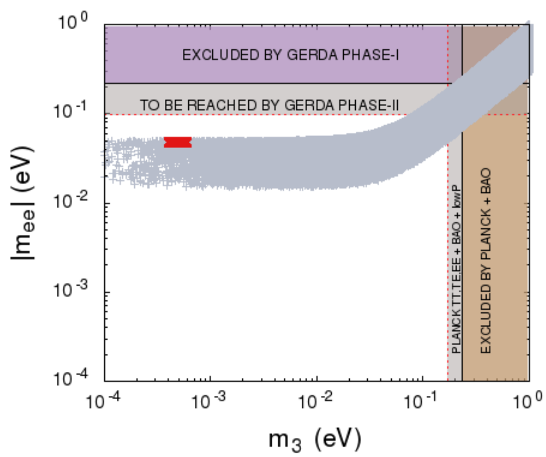

Figure 3.11: *(colour online) Lightest eigenvalue (m_3) Vs $|m_{11}|$ plot. The gray band shows the range of $|m_{11}|$ allowed by the present oscillation data with all the CP phases within the range $0 - 2\pi$. The small red coloured band is allowed in our model.*

The model predicts inverted hierarchy of the neutrino masses which is explicit from the second figure of Fig.3.10. We also obtain a range on the sum of three light neutrino masses as 0.0953 eV $< \Sigma_i m_i <$ 0.1026 eV and a range of $|m_{11}|$ as 0.03 eV $< |m_{11}| <$ 0.048 eV which are well bellow the present experimental upper bound 0.23 eV and 0.35 eV respectively [185].

Before closing the discussion we would like to mention that although charged lepton correction to $\mu\tau$ symmetric matrix is studied before [155, 192–194], here we consider a two parameter structure of a $\mu\tau$ symmetric matrix which is much more predictive than the previous ones. As for example in our model CP violation arises completely from the charged lepton sector as our mass matrix consist of two real parameters. Thus mixing in the charged lepton sector dictates a common origin of θ_{13} and the CP-violating phases. In our analysis the Dirac and Majorana phases are significantly correlated. Thus only the measurement of CP violating phases can challenge the viability of the present model [134]. With the recent hint of T2K, nearly maximal CP violation is also allowed here which in turn fixes the Majorana phases and thus the double beta decay parameter $|m_{11}|$. The allowed occurrence of inverted hierarchy puts a lower limit to $|m_{11}|$ as shown in Fig.3.11. One can see a very narrow range of $|m_{11}|$ is allowed. Thus significant development of the experiments like GERDA and EXO can test the viability of the model. Finally the constraint range of the sum of the light neutrino masses is also a major result of the analysis as $\Sigma_i m_i \sim 0.1$ eV at 4σ level is expected to be probed by the future astrophysical experiments.

ii) All nondegenerate eigenvalues of M_{RS}

In this category there are 9 structures of effective M_ν matrices. We diagonalize them through a direct diagonalization procedure [130] and calculate the eigenvalues, mixing angles. It is seen that the matrices $m^1_{\nu f23}$, $m^2_{\nu f23}$ and $m^3_{\nu f23}$ are phenomenologically ruled out. To be more specific one needs $\lambda_{23} \gg 1$ which is not be the case. Proceeding in the same way as that of the previous section we estimate the ranges of J_{CP}, δ_{CP}, α, β, $|m_{11}|$ and $|\Sigma_i m_i|$ for the survived matrices. The hierarchy of the neutrino masses for all the cases is inverted. The predictions of the viable matrices are listed in Table 3.13. In Fig.3.12 we plot the lightest eigenvalue with $|m_{11}|$.

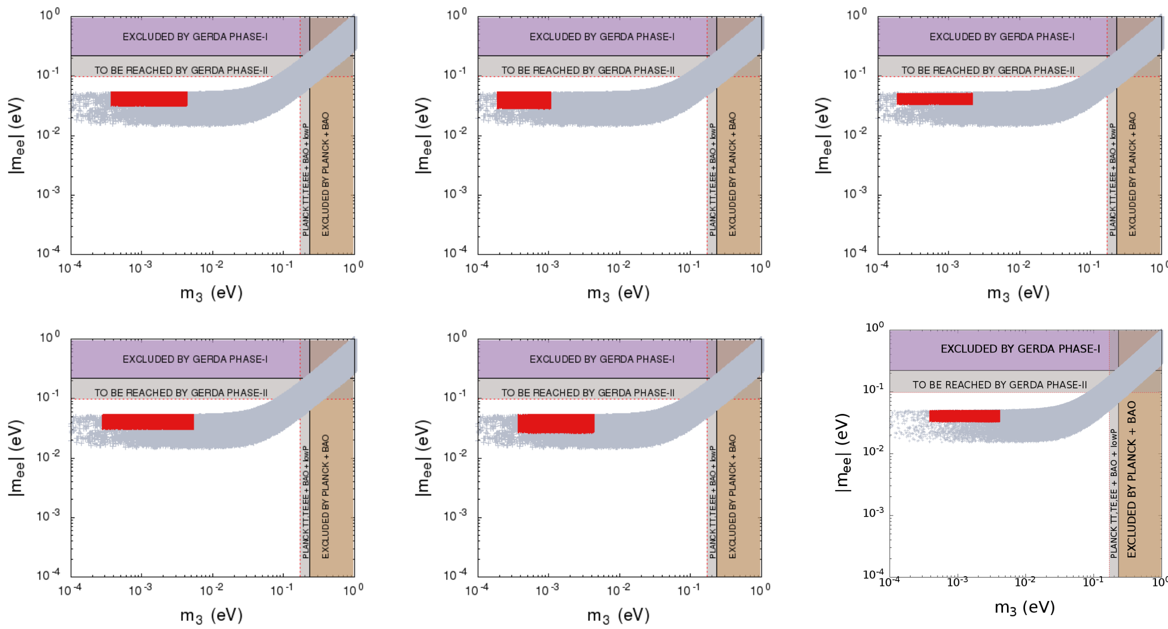

Figure 3.12: *(colour online) Lightest eigenvalue (m_3) Vs $|m_{11}|$ plot: For all nondegenerate eigenvalues of M_{RS}. The first three figures of the first row are shown for the matrices $m_{\nu f12}^{i(=1,2,3)}$ and the figures in the second row are shown for the matrices $m_{\nu f13}^{i(=1,2,3)}$.*

Before concluding this section we would like to mention that the charged lepton correction to the matrices given in (3.74) (with all diagonal entries zero) are also studied in Ref. [4]. Particularly the classes 4_4 and 3_1 [4] respectively resemble m_l and M_ν matrices considered here in the present work. However, in Ref. [4] these cases are categorized as less predictive due to large number of parameters (10 real parameters) and hence the results are not presented. However in the present work, those cases contain less number of parameters (7 real parameters) since the structure of M_{RS} matrix is flavour diagonal (p and q parameters defined in Sec.3.7 are real) and we estimate the prediction for these cases regarding $|m_{11}|$, $\Sigma_i m_i$, δ_{CP} etc.

Table 3.13: Predictions of the viable matrices.

	Six predicted quantities					
	$\lvert\delta_{CP}\rvert$ (deg.)	$\lvert\alpha\rvert$ (deg.)	$\lvert\beta\rvert$ (deg.)	$\lvert J_{CP}\rvert$	$\Sigma_i m_i$ (eV)	$\lvert m_{11}\rvert$ (eV)
$m^1_{\nu f12}$	$100-23$	$80-12$	$63-23$	$0.01-0.04$	$0.09-0.12$	$0.026-0.048$
$m^2_{\nu f12}$	$98-34$	$92-18$	$78-0$	$0.015-0.38$	$0.07-0.108$	$0.029-0.049$
$m^3_{\nu f12}$	$88-0$	$71-37$	$62-35$	$0.012-0.036$	$0.07-0.1$	$0.029-0.048$
$m^1_{\nu f13}$	$100-20$	$85-10$	$60-20$	$0.01-0.04$	$0.09-0.14$	$0.031-0.05$
$m^2_{\nu f13}$	$94-35$	$100-18$	$81-14$	$0.012-0.038$	$0.07-0.132$	$0.032-0.049$
$m^3_{\nu f13}$	$102-17$	$82-26$	$62-21$	$0.017-0.04$	$0.08-0.15$	$0.028-0.048$

3.9 Summary

Within the framework of inverse seesaw, we study the phenomenology of maximal zero textures with scaling ansatz and cyclic symmetry in the neutrino matrices. Through out the analysis we focus on the effective structures of the low energy light neutrino mass matrices that lead to some intriguing testable predictions. These effective symmetries might arise from larger groups such as D_4, A_4 etc. as discussed in the chapter 1. We also present an explicit model with A_4 symmetry to realize one of the textures of the mass matrices under consideration. Both the symmetries, i.e. the scaling ansatz and the cyclic symmetry have to be broken softly due their inconsistency with oscillation data in the unbroken schemes. Each of the cases predicts a highly constrained ranges of CP violating phases, $|m_{11}|$ and $\Sigma_i m_i$ along with an inverted ordering of light neutrino masses. Thus our results are likely to be tested in the planned and forthwith experiments.

Chapter 4

Complex Scaling and residual symmetry

4.1 Introduction

The masses and mixing properties of the three light neutrinos are beginning to get pinned down. Though the precise mass values are still unknown, upper limits on them have been pushed down to fractions of electron volts. Furthermore, it is already known that at least one of the neutrinos must be heavier than about 50 meV. Additionally, the three angles which describe their mixing have become reasonably well-known with $\theta_{12} \sim 34^o$, $\theta_{23} \sim 45^o$ and $\theta_{13} \sim 8^o$. Understanding this mixing phenomenon (with one small and two large angles) has emerged as a major challenge. As ongoing experiments feed in more and more information on neutrino masses and mixing, the flavor structure of the 3×3 neutrino mass matrix M_ν is being slowly uncovered. Many of its features still remain unknown nonetheless and continue to intrigue theoretical investigators. (Uptodate overviews of these issues and their investigations along with original references may be found in the two review articles quoted in Ref. [104, 197]). Especially tantalizing is the predicted phenomenon of leptonic CP-violation which likely to have implications for leptogenesis [90,103,198]. As yet, there is no statistically reliable definitive experimental result on leptonic CP-violation. However, hints of a near-maximal CP-violation, with the phase δ being $\simeq 3\pi/2$, have emerged from results reported by the T2K [17] and NOνA [199] experiments. Similarly, a recent global analysis [30] of all neutrino data is hinting at a nonmaximal value of $\sin^2 2\theta_{23}$. Another yet unresolved question of great interest is that of neutrino mass ordering : normal vs. inverted. In addition, one would like to know if the three neutrinos are Majorana or Dirac particles – to be presumably determined by a future observation of nuclear $0\nu\beta\beta$ decay [200].

Let us start with the minimal supposition that there are only three light and flavored left-chiral neutrinos and that they are Majorana in character. The neutrino mass term in the Lagrangian density now reads

$$-\mathcal{L}^{\nu}_{mass} = \frac{1}{2}\bar{\nu_l^C}(M_\nu)_{lm}\nu_m + h.c. \tag{4.1}$$

with $\nu_l^C = C\bar{\nu_l}^T$ and the subscripts l, m spanning the lepton flavor indices e, μ, τ. M_ν is a complex symmetric matrix ($M_\nu^* \neq M_\nu = M_\nu^T$) which can be put into a diagonal form by a similarity transformation with a unitary matrix U:

$$U^T M_\nu U = M_\nu^d \equiv \text{diag}\,(\mathrm{m}_1, \mathrm{m}_2, \mathrm{m}_3). \tag{4.2}$$

Here m_i ($i = 1, 2, 3$) are real and positive masses. We choose to work in a Weak Basis in which the charged lepton mass matrix is diagonal with real and positive elements, i.e. $M_l = \text{diag.}\,(\mathrm{m_e}, \mathrm{m}_\mu, \mathrm{m}_\tau)$ and the unphysical phases of U are absorbed into the neutrino fields. Now

$$U = U_{PMNS} \equiv \begin{pmatrix} c_{12}c_{13} & e^{i\frac{\alpha}{2}}s_{12}c_{13} & s_{13}e^{-i(\delta-\frac{\beta}{2})} \\ -s_{12}c_{23} - c_{12}s_{23}s_{13}e^{i\delta} & e^{i\frac{\alpha}{2}}(c_{12}c_{23} - s_{12}s_{13}s_{23}e^{i\delta}) & c_{13}s_{23}e^{i\frac{\beta}{2}} \\ s_{12}s_{23} - c_{12}s_{13}c_{23}e^{i\delta} & e^{i\frac{\alpha}{2}}(-c_{12}s_{23} - s_{12}s_{13}c_{23}e^{i\delta}) & c_{13}c_{23}e^{i\frac{\beta}{2}} \end{pmatrix} \tag{4.3}$$

with $c_{ij} \equiv \cos\theta_{ij}$, $s_{ij} \equiv \sin\theta_{ij}$ and $\theta_{ij} = [0, \pi/2]$. CP-violation enters through nontrivial values of the Dirac phase δ and of the Majorana phases α, β with $\delta, \alpha, \beta = [0, 2\pi]$. We follow the PDG convention [201] on these angles and phases except that we denote the Majorana phases by α and β. In principle there could also be a phase matrix with U_{PMNS} if we work in a Weak Basis where M_l is diagonal but where the unphysical phases are not absorbed in the neutrino fields. It is demonstrated later that even if we include the unphysical phase matrix, our result remains the same which is obvious, since physical results are basis independent.

Quite a few different hypotheses have been advanced over several decades on the flavor structure of M_ν, as reviewed in the first article of Ref. [104]. We zero in on an ansatz made some years ago [15, 16] that we call Simple Real Scaling (SRS). This posits the relations

$$\frac{(M_\nu^{SRS})_{e\mu}}{(-M_\nu^{SRS})_{e\tau}} = \frac{(M_\nu^{SRS})_{\mu\mu}}{(-M_\nu^{SRS})_{\mu\tau}} = \frac{(M_\nu^{SRS})_{\tau\mu}}{(-M_\nu^{SRS})_{\tau\tau}} = k, \tag{4.4}$$

where k is a real and positive dimensionless scaling factor. It is straightforward to induce from (4.4) the form of the neutrino Majorana mass matrix:

$$M_\nu^{SRS} = \begin{pmatrix} X & -Yk & Y \\ -Yk & Zk^2 & -Zk \\ Y & -Zk & Z \end{pmatrix}. \tag{4.5}$$

Here X, Y, Z are complex mass dimensional quantities that are a priori unknown. We consistently denote complex (real) quantities by capital (small) letters throughout. We have chosen appropriate negative signs in (4.4) and (4.5) to be in conformity with the PDG convention [201] on the form of U_{PMNS} that emerges from (4.5). It was pointed out by Mohapatra and Rodejohann [16] that - in the basis where the charged lepton mass matrix is diagonal - (4.5) can be realized from the larger symmetry group $D_4 \times \mathbb{Z}_2$. This ansatz of Simple Real Scaling led to a sizable body of research as we cited in the earlier chapters. But it predicts a vanishing s_{13} (and hence no measurable leptonic Dirac CP-violation) as well as an inverted neutrino mass hierarchy (i.e. $m_{2,1} > m_3$) with $m_3 = 0$. While the latter result is still allowed within current experimental bounds, a null value of s_{13} has been ruled out at more than 10σ [191]. Thus SRS, as it stands, has to be abandoned.

We want to consider an extended version of (4.5) which allows a nonvanishing s_{13}. To this end, we employ the method of complex extension which in turn is based on the idea of the residual symmetry $\mathbb{Z}_2 \times \mathbb{Z}_2$ [7–9] of M_ν. This is explained in Sec. 4.3 below. As detailed in the subsequent Sec. 4.4, the complex extension (CES for Complex Extended Scaling) leads to the neutrino mass matrix

$$M_\nu^{CES} = \begin{pmatrix} x & -y_1 k + i y_2 k^{-1} & y_1 + i y_2 \\ -y_1 k + i y_2 k^{-1} & z_1 - w k^{-1}(k^2-1) - i z_2 & w - i z_2 (2k)^{-1}(k^2-1) \\ y_1 + i y_2 & w - i z_2 (2k)^{-1}(k^2-1) & z_1 + i z_2 \end{pmatrix}. \quad (4.6)$$

Here x, $y_{1,2}$, $z_{1,2}$ and w are real mass dimensional quantities that are a priori unknown. It will be shown that M_ν^{CES} of (4.6) can accommodate a nonzero value for each of m_1, m_2, m_3 and can fit the extant data on $\Delta m_{21}^2 \equiv m_2^2 - m_1^2$, $|\Delta m_{32}^2| \equiv |m_3^2 - m_2^2|$ as well as on θ_{12} and θ_{13}. The relation $\tan\theta_{23} = k^{-1}$ is a consequence so that the presently allowed range of $\tan\theta_{23}$ around unity would yield the permitted domain of the variation of the scaling parameter k close to 1. Furthermore, (4.6) leads to the result that $\alpha, \beta = 0$ or π, i.e. there is no Majorana CP-violation, and the verifiable/falsifiable prediction that $\cos\delta = 0$, i.e. leptonic Dirac CP-violation is maximal. We have no statement on the sign of $\sin\delta$ so that δ can be either $\pi/2$ or $3\pi/2$. Furthermore, we show that a normal mass ordering (with $m_{2,1} < m_3$) is allowed in addition to an inverted one ($m_{2,1} > m_3$) in the parameter space of the model.

The rest of the paper is organized as follows. In Sec.4.2 we elucidate the meaning of the residual $\mathbb{Z}_2 \times \mathbb{Z}_2$ discrete symmetry of M_ν in terms of its invariance under two separate similarity transformations. Simple real scaling and its real generalization are discussed in Sec.4.3. Sec.4.4 contains a presentation of the procedure of complex extension; this is first illustrated for $\mu\tau$ interchange symmetry and then applied to the scaling transformation to lead to the proposed M_ν^{CES} of (4.6) as well as its main consequences, namely $\tan\theta_{23} = k^{-1}$ and $\cos\delta = 0$ plus the allowed occurrence of a normal mass ordering. The origin of the neutrino mass matrix M_ν^{CES} in our scheme from type-I seesaw mechanism is shown in Sec.4.5. Detailed phenomenological implications of M_ν^{CES} are worked out numerically in Sec.4.6 and fitted with the current data yielding various 3σ-allowed regions in the parameter space; the application of our results to forthcoming experiments on nuclear $0\nu\beta\beta$ decay and neutrino oscillations is also discussed in the same section. Sec.4.8 summarizes our conclusions.

4.2 Meaning of residual flavor symmetry of M_ν

It would be useful to focus on the feature [7–9] of M_ν that it has a residual (sometimes called 'remnant' [202]) $\mathbb{Z}_2 \times \mathbb{Z}_2$ flavor symmetry and at the same time review the representation content of the latter. Such an exercise will enable us to set up the theoretical machinery needed to apply the idea to Simple Real Scaling. In addition, this will lead us to its real generalization as well as to its complex extension.

Let G be a generic 3×3 unitary matrix representation of some horizontal symmetry of M_ν effected through the similarity transformation

$$G^T M_\nu G = M_\nu. \tag{4.7}$$

Eqs. (4.2) and (4.7) lead to the conclusion that the unitary matrix $U' \equiv GU$ also puts M_ν into a diagonal form by a similarity transformation, i.e. $U'^T M_\nu U' = M_\nu^d$. It can then be shown [7] that, if m_1, m_2 and m_3 are nondegenerate, G has eigenvalues ± 1 and is diagonalized by U. Thus

$$GU = Ud, \tag{4.8}$$

$$d^2 = I. \tag{4.9}$$

Here d is a 3×3 diagonal matrix in flavor space with $d_{lm} = \pm\delta_{lm}$. There are eight possible distinct forms for d. Two of these are trivial ˘ being the unit and the negative unit matrices. Of the remaining six, three are negatives of the other three. Finally, we have three G_a's (a = 1, 2, 3) but it is sufficient to consider any two of those as independent on account of the relation $G_a = \epsilon_{abc} G_b G_c$. The two independent G_a's (chosen here as $G_{2,3}$) are representations of a residual $\mathbb{Z}_2 \times \mathbb{Z}_2$ symmetry in the Majorana mass term of the neutrino Lagrangian. It follows from (4.8) and (4.9) that

$$G^2 = I, \ \text{det G} = \pm 1. \tag{4.10}$$

The eigenvalue equation (4.8) needs to be considered for the two independent d's, i.e. d_2 and d_3, corresponding respectively to G_2 and G_3. Suppose we choose

$$d_2 = \text{diag}\,(-1, 1, -1), \tag{4.11}$$

$$d_3 = \text{diag}\,(-1, -1, 1) \tag{4.12}$$

for det G =1. (The choice for the case det $G = -1$ is a trivial extension with $-d_2$ and $-d_3$.) Now

$$G_{2,3} = U d_{2,3} U^\dagger \tag{4.13}$$

can be obtained by use of the explicit form of U as given in (4.3). For instance, let us consider the situation for $\mu\tau$ interchange symmetry [10] which implies $\theta_{23} = \pi/4$ and $\theta_{13} = 0$. Now we obtain

$$G_2 = \begin{pmatrix} -\cos 2\theta_{12} & 2^{-\frac{1}{2}}\sin 2\theta_{12} & -2^{-\frac{1}{2}}\sin 2\theta_{12} \\ 2^{-\frac{1}{2}}\sin 2\theta_{12} & -\frac{1}{2}(1-\cos 2\theta_{12}) & -\frac{1}{2}(1+\cos 2\theta_{12}) \\ -2^{-\frac{1}{2}}\sin 2\theta_{12} & -\frac{1}{2}(1+\cos 2\theta_{12}) & -\frac{1}{2}(1-\cos 2\theta_{12}) \end{pmatrix}, G_3^{\mu\tau} = \begin{pmatrix} -1 & 0 & 0 \\ 0 & 0 & 1 \\ 0 & 1 & 0 \end{pmatrix} \tag{4.14}$$

The above G_3 explicitly implements $\mu\tau$ interchange in the neutrino flavor basis and hence has been labeled with the superscript $\mu\tau$. Thus one can now identify one of the two residual $\mathbb{Z}_2$'s as $\mathbb{Z}_2^{\mu\tau}$. The full residual symmetry in this case is $\mathbb{Z}_2 \times \mathbb{Z}_2^{\mu\tau}$. Our aim would be to undertake a similar task with scaling symmetry in obtaining a $\mathbb{Z}_2^{scaling}$. It may be mentioned that some authors [203] have generalized $G_3^{\mu\tau}$ to

$$G_3^{G\mu\tau} = \begin{pmatrix} -1 & 0 & 0 \\ 0 & \cos 2\theta_{23} & \sin 2\theta_{23} \\ 0 & \sin 2\theta_{23} & \cos 2\theta_{23} \end{pmatrix} \tag{4.15}$$

which can accommodate an arbitrary θ_{23} but still has $\theta_{13} = 0$. A somewhat different use of the residual symmetry approach with another pair of $\mathbb{Z}_2$'s was made in Ref. [204–206].

A comment on the use of the residual $\mathbb{Z}_2 \times \mathbb{Z}_2$ symmetry would be in order. One could start from any arbitrary ansatz on U_{PMNS}, reconstruct the residual $\mathbb{Z}_2 \times \mathbb{Z}_2$ symmetry and work out the consequences. However, the $\mathbb{Z}_2 \times \mathbb{Z}_2$ symmetry emerging from an arbitrary ansatz may not follow from a larger symmetry group or have some deeper flavor meaning. The SRS ansatz has been shown to follow [15,16] from a larger flavor symmetry group $D_4 \times \mathbb{Z}_2$.

4.3 Simple Real Scaling and its real generalization

Simple Real Scaling and the corresponding M_ν^{SRS}, cf. (4.5), were already introduced in Sec.4.1. It is evident from (4.5) that the latter has a vanishing determinant, i.e. one null eigenvalue. The corresponding eigenvector, given that θ_{12} and θ_{23} are known to be hugely nonzero, can be identified only with the third column of U^{SRS} and written as

$$C_3^{SRS} = \left[0, (1+k^2)^{-\frac{1}{2}} e^{i\frac{\beta}{2}}, k(1+k^2)^{-\frac{1}{2}} e^{i\frac{\beta}{2}}\right]^T. \tag{4.16}$$

Two immediate consequences are that $m_3 = 0$, i.e. the neutrino mass ordering is inverted ($m_{2,1} > m_3$), and $\theta_{13} = 0$. The full U^{SRS} can be written with an undetermined angle θ_{12} and the corresponding c_{12}, s_{12} as

$$U^{SRS} = \begin{pmatrix} c_{12} & s_{12} e^{i\frac{\alpha}{2}} & 0 \\ -k(1+k^2)^{-\frac{1}{2}} s_{12} & k(1+k^2)^{-\frac{1}{2}} c_{12} e^{i\frac{\alpha}{2}} & (1+k^2)^{-\frac{1}{2}} e^{i\frac{\beta}{2}} \\ (1+k^2)^{-\frac{1}{2}} s_{12} & -(1+k^2)^{-\frac{1}{2}} c_{12} e^{i\frac{\alpha}{2}} & k(1+k^2)^{-\frac{1}{2}} e^{i\frac{\beta}{2}} \end{pmatrix}. \tag{4.17}$$

A comparison between (4.3) and (4.17) immediately yields

$$\tan\theta_{23} = k^{-1}. \tag{4.18}$$

As we shall see, (4.18) is going to survive both the real generalization and the complex CP-transformed extension of SRS. An expression for $G_3^{scaling}$ as a representation for

$\mathbb{Z}_2^{scaling}$ can now be derived by use of (4.13) . On utilizing U^{SRS} from (4.17) and d_3 from (4.12), we have

$$G_3^{scaling} = \begin{pmatrix} -1 & 0 & 0 \\ 0 & (1-k^2)(1+k^2)^{-1} & 2k(1+k^2)^{-1} \\ 0 & 2k(1+k^2)^{-1} & -(1-k^2)(1+k^2)^{-1} \end{pmatrix} = (G_3^{scaling})^T. \quad (4.19)$$

The $\mathbb{Z}_2^{scaling}$ symmetry of M_ν^{SRS} ensures that

$$(G_3^{scaling})^T M_\nu^{SRS} G_3^{scaling} = M_\nu^{SRS}. \quad (4.20)$$

It may be noted that (4.20) does not lead uniquely to the form (4.5). Further, while the form of $G_3^{scaling}$ follows uniquely from U^{SRS} of (4.17) via the relation been G_3 and d_3, the reverse is not the case. Indeed, though the third column of U, reconstructed from $G_3^{scaling}$, must be C_3^{SRS} of (4.16) since $(d_3)_{33} = 1$, its first two columns could be an arbitrary orthogonal pair. That occurs because of the degeneracy of the (1,1) and (2,2) elements in d_3. The full residual symmetry of M_ν^{SRS} is $\mathbb{Z}_2^k \times \mathbb{Z}_2^{scaling}$, where a representation for $\mathbb{Z}_2^k$ is $G_2^k = U^{SRS} d_2 U^{SRS\dagger}$. Explicitly,

$$G_2^k = \begin{pmatrix} -\cos 2\theta_{12} & k(1+k^2)^{-1/2}\sin 2\theta_{12} & -(1+k^2)^{-1/2}\sin 2\theta_{12} \\ k(1+k^2)^{-1/2}\sin 2\theta_{12} & -(1+k^2)^{-1}(1-k^2\cos 2\theta_{12}) & -k(1+k^2)^{-1}(1+\cos 2\theta_{12}) \\ -(1+k^2)^{-1/2}\sin 2\theta_{12} & -k(1+k^2)^{-1}(1+\cos 2\theta_{12}) & -(1+k^2)^{-1}(k^2-\cos 2\theta_{12}) \end{pmatrix} \quad (4.21)$$

which obeys

$$(G_2^k)^T M_\nu^{SRS} G_2^k = M_\nu^{SRS}. \quad (4.22)$$

A good check is that, for $k = 1$, the scaling procedure just reduces to $\mu\tau$ interchange with the additional constraint $M^\nu_{\mu\mu} = M^\nu_{\mu\tau}$. But the point of real interest is that M_ν^{SRS} of (4.5) is not the most general form obeying (4.20). The latter may be worked out to be

$$M_\nu^{GRS} = \begin{pmatrix} x & -Yk & Y \\ -Yk & Z - Wk^{-1}(k^2-1) & W \\ Y & W & Z \end{pmatrix}, \tag{4.23}$$

where W is another a priori unknown mass dimensional complex quantity. We call this form of M_ν the Generalized Real Scaling ansatz and denote it by the superscript GRS. Evidently, the specific choice $W = -Zk$ reduces M_ν^{GRS} to M_ν^{SRS}. The neutrino mass matrix M_ν^{GRS} of (4.23) has interesting properties. For one thing, it has a determinant which does not appear to vanish. Therefore, we take all neutrino masses to be nonzero and can accommodate a nonzero m_3 and in principle a normal mass ordering with $m_{2,1} < m_3$. However, being invariant under a similarity transformation by $G_3^{scaling}$ of (4.19), the third column of the corresponding U^{GRS} is constrained to be C_3^{SRS} of (4.16). Consequently, one obtains a vanishing θ_{13} which is now experimentally known to be nonzero. Thus M_ν^{GRS} of (4.23) is unacceptable. A more extended version of scaling in the neutrino mass matrix is needed to describe nature. This is what will be provided in the next section.

4.4 Complex extension of scaling ansatz

It would be useful to first recall how the complex extension of $\mu\tau$ interchange symmetry was originally made [10]. The $\mu\tau$ interchange invariant $M_\nu^{\mu\tau}$ obeys the condition

$$(G_3^{\mu\tau})^T M_\nu^{\mu\tau} G_3^{\mu\tau} = M_\nu^{\mu\tau} \tag{4.24}$$

with $G_3^{\mu\tau}$ given by (4.14). Eq. (4.24) forces $M_\nu^{\mu\tau}$ to have the form

$$M_\nu^{\mu\tau} = \begin{pmatrix} A & B & -B \\ B & C & D \\ -B & D & C \end{pmatrix}, \tag{4.25}$$

with A, B, C, D as mass dimensional complex quantities. It is well-known that (4.25) leads to $\theta_{13} = 0$ and cannot be accepted as it stands.

Grimus and Lavoura made an alternative proposal, namely the complex-extended invariance relation

$$(G_3^{\mu\tau})^T M_\nu G_3^{\mu\tau} = M_\nu^*. \tag{4.26}$$

This was justified [10] by means of a non-standard CP-transformation [112, 207, 208] on the ν_α field which is generally represented as[1]

$$\nu_{L\alpha} \to i G_{\alpha\beta} \gamma^0 \nu_{L\beta}^C \tag{4.27}$$

with $G_{\alpha\beta}$ as the matrix element of the flavor symmetry. Eq. (4.27) along with (4.1) leads to (4.26) if $G_{\alpha\beta}$ is considered as $G_3^{\mu\tau}$. Suffice it to say that (4.26) leads to a

[1]It is a theoretically interesting question whether such an extended CP-invariance can arise from an automorphism of a larger flavor symmetry like in the top-down approach of Ref. [11]. But we do not explore this possibility here.

complex-extended $\mu\tau$ ($CE\mu\tau$) symmetric form of M_ν:

$$M_\nu^{CE\mu\tau} = \begin{pmatrix} a & B & B^* \\ B & C & d \\ B^* & d & C^* \end{pmatrix}, \tag{4.28}$$

where a, d are real and B, C are complex mass dimensional quantities in general. Once again, since the determinant does not vanish, we take all neutrino masses to be nonzero. The observable consequences of (4.28) are: $\theta_{23} = \pi/4$, $\cos\delta = 0$, α, $\beta = 0$ or π while θ_{13} is in general nonzero. A further extension of this approach has recently been made [202, 209] allowing nonmaximal values for θ_{23} and Dirac CP-violation.

We have derived (4.18), i.e. $\tan\theta_{23} = k^{-1}$, so that atmospheric neutrino mixing is not forced to be strictly maximal. On the other hand, the observed fact that $\tan\theta_{23}$ is not far from unity implies that so is k. Our proposed relation, in place of (4.26), is

$$(G_3^{scaling})^T M_\nu G_3^{scaling} = M_\nu^*, \tag{4.29}$$

with $G_3^{scaling}$ as given in (4.19) and, as stated earlier, in the basis where the charged lepton mass matrix is diagonal and positive. The general form of M_ν^{CES}, as given in (4.6), follows in consequence. It is important to note that M_ν^{CES} of (4.6) has a structure that is quite different from that of either M_ν^{SRS} of (4.5) or M_ν^{GRS} of (4.23). If all imaginary parts in M_ν^{CES} are set equal to zero, a form similar to that of M_ν^{GRS} is recovered but with all real entries while those in M_ν^{GRS} of (4.23) are in general complex. Therefore, no special choice in M_ν^{CES} can yield M_ν^{SRS} or M_ν^{GRS} in their respective generalities.

Grimus and Lavoura [10] had proved a corollary of complex-extended invariance.

This can be stated with respect to a relation such as (4.26) or (4.29) as

$$G_3^{scaling} U^* = U\tilde{d} \tag{4.30}$$

with $\tilde{d}$ as a diagonal matrix. Once again, $\tilde{d}_{lm} = \pm\, \delta_{lm}$ if the neutrino masses m_1, m_2, m_3 are all nonzero and nondegenerate. The key difference between (4.30) and (4.8) is the complex conjugation of U in the LHS. Let us take

$$\tilde{d} = \mathrm{diag}\,(\tilde{\mathrm{d}}_1, \tilde{\mathrm{d}}_2, \tilde{\mathrm{d}}_3), \tag{4.31}$$

where each $\tilde{d}_i$ $(i = 1, 2, 3)$ can be $+1$ or -1. With $G_3 = G_3^{scaling}$, (4.30) can be written explicitly :

$$\begin{pmatrix} -(U_{e1}^{CES})^* & -(U_{e2}^{CES})^* & -(U_{e3}^{CES})^* \\ \frac{1-k^2}{1+k^2}(U_{\mu 1}^{CES})^* + \frac{2k}{1+k^2}(U_{\tau 1}^{CES})^* & \frac{1-k^2}{1+k^2}(U_{\mu 2}^{CES})^* + \frac{2k}{1+k^2}(U_{\tau 2}^{CES})^* & \frac{1-k^2}{1+k^2}(U_{\mu 3}^{CES})^* + \frac{2k}{1+k^2}(U_{\tau 3}^{CES})^* \\ \frac{2k}{1+k^2}(U_{\mu 1}^{CES})^* - \frac{1-k^2}{1+k^2}(U_{\tau 1}^{CES})^* & \frac{2k}{1+k^2}(U_{\mu 2}^{CES})^* - \frac{1-k^2}{1+k^2}(U_{\tau 2}^{CES})^* & \frac{2k}{1+k^2}(U_{\mu 3}^{CES})^* - \frac{1-k^2}{1+k^2}(U_{\tau 3}^{CES})^* \end{pmatrix}$$

$$= \begin{pmatrix} \tilde{d}_1 U_{e1}^{CES} & \tilde{d}_2 U_{e2}^{CES} & \tilde{d}_3 U_{e3}^{CES} \\ \tilde{d}_1 U_{\mu 1}^{CES} & \tilde{d}_2 U_{\mu 2}^{CES} & \tilde{d}_3 U_{\mu 3}^{CES} \\ \tilde{d}_1 U_{\tau 1}^{CES} & \tilde{d}_2 U_{\tau 2}^{CES} & \tilde{d}_3 U_{\tau 3}^{CES} \end{pmatrix}. \tag{4.32}$$

It is evident from (4.32) that the choice $\tilde{d}_1 = 1$ leads to an imaginary U_{e1} in contradiction with the real (1,1) element of (4.3); this choice is hence excluded. Note that the choice of U_{PMNS} in (4.3) is simply due to the choice of the Weak Basis where the neutrino fields are phase rotated. However, in Sec. 4.7, we demonstrate that the physical results derived here are basis independent, i.e., the inclusion of an unphysical phase matrix does not impair our predictions. There are now four permitted cases a,

b, c, d with the following four combinations allowed for $\tilde{d}$:

$$\tilde{d}_a \equiv \text{diag}\,(-1, 1, 1), \tag{4.33}$$

$$\tilde{d}_b \equiv \text{diag}\,(-1, 1, -1), \tag{4.34}$$

$$\tilde{d}_c \equiv \text{diag}\,(-1, -1, 1), \tag{4.35}$$

$$\tilde{d}_d \equiv \text{diag}\,(-1, -1, -1). \tag{4.36}$$

The above can be written compactly as

$$\tilde{d}_{a,b,c,d} = \text{diag}\,(-1, \eta, \xi) \tag{4.37}$$

$$\eta_{a,b} = 1, \eta_{c,d} = -1, \tag{4.38}$$

$$\xi_{a,c} = 1, \xi_{b,d} = -1. \tag{4.39}$$

Comparing with (4.3), we obtain

$$e^{-i\alpha} = -\eta \tag{4.40}$$

$$e^{i(2\delta-\beta)} = -\xi. \tag{4.41}$$

Thus we are led to the result that $\alpha = \pi, 0$ for $\eta = +1, -1$ respectively; in a similar manner $2\delta - \beta = \pi, 0$ for $\xi = +1, -1$ respectively. We can derive from (4.32) altogether six independent constraint conditions as linear relations among various elements of U^{CES} and $(U^{CES})^*$. These are listed in Table 4.1. More information is obtained by use of the explicit expressions of $U^{CES}_{l\alpha}$ from (4.3). Consider the real and imaginary parts of the constraint condition on $U^{CES}_{\tau 3}$ given in the bottom line in Table 4.1.

Since c_{13} is known to be nonzero, it can be canceled from both sides. Now, from the respective real and imaginary parts, we have the relations

$$2kc_{23}\cos\frac{\beta}{2} = [k^2(1+\xi)-1+\xi]s_{23}cos\frac{\beta}{2}, \tag{4.42}$$

$$2kc_{23}\sin\frac{\beta}{2} = [k^2(1-\xi)-1-\xi]s_{23}\sin\frac{\beta}{2}. \tag{4.43}$$

Table 4.1: Constraint equations on elements of the mixing matrix

Element of U^{CES}	Constraint condition
$\mu 1$	$2kU^{CES}_{\mu 1} = (1-k^2)U^{CES}_{\tau 1} - (1+k^2)(U^{CES}_{\tau 1})^*$
$\tau 1$	$2kU^{CES}_{\tau 1} = -(1-k^2)U^{CES}_{\mu 1} - (1+k^2)(U^{CES}_{\mu 1})^*$
$\mu 2$	$2kU^{CES}_{\mu 2} = (1-k^2)U^{CES}_{\tau 2} + \eta(1+k^2)(U^{CES}_{\tau 2})^*$
$\tau 2$	$2kU^{CES}_{\tau 2} = -(1-k^2)U^{CES}_{\mu 2} + \eta(1+k^2)(U^{CES}_{\mu 2})^*$
$\mu 3$	$2kU^{CES}_{\mu 3} = (1-k^2)U^{CES}_{\tau 3} + \xi(1+k^2)(U^{CES}_{\tau 3})^*$
$\tau 3$	$2kU^{CES}_{\tau 3} = -(1-k^2)U^{CES}_{\mu 3} + \eta(1+k^2)(U^{CES}_{\mu 3})^*$

Since $\xi^2 = 1$, the product of the above two equations leads to the result

$$\sin\beta = 0, \tag{4.44}$$

or $\beta = 0$ or π. There are now four options:

$$\beta = 0, \xi = 1 \Rightarrow \tan\theta_{23} = k^{-1}, \tag{4.45}$$

$$\beta = 0, \xi = -1 \Rightarrow \tan\theta_{23} = -k, \tag{4.46}$$

$$\beta = \pi, \xi = 1 \Rightarrow \tan\theta_{23} = -k, \tag{4.47}$$

$$\beta = \pi, \xi = -1 \Rightarrow \tan\theta_{23} = k^{-1}. \tag{4.48}$$

The option $\beta = 0$, $\xi = 1$ for cases a and c, cf. (4.33) and (4.35), as well as $\beta = \pi$, $\xi = 1$ for cases b and d, cf. (4.34) and (4.36), yield the scaling relation (4.18) while the other two options require $\tan\theta_{23}$ to equal $-k$. As will be shown below, the latter possibility is inconsistent with other constraint conditions. Our final result on the Majorana phases is that both α and β are restricted to be 0 or π. A combination of information from $0\nu\beta\beta$ decay, the cosmological upper bound on $\Sigma_i m_i$ and the effective mass $\Sigma_i|U_{ei}|^2 m_i$ measured in single β-decay is expected to experimentally constrain [127] these phases.

To proceed further, consider the constraint condition on $U^{CES}_{\tau 2}$ given in the 4th line from the top of Table 4.1. The corresponding real and imaginary parts respectively yield

$$\begin{aligned}
&2k[c_{12}s_{23}\cos\frac{\alpha}{2} + s_{12}s_{13}c_{23}\cos(\delta + \frac{\alpha}{2})] \\
&= [1 - k^2 - \eta(1 + k^2)][c_{12}c_{23}\cos\frac{\alpha}{2} - s_{12}s_{13}s_{23}\cos(\delta + \frac{\alpha}{2})], \qquad (4.49)\\
&2k[c_{12}s_{23}\sin\frac{\alpha}{2} + s_{12}s_{13}c_{23}\sin(\delta + \frac{\alpha}{2})] \\
&= [1 - k^2 - \eta(1 + k^2)][c_{12}c_{23}\sin\frac{\alpha}{2} - s_{12}s_{13}s_{23}\sin(\delta + \frac{\alpha}{2})]. \qquad (4.50)
\end{aligned}$$

Let us now take the two cases at hand.

Case 1: $\eta = 1$, $\alpha = \pi$

On utilizing that each of s_{12}, s_{13} and c_{23} is nonzero, one obtains from (4.49) and (4.50) the respective relations

$$(\tan\theta_{23} - k^{-1})\sin\delta = 0, \qquad (4.51)$$

$$c_{12}(\tan\theta_{23} - k^{-1}) + s_{12}s_{13}(1 + k^{-1}\tan\theta_{23})\cos\delta = 0. \qquad (4.52)$$

Case 2: $\eta = -1$, $\alpha = 0$

It is easy to see that here one obtains the same pair of equations, namely (4.51) and

(4.52), but in a reverse sequence.

Eq. (4.52) has important implications. If $\tan\theta_{23}$ is put equal to $-k$, instead of k^{-1}, one is led to $c_{12} = 0$ in contradiction with experiment [30]. Therefore, the two options $\beta = 0$, $\xi = 1$ and $\beta = \pi$, $\xi = -1$ need to be retained with the other two options $\beta = 0$, $\xi = -1$ and $\beta = \pi$, $\xi = 1$ discarded. Now that $\tan\theta_{23}$ does equal k^{-1}, i.e. (4.18) holds, from (4.52) we have

$$\cos\delta = 0, \tag{4.53}$$

i.e. leptonic Dirac CP-violation is maximal with δ being either $\pi/2$ or $3\pi/2$. However, we are unable to distinguish between these two options since we have no statement on the sign of $\sin\delta$.

Table 4.2: Predictions of the CP phases

$\tilde{d}$	α	β	$\cos\delta$
$\tilde{d}_a = \text{diag}\,(-1, +1, +1)$	π	0	0
$\tilde{d}_b = \text{diag}\,(-1, +1, -1)$	π	π	0
$\tilde{d}_c = \text{diag}\,(-1, -1, +1)$	0	0	0
$\tilde{d}_d = \text{diag}\,(-1, -1, -1)$	0	π	0

We have checked that (4.53) consistently follows from the remaining four constraint equations of Table 4.1 and that no new condition emerges. Finally, we are left with four options, as shown in Table 4.2. Each of these implies (4.53), i.e. the maximality of leptonic Dirac CP violation which enters via U_{PMNS}.

4.5 Origin of neutrino masses from type-I seesaw

So far the analysis was based on an effective light neutrino mass matrix; no specific origin of neutrino masses has been considered. There are plenty of neutrino mass models that deal with Majorana neutrinos. However, here we discuss the realization of the complex extended scaling neutrino mass matrix M_ν^{CES} through the type-I seesaw mechanism via three heavy right-handed neutrino fields $N_{lR}\,(l=1,2,3)$ with a Majorana mass matrix M_R. We choose a Weak Basis in which the charged lepton and the right-handed neutrino mass matrices are diagonal and nondegenarate. With m_D as the Dirac mass matrix and $M_R = \mathrm{diag}\,(\mathrm{M}_1, \mathrm{M}_2, \mathrm{M}_3)$, the neutrino mass terms read

$$-\mathcal{L}^{\nu,N}_{mass} = \bar{N}_{lR}(m_D)_{l\alpha}L_\alpha + \frac{1}{2}\bar{N}_{lR}(M_R)_l\delta_{lm}N^C_{mR} + \text{h.c.} \tag{4.54}$$

The effective light neutrino mass matrix is given by the standard seesaw relation

$$M_\nu = -m_D^T M_R^{-1} m_D. \tag{4.55}$$

We represent the G's, introduced earlier for left handed fields, generically by G_L and define a corresponding G_R for N_R. The residual CP transformations on the neutrino fields are defined as [209]

$$\nu_{L\alpha} \rightarrow i(G_L)_{\alpha\beta}\gamma^0\nu^C_{L\beta}, \quad N_{R\alpha} \rightarrow i(G_R)_{\alpha\beta}\gamma^0 N^C_{R\beta}. \tag{4.56}$$

The invariance of the mass terms of (4.54) under the CP transformations defined in (4.56) leads to the relations

$$G_R^\dagger m_D G_L = m_D^*, \quad G_R^\dagger M_R G_R^* = M_R^*. \tag{4.57}$$

Eqs. (4.55) and (4.57) together imply $G_L^T M_\nu G_L = M_\nu^*$. Now, specifying G_L by $G_3^{scaling}$, we obtain the key equation

$$(G_3^{scaling})^T M_\nu G_3^{scaling} = M_\nu^*. \tag{4.58}$$

Since we choose the right handed neutrino mass matrix M_R to be diagonal, the symmetry matrix G_R is diagonal with entries ± 1, i.e.

$$G_R = \text{diag}\,(\pm 1, \pm 1, \pm 1). \tag{4.59}$$

Hence there are eight different structures of G_R. Correspondingly, from the first relation of (4.57), there are eight different structures of m_D. Unlike the complex transformations of m_D and M_R in (4.57), we now have real symmetry transformations $G_R^\dagger m_D G_L = m_D$ and $G_R^\dagger M_R G_R^* = M_R$. It can be shown by tedious algebra that, except for $G_R = \text{diag}(-1,-1,-1)$, all other structures of G_R are incompatible with scaling symmetry, i.e. cannot generate M_ν^{GRS}. Thus we take $G_R = \text{diag}(-1,-1,-1)$ as the only viable residual symmetry on the right-handed neutrino field. Now, $G_R^\dagger m_D G_L = m_D^*$ can be written as$m_D G_L = -m_D^*$ which is basically a complex extension of the Joshipura-Rodejohann result $m_D G_L = -m_D$ [210]. In our context, this can be rewritten as

$$m_D G_3^{scaling} = -m_D^*. \tag{4.60}$$

The most general m_D that satisfies (4.60) is

$$m_D^{CES} = \begin{pmatrix} a & b_1 + ib_2 & -b_1/k + ib_2 k \\ e & c_1 + ic_2 & -c_1/k + ic_2 k \\ f & d_1 + id_2 & -d_1/k + id_2 k \end{pmatrix}, \tag{4.61}$$

where a, $b_{1,2}$, $c_{1,2}$, $d_{1,2}$, e and f are arbitrary real mass dimensional quantities. Using (4.55), M_ν^{CES} of (4.6) is obtained with the parameters as given in Table 4.3. Some detailed interesting consequences of m_D^{CES}, specifically with respect to leptogenesis, will be studied elsewhere.

Table 4.3: Parameters of M_ν^{CES} in terms of the parameters of m_D and M_R

$x = -(\frac{a^2}{M_1} + \frac{e^2}{M_2} + \frac{f^2}{M_3})$
$y_1 = \frac{1}{k}(\frac{ab_1}{M_1} + \frac{ec_1}{M_2} + \frac{fd_1}{M_3})$
$y_2 = k(\frac{ab_2}{M_1} + \frac{ec_2}{M_2} + \frac{fd_2}{M_3})$
$z_1 = -\frac{1}{k^2}(\frac{b_1^2}{M_1} + \frac{c_1^2}{M_2} + \frac{d_1^2}{M_3}) + k^2(\frac{b_2^2}{M_1} + \frac{c_2^2}{M_2} + \frac{d_2^2}{M_3})$
$z_2 = \frac{2b_1b_2}{M_1} + \frac{2c_1c_2}{M_2} + \frac{2d_1d_2}{M_3}$
$w = \frac{1}{k}(\frac{b_1^2}{M_1} + \frac{c_1^2}{M_2} + \frac{d_1^2}{M_3}) + k(\frac{b_2^2}{M_1} + \frac{c_2^2}{M_2} + \frac{d_2^2}{M_3})$

4.6 Phenomenological constraints and consequences

We need to numerically pin down the mass dimensional six real parameters x, y_1, y_2, z_1, z_2 and w of M_ν^{CES} by inputting the 3σ ranges of quantities measured in neutrino oscillation experiments. To that end, we use the values from a recent global analysis [30]. In addition, we use the cosmological upper limit [20] of 0.23 eV on the sum $m_1 + m_2 + m_3$ of the masses of the neutrinos. These input numbers are shown

Table 4.4: Input values used

θ_{12} (deg)	θ_{23} (deg)	θ_{13} (deg)	Δm^2_{21} $\times 10^5 \mathrm{eV}^2$	$\lvert\Delta m^2_{31}\rvert$ $\times 10^3(\mathrm{eV}^2)$	$\Sigma_i m_i$ (eV)
$31.29 - 35.91$	$38.3 - 53.3$	$7.87 - 9.11$	$7.02 - 8.09$	$2.32 - 2.59$	< 0.23

in Table 4.4. In terms of output, we obtain the 3σ allowed intervals of the above mentioned six real parameters and from those the 3σ allowed ranges of the individual neutrino masses m_1, m_2, m_3. Both types of neutrino mass ordering, normal as well as inverted, are found to be allowed. All these values are listed in Tables 4.5 and 4.6 respectively for the two separate categories of mass ordering. We notice that, for

Table 4.5: Output values obtained for normal mass ordering with the best fit m's given within brackets

x (eV)	y_1 (eV)	y_2 (eV)	z_1 (eV)	z_2 (eV)	w (eV)
-0.20 – $+0.21$	-0.12 – $+0.11$	-0.05 – $+0.05$	-0.17 – $+0.17$	-0.18 – $+0.17$	-0.16 – $+0.15$
m_1 (eV)		m_2 (eV)		m_3 (eV)	
$9.2 \times 10^{-5} - 0.071$ (0.052)		$0.01 - 0.077$ (0.054)		$0.051 - 0.082$ (0.072)	

Table 4.6: Output values obtained for inverted mass ordering with the best fit m's given within brackets

x (eV)	y_1 (eV)	y_2 (eV)	z_1 (eV)	z_2 (eV)	w (eV)
-0.44 – $+0.46$	-0.16 – $+0.16$	-0.14 – $+0.14$	-0.01 – $+0.01$	-0.01 – $+0.01$	-0.05 – $+0.06$
m_1 (eV)		m_2 (eV)		m_3 (eV)	
$0.049 - 0.079$ (0.068)		$0.051 - 0.085$ (0.069)		$8.2 \times 10^{-5} - 0.068$ (0.048)	

both types of ordering, the neutrino masses become hierarchical, i.e. $m_{2,1} << m_3$ for normal ordering and $m_{2,1} >> m_3$ for inverted ordering, for low values of the lightest neutrino mass. However they tend towards quasi-degeneracy $m_1 \sim m_2 \sim m_3$ as the latter increases to its permitted maximum value ~ 0.07 eV. This is clear from the mass bands shown in Fig. 4.1.

Neutrinoless double beta decay $0\nu\beta\beta$:

This is the lepton number violating process

$$(A, Z) \longrightarrow (A, Z+2) + 2e^- \tag{4.62}$$

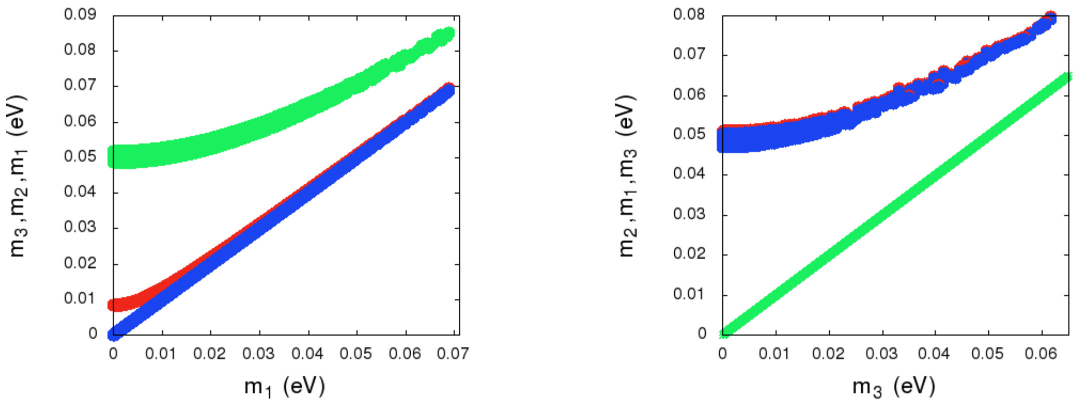

Figure 4.1: *Plots of the mass band for normal (left) and inverted (right) mass ordering. We have choosen to plot the lightest eigenvalue also in the ordinate to bring three mass bands together. Color code: green (m_3), red (m_2) and blue (m_1).*

with no final state neutrinos. An observation of the decay will confirm the Majorana nature of neutrinos which is yet to be established. The corresponding the half-life [211] is given by

$$\frac{1}{T_1^{0\nu}/2} = G_{0\nu}|M_{0\nu}|^2|M_{ee}^\nu|^2 m_e^{-2}. \tag{4.63}$$

where $G_{0\nu}$ is a phase space factor, $M_{0\nu}$ is the nuclear matrix element (NME), m_e is the electron mass and finally $|M_{ee}^\nu|$ is the (1,1) element of M^ν which can also be written as $\Sigma_i m_i U_{ei}^2$. Following the PDG parametrization of the mixing matrix U_{PMNS}, one can write M_{ee}^ν as

$$M_{ee}^\nu = c_{12}^2 c_{13}^2 m_1 + s_{12}^2 c_{13}^2 m_2 e^{i\alpha} + s_{13}^2 m_3 e^{i(\beta-2\delta)}. \tag{4.64}$$

There are several ongoing experiments which have put significant upper limits on $|M_{ee}^\nu|$. Some recent experiments like KamLAND-Zen [26] and EXO [25] have improved this upper bound to 0.35 eV. However, the most significant upper bound on $|M_{ee}^\nu|$ to date is put by GERDA phase-I data [21] to be 0.22 eV; this is likely to be lowered by GERDA phase -II data [27] to around 0.098 eV.

In our model there are four sets of values of the CP-violating phases α and β for each neutrino mass ordering . Since $|M^{\nu}_{ee}|$ is sensitive to the CP phases, we get four different plots for each mass ordering as shown in Fig. 4.2. The same plots are valid for both types of mass ordering provided the horizontal axis is taken to represent the lightest neutrino mass m_1 or m_3 - depending on the ordering. As

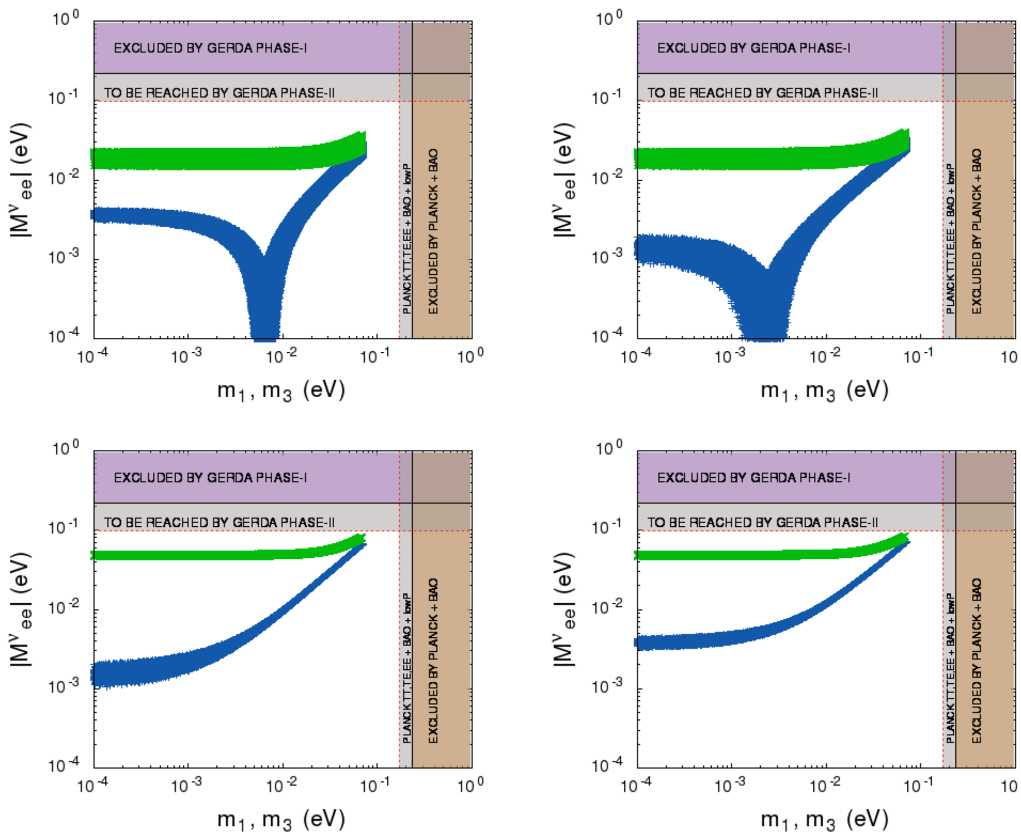

Figure 4.2: *Plot of $|M^{\nu}_{ee}|$ vs. the lightest neutrino mass: the top two figures represent Case A (left) and Case B (right) while the figures in the lower panel represent Case C (left) and Case D (right).*

mentioned earlier, we have used the upper bound of 0.23 eV on $\Sigma_i m_i$. These plots lead to upper bounds on the lightest neutrino mass for both cases of mass ordering. For hierarchical neutrinos, $|M^{\nu}_{ee}|$ is found to lead to an upper limit which is below the reach of the GERDA phase-II data. The latter appears close to being obtainable only for a quasidegenerate neutrino mass spectrum ($m_{lightest} > 0.07$ eV). However the value predicted in our model could be probed by a combination of GERDA and MAJORANA experiments [212]. In order to explain the nature of the plots analytically, let us first consider the inverted mass ordering: In this case, with the approximations $m_3 \simeq 0$ and $m_1 \simeq m_2$, the probed effective mass $|M^\nu_{ee}|$ simplifies to

$$|M^\nu_{ee}| = \sqrt{|\Delta m_{32}|^2} c^2_{13} [\{1 - s^2_{12}(1 - \cos\alpha)\}^2 + s^4_{12} \sin^2\alpha]^{1/2}. \tag{4.65}$$

Clearly, $|M^\nu_{ee}|$ is insensitive to the phases β and δ. On the other hand, for $\alpha = 0$ and π (4.65) simplifies to

$$|M^\nu_{ee}| = \sqrt{|\Delta m_{32}|^2} c^2_{13} \tag{4.66}$$

and

$$|M^\nu_{ee}| = \sqrt{|\Delta m_{32}|^2} c^2_{13} [\{1 - 2s^2_{12}\}^2] \tag{4.67}$$

respectively. Hence, for $\alpha = \pi$ (cases A, B), $|M^\nu_{ee}|$ is suppressed as compared to the case $\alpha = 0$ (C, D). For a normal mass ordering, in addition to the s_{13} suppression, there is a significant interference between the first two terms, thus lowering the value of $|M^\nu_{ee}|$. However, if $\alpha = 0$, the first two terms interfere constructively and then we obtain a lower bound ($\sim 10^{-3}$ eV for Case C and $\sim 5 \times 10^{-3}$ eV for Case D) despite this being a case of normal mass ordering. This is one of the remarkable results of the present analysis. On the other hand, for $\alpha = \pi$, the first two terms interfere destructively, for the case of a normal mass ordering; consequently, a sizable cancellation between them brings down the value of $|M^\nu_{ee}|$ and results in the kinks shown by the lower curves in the top two figures.

CP asymmetry in neutrino oscillations:

Here we discuss the determination of our predicted maximal Dirac CP-violating phase δ by means of neutrino oscillation studies. This δ will show up in the asymmetry parameter $A_{\alpha\beta}$, defined as

$$A_{\alpha\beta} = P(\nu_\alpha \to \nu_\beta) - P(\bar{\nu_\alpha} \to \bar{\nu_\beta}), \tag{4.68}$$

where $\alpha, \beta = (e, \mu, \tau)$ are flavor indices and the P's are transition probabilities. Let us consider first $\nu_\mu \to \nu_e$ oscillation in vacuum. The transition probability can now be written (with the superscript zero indicating oscillations in vacuum) as

$$P^0_{\mu e} \equiv P^0(\nu_\mu \to \nu_e) = P^0_{atm} + P^0_{sol} + 2\sqrt{P^0_{atm}}\sqrt{P^0_{sol}}\cos(\Delta_{32} + \delta), \tag{4.69}$$

where $\Delta_{ij} = \frac{\Delta m^2_{ij} L}{4E}$ is the kinematic phase factor (L being the baseline length and E being the beam energy) and P^0_{atm}, P^0_{sol} are respectively defined as

$$\sqrt{P^0_{atm}} = \sin\theta_{23}\sin 2\theta_{13}\sin\Delta_{31}, \tag{4.70}$$

$$\sqrt{P^0_{sol}} = \cos\theta_{23}\cos\theta_{13}\sin 2\theta_{12}\sin\Delta_{21}. \tag{4.71}$$

For an antineutrino beam, δ is replaced by $-\delta$ and thus we have

$$\bar{P}^0_{\mu e} \equiv P^0(\bar{\nu_\mu} \to \bar{\nu_e}) = P^0_{atm} + P^0_{sol} + 2\sqrt{P^0_{atm}}\sqrt{P^0_{sol}}\cos(\Delta_{32} - \delta). \tag{4.72}$$

Now the CP asymmetry parameter $A^0_{\mu e}$ in vacuum [213] can be calculated as

$$A^0_{\mu e} = \frac{P^0_{\mu e} - \bar{P}^0_{\mu e}}{P^0_{\mu e} + \bar{P}^0_{\mu e}} = \frac{2\sqrt{P^0_{atm}}\sqrt{P^0_{sol}}\sin\Delta_{32}\sin\delta}{P^0_{atm} + P^0_{sol} + 2\sqrt{P^0_{atm}}\sqrt{P^0_{sol}}\cos\Delta_{32}\cos\delta}. \tag{4.73}$$

With our prediction $\cos\delta = 0$, (4.73) can be rewritten as

$$A^0_{\mu e} = \pm\frac{2\sqrt{P^0_{atm}}\sqrt{P^0_{sol}}\sin\Delta_{32}}{P^0_{atm} + P^0_{sol}}, \tag{4.74}$$

with a $+$ $(-)$ sign for $\delta = \pi/2$ $(3\pi/2)$.

In order to realistically describe neutrino oscillations in long baseline experiments, matter effects in neutrino propagation through the earth need to be taken into account. In that case P^0_{atm} and P^0_{sol} will be modified to

$$\sqrt{P_{atm}} = \sin\theta_{23}\sin 2\theta_{13}\frac{\sin(\Delta_{31} - aL)}{\Delta_{31} - aL}\Delta_{31}, \tag{4.75}$$

and

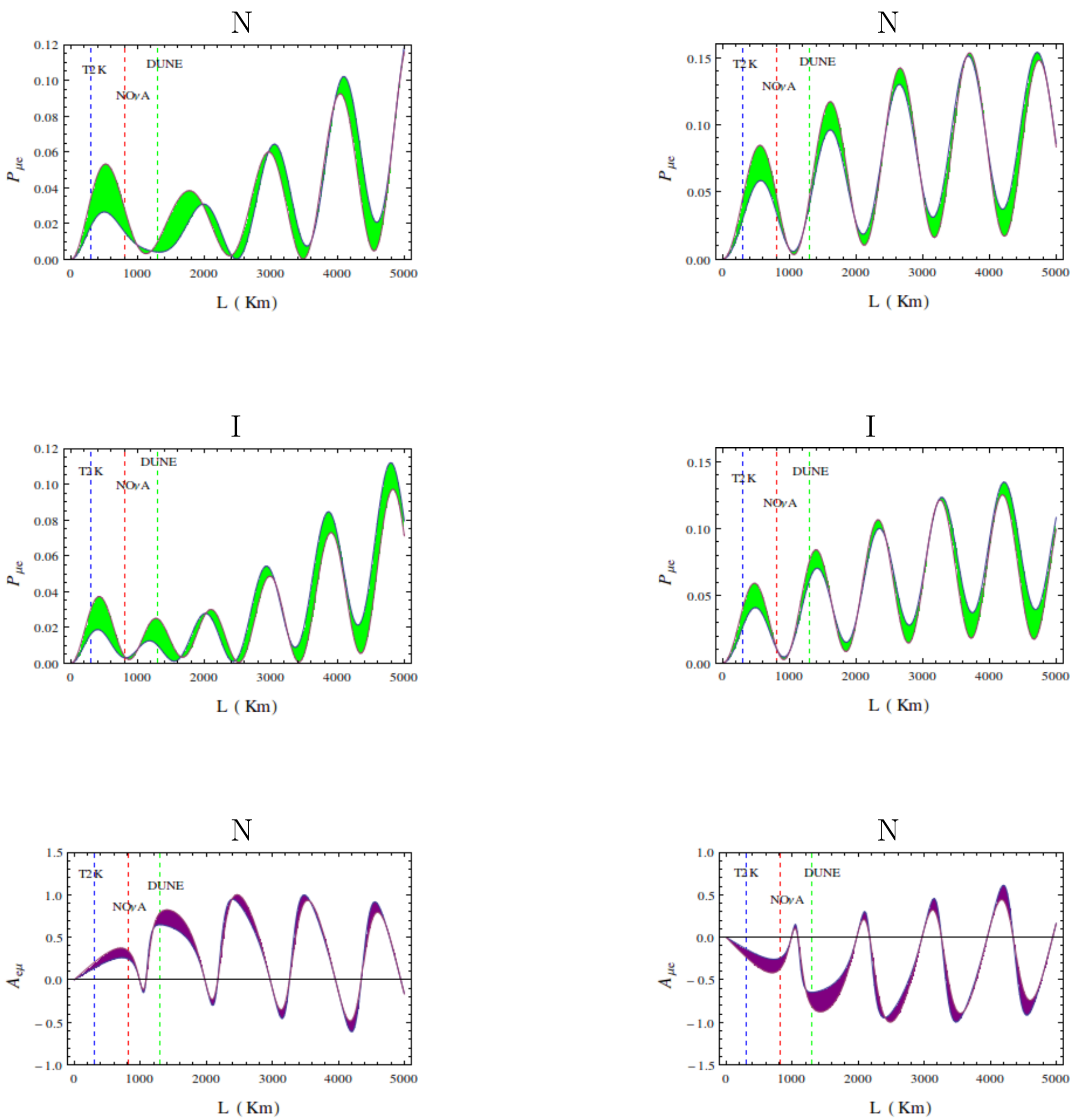

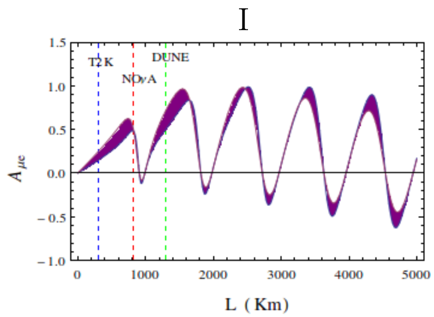

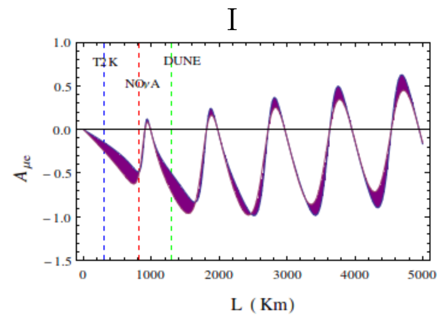

Figure 4.3: *Plots of the transition probability ($P_{\mu e}$) and CP asymmetry parameter ($A_{\mu e}$) with baseline length L for $\delta = \pi/2$ (left panel) and $\delta = 3\pi/2$ (right panel) with $E = 1$ GeV. Cases for normal (inverted) mass ordering have been labelled on top by N (I). The bands are caused by the atmospheric mixing angle θ_{23} being allowed to vary within the 3σ region while the other parameters are kept at their best fit values.*

$$\sqrt{P_{sol}} = \cos\theta_{23}\cos\theta_{13}\sin 2\theta_{12}\frac{\sin aL}{aL}\sin\Delta_{21} \tag{4.76}$$

respectively. Here $a = G_F N_e/\sqrt{2}$ with G_F as the Fermi constant and N_e as the number density of electrons in the medium of propagation. An approximate value of a for the earth is 3500 km^{-1} [213]. Now the same formulae for $P_{\mu e}$, $\bar{P}_{\mu e}$ and $A_{\mu e}$ will hold as in (4.69), (4.72) and (4.73) but with P^0_{atm} and P^0_{sol} replaced by P_{atm} and P_{sol} respectively. In Fig.4.3 we plot $P_{\mu e}$ and $A_{\mu e}$ against the baseline length L in the two cases $\delta = \pi/2$ and $\delta = 3\pi/2$ for both normal and inverted mass ordering. The lengths corresponding to T2K, NOνA and DUNE are indicated in these figures. In Fig.4.4 the CP asymmetry $A_{\mu e}$ is plotted against the beam energy E again for the cases $\delta = \pi/2$ and $\delta = 3\pi/2$ separately for the three above cited experiments; both normal and inverted mass ordering cases are included. As expected, $A_{\mu e}$ has opposite signs for $\delta = \pi/2$ and $\delta = 3\pi/2$.

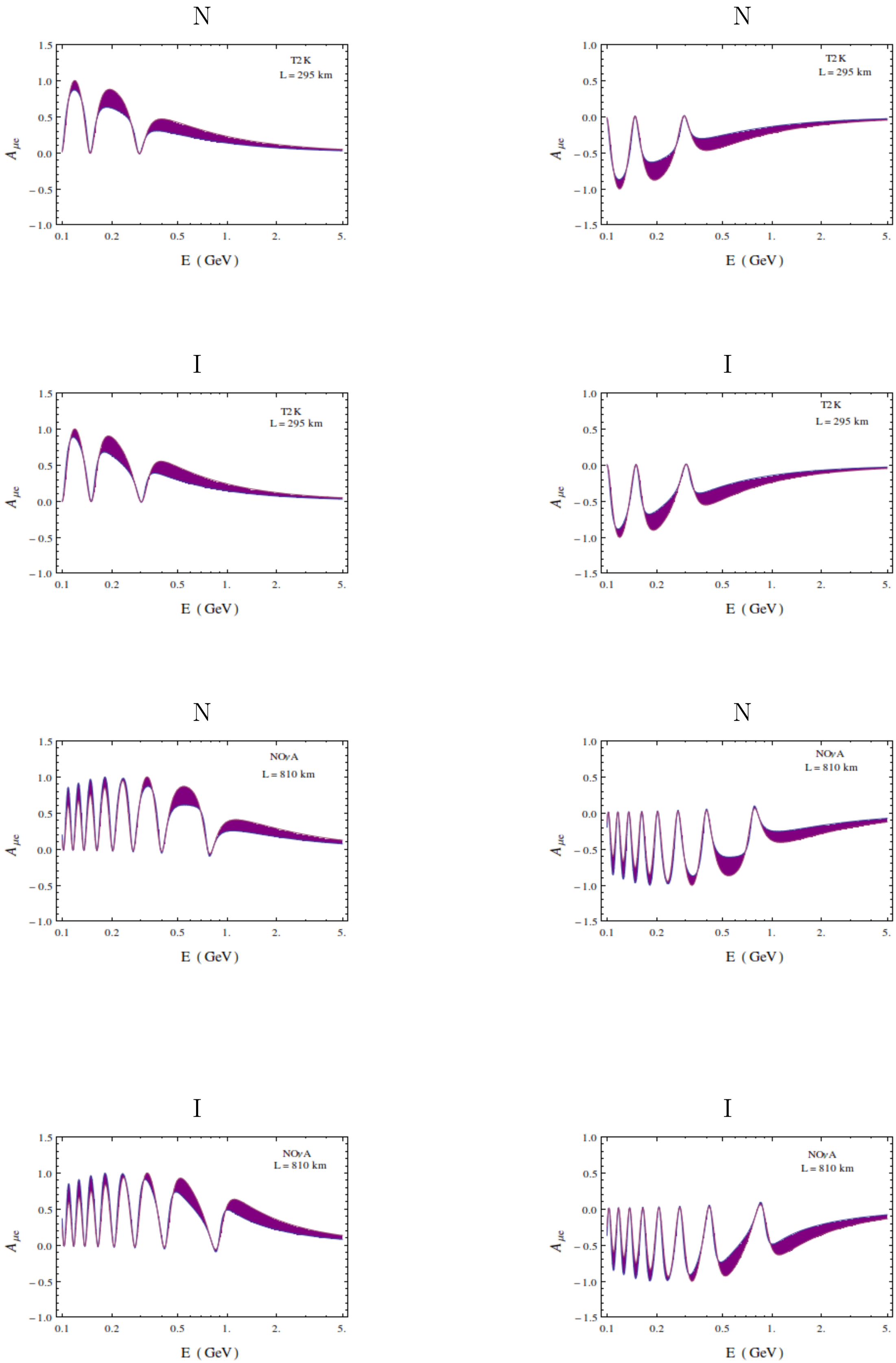
N
N
T2K
L = 295 km
$A_{\mu e}$
E (GeV)
I
I
NOνA
L = 810 km

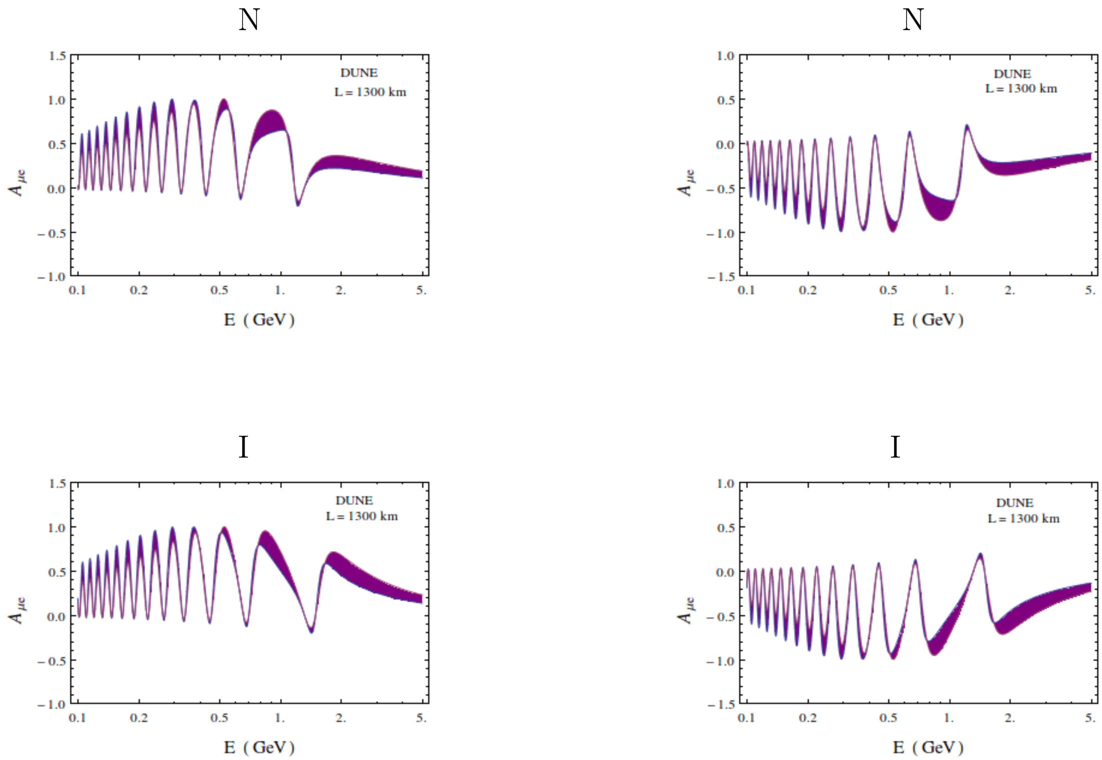

Figure 4.4: *Plots of the CP asymmetry parameter $A_{\mu e}$ against beam energy E for $\delta = \pi/2$ (left panel) and $\delta = 3\pi/2$ (right panel) for various experiments as shown. Cases for normal (inverted) mass ordering have been labelled on top by N (I). The atmospheric mixing angle θ_{23} is allowed to vary within the 3σ region, leading to the bands, while the other parameters are kept at their best fit values.*

It is further interesting that the extrema of the CP-asymmetry parameter exhibit opposite behavior as a function of E for $\delta = \pi/2$ and $\delta = 3\pi/2$.

4.7 Inclusion of unphysical phase

As mentioned in Sec.4.1, our calculations have been done in a Weak Basis where the unphysical phases are absorbed in the neutrino fields. However, one can also reproduce our results including this unphysical phase matrix in the calculation. In that case the U_{PMNS} of (4.3) writes as

$$U_{PMNS} = P_\phi U, \tag{4.77}$$

with $P_\phi = \text{diag.}\ (e^{i\phi}, 1, 1)$. Note that there is only a single unphysical phase in the phase matrix P_ϕ, since the symmetry under consideration dictates M_ν^{CES} in (4.6) to contain seven real parameters which correspond to three nonzero masses, three mixing angles and an unphysical phase. Now for $\tilde{d}_1 = -1$, Eq. (4.32) and (1,1) element of the U_{PMNS} in (4.77) gives

$$e^{-2i\phi} = 1, \tag{4.78}$$

therefore, $\phi = 0$ or π. From (1,2) element we get

$$e^{-i(\alpha+2\phi)} = -\eta. \tag{4.79}$$

Thus for both the values of ϕ, (4.79) leads to (4.40); therefore, for each $\tilde{d}$ matrix with $\tilde{d}_1 = -1$, the prediction for α, i.e, $\alpha = 0$ or π remain the same. Now, following the same way as in Sec.4.4, the results presented in Table 4.2 can be reproduced.

Unlike the previous case, now $\tilde{d}_1 = 1$ cannot be ruled out. In this case, from the (1,1) element of U_{PMNS} in (4.77), we get $\phi = \pi/2$ or $3\pi/2$. Now, for both the values of ϕ, Eq. (4.79) with $\eta = 1$ leads to $\alpha = 0$, and with $\eta = -1$ leads to $\alpha = \pi$. Since the predictions for α remain the same, so do the other parameters which are solved exactly in the same way as in Sec.4.4, by use of *both* real and imaginary parts of the relevant complex equations. We put the more general statements regarding the CP phases for each $\tilde{d}$ with $\tilde{d}_1 = 1$ in Table 4.7. In comparison with Table 4.2, the values

Table 4.7: Predictions of the CP phases for $\tilde{d}_1 = 1$

$\tilde{d}$	α	β	$\cos\delta$
$\tilde{d}_e = \text{diag}\,(-1,+1,+1)$	0	0	0
$\tilde{d}_f = \text{diag}\,(-1,+1,-1)$	0	π	0
$\tilde{d}_g = \text{diag}\,(-1,-1,+1)$	π	0	0
$\tilde{d}_h = \text{diag}\,(-1,-1,-1)$	π	π	0

of α have changed relative to those of β, but the final result that both α and β are either 0 or π remain the same, though the value of $\tilde{d}_1$ has changed.

4.8 Summary

In this paper we have proposed a complex extension of the scaling ansatz for the neutrino Majorana mass matrix M^ν. To that end, we have made use of the residual $\mathbb{Z}_2 \times \mathbb{Z}_2^{scaling}$ symmetry of M^ν by obtaining the representation $G_3^{scaling}$ from the original simple scaling ansatz on M^ν. The resultant form of the neutrino Majorana matrix is given by M_ν^{CES} of (4.6). We have shown that it admits nonzero values of all the physical neutrino masses as well as both normal and inverted types of mass ordering. We have shown how a nonvanishing θ_{13} emerges from M_ν^{CES}. The additional result $k^{-1} = \tan\theta_{23}$, k being the real positive scaling factor, has also been derived. Dirac CP-violation has been shown to be maximal with $\cos\delta = 0$ while Majorana CP-violation has been demonstrated to be absent with $\alpha, \beta = 0$ or π. The type-I seesaw mechanism which yields nonzero neutrino masses within our scheme has also been constructed. Phenomenological implications for both $0\nu\beta\beta$ decay and neutrino/antineutrino oscillation studies at long baselines have been worked out and projections made that will be testable in forthcoming experiments.

Chapter 5

Complex Scaling and flavored leptogenesis

5.1 Introduction

Much effort has already been made towards understanding the origin of the baryon asymmetry of the universe $Y_B = (n_B - n_{\bar{B}})/s \simeq (8.7 \pm 0.1) \times 10^{-11}$ [20] – the number density (n_B) of baryons minus that ($n_{\bar{B}}$) of antibaryons normalized to the entropy density s. A comprehensive review with references may be found in Ref. [29]. Various possible mechanisms have been considered for this purpose, e.g. GUT baryogenesis, electroweak baryogenesis, the Affleck-Dine mechanism and baryogenesis via leptogenesis. We concentrate on the last-mentioned possibility [90, 99, 103, 214–216] which has been elaborated in section 1. Here a CP odd particle-antiparticle asymmetry is first generated at a high scale in the leptonic sector; that is thereafter converted into a baryon asymmetry by sphaleron processes during the electroweak phase transition. In the most popular extension of the Standard Model

(SM) for generating light neutrino masses, three[1] heavy right-chiral (RH) singlet neutrinos are added to induce tiny neutrino masses and their mixing angles through the type-1 seesaw mechanism [142,217–219]. The complex Yukawa couplings $f^N_{i\alpha}$, that connect those singlet RH neutrinos N_i to the SM-doublet left-chiral leptons of flavor α, generate the necessary CP violation in the decays of those heavy RH neutrinos into the Higgs scalar plus the SM leptons. The occurrence of Majorana mass terms for the heavy neutrinos in the Lagrangian provides the required lepton nonconservation. The rate of interaction with those Yukawa couplings being smaller than the Hubble expansion rate, departure from thermal equilibrium ensues. Hence all the Sakarav conditions [220] are fulfilled for generating Y_B. The present work is devoted to a quantitative study of the origin of Y_B via leptogenesis in a model [22] of neutrino masses with complex scaling – proposed by some of us. As a step towards that, we shall summarize the relevant features of the concerned model in the next Sec. 5.2.

First, let us establish our notation and convention by choosing without loss of generality the Weak Basis (sometimes called the leptogenesis basis [209]) in which the 3×3 mass matrices, not only of the charged leptons but also of the heavy RH neutrinos, are diagonal with nondegenerate real and positive entries, e.g. $M_R = \text{diag}\,(M_1, M_2, M_3)$, $M_i\,(i = 1, 2, 3) > 0$. We shall work in the strongly hierarchical scenario in the right-chiral neutrino sector in which those masses will be taken to be widely spaced. Specifically, we assume that $M_1 << M_2 << M_3$. A crucial input into these scenarios is the flavor structure of the neutrino Dirac mass matrix m_D. The latter appears in the neutrino mass terms of the Lagrangian as

$$-\mathcal{L}^{\nu,N}_{mass} = \bar{N}_{iR}(m_D)_{i\alpha}\nu_{L\alpha} + \frac{1}{2}\bar{N}_{iR}(M_R)_i\delta_{ij}N^C_{jR} + \text{h.c.} \tag{5.1}$$

with $N^C_j = C\bar{N}^T_j$. The effective light neutrino Majorana mass matrix M_ν is then

[1] This can be done with two heavy RH singlet neutrinos but not with just one.

given by the standard seesaw result

$$M_\nu = -m_D^T M_R^{-1} m_D. \tag{5.2}$$

This M_ν enters the effective low energy neutrino mass term in the Lagrangian as

$$-\mathcal{L}^\nu_{mass} = \frac{1}{2}\bar{\nu^C_{L\alpha}}(M_\nu)_{\alpha\beta}\nu_{L\beta} + \text{h.c.} \tag{5.3}$$

It is a complex symmetric 3×3 matrix $(M_\nu^* \neq M_\nu = M_\nu^T)$ which can be put into a diagonal form by a similarity transformation with a unitary matrix U:

$$U^T M_\nu U = M_\nu^d \equiv \text{diag}\,(\text{m}_1, \text{m}_2, \text{m}_3) \tag{5.4}$$

with m_i $(i = 1, 2, 3)$ taken to be nonzero, real and small positive masses $< \mathcal{O}(\text{eV})$. In our Weak Basis we can take same U as defined in (4.3) of the previous chapter.

In the main body of this analysis we calculate the CP asymmetry originating from the decays $N_i \to \not{L}_\alpha\phi$, $\not{L}^C_\alpha\phi^\dagger$ where $\not{L}_\alpha$ and ϕ are the respective fields of the SM left-chiral lepton doublet of flavor α and the Higgs doublet. This is done in terms of the imaginary parts of appropriately defined quartic products of the neutrino Dirac mass matrix m_D and its hermitian conjugate $m_D^\dagger$, as well as of an explicit function of the variable $x_{ij} \equiv M_j^2/M_i^2$. Clearly, the calculation depends sensitively on the flavor structure of m_D and hence on the specific neutrino mass model under consideration. The CP asymmetries (and therefore leptogenesis as a whole) may be flavor dependent or independent according to the temperature regime in which the CP violating decays take place. For an evolution down to the electroweak scale, one needs to solve the corresponding Boltzmann Equations. We therefore consider the Boltzmann evolution equation for the number density n_a of a particle of type a (either a right-chiral heavy neutrino N_i or a left-chiral lepton doublet $\not{L}_\alpha$) normalized to the photon number density n_γ. For this purpose, we take

$$\eta_a(z) = \frac{n_a(z)}{n_\gamma(z)}, n_\gamma(z) = \frac{2M_1^3}{\pi^2 z^3} \tag{5.5}$$

as functions of $z \equiv M_1/T$. We rewrite these equations for the variable Y_a where

$$Y_a = n_a/s = \frac{n_\gamma}{s}\eta_a = 1.8 g_{*s}\eta_a, \tag{5.6}$$

g_{*s} being the total number of effective and independent massless degrees of freedom at the concerned temperature. The evolution of Y_a is studied for different a's from a temperature of the order of the lightest right-chiral neutrino mass M_1 to that of the electroweak phase transition where sphaleron-induced processes take place converting the lepton asymmetry into a baryon asymmetry Y_B.

In pursuing Y_B, we need to zero in on Y_{Δ_λ} where $\Delta_\lambda = \frac{1}{3}B - L_\lambda$ with B being the baryon number and L_λ the lepton number of the active flavor λ. The analysis is done numerically but in three different regimes [99, 216] depending on where M_1 lies: (1) $M_1 < 10^9$ GeV where all the lepton flavor are distinctly active, (2) 10^9 GeV $< M_1 < 10^{12}$ GeV where e and μ flavors are indistinguishable but the τ-flavor is separately active and (3) $M_1 > 10^{12}$ GeV where all lepton flavors are indistinguishable. The quantity Y_B and Y_{Δ_λ} are linearly related but with different numerical coefficients for the three different regimes. In our numerical analysis, six constraints from experimental and observational data are inputted: the 3σ ranges of the solar and atmospheric neutrino mass squared differences as well as of the three neutrino mixing angles plus the cosmological upper bound on the sum of the three light neutrino masses. The analysis is done separately in each regime for a normal mass ordering ($m_3 > m_2 > m_1$) as well as for an inverted ordering ($m_2 > m_1 > m_3$) of the light neutrinos. The final results are tabulated numerically as well as displayed graphically.

We have already mentioned the content of Section 5.2. The rest of the chapter is organized as follows. In Section 5.3 we calculate the CP asymmetry parameters generated in the decays of N_i into $\not{L}_\alpha \phi$ and $\not{L}_\alpha^C \phi^\dagger$. The numerical analysis that follows is detailed with a discussion of its consequences in Section 5.4. Section 5.5 addresses the possible role played by the heavier neutrinos $N_{2,3}$. A summary of our work is given in the last Section 5.6.

5.2 Complex scaling with Type-I seesaw

Let's recall the application of complex scaling in the case of Type-I seesaw. A key feature of M_ν is the $\mathbb{Z}_2 \times \mathbb{Z}_2$ residual symmetry [7] that it possesses. This is implemented in the effective M_ν by considering the nonstandard CP transformations

$$\nu_{L\alpha} \to i(G_L)_{\alpha\beta}\gamma^0 \nu_{L\beta}^C, \quad N_{Ri} \to i(G_R)_{ij}\gamma^0 N_{Rj}^C \tag{5.7}$$

and demanding the invariance relations

$$G_R^\dagger m_D G_L = m_D^*, \quad G_R^\dagger M_R G_R^* = M_R^*. \tag{5.8}$$

Eqs. (5.2) and (5.8) together imply

$$G_L^T M_\nu G_L = M_\nu^* \tag{5.9}$$

which is our complex-extended invariance statement on the low energy neutrino

Majorana mass matrix M_ν. At this point, G_L is taken to be [22]

$$G_L = G_3^{\rm scaling} = \begin{pmatrix} -1 & 0 & 0 \\ 0 & (1-k^2)(1+k^2)^{-1} & 2k(1+k^2)^{-1} \\ 0 & 2k(1+k^2)^{-1} & -(1-k^2)(1+k^2)^{-1} \end{pmatrix}, \tag{5.10}$$

k being a real scaling factor. This $G_3^{\rm scaling}$ is the operative residual symmetry generator for the original scaling ansatz [16]. It now obeys the relation

$$G_3^{\rm scaling} U^* = U\tilde{d}, \tag{5.11}$$

where $\tilde{d}_{\alpha\beta}$ equals $\pm\delta_{\alpha\beta}$ and hence admits eight possibilities. Only four of these were shown [22] to be viable and led independently to the results

$$\tan\theta_{23} = k^{-1}, \tag{5.12}$$

$$\sin\alpha = \sin\beta = \cos\delta = 0. \tag{5.13}$$

The detailed phenomenological consequences of (5.12) and (5.13) were worked out in Ref. [22]. The most general M_ν, that satisfies

$$(G_3^{\rm scaling})^T M_\nu G_3^{\rm scaling} = M_\nu^*, \tag{5.14}$$

is given by the complex-extended scaling (CES) form of M_ν which has been discussed in the previous chapter.

Since M_R has been taken to be diagonal, the corresponding symmetry generator matrix G_R, cf. the second of Eqs. (5.8), is diagonal with entries ± 1, i.e.

$$G_R = \text{diag}\,(\pm 1, \pm 1, \pm 1). \tag{5.15}$$

Thus there are eight different structures of G_R. Correspondingly, from the first relation of (5.8), there could be eight possible different structures of m_D. It can be shown by tedious algebra that all other structures of G_R, except for

$$G_R = \text{diag}\,(-1, -1, -1), \tag{5.16}$$

are incompatible with scaling symmetry. Thus we take G_R of (5.16) as the only viable residual symmetry of M_R. We can now write the first of (5.8) as

$$m_D G_L = -m_D^* \tag{5.17}$$

which is really a complex extension of the Joshipura-Rodejohann result[2] [210] $m_D G_L = -m_D$.

The most general form of m_D that satisfies (5.17) is

$$m_D^{CES} = \begin{pmatrix} a & b_1 + ib_2 & -b_1/k + ib_2 k \\ e & c_1 + ic_2 & -c_1/k + ic_2 k \\ f & d_1 + id_2 & -d_1/k + id_2 k \end{pmatrix}, \tag{5.18}$$

where a, $b_{1,2}$, $c_{1,2}$, $d_{1,2}$, e and f are nine a priori unknown real mass dimensional quantities apart from the real, positive, dimensionless k. Using (5.2), M_ν^{CES} of (4.4) obtains with the real mass parameters x, $y_{1,2}$, $z_{1,2}$ and w related to those of (5.18),

[2]Those authors followed a different phase convention; they obtained $m_D G_L = m_D$ instead of $m_D G_L = -m_D$.

as given in Table 5.1. It is noteworthy that whereas m_D^{CES} has ten real parameters,

Table 5.1: Parameters of M_ν^{CES} in terms of the parameters of m_D and M_R.

$x = -(\frac{a^2}{M_1} + \frac{e^2}{M_2} + \frac{f^2}{M_3})$
$y_1 = \frac{1}{k}(\frac{ab_1}{M_1} + \frac{ec_1}{M_2} + \frac{fd_1}{M_3})$
$y_2 = k(\frac{ab_2}{M_1} + \frac{ec_2}{M_2} + \frac{fd_2}{M_3})$
$z_1 = -\frac{1}{k^2}(\frac{b_1^2}{M_1} + \frac{c_1^2}{M_2} + \frac{d_1^2}{M_3}) + k^2(\frac{b_2^2}{M_1} + \frac{c_2^2}{M_2} + \frac{d_2^2}{M_3})$
$z_2 = \frac{2b_1b_2}{M_1} + \frac{2c_1c_2}{M_2} + \frac{2d_1d_2}{M_3}$
$w = \frac{1}{k}(\frac{b_1^2}{M_1} + \frac{c_1^2}{M_2} + \frac{d_1^2}{M_3}) + k(\frac{b_2^2}{M_1} + \frac{c_2^2}{M_2} + \frac{d_2^2}{M_3})$

M_ν^{CES} has only seven. One can count the real parameters, as given in m_D of (5.18). Along with the RH neutrino masses M_1, M_2, M_3, one obtains a set of thirteen real parameters for M_ν. In order to reduce the number of parameters towards attaining the goal of a tractable result, we first use the assumed hierarchical nature of the RH neutrino masses $M_1 << M_2 << M_3$. We then take the parameters $d_{1,2}$, e and f in Table 5.1 to be of the same order of magnitude as a, $b_{1,2}$ and $c_{1,2}$. That enables us to neglect all terms in Table 5.1 with M_3 in the denominator. Now we rescale the remaining parameters of Table 5.1 as follows:

$$a \longrightarrow a' = \frac{a}{\sqrt{M_1}}, \tag{5.19}$$

$$b_{1,2} \longrightarrow b'_{1,2} = \frac{b_{1,2}}{\sqrt{M_1}}, \tag{5.20}$$

$$c_{1,2} \longrightarrow c'_{1,2} = \frac{c_{1,2}}{\sqrt{M_2}}, \tag{5.21}$$

$$e \longrightarrow e' = \frac{e}{\sqrt{M_2}}. \tag{5.22}$$

Consequently, the entries of Table 5.1 can be written in terms of the rescaled parameters as in Table 5.2. We are now left with a six-dimensional parameter space with the real parameters x, $y_{1,2}$, $z_{1,2}$ and w as given in Table 5.2. Note that, had we

Table 5.2: Parameters of m_D^{CES} in the rescaled version.

$x = -(a'^2 + e'^2)$
$y_1 = \frac{1}{k}(a'b'_1 + e'c'_1)$
$y_2 = -k(a'b'_2 + e'c'_2)$
$z_1 = -\frac{1}{k^2}({b'_1}^2 + {c'_1}^2) + k^2({b'_2}^2 + {c'_2}^2)$
$z_2 = 2b'_1b'_2 + 2c'_1c'_2$
$w = \frac{1}{k}({b'_1}^2 + {c'_1}^2) + k({b'_2}^2 + {c'_2}^2)$

neglected the terms with M_2 in the denominator too, we would have been left with a three dimensional parameter space which would have been in a danger of being overdetermined by the six experimental and observational constraints mentioned in the Introduction. We shall latter discuss how to estimate the missing parameters f and $d_{1,2}$.

Before concluding this section, let us make an important point. In the absence of of any imaginary part of the matrix m_D^{CES} of (5.18), the seesaw relation (5.2) gives rise to the Generalized Real Scaling form of M_ν, namely [22]

$$M_\nu^{GRS} = \begin{pmatrix} x & -y_1 k & y_1 \\ -y_1 k & z_1 - wk^{-1}(k^2-1) & w \\ y_1 & w & z_1 \end{pmatrix} \tag{5.23}$$

with real mass-dimensional entries. However, as was explained in Ref. [22], in this case θ_{13} vanishes and so information about the Dirac CP violating phase δ is lost. Moreover, owing to the real nature of the associated m_D^{GRS}, there is no Majorana CP violation either. Thus we see that the imaginary part of m_D^{CES} is the common source of an operative nonzero θ_{13} as well as CP violation in leptonic sector. The latter is in fact crucial to leptogenesis which is effected through a nonzero value of the CP asymmetry parameter ϵ, as explained in the next section. It is through the nonvanishing nature of Im m_D^{CES} that the final matter-antimatter asymmetry in the universe gets directly related to the low energy parameters θ_{13} and δ.

5.3 Calculation of CP asymmetry parameter and relevant Boltzmann equations

A general discussion regarding the CP asymmetry parameter ε_i has been presented in chapter 1 where the simplified expression for ε_i is given by

$$\begin{aligned} \varepsilon_i &= \sum_\alpha \varepsilon_i^\alpha \\ &= \frac{1}{4\pi v^2 \mathcal{H}_{ii}} \sum_{j\neq i} \left[f(x_{ij}) + \frac{\sqrt{x_{ij}}}{(1-x_{ij})} \right] \mathrm{Im}\, \mathcal{H}_{ij}\mathcal{H}_{ij}. \end{aligned} \tag{5.24}$$

In the mass model being considered, it follows from (5.18) that

$$\mathcal{H}^{CES} = \begin{pmatrix} a^2+b_1^2p+b_2^2q & ae+b_1c_1p+b_2c_2q & af+b_1d_1p+b_2d_2q \\ ae+b_1c_1p+b_2c_2q & e^2+c_1^2p+c_2^2q & ef+c_1d_1p+c_2d_2q \\ af+b_1d_1p+b_2d_2q & ef+c_1d_1p+c_2d_2q & f^2+d_1^2p+d_2^2q \end{pmatrix} \tag{5.25}$$

with $p = 1 + k^{-2}$ and $q = 1 + k^2$. Since (5.25) implies that Im $\mathcal{H}^{CES}$=0, it follows from (5.24) that

$$\varepsilon_i = 0, \tag{5.26}$$

i.e.flavored-summed leptogenesis does not take place for any N_i. With the assumption that only the decay of N_1 matters in generating the CP asymmetry, ε_1 is the pertinent quantity for unflavored leptogenesis, but it vanishes. This nonoccurrence of unflavored leptogenesis is one of the robust predictions of the model.

Next, we focus on the calculation of the α-flavored CP asymmetry in terms of x_{12}, x_{13} and the elements of m_D^{CES}. These are relevant for the fully flavored as well as the τ-flavored regimes. We find that

$$\varepsilon_1^e = 0, \tag{5.27}$$

while

$$\varepsilon_1^\mu = \xi[b_2k^2(\chi_1+\chi_2)+b_1(\chi_3+\chi_4)-b_1^2\chi_5] = -\varepsilon_1^\tau. \tag{5.28}$$

In (5.28) the real parameters ξ and χ_i $(i=1-5)$ are defined as

$$\begin{aligned}
\xi &= \frac{1}{4[b_1^2+(a^2+b_1^2+b_2^2)k^2+b_2^2k^4]\pi v^2},\\
\chi_1 &= b_2(1+k^2)[c_1c_2\{1+g(x_{12})-x_{12}\}+d_1d_2\{1+g(x_{13})-x_{13}\}],\\
\chi_2 &= a[c_1e\{1+g(x_{12})-x_{12}\}+d_1f\{1+g(x_{13})-x_{13}\}],\\
\chi_3 &= b_2(1+k^2)[c_1^2\{1+g(x_{12})-x_{12}\}-k^2[c_2^2\{1+g(x_{12})\\
&- x_{12}\}+d_2^2\{1+g(x_{13})-x_{13}\}]+d_1^2\{1+g(x_{13})-x_{13}\}],\\
\chi_4 &= -ak^2[c_2e\{1+g(x_{12})-x_{12}\}+d_2f\{1+g(x_{13})-x_{13}\}],\\
\chi_5 &= ((1+k^2)[c_1c_2\{1+g(x_{12})-x_{12}\}+d_1d_2\{1+g(x_{13})-x_{13}\}].
\end{aligned} \tag{5.29}$$

Thus the nonzero leptonic CP asymmetry parameter $\varepsilon_1^\mu = -\varepsilon_1^\tau$ depends on all ten parameters of m_D^{CES} as well as on x_{12} and x_{13}.

We had earlier identified Im m_D^{CES} as the common source of the origin of a nonzero θ_{13} and leptonic CP violation. A real m_D^{CES} implies vanishing values for b_2,

c_2 and d_2 in which case $\varepsilon_1^\mu = -\varepsilon_1^\tau$ vanishes identically and, as explained in Ref. [22], so does θ_{13}. However, the reverse statement is not true. One could have a vanishing leptonic CP asymmetry simply by setting $b_{1,2}$ to zero in (5.28). But, so long as Im m_D^{CES} is nonzero, e.g. through nonvanishing values of c_2 and d_2, θ_{13} need not vanish. Indeed, the leptonic CP asymmetry depends rather sensitively on $b_{1,2}$. We shall elaborate on this later in our numerical discussion.

A major simplification (1.118) occurs in our model when the active flavor λ equals e since $\varepsilon_1^e = 0$ and only the second RHS term contributes to the evolution of η^λ. Then the solution of the equation becomes [221]

$$\eta_L^e(z) = \eta_L^e(z=0)\exp[-\frac{1}{4}\int_0^z W^e(z')dz'], \tag{5.30}$$

where $W^e(z) = \frac{1}{2}D_1^e(z)z^2K_2(z) + D_1^{e\mathrm{YW}}(z) + D_1^{e\mathrm{GW}}(z)$. However, at a very high temperature, the lepton asymmetries get efficiently washed out. Therefore $\eta_L^e(z\to 0)$ vanishes and from (5.30) $\eta_L^e(z) = 0$ for all z. Similarly, for an unflavored (i.e flavor-summed) leptogenesis in our model, $\eta^e + \eta^\mu + \eta^\tau = 0$ since $\varepsilon_1^\mu = -\varepsilon_1^\tau$.

We have to focus on Y_{Δ_λ}, defined as $s^{-1}\{1/3(n_B - n_{\bar{B}}) - (n_L - n_{\bar{L}})\}$ as mentioned in the Introduction. We consider the BE of (1.139) for the evolution of Y_{Δ_λ}, for convenience which is written again as

$$\begin{aligned}\frac{dY_{\Delta_\lambda}}{dz} &= \sum_{i=1}^{3}[\varepsilon_i^\lambda\{D_i(z) + D_i^{\mathrm{SY}}(z) + D_i^{\mathrm{SG}}(z)\}\{Y_{N_i}^{\mathrm{eq}}(z) - Y_{N_i}(z)\}] \\ &+ \frac{1}{4}\sum_\rho A_{\lambda\rho}Y_{\Delta_\rho}\sum_{i=1}^{3}\{\frac{1}{2}D_i^\lambda(z)z^2K_2(z) + D_i^{\lambda\ \mathrm{YW}}(z) + D_i^{\lambda\ \mathrm{GW}}(z)\}.\end{aligned} \tag{5.31}$$

We need to solve (1.130) and (5.31) and evolve Y_{N_i} as well as Y_{Δ_λ} upto a value of z where the quantities Y_{Δ_λ} become constant with z, i.e. do not change as z is varied. The final baryon asymmetry Y_B is obtained [222] linearly in terms Y_{Δ_λ}, the coefficient depending on the mass regime in which M_1 is located, as explained in chapter 1.

A complete and detail numerical discussion of the present work is given in the following section.

5.4 Numerical analysis: methodology and discussion

In order to numerically check the viability of our theoretical results, the allowed (3σ) values of globally fitted neutrino oscillation data [30] and the upper bound of 0.23 eV on the sum of the light neutrino masses have been used, cf. Table 5.3. We first constrain the parameter space constructed with the six rescaled parameters defined in Eqs. (5.19) - (5.22). Both normal and inverted types of light neutrino mass ordering are found to be allowed over a sizable region of the parameter space consistent with the input constraints. The ranges of

Table 5.3: Input values used

Parameters	θ_{12} degrees	θ_{23} (deg)	θ_{13} (deg)	Δm^2_{21} $\times 10^5 \text{eV}^2$	$\lvert\Delta m^2_{31}\rvert$ $\times 10^3 (\text{eV}^2)$	$\Sigma_i m_i$ (eV)
3σ/others	31.29 − 35.91	38.3−53.3	7.87−9.11	7.02−8.09	2.32−2.59	< 0.23
Bfp(NO)	33.48	42.3	8.50	7.50	2.46	−
Bfp(IO)	33.48	49.5	8.51	7.50	2.45	−

the rescaled parameters are graphically shown in Fig.5.1 and Fig.5.2 respectively for the normal and the inverted ordering of the light neutrino masses. This is the primary constraining procedure since the CP asymmetry parameters ε_i^α and the different Γ's

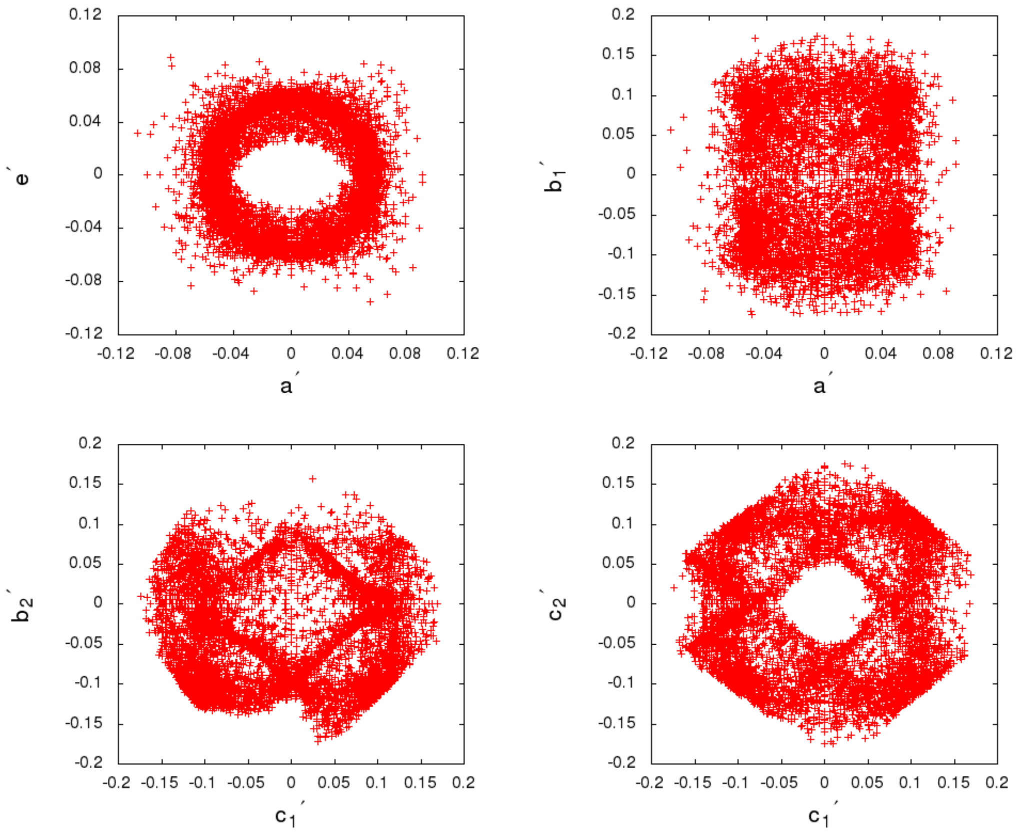

Figure 5.1: *Plots of the reduced parameters for a normal mass ordering of the light neutrinos.*

of the Boltzmann equations depend individually upon the elements of m_D and the RH neutrino masses M_i ($i = 1, 2, 3$). Therefore, merely restricting the rescaled parameters is not sufficient for the computation of the final baryon asymmetry. In order to obtain the allowed ranges of the parameters a, $b_{1,2}$, $c_{1,2}$ and e, included in m_D, we incorporate the strong hierarchy assumption of the RH neutrino masses ($M_1 << M_2 << M_3$), as mentioned in earlier sections. For numerical purposes, we arbitrarily choose M_2/M_1 $= M_3/M_2 = 10^3$. We shall later discuss in Section 5.5 the effects of changing these mass ratios. Depending upon the mass regime, for a fixed value of M_1, we then obtain the allowed ranges of the parameters of m_D from the relations defined in Eqs. (5.19) - (5.22).

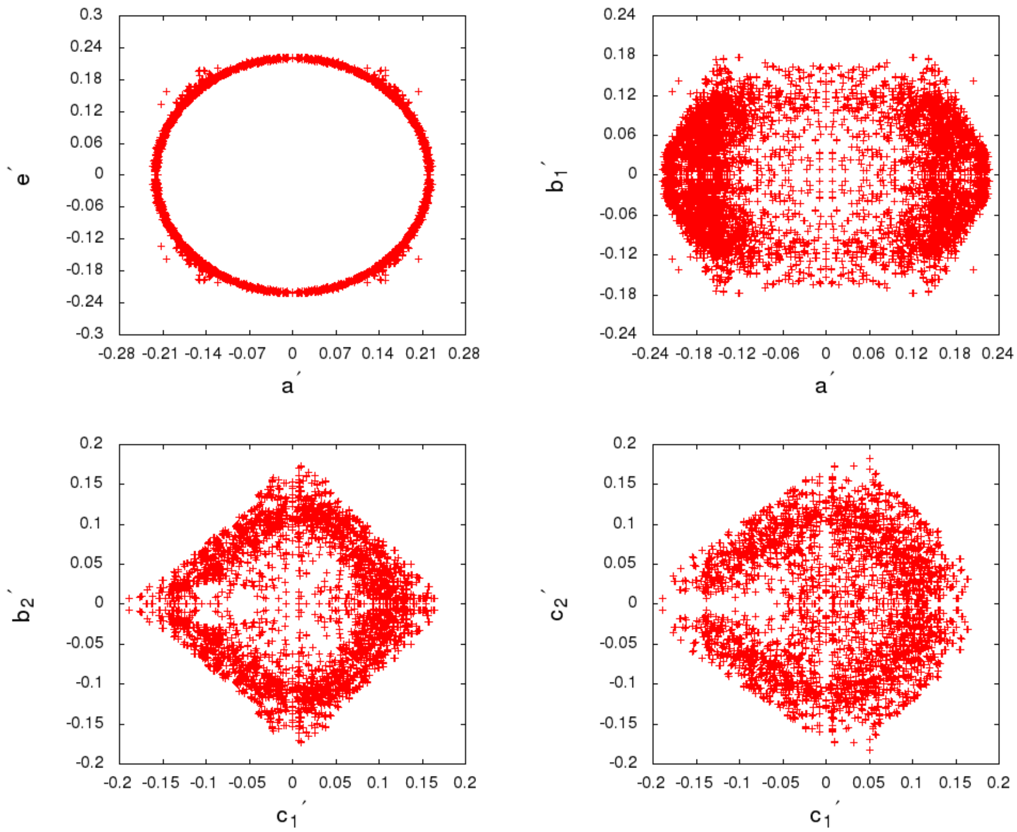

Figure 5.2: *Plots of the reduced parameters for an inverted mass ordering of the light neutrinos.*

Even after constraining the six unprimed parameters of m_D and the masses of the three right handed heavy neutrinos, three undetermined parameters remain – namely f, d_1 and d_2. The latter have been neglected earlier in the primary implementation of the input constraints since their contributions to the light neutrino mass matrix M_ν are suppressed by the heaviest RH neutrino mass M_3. However, for a quantitatively successful treatment of leptogenesis, one needs to estimate these missing parameters too, as mentioned in Sec. 5.2. We discuss here some technical details regarding this estimation. For example, let us consider the first equation of Table 5.1, namely

$$x = -\left(\frac{a^2}{M_1} + \frac{e^2}{M_2} + \frac{f^2}{M_3}\right). \tag{5.32}$$

The last RHS term was earlier neglected on the grounds that the parameter f, which is presumably of same the order of magnitude as a or e, is suppressed by M_3. Now, in order to estimate f, we first set it at a value which is larger i.e. between a and e. Then we keep on decreasing it until the quantity $f^2 M_3^{-1}/(a^2 M_1^{-1} + e^2 M_2^{-1})$ becomes less than a very small number which we choose to be 10^{-5}. In a similar manner one can estimate approximate values of d_1 and d_2. Thus, knowing the numerical values of all the parameters of m_D as well as those of M_R, we can make a realistic estimate of the final value of the baryon asymmetry. The first step towards the last-mentioned goal is the estimation of ε_1^λ in the three mass regimes of M_1. We have carried out our numerical analysis over a wide range of values of M_1 in the τ-flavored and in the fully flavored regimes. As mentioned in the last paragraph of Sec. 5.3, $\varepsilon_1^{\mu,\tau}$ are mostly sensitive to $b_{1,2}$. In order to see the nature of the variation of $\varepsilon_1^{\mu,\tau}$ with $b_{1,2}$ for constant values of c_2 and d_2, we first set c_2 and d_2 to be zero.

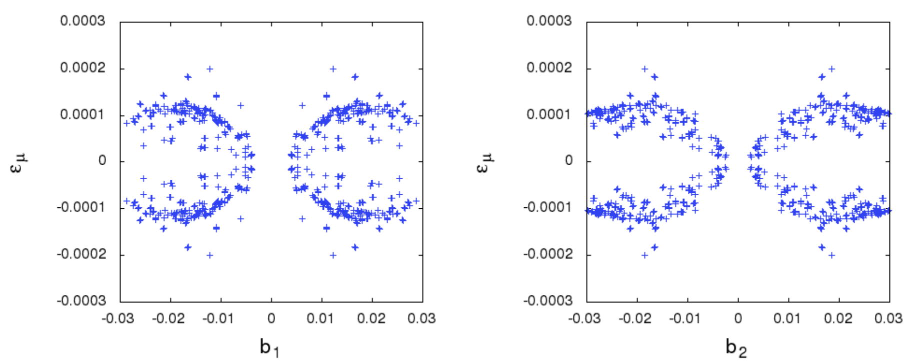

Figure 5.3: *Plot of ε_1^μ with b_1 (left), b_2 (right) for a normal light neutrino mass ordering . A sample value of $M_1 = 3.62 \times 10^{11}$ GeV has been chosen.*

Now the simplified expression of the relevant CP asymmetry parameter becomes

$$\varepsilon_1^\mu = \xi(b_2 k^2 \chi_2 + b_1 \chi_3') = -\varepsilon_1^\tau, \tag{5.33}$$

where ξ and χ_2 as are defined in (5.29), and χ_3' is given by

$$\chi_3' = b_2(1+k^2)[c_1^2\{1+g(x_{12})-x_{12}) + d_1^2(1+g(x_{13})-x_{13}\}]. \tag{5.34}$$

For a graphical representation of the variation of the CP asymmetry parameter ε_1^μ with $b_{1,2}$, we choose a sample value of $M_1 = 3.62 \times 10^{11}$ GeV and assume a normal mass ordering[3] of the light neutrinos. The corresponding scatter plots are shown in Fig. 5.3. The vanishing of $b_{1,2}$ implies $\varepsilon_1^\mu = 0$; therefore, in our numerical computation, only those values of ε_1^μ are allowed which correspond to $b_{1,2} \neq 0$. One can have a similar plot for ε_1^τ since $\varepsilon_1^\mu = -\varepsilon_1^\tau$ and the plots in Fig. 5.3 are symmetric about the origin. The corresponding plots for an inverted mass ordering of the light neutrinos can also be generated. However, with the same computational technique as used for normal ordering, we find a much smaller number of allowed points which hardly show a fair variation of ε_1^μ with $b_{1,2}$.

Finally, knowing the numerical range of ε_1^λ is the last step needed to solve the Boltzmann equations given in (1.130) and (5.31) leading to the parameter Y_{Δ_λ} upto a fairly large value of z where Y_{Δ_λ} becomes constant. Then, using the suitable equations (1.141), (1.144), depending upon the energy regime, one can compute the final value of Y_B. However, this final step needs to overcome the following hurdle. Unlike estimating ε_1^λ for the entire allowed parameter ranges of m_D and M_R, it becomes impractical in terms of computer time to solve the Boltzmann equations for this huge data set even if M_1 is fixed to a constant value. So we were obliged to use only those values of the members of parameter set for which the neutrino oscillation observables are restricted close to their best fit values. For this purpose we choose a χ^2 for every observable

[3] As we shall see later, in our model an inverted mass ordering is disfavored in terms of a realistic baryogenesis.

deviating from its experimentally measured best fit value as

$$\chi^2 = \sum_{i=1}^{5} \Big[\frac{O_i(th) - O_i(bf)}{\Delta O_i}\Big]^2. \tag{5.35}$$

In (5.35) O_i denotes the ith neutrino oscillation observable from among $(\Delta m^2_{21}, \Delta m^2_{32}, \theta_{12}, \theta_{23}, \theta_{13})$ and the summation runs over all the five observables. The parenthetical th stands for the theoretical prediction, i.e the numerical value of the observable given by our model, whereas bf denotes the best fit value (cf. Table 5.3). ΔO_i in the denominator stands for the measured 1σ range of O_i. After calculating χ^2 for all the points $\{a', e', b'_1, c'_1, b'_2, c'_2\}$, as allowed by the oscillation data, we start from the minimum value of the χ^2 $(=\chi^2_{min})$ and keep on increasing the latter until we get Y_B to be positive as well as in the observed range. It is to be noted that for a particular value of χ^2, i.e. for a particular primed data set, we are able to generate a large number of unprimed points (parameters of m_D) by varying the values of M_1 in Eqs.(5.19)-(5.22). To be more precise, 'n' values of M_1 lead to 'n' values of the unprimed set of parameters for the particular primed set under consideration. The other three parameters f, d_1 and d_2 are again computed by means of the previously mentioned approximation technique. We vary M_1 over a wide range in the relevant mass regimes for both types of mass ordering and present our final result systematically in the following way.

Y_B for normal mass ordering of light neutrinos:

$\mathbf{M_1 < 10^9}$ GeV: In this regime all lepton flavors (e, μ, τ) act distinguishably. However, since $\varepsilon_1^e = 0$, we first need to evaluate $\varepsilon_1^{\mu,\tau}$ individually. It is found that $|\varepsilon_1^{\mu,\tau}|$ can have values at most $\sim 10^{-8}$. Y_B of the right amount cannot be generated with such a small CP asymmetry parameter [103].

10^9 GeV $<$ $\mathbf{M_1}$ $<$ $\mathbf{10^{12}}$ GeV: After carrying out the χ^2 analysis for this regime, we first calculate the final Y_B for $\chi^2_{min}(=0.002)$. It is found that the final Y_B saturates to a negative value. Then we keep on increasing χ^2 and find that a positive value for the final Y_B within the observed range may be obtained for $\chi^2 = 0.003$ which is close enough to the best-fit value of $\chi^2 = 0.002$. In the entire analysis, for each value of χ^2, i.e. for this single primed set, M_1 is varied over a wide range. Then, for each value of M_1, a set of values of the unprimed parameters $\{a, e, f, b_1, c_1, d_1, b_2, c_2, d_2\}$ is generated. The Boltzmann equations are solved for each set of values of M_1. Since, in this regime, the τ flavor acts distinguishably, we need to solve

Table 5.4: parameters corresponding $\chi^2 = 0.003$ for normal mass ordering.

a'	e'	b'_1	c'_1	b'_2	c'_2	χ^2
0.026	0.054	0.019	0.095	-0.080	0.095	0.003

the Boltzmann equations for two flavors (τ and 2) in order to obtain the variation of $Y_{\Delta_{\tau,2}}$ or of Y_B with z. For each set of the primed parameters, we take thirty values of M_1 within the range 10^9 GeV to 10^{12} GeV and solve the Boltzmann equations thirty times for each M_1 along with the corresponding unprimed set of rescaled parameters. For a concise presentation, in Table 5.5, we tabulate only ten such values of M_1 for which Y_B is near or inside the observed range.

Table 5.5: Y_B for different masses of lightest right handed neutrino.

$\frac{M_1}{10^{11}}$ (GeV)	3.57	3.58	3.59	3.60	3.61	3.62	3.63	3.64	3.65	3.66
$Y_B \times 10^{11}$	8.55	8.57	8.59	8.61	8.64	8.66	8.69	8.71	8.74	8.77

Fig.5.4 contains a graphical presentation of the variation of the asymmetries

Y_{Δ_2}, Y_{Δ_τ} and Y_B with z for a definite value of M_1 which is taken to be 3.62×10^{11} GeV. It may be seen that Y_B is inside the observed range [20] for large z corresponding to the present epoch.

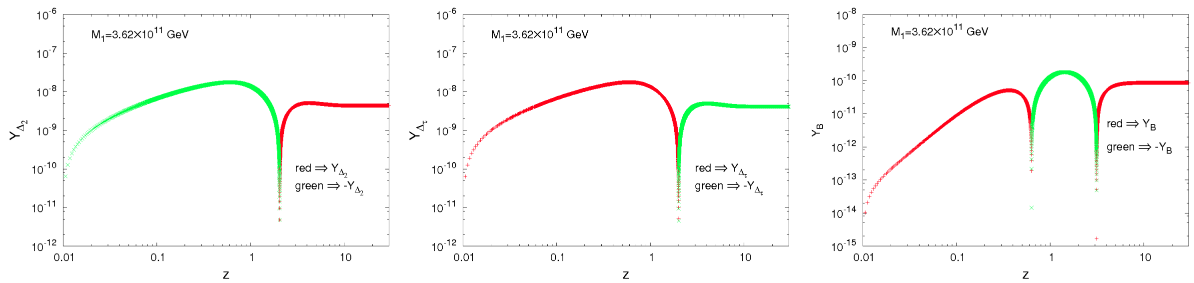

Figure 5.4: *Variation of Y_{Δ_μ} (left), Y_{Δ_τ} (middle), Y_B (right) with z in the mass regime (2) for a definite value of M_1. N.B. since these become negative for certain values of z, their negatives have been plotted on the log scale for those values of z. A normal mass ordering for the light neutrinos has been assumed.*

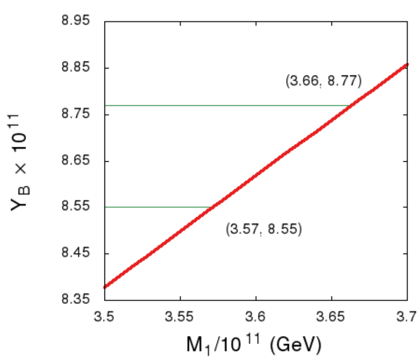

Figure 5.5: *A plot of the final Y_B for different values of M_1 for a normal light neutrino mass ordering.*

A careful surveillance of Table 5.5 leads to the conclusion that we can obtain upper and lower bounds on M_1 due to the constraint from the observed range of Y_B. One can appreciate this fact more clearly from the plot of Y_B vs. M_1 in Fig.5.5. Two straight lines have been drawn parallel to the abscissa in Fig.5.5: one at $Y_B =$

8.55×10^{-11} and the other at $Y_B = 8.77 \times 10^{-11}$. The values of M_1, where the straight lines meet the Y_B vs z curve, yield the allowed lower and upper bounds on M_1, namely $(M_1)_{lower} = 3.57 \times 10^{11}$ GeV and $(M_1)_{upper} = 3.66 \times 10^{11}$ GeV.

$\mathbf{M_1 > 10^{12}}$ GeV: It has been shown that $Y_B = 0$ here for our model.

Y_B for inverted mass ordering of light neutrinos:
In this case too the numerical estimation of the baryon asymmetry parameter has been made exactly in the same manner as for a normal mass ordering. A final discussion for each regime goes as follows.

$\mathbf{M_1 < 10^9}$ GeV: As in the case of normal ordering, the values of $\varepsilon_1^{\mu,\tau}$ can reach up to at most the order of 10^{-8} which is not adequate to let Y_B come within its observed range.

$\mathbf{10^9}$ GeV $< \mathbf{M_1} < \mathbf{10^{12}}$ GeV: In this regime we first calculate the minimum value of χ^2 for the full set of primed parameters constrained by the oscillation data. We find that for $\chi^2_{min} = 0.246$ the final baryon asymmetry saturates to a negative value. As in the previous case we then keep on increasing the value of χ^2 and check the final Y_B by varying M_1 over a wide range for each value of χ^2. It turns out that though Y_B attains a positive value for $\chi^2 = 0.952$, it is below the observed range. Then, using the χ^2 enhancement technique, for Y_B to be in the observed range the minimum value of χ^2 is found to be 1.67 which is far away from the best-fit point. The set of primed parameters for $\chi^2 = 1.67$ is tabulated in Table 5.6.

Table 5.6: parameters corresponding $\chi^2 = 1.67$ for inverted hierarchy

a'	e'	b'_1	c'_1	b'_2	c'_2	χ^2
0.15	0.16	-0.017	-0.022	0.10	-0.096	1.67

$\mathbf{M_1 > 10^{12}}$ **GeV:** Once again, $Y_B = 0$ here for the present model.

A compact presentation of the final conclusions regarding Y_B from the numerical analysis is given in Table 5.7 where only the results on Y_B for the regimes $M_1 < 10^9$ GeV and 10^9 GeV $< M_1 < 10^{12}$ GeV are shown since $M_1 > 10^{12}$ GeV regime is theoretically ruled out due the vanishing CP asymmetry parameter.

Table 5.7: Final statements on Y_B for two mass regimes.

Type	$M_1 < 10^9$ GeV	10^9 GeV $< M_1 < 10^{12}$ GeV
Normal Ordering	Ruled out since Y_B is below the observed range for any χ^2.	Y_B within the observed range for χ^2=0.003 close to $\chi^2_{min} = 0.002$.
Inverted Ordering	Ruled out since Y_B is below the observed range for any χ^2.	Y_B within the observed range for χ^2=1.67 far away from $\chi^2_{min} = 0.246$.

We would like to make a further statement before finishing this numerical discussion . Though we had earlier enumerated the difficulties in numerically solving the Boltzmann equations for each data point within the entire 3σ parameter range of m_D, we have been able to perform the task only for a few data points in that range. We actually find that there is no monotonic variation of Y_B with the chosen data points. For example, given a normal ordering of the light neutrino masses, suppose we take the data set that corresponds to the worst fit point (χ^2_{max}) and solve the Boltzmann equations for 10^9 GeV $< M_1 < 10^{12}$ GeV. Such a procedure yields a negative final value of Y_B contrary to the result obtained in the $\chi^2 = 0.003$ case. For the other data points also, Y_B varies widely with the parameters of m_D from one neutrino mass model to another [223–226]. This conclusion is true for all mass regimes (except for $M_1 > 10^{12}$ GeV, where $\sum_\lambda \varepsilon_1^\lambda = 0$ and hence Y_B vanishes) as well as for an inverted mass ordering of the light neutrinos. Table 5.7 shows that, for data points close to the best fit values, an inverted mass ordering is not favored in this model. However, *we cannot completely rule out this mass ordering here since such is not the case as one moves further away from the best-fit values while still remaining within the* 3σ *range*. There may exist certain data sets (e.g. $\chi^2 = 1.67$) in the allowed 3σ ranges for which the proper value of Y_B can be generated even with an inverted light neutrino mass ordering.

5.5 Sensitivity to the heavier neutrinos

In our analysis so far, the effect of the two heavier neutrinos (N_2, N_3) on the produced final lepton asymmetry has been neglected. We have assumed that the asymmetries produced by the decays of both of them get washed out [227]. We examine this issue in this section. Is Y_B sensitive to N_2 and N_3? There are two ways that such a sensitivity might arise: (1) directly, if the contributions to Y_λ from $N_{2,3}$ decays do not get washed out for some reason and (2) indirectly, even if those do get washed out, a dependence of Y_B on the heavier RH neutrino masses might persist through the CP asymmetry parameter ε_1^α.

- **Indirect effect of $N_{2,3}$:**

  Though the neutrino oscillation data have been fitted with the primed parameters, cf (5.19)–(5.22), for computing the quantities related to leptogenesis, we need to examine the unprimed ones, i.e. the Dirac mass matrix elements. Is the final baryon asymmetry affected by the chosen hierarchies of the RH neutrinos? Interestingly, we find that the final Y_B is not so sensitive to $M_{2,3}$. One can justify this statement by simplifying the CP asymmetry parameters of (1.111) to

$$\varepsilon_1^{\alpha} = -\kappa\Big[\sum_{j=2,3}\frac{3M_1}{2M_j}\,\mathrm{Im}[\,\mathcal{H}_{1j}(m_D)_{1\alpha}(m_D^*)_{j\alpha}] - \sum_{j=2,3}\frac{M_1^2}{M_j^2}\mathrm{Im}[\,\mathcal{H}_{j1}(m_D)_{1\alpha}({m_D}^*)_{j\alpha}]\Big] \tag{5.36}$$

with $\kappa = \frac{1}{4\pi v^2\mathcal{H}_{11}}$. Here we approximate $g(x_{1j})$ of Eqs. (1.111) to be $g(x_{1j}) = -\frac{3}{2\sqrt{x_{1j}}}$ for $x_{1j} \gg 1$. The last term of Eq. (5.36) is much suppressed since it is of second order in x_{1j}^{-1}. The first term has two parts for $j = 2, 3$. However, since M_3 is much larger than M_1 and f, d_1 and d_2 are taken to have values of the order of the other Dirac components, the $j = 3$ term has a negligible effect on ε_1^{α}. Now, for $j = 2$, ε_1^{α} is simplified as

$$\varepsilon_1^{\mu} = -\frac{3M_1}{8\pi v^2\mathcal{H}_{11}}[(ae' + b_1c_1' + b_2c_2')(b_2c_1' + b_1c_2')] = -\varepsilon_1^{\tau} \tag{5.37}$$

with $\varepsilon_1^e = 0$. Since e' and $c_{1,2}'$ are fixed by the oscillation data, $\varepsilon_1^{\mu,\tau}$ are insensitive to the value of M_2. In order to numerically compute the final baryon asymmetry for a normal mass ordering of the light neutrinos, we consider each term in (5.37) and two different mass hierarchical schemes for the RH neutrinos, e.g, $M_{i+1}/M_i = 10^2$ and $M_{i+1}/M_i = 10^4$ where i can take the values 1,2. Recall that in the previous section we have presented Y_B for $M_{i+1}/M_i = 10^3$. A careful inspection of Fig.5.5 and Fig.5.6 reveals an interesting fact. Though the chosen mass ratios of the RH neutrinos have been altered, changes in the lower and upper bounds on M_1 are not significant for the observed range of Y_B. For convenience, we present in Table 5.8 the variation of Y_B with M_1 for different mass ratios.

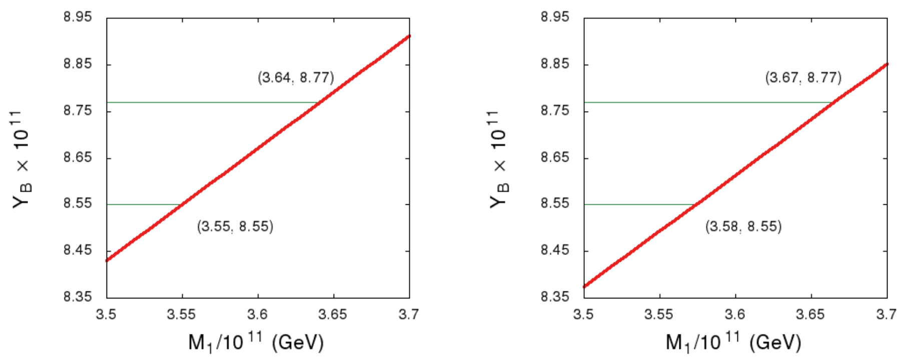

Figure 5.6: *Plots of final Y_B for different values of M_1 for $M_{i+1}/M_i = 10^2$ (left) and $M_{i+1}/M_i = 10^4$ (right).*

Table 5.8: Lower and upper bounds on M_1 for different mass ratios of the RH neutrinos ($i = 1, 2$).

Hierarchies $\rightarrow$	$M_{i+1}/M_i = 10^2$	$M_{i+1}/M_i = 10^3$	$M_{i+1}/M_i = 10^4$
Upper bound (GeV)	3.64×10^{11}	3.66×10^{11}	3.67×10^{11}
Lower bound (GeV)	3.55×10^{11}	3.57×10^{11}	3.58×10^{11}

- **Direct effect of N_2:**

  Here we consider only N_2, neglecting N_3 for simplicity. It is argued in Ref. [228] that, due to a decoherence effect, a finite lepton asymmetry generated by N_2 decays might remain protected against N_1-washout and could survive down to the electroweak scale. Thus it itself might generate the final baryon asymmetry if a sizable amount of lepton asymmetry survives. This procedure is subject to the condition that two washout factors K_1 (related to N_1-washout) and K_2 (related to N_2-washout) need not be of the same order. These are defined as

$$K_1 = \frac{\mathcal{H}_{11}}{M_1 m^*}, \; K_2 = \frac{\mathcal{H}_{22}}{M_2 m^*}, \tag{5.38}$$

where $m^* = 1.66\sqrt{g^*}\pi v^2/M_{Pl} \approx 10^{-3}$ eV.

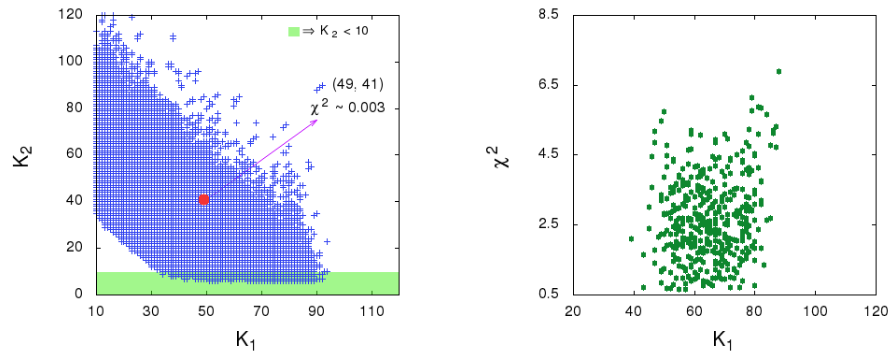

Figure 5.7: *A plot of the two washout parameters K_1 and K_2 appears in the left panel. The red dot corresponds to $\chi^2 = 0.003$ for which we estimate Y_B. The green shaded area indicates a possibility of N_2 leptogenesis. A plot of χ^2 with K_1 for $K_2 < 10$ is given in the right panel. A normal mass ordering for the light neutrinos has been assumed.*

The conditions that are needed can be stated as [228]

$$K_1 \gg 1 \text{ and } K_2 \not\gg 1. \tag{5.39}$$

Here $K_1 \gg 1$ indicates that faster N_1 interactions break coherence among the states produced by N_2, i.e. a part of the lepton asymmetry produced by N_2 gets protected against N_1-washout. On the other hand, $K_2 \not\gg 1$ implies a mild washout of the lepton asymmetry produced by N_2 from N_2-related interactions in a way that a sizable N_2-generated lepton asymmetry survives during the N_1-leptogenesis phase. Quantitatively, our allowed parametric region (blue shaded area in the K_2 vs. K_1 plot in the left panel of Fig.5.7) prefers large values of K_2 in excess of 10 except at the bottom (green band). Thus the $K_2 \not\gg 1$ condition is strongly violated in most of the region. On the other hand, the few allowed points with $K_2 < 10$, displayed in a χ^2 vs. K_1 plot in the right panel of Fig.5.7, correspond to values of χ^2 above 0.5 far in excess of $\chi^2 = 0.003$ for which we obtain Y_B in the observed range. Therefore, for our calculation, any direct effect of N_2 does not appear to be relevant.

5.6 Summary

Some of us has recently proposed a complex-extended scaling model of the light neutrino Majorana mass matrix M_ν, generated by a type-1 seesaw induced by heavy RH neutrinos. Unlike the Simple Real Scaling model advanced earlier, this new model can accommodate a nonzero θ_{13} and has a sizable region of parameter space allowed by all current and relevant experimental data. The atmospheric mixing angle θ_{23} is given by $\tan^{-1}(1/k)$, k being a real positive scaling factor which can be either greater or less than unity. Most interesting are the predictions of the model in regard to CP violation: maximal ($\cos\delta = 0$) for the Dirac type and absent (α, $\beta = 0$ or π) for the Majorana type. Since CP violation is crucially related to baryogenesis, we have been motivated in this paper to investigate the latter quantitatively in the model under consideration.

We first performed a general calculation of the CP asymmetries ε_i^α in the decays $N_i \to \not{L}_\alpha \phi, \not{L}_\alpha^C \phi^\dagger$ in terms of the parameters of the model. This led to a vanishing value of ε_i^e with a generally nonvanishing $\varepsilon_i^\mu = -\varepsilon_i^\tau$. A common source of the origin of a nonzero θ_{13} and these CP asymmetries was found in the imaginary part of m_D. We then evolved $Y_2 = Y_e + Y_\mu$ and Y_τ, respectively equal to $(n_L^{(2)} - n_{\bar{L}}^{(2)})/s$ and $(n_L^\tau - n_{\bar{L}}^\tau)/s$, from a high temperature (depending on the mass regime in which M_1 lies) down to that of the electroweak phase transition. In doing so we have had to consider the Boltzmann equations for Y_{N_i} and Y_λ, respectively equal to n_{N_i}/s and $(n_L^\lambda - n_{\bar{L}}^\lambda)/s$, λ

being an active lepton flavor index which can sometimes be a combination of e, μ, τ. We then utilized the different linear relations between Y_λ and Y_{Δ_λ}, with $\Delta_\lambda = \frac{1}{3}B - L_\lambda$, for the three different specified regimes of M_1 to arrive at the baryon asymmetry of the universe for each regime. The latter values have been evaluated numerically and their implications discussed.

In a nutshell, realistic baryogenesis has been found to be possible in this model for values close to best fit values of the input neutrino oscillation observables only in the 10^9 GeV $< M_1 < 10^{12}$ GeV regime and for a normal mass ordering of the light neutrinos. This analysis excludes (from a baryogenesis standpoint) the regimes $M_1 < 10^9$ GeV and $M_1 > 10^{12}$ GeV and disfavors an inverted mass ordering of the light neutrinos. However, the latter is still allowed for values of the input parameters away from their best-fit numbers but within a 3σ range. As neutrino oscillation data improve, the conclusions from our analysis will be sharpened.

Chapter 6

Summary and conclusions

Masses and mixing of light neutrinos are well established now by the neutrino oscillation experiments. The required various extensions of the SM to explain these small masses open up the possibility to explore new physics beyond the standard model. Despite the measurements of the low energy neutrino parameters at a great significant level, there are some low energy observable, such as the Dirac CP phase and the Majorana phases which are yet to be determined. The mass ordering of the neutrinos–normal or inverted has not been fixed yet. A more fundamental question–the nature of the neutrinos; whether they are Dirac or Majorana type has not been answered. To probe a Majorana neutrino through $\beta\beta0\nu$ decay several efficient experiments are going on and planned. This is a high time in neutrino physics as far as the experimental confrontation of a predictive neutrino mass model is concerned. In this thesis, we have presented some highly testable neutrino mass models based on some BSM framework such as Type-I and Inverse seesaw mechanisms with some interesting discrete residual symmetries as an added feature.

Before describing the models in detail, we have developed a general methodology for the evaluation of Majorana phases in a model independent way. In chapter 2, we have shown that with the construction of some rephasing invariants by the elements of M_ν, one can calculate the CP violating phases. Our methodology is valid for any hierarchical neutrino mass model even if it possesses a vanishing eigenvalue. We have also constrained the Majorana phases of a general mass matrix using the constraints on $|M_{ee}|$ and the upper bounds on the sum of the light neutrino masses $(\sum_i m_i)$ in addition to the standard oscillation constraints. To exemplify our methodology, we have also presented two predictive mass models for each mass ordering and demonstrated the application of the developed general methodology.

In chapter 3, we have presented two mass models based on scaling ansatz and cyclic symmetry as an effective residual symmetry along with some vanishing elements in M_ν. As an immediate consequence, the number of parameters are drastically reduced and we end up with some interesting predictions for the low energy parameters in each of the cases. For example, both the models predict a constraint ranges of δ which will be tested in the various ongoing experiments like T2K etc.. Each of the models predicts a particular mass ordering along with a constraint range of $|M_{ee}|$.

In chapter 4, we have investigated a model based on a residual $\mathbb{Z}_2 \times \mathbb{Z}_2$ symmetry complemented by a nonstandard CP transformation. We have presented the scaling hypothesis as a residual $\mathbb{Z}_2 \times \mathbb{Z}_2$ symmetry. We have then extended the latter to its complex version with a CP transformation, since the real invariance could predict a vanishing θ_{13} and hence undetermined Dirac CP violation. As a consequence, we have obtained a maximally violating value $3\pi/2$ for δ with θ_{23} not being maximal in general. The Majorana phases are found to be either 0 or π.

In chapter 5 we have extended this discussion to a Type-I seesaw framework and examined the impact of this symmetry on leptogenesis in detail. Due to a typical structure of m_D, a common origin of nonzero θ_{13}, CP violation in the leptonic sector and matter antimatter asymmetry has been found.

At the end, neutrino physics is now playing a pivotal role to probe physics beyond the standard model. Within the purview of different experimental results this is our endeavour to investigate the central role played by the neutrinos in the other issues of BSM physics.

Bibliography

[1] G. Altarelli and F. Feruglio, "Discrete Flavor Symmetries and Models of Neutrino Mixing," *Rev. Mod. Phys.*, vol. 82, pp. 2701–2729, 2010.

[2] H. Ishimori, T. Kobayashi, H. Ohki, Y. Shimizu, H. Okada, and M. Tanimoto, "Non-Abelian Discrete Symmetries in Particle Physics," *Prog. Theor. Phys. Suppl.*, vol. 183, pp. 1–163, 2010.

[3] S. F. King and C. Luhn, "Neutrino Mass and Mixing with Discrete Symmetry," *Rept. Prog. Phys.*, vol. 76, p. 056201, 2013.

[4] P. O. Ludl and W. Grimus, "A complete survey of texture zeros in the lepton mass matrices," *JHEP*, vol. 07, p. 090, 2014. [Erratum: JHEP10,126(2014)].

[5] B. Adhikary, B. Brahmachari, A. Ghosal, E. Ma, and M. K. Parida, "A(4) symmetry and prediction of U(e3) in a modified Altarelli-Feruglio model," *Phys. Lett.*, vol. B638, pp. 345–349, 2006.

[6] S.-F. Ge, H.-J. He, and F.-R. Yin, "Common Origin of Soft mu-tau and CP Breaking in Neutrino Seesaw and the Origin of Matter," *JCAP*, vol. 1005, p. 017, 2010.

[7] C. S. Lam, "Symmetry of Lepton Mixing," *Phys. Lett.*, vol. B656, pp. 193–198, 2007.

[8] C. S. Lam, "Determining Horizontal Symmetry from Neutrino Mixing," *Phys. Rev. Lett.*, vol. 101, p. 121602, 2008.

[9] C. S. Lam, "The Unique Horizontal Symmetry of Leptons," *Phys. Rev.*, vol. D78, p. 073015, 2008.

[10] W. Grimus and L. Lavoura, "A Nonstandard CP transformation leading to maximal atmospheric neutrino mixing," *Phys. Lett.*, vol. B579, pp. 113–122, 2004.

[11] F. Feruglio, C. Hagedorn, and R. Ziegler, "Lepton Mixing Parameters from Discrete and CP Symmetries," *JHEP*, vol. 07, p. 027, 2013.

[12] R. N. Mohapatra and C. C. Nishi, "Implications of mu-tau flavored CP symmetry of leptons," *JHEP*, vol. 08, p. 092, 2015.

[13] A. Ghosal and R. Samanta, "Probing texture zeros with scaling ansatz in inverse seesaw," *JHEP*, vol. 05, p. 077, 2015.

[14] R. Samanta and A. Ghosal, "Probing maximal zero textures with broken cyclic symmetry in inverse seesaw," *Nucl. Phys.*, vol. B911, pp. 846–862, 2016.

[15] L. Lavoura, "New model for the neutrino mass matrix," *Phys. Rev.*, vol. D62, p. 093011, 2000.

[16] R. N. Mohapatra and W. Rodejohann, "Scaling in the neutrino mass matrix," *Phys. Lett.*, vol. B644, pp. 59–66, 2007.

[17] K. Abe *et al.*, "Measurements of neutrino oscillation in appearance and disappearance channels by the T2K experiment with 6.6ÃŮ10^{20} protons on target," *Phys. Rev.*, vol. D91, no. 7, p. 072010, 2015.

[18] R. Samanta, M. Chakraborty, and A. Ghosal, "Evaluation of the Majorana Phases of a General Majorana Neutrino Mass Matrix: Testability of hierarchical Flavour Models," *Nucl. Phys.*, vol. B904, pp. 86–105, 2016.

[19] U. Sarkar and S. K. Singh, "CP violation in neutrino mass matrix," *Nucl. Phys.*, vol. B771, pp. 28–39, 2007.

[20] P. A. R. Ade *et al.*, "Planck 2015 results. XIII. Cosmological parameters," *Astron. Astrophys.*, vol. 594, p. A13, 2016.

[21] M. Agostini *et al.*, "Results on Neutrinoless Double-β Decay of ^{76}Ge from Phase I of the GERDA Experiment," *Phys. Rev. Lett.*, vol. 111, no. 12, p. 122503, 2013.

[22] R. Samanta, P. Roy, and A. Ghosal, "Extended scaling and residual flavor symmetry in the neutrino Majorana mass matrix," *Eur. Phys. J.*, vol. C76, no. 12, p. 662, 2016.

[23] R. Samanta, M. Chakraborty, P. Roy, and A. Ghosal, "Baryon asymmetry via leptogenesis in a neutrino mass model with complex scaling," *JCAP*, vol. 1703, no. 03, p. 025, 2017.

[24] Z.-z. Xing, "Properties of CP Violation in Neutrino-Antineutrino Oscillations," *Phys. Rev.*, vol. D87, no. 5, p. 053019, 2013.

[25] M. Auger *et al.*, "Search for Neutrinoless Double-Beta Decay in ^{136}Xe with EXO-200," *Phys. Rev. Lett.*, vol. 109, p. 032505, 2012.

[26] K. Asakura *et al.*, "Search for double-beta decay of ^{136}Xe to excited states of ^{136}Ba with the KamLAND-Zen experiment," *Nucl. Phys.*, vol. A946, pp. 171–181, 2016.

[27] B. Majorovits, "The search for 0Î¡ÎšÎš decay with the GERDA experiment: Status and prospects," *AIP Conf. Proc.*, vol. 1672, p. 110003, 2015.

[28] M.-C. Chen, "TASI 2006 Lectures on Leptogenesis," in *Proceedings of Theoretical Advanced Study Institute in Elementary Particle Physics : Exploring New Frontiers Using Colliders and Neutrinos (TASI 2006): Boulder, Colorado, June 4-30, 2006*, pp. 123–176, 2007.

[29] J. M. Cline, "Baryogenesis," in *Les Houches Summer School - Session 86: Particle Physics and Cosmology: The Fabric of Spacetime Les Houches, France, July 31-August 25, 2006*, 2006.

[30] M. C. Gonzalez-Garcia, M. Maltoni, and T. Schwetz, "Global Analyses of Neutrino Oscillation Experiments," *Nucl. Phys.*, vol. B908, pp. 199–217, 2016.

[31] D. V. Forero, M. Tortola, and J. W. F. Valle, "Global status of neutrino oscillation parameters after Neutrino-2012," *Phys. Rev.*, vol. D86, p. 073012, 2012.

[32] Y. Fukuda *et al.*, "Evidence for oscillation of atmospheric neutrinos," *Phys. Rev. Lett.*, vol. 81, pp. 1562–1567, 1998.

[33] F. Reines and C. L. Cowan *Nature*, vol. 178 (446), 1956.

[34] B. Pontecorv *Sov. Phys. JETP*, vol. 6, 1957.

[35] B. Pontecorv *Sov. Phys. JETP*, vol. 7, 1958.

[36] M. N. Z. Maki and S. Sakata *Prog. Theor. Phys*, vol. 28, 1962.

[37] K. A. G. L. M. L. N. B. M. i.-t. M. S. G. Danby, J. M. Gaillard and J. Steinberge *Phys. Rev. Lett.*, vol. 9 (36), 1962.

[38] S. A. Bludman, N. Hata, and P. Langacker, "Astrophysical solutions are incompatible with the solar neutrino data," *Phys. Rev.*, vol. D49, pp. 3622–3625, 1994.

[39] N. Hata and P. Langacker, "Solutions to the solar neutrino anomaly," *Phys. Rev.*, vol. D56, pp. 6107–6116, 1997.

[40] S. J. Parke, "Status of the solar neutrino puzzle," *Phys. Rev. Lett.*, vol. 74, pp. 839–841, 1995.

[41] K. S. H. et al. (KAMIOKANDE-II) *Phys. Lett B205.*, vol. 416, 1988.

[42] M. C. Goodman, "The Atmospheric neutrino anomaly in Soudan-2," *Nucl. Phys. Proc. Suppl.*, vol. 38, pp. 337–342, 1995.

[43] Y. Fukuda *et al.*, "Solar neutrino data covering solar cycle 22," *Phys. Rev. Lett.*, vol. 77, pp. 1683–1686, 1996.

[44] P. Anselmann *et al.*, "Solar neutrinos observed by GALLEX at Gran Sasso.," *Phys. Lett.*, vol. B285, pp. 376–389, 1992.

[45] D. Abdurashitov *et al.*, "Results from SAGE," *Phys. Lett.*, vol. B328, pp. 234–248, 1994.

[46] J. Hosaka *et al.*, "Solar neutrino measurements in super-Kamiokande-I," *Phys. Rev.*, vol. D73, p. 112001, 2006.

[47] M. Acciarri *et al.*, "Determination of the number of light neutrino species from single photon production at LEP," *Phys. Lett.*, vol. B431, pp. 199–208, 1998.

[48] K. Kodama *et al.*, "Observation of tau neutrino interactions," *Phys. Lett.*, vol. B504, pp. 218–224, 2001.

[49] Q. R. Ahmad *et al.*, "Direct evidence for neutrino flavor transformation from neutral current interactions in the Sudbury Neutrino Observatory," *Phys. Rev. Lett.*, vol. 89, p. 011301, 2002.

[50] A. Aguilar-Arevalo *et al.*, "Evidence for neutrino oscillations from the observation of anti-neutrino(electron) appearance in a anti-neutrino(muon) beam," *Phys. Rev.*, vol. D64, p. 112007, 2001.

[51] V. A. KosteleckÃ¡, ed., *Proceedings, 5th Meeting on CPT and Lorentz Symmetry (CPT 10)*, (Singapore), World Scientific, World Scientific, 2010.

[52] J. Beringer *et al.*, "Review of Particle Physics (RPP)," *Phys. Rev.*, vol. D86, p. 010001, 2012.

[53] S. M. Bilenky and S. T. Petcov, "Massive Neutrinos and Neutrino Oscillations," *Rev. Mod. Phys.*, vol. 59, p. 671, 1987. [Erratum: Rev. Mod. Phys.60,575(1988)].

[54] L. Wolfenstein, "Neutrino Oscillations in Matter," *Phys. Rev.*, vol. D17, pp. 2369–2374, 1978.

[55] S. P. Mikheev and A. Yu. Smirnov, "Resonance Amplification of Oscillations in Matter and Spectroscopy of Solar Neutrinos," *Sov. J. Nucl. Phys.*, vol. 42, pp. 913–917, 1985. [Yad. Fiz.42,1441(1985)].

[56] S. Choubey and P. Roy, "Testing maximality in muon neutrino flavor mixing," *Phys. Rev. Lett.*, vol. 93, p. 021803, 2004.

[57] E. K. Akhmedov, R. Johansson, M. Lindner, T. Ohlsson, and T. Schwetz, "Series expansions for three flavor neutrino oscillation probabilities in matter," *JHEP*, vol. 04, p. 078, 2004.

[58] R. Davis, Jr., D. S. Harmer, and K. C. Hoffman, "Search for neutrinos from the sun," *Phys. Rev. Lett.*, vol. 20, pp. 1205–1209, 1968.

[59] B. T. Cleveland, T. Daily, R. Davis, Jr., J. R. Distel, K. Lande, C. K. Lee, P. S. Wildenhain, and J. Ullman, "Measurement of the solar electron neutrino flux

with the Homestake chlorine detector," *Astrophys. J.*, vol. 496, pp. 505–526, 1998.

[60] C. Arpesella *et al.*, "Direct Measurement of the Be-7 Solar Neutrino Flux with 192 Days of Borexino Data," *Phys. Rev. Lett.*, vol. 101, p. 091302, 2008.

[61] M. Altmann *et al.*, "GNO solar neutrino observations: Results for GNO I," *Phys. Lett.*, vol. B490, pp. 16–26, 2000.

[62] S. Abe *et al.*, "Precision Measurement of Neutrino Oscillation Parameters with KamLAND," *Phys. Rev. Lett.*, vol. 100, p. 221803, 2008.

[63] M. H. Ahn *et al.*, "Measurement of Neutrino Oscillation by the K2K Experiment," *Phys. Rev.*, vol. D74, p. 072003, 2006.

[64] P. Adamson *et al.*, "Improved search for muon-neutrino to electron-neutrino oscillations in MINOS," *Phys. Rev. Lett.*, vol. 107, p. 181802, 2011.

[65] F. Ardellier *et al.*, "Double Chooz: A Search for the neutrino mixing angle theta(13)," 2006.

[66] X. Guo *et al.*, "A Precision measurement of the neutrino mixing angle θ_{13} using reactor antineutrinos at Daya-Bay," 2007.

[67] S.-B. Kim, "RENO: Reactor experiment for neutrino oscillation at Yonggwang," *AIP Conf. Proc.*, vol. 981, pp. 205–207, 2008. [J. Phys. Conf. Ser.120,052025(2008)].

[68] G. 't Hooft, "Symmetry Breaking Through Bell-Jackiw Anomalies," *Phys. Rev. Lett.*, vol. 37, pp. 8–11, 1976.

[69] H. Hettmansperger, M. Lindner, and W. Rodejohann, "Phenomenological Consequences of sub-leading Terms in See-Saw Formulas," *JHEP*, vol. 04, p. 123, 2011.

[70] T. P. Cheng and L.-F. Li, “$\mu \to e\gamma$ in Theories With Dirac and Majorana Neutrino Mass Terms,” *Phys. Rev. Lett.*, vol. 45, p. 1908, 1980.

[71] M. Hirsch, S. Morisi, and J. W. F. Valle, “A4-based tri-bimaximal mixing within inverse and linear seesaw schemes,” *Phys. Lett.*, vol. B679, pp. 454–459, 2009.

[72] Y. Chikashige, R. N. Mohapatra, and R. D. Peccei, “Are There Real Goldstone Bosons Associated with Broken Lepton Number?,” *Phys. Lett.*, vol. 98B, pp. 265–268, 1981.

[73] Y. Chikashige, R. N. Mohapatra, and R. D. Peccei, “Spontaneously Broken Lepton Number and Cosmological Constraints on the Neutrino Mass Spectrum,” *Phys. Rev. Lett.*, vol. 45, p. 1926, 1980.

[74] E. K. Akhmedov, “Neutrino physics,” in *Proceedings, Summer School in Particle Physics: Trieste, Italy, June 21-July 9, 1999*, pp. 103–164, 1999.

[75] A. Melfo, M. Nemevsek, F. Nesti, G. Senjanovic, and Y. Zhang, “Type II Seesaw at LHC: The Roadmap,” *Phys. Rev.*, vol. D85, p. 055018, 2012.

[76] E. Ma and U. Sarkar, “Neutrino masses and leptogenesis with heavy Higgs triplets,” *Phys. Rev. Lett.*, vol. 80, pp. 5716–5719, 1998.

[77] D. Aristizabal Sierra, M. Dhen, and T. Hambye, “Scalar triplet flavored leptogenesis: a systematic approach,” *JCAP*, vol. 1408, p. 003, 2014.

[78] A. Zee, “A Theory of Lepton Number Violation, Neutrino Majorana Mass, and Oscillation,” *Phys. Lett.*, vol. 93B, p. 389, 1980. [Erratum: Phys. Lett.95B,461(1980)].

[79] L. Wolfenstein, “A Theoretical Pattern for Neutrino Oscillations,” *Nucl. Phys.*, vol. B175, pp. 93–96, 1980.

[80] K. S. Babu, "Model of 'Calculable' Majorana Neutrino Masses," *Phys. Lett.*, vol. B203, pp. 132–136, 1988.

[81] E. Ma, "Verifiable radiative seesaw mechanism of neutrino mass and dark matter," *Phys. Rev.*, vol. D73, p. 077301, 2006.

[82] R. Franceschini, T. Hambye, and A. Strumia, "Type-III see-saw at LHC," *Phys. Rev.*, vol. D78, p. 033002, 2008.

[83] R. N. Mohapatra and G. Senjanovic, "Neutrino Mass and Spontaneous Parity Violation," *Phys. Rev. Lett.*, vol. 44, p. 912, 1980.

[84] R. N. Mohapatra and G. Senjanovic, "Neutrino Masses and Mixings in Gauge Models with Spontaneous Parity Violation," *Phys. Rev.*, vol. D23, p. 165, 1981.

[85] H. Georgi and S. L. Glashow, "Unity of All Elementary Particle Forces," *Phys. Rev. Lett.*, vol. 32, pp. 438–441, 1974.

[86] D. Chang, R. N. Mohapatra, and M. K. Parida, "A New Approach to Left-Right Symmetry Breaking in Unified Gauge Theories," *Phys. Rev.*, vol. D30, p. 1052, 1984.

[87] D. Chang, R. N. Mohapatra, and M. K. Parida, "Decoupling Parity and SU(2)-R Breaking Scales: A New Approach to Left-Right Symmetric Models," *Phys. Rev. Lett.*, vol. 52, p. 1072, 1984.

[88] R. N. Mohapatra, *UNIFICATION AND SUPERSYMMETRY. THE FRONTIERS OF QUARK - LEPTON PHYSICS.* Berlin: Springer, 1986.

[89] A. Sakharov *JETP Lett..*, vol. 91B, 1967.

[90] M. Fukugita and T. Yanagida, "Baryogenesis Without Grand Unification," *Phys. Lett.*, vol. B174, pp. 45–47, 1986.

[91] N. S. Manton, “Topology in the Weinberg-Salam Theory,” *Phys. Rev.*, vol. D28, p. 2019, 1983.

[92] S. L. Adler, “Axial vector vertex in spinor electrodynamics,” *Phys. Rev.*, vol. 177, pp. 2426–2438, 1969.

[93] V. A. Kuzmin, V. A. Rubakov, and M. E. Shaposhnikov, “On the Anomalous Electroweak Baryon Number Nonconservation in the Early Universe,” *Phys. Lett.*, vol. 155B, p. 36, 1985.

[94] F. R. Klinkhamer and N. S. Manton, “A Saddle Point Solution in the Weinberg-Salam Theory,” *Phys. Rev.*, vol. D30, p. 2212, 1984.

[95] P. B. Arnold and L. D. McLerran, “Sphalerons, Small Fluctuations and Baryon Number Violation in Electroweak Theory,” *Phys. Rev.*, vol. D36, p. 581, 1987.

[96] P. B. Arnold, D. Son, and L. G. Yaffe, “The Hot baryon violation rate is O (alpha-w**5 T**4),” *Phys. Rev.*, vol. D55, pp. 6264–6273, 1997.

[97] P. B. Arnold, D. T. Son, and L. G. Yaffe, “Effective dynamics of hot, soft nonAbelian gauge fields. Color conductivity and log(1/alpha) effects,” *Phys. Rev.*, vol. D59, p. 105020, 1999.

[98] A. Pilaftsis and T. E. J. Underwood, “Resonant leptogenesis,” *Nucl. Phys.*, vol. B692, pp. 303–345, 2004.

[99] A. Abada, S. Davidson, A. Ibarra, F. X. Josse-Michaux, M. Losada, and A. Riotto, “Flavour Matters in Leptogenesis,” *JHEP*, vol. 09, p. 010, 2006.

[100] J. Edsjo and P. Gondolo, “Neutralino relic density including coannihilations,” *Phys. Rev.*, vol. D56, pp. 1879–1894, 1997.

[101] B. Adhikary, M. Chakraborty, and A. Ghosal, "Flavored leptogenesis with quasidegenerate neutrinos in a broken cyclic symmetric model," *Phys. Rev.*, vol. D93, no. 11, p. 113001, 2016.

[102] E. W. Kolb and M. S. Turner, "The Early Universe," *Front. Phys.*, vol. 69, pp. 1–547, 1990.

[103] S. Davidson, E. Nardi, and Y. Nir, "Leptogenesis," *Phys. Rept.*, vol. 466, pp. 105–177, 2008.

[104] S. F. King, "Models of Neutrino Mass, Mixing and CP Violation," *J. Phys.*, vol. G42, p. 123001, 2015.

[105] S. F. King, "Neutrino mass models," *Rept. Prog. Phys.*, vol. 67, pp. 107–158, 2004.

[106] R. N. Mohapatra and A. Y. Smirnov, "Neutrino Mass and New Physics," *Ann. Rev. Nucl. Part. Sci.*, vol. 56, pp. 569–628, 2006.

[107] G. Altarelli and F. Feruglio, "Theoretical models of neutrino masses and mixings," *Springer Tracts Mod. Phys.*, vol. 190, pp. 169–207, 2003.

[108] J. W. F. Valle, "Neutrino physics overview," *J. Phys. Conf. Ser.*, vol. 53, pp. 473–505, 2006.

[109] E. Ma, "Plato's fire and the neutrino mass matrix," *Mod. Phys. Lett.*, vol. A17, pp. 2361–2370, 2002.

[110] M. Tanimoto, "Generation of neutrino masses and mixings in gauge theories," in *Weak interactions and neutrinos. Proceedings, 17th International Workshop, WIN'99, Cape Town, South Africa, January 24-30, 1999*, pp. 345–349, 1999.

[111] S. F. King, "Unified Models of Neutrinos, Flavour and CP Violation (references therein)," *Prog. Part. Nucl. Phys.*, vol. 94, pp. 217–256, 2017.

[112] W. Grimus and M. N. Rebelo, “Automorphisms in gauge theories and the definition of CP and P,” *Phys. Rept.*, vol. 281, pp. 239–308, 1997.

[113] P. Chen, C.-C. Li, and G.-J. Ding, “Lepton Flavor Mixing and CP Symmetry,” *Phys. Rev.*, vol. D91, p. 033003, 2015.

[114] F. Feruglio, C. Hagedorn, and R. Ziegler, “A realistic pattern of lepton mixing and masses from S_4 and CP,” *Eur. Phys. J.*, vol. C74, p. 2753, 2014.

[115] M. Agostini *et al.*, “Limit on Neutrinoless Double Beta Decay of ^{76}Ge by GERDA,” *Phys. Procedia*, vol. 61, pp. 828–837, 2015.

[116] W. Xu *et al.*, “The *MAJORANA DEMONSTRATOR*: A Search for Neutrinoless Double-beta Decay of ^{76}Ge,” *J. Phys. Conf. Ser.*, vol. 606, no. 1, p. 012004, 2015.

[117] F. Simkovic, S. M. Bilenky, A. Faessler, and T. Gutsche, “Possibility of measuring the CP Majorana phases in 0Î¡ÎšÎš decay,” *Phys. Rev.*, vol. D87, no. 7, p. 073002, 2013.

[118] J. J. GÃşmez-Cadenas and J. MartÃŋn-Albo, “Phenomenology of neutrinoless double beta decay,” *PoS*, vol. GSSI14, p. 004, 2015.

[119] W. Tornow, “Search for Neutrinoless Double-Beta Decay,” in *34th International Symposium on Physics in Collision (PIC 2014) Bloomington, Indiana, United States, September 16-20, 2014*, 2014.

[120] S. M. Bilenky and C. Giunti, “Neutrinoless Double-Beta Decay: a Probe of Physics Beyond the Standard Model,” *Int. J. Mod. Phys.*, vol. A30, no. 04n05, p. 1530001, 2015.

[121] E. W. Hennecke, O. K. Manuel, and D. D. Sabu, “Double beta decay of Te-128,” *Phys. Rev.*, vol. C11, pp. 1378–1384, 1975.

[122] K. Zuber, "Status and perspectives of double beta decay searches," *J. Phys. Conf. Ser.*, vol. 578, no. 1, p. 012007, 2015.

[123] B. Schwingenheuer, "Status and prospects of searches for neutrinoless double beta decay," *Annalen Phys.*, vol. 525, pp. 269–280, 2013.

[124] D. Lorca, "The Hunt for neutrinoless double beta decay with the NEXT experiment," in *Proceedings, 20th International Conference on Particles and Nuclei (PANIC 14): Hamburg, Germany, August 24-29, 2014*, pp. 321–324, 2014.

[125] Z.-z. Xing and Y.-L. Zhou, "Majorana CP-violating phases in neutrino-antineutrino oscillations and other lepton-number-violating processes," *Phys. Rev.*, vol. D88, p. 033002, 2013.

[126] S. Gupta, S. K. Kang, and C. S. Kim, "Renormalization Group Evolution of Neutrino Parameters in Presence of Seesaw Threshold Effects and Majorana Phases," *Nucl. Phys.*, vol. B893, pp. 89–106, 2015.

[127] H. Minakata, H. Nunokawa, and A. A. Quiroga, "Constraining Majorana CP phase in the precision era of cosmology and the double beta decay experiment," *PTEP*, vol. 2015, p. 033B03, 2015.

[128] S. M. Bilenky, J. Hosek, and S. T. Petcov, "On Oscillations of Neutrinos with Dirac and Majorana Masses," *Phys. Lett.*, vol. B94, pp. 495–498, 1980.

[129] C. Giunti, "No Effect of Majorana Phases in Neutrino Oscillations," *Phys. Lett.*, vol. B686, pp. 41–43, 2010.

[130] B. Adhikary, M. Chakraborty, and A. Ghosal, "Masses, mixing angles and phases of general Majorana neutrino mass matrix," *JHEP*, vol. 10, p. 043, 2013. [Erratum: JHEP09,180(2014)].

[131] Z.-Z. Xing, "Majorana phases and neutrino-antineutrino oscillations," *Int. J. Mod. Phys.*, vol. A29, p. 1444003, 2014.

[132] D. Delepine, V. Gonzalez Macias, S. Khalil, and G. L. Castro, "Probing Majorana neutrino CP phases and masses in neutrino-antineutrino conversion," *Phys. Lett.*, vol. B693, pp. 438–442, 2010.

[133] F. Beutler *et al.*, "The clustering of galaxies in the SDSS-III Baryon Oscillation Spectroscopic Survey: signs of neutrino mass in current cosmological data sets," *Mon. Not. Roy. Astron. Soc.*, vol. 444, no. 4, pp. 3501–3516, 2014.

[134] Y. Shimizu and M. Tanimoto, "Testing the minimal S_4 model of neutrinos with the Dirac and Majorana phases," *JHEP*, vol. 12, p. 132, 2015.

[135] B. Adhikary, A. Ghosal, and P. Roy, "Maximal zero textures of the inverse seesaw with broken $\mu\tau$ symmetry," *Indian J. Phys.*, vol. 88, pp. 979–989, 2014.

[136] M. Chakraborty, H. Z. Devi, and A. Ghosal, "Scaling ansatz with texture zeros in linear seesaw," *Phys. Lett.*, vol. B741, pp. 210–216, 2015.

[137] B. Adhikary, M. Chakraborty, and A. Ghosal, "Scaling ansatz, four zero Yukawa textures and large θ_{13}," *Phys. Rev.*, vol. D86, p. 013015, 2012.

[138] P. F. Harrison, D. H. Perkins, and W. G. Scott, "Threefold maximal lepton mixing and the solar and atmospheric neutrino deficits," *Phys. Lett.*, vol. B349, pp. 137–144, 1995.

[139] C.-Y. Chen and L. Wolfenstein, "Consequences of approximate S(3) symmetry of the neutrino mass matrix," *Phys. Rev.*, vol. D77, p. 093009, 2008.

[140] R. N. Mohapatra and J. W. F. Valle, "Neutrino Mass and Baryon Number Nonconservation in Superstring Models," *Phys. Rev.*, vol. D34, p. 1642, 1986.

[141] J. Bernabeu, A. Santamaria, J. Vidal, A. Mendez, and J. W. F. Valle, "Lepton Flavor Nonconservation at High-Energies in a Superstring Inspired Standard Model," *Phys. Lett.*, vol. B187, pp. 303–308, 1987.

[142] R. N. Mohapatra, "Mechanism for Understanding Small Neutrino Mass in Superstring Theories," *Phys. Rev. Lett.*, vol. 56, pp. 561–563, 1986.

[143] J. Schechter and J. W. F. Valle, "Neutrino Decay and Spontaneous Violation of Lepton Number," *Phys. Rev.*, vol. D25, p. 774, 1982.

[144] P. S. B. Dev and R. N. Mohapatra, "TeV Scale Inverse Seesaw in SO(10) and Leptonic Non-Unitarity Effects," *Phys. Rev.*, vol. D81, p. 013001, 2010.

[145] R. L. Awasthi, M. K. Parida, and S. Patra, "Neutrino masses, dominant neutrinoless double beta decay, and observable lepton flavor violation in left-right models and SO(10) grand unification with low mass W_R, Z_R bosons," *JHEP*, vol. 08, p. 122, 2013.

[146] A. Abada and M. Lucente, "Looking for the minimal inverse seesaw realisation," *Nucl. Phys.*, vol. B885, pp. 651–678, 2014.

[147] A. Palcu, "A straightforward realization of a quasi-inverse seesaw mechanism at TeV scale," *Rom. Rep. Phys.*, vol. 68, no. 1, p. 128, 2016.

[148] J. Schechter and J. W. F. Valle, "Neutrino Masses in SU(2) x U(1) Theories," *Phys. Rev.*, vol. D22, p. 2227, 1980.

[149] S. Fraser, E. Ma, and O. Popov, "Scotogenic Inverse Seesaw Model of Neutrino Mass," *Phys. Lett.*, vol. B737, pp. 280–282, 2014.

[150] S. S. C. Law and K. L. McDonald, "Generalized inverse seesaw mechanisms," *Phys. Rev.*, vol. D87, no. 11, p. 113003, 2013.

[151] A. Blum, R. N. Mohapatra, and W. Rodejohann, “Inverted mass hierarchy from scaling in the neutrino mass matrix: Low and high energy phenomenology,” *Phys. Rev.*, vol. D76, p. 053003, 2007.

[152] M. Obara, “The Possible Textures in the Seesaw Realization of the Strong Scaling Ansatz and the Implications for Thermal Leptogenesis,” 2007.

[153] A. Damanik, M. Satriawan, Muslim, and P. Anggraita, “Neutrino mass matrix from seesaw mechanism subjected to texture zero and invariant under a cyclic permutation,” 2007.

[154] W. Grimus and L. Lavoura, “Softly broken lepton number L(e) - L(mu) - L(tau) with non-maximal solar neutrino mixing,” *J. Phys.*, vol. G31, pp. 683–692, 2005.

[155] S. Dev, R. R. Gautam, and L. Singh, “Charged Lepton Corrections to Scaling Neutrino Mixing,” *Phys. Rev.*, vol. D89, no. 1, p. 013006, 2014.

[156] P. H. Frampton, S. L. Glashow, and D. Marfatia, “Zeroes of the neutrino mass matrix,” *Phys. Lett.*, vol. B536, pp. 79–82, 2002.

[157] K. Whisnant, J. Liao, and D. Marfatia, “Constraints on texture zero and cofactor zero models for neutrino mass,” *AIP Conf. Proc.*, vol. 1604, pp. 273–278, 2014.

[158] P. O. Ludl and W. Grimus, “A complete survey of texture zeros in general and symmetric quark mass matrices,” *Phys. Lett.*, vol. B744, pp. 38–42, 2015.

[159] W. Grimus and P. O. Ludl, “Correlations and textures in the neutrino mass matrix,” *PoS*, vol. EPS-HEP2013, p. 075, 2013.

[160] L. Lavoura, “New texture-zero patterns for lepton mixing,” *J. Phys.*, vol. G42, p. 105004, 2015.

[161] P. M. Ferreira and L. Lavoura, “New textures for the lepton mass matrices,” *Nucl. Phys.*, vol. B891, pp. 378–400, 2015.

[162] Z.-z. Xing and Z.-h. Zhao, “On the four-zero texture of quark mass matrices and its stability,” *Nucl. Phys.*, vol. B897, pp. 302–325, 2015.

[163] Z.-z. Xing, “Texture zeros and Majorana phases of the neutrino mass matrix,” *Phys. Lett.*, vol. B530, pp. 159–166, 2002.

[164] J. Liao, D. Marfatia, and K. Whisnant, “Texture and Cofactor Zeros of the Neutrino Mass Matrix,” *JHEP*, vol. 09, p. 013, 2014.

[165] H. Fritzsch, Z.-z. Xing, and S. Zhou, “Two-zero Textures of the Majorana Neutrino Mass Matrix and Current Experimental Tests,” *JHEP*, vol. 09, p. 083, 2011.

[166] A. Merle and W. Rodejohann, “The Elements of the neutrino mass matrix: Allowed ranges and implications of texture zeros,” *Phys. Rev.*, vol. D73, p. 073012, 2006.

[167] W. Wang, “Neutrino mass textures with one vanishing minor and two equal cofactors,” *Eur. Phys. J.*, vol. C73, p. 2551, 2013.

[168] W. Wang, “Parallel Texture Structures with Cofactor Zeros in Lepton Sector,” *Phys. Lett.*, vol. B733, pp. 320–327, 2014. [Erratum: Phys. Lett.B738,524(2014)].

[169] L. Lavoura, “Zeros of the inverted neutrino mass matrix,” *Phys. Lett.*, vol. B609, pp. 317–322, 2005.

[170] A. Kageyama, S. Kaneko, N. Shimoyama, and M. Tanimoto, “Seesaw realization of the texture zeros in the neutrino mass matrix,” *Phys. Lett.*, vol. B538, pp. 96–106, 2002.

[171] W. Wang, "Parallel Lepton Mass Matrices with Texture and Cofactor Zeros," *Phys. Rev.*, vol. D90, no. 3, p. 033014, 2014.

[172] G. C. Branco, D. Emmanuel-Costa, M. N. Rebelo, and P. Roy, "Four Zero Neutrino Yukawa Textures in the Minimal Seesaw Framework," *Phys. Rev.*, vol. D77, p. 053011, 2008.

[173] S. Choubey, W. Rodejohann, and P. Roy, "Phenomenological consequences of four zero neutrino Yukawa textures," *Nucl. Phys.*, vol. B808, pp. 272–291, 2009. [Erratum: Nucl. Phys.B818,136(2009)].

[174] B. Adhikary, A. Ghosal, and P. Roy, "mu tau symmetry, tribimaximal mixing and four zero neutrino Yukawa textures," *JHEP*, vol. 10, p. 040, 2009.

[175] B. Adhikary, A. Ghosal, and P. Roy, "Baryon asymmetry from leptogenesis with four zero neutrino Yukawa textures," *JCAP*, vol. 1101, p. 025, 2011.

[176] B. Adhikary, A. Ghosal, and P. Roy, "Neutrino Masses, Cosmological Bound and Four Zero Yukawa Textures," *Mod. Phys. Lett.*, vol. A26, pp. 2427–2435, 2011.

[177] P. S. B. Dev and A. Pilaftsis, "Minimal Radiative Neutrino Mass Mechanism for Inverse Seesaw Models," *Phys. Rev.*, vol. D86, p. 113001, 2012.

[178] M. Malinsky, "Non-unitarity effects in the minimal inverse seesaw model," *PoS*, vol. EPS-HEP2009, p. 288, 2009.

[179] D. V. Forero, M. Tortola, and J. W. F. Valle, "Neutrino oscillations refitted," *Phys. Rev.*, vol. D90, no. 9, p. 093006, 2014.

[180] M. C. Gonzalez-Garcia, M. Maltoni, J. Salvado, and T. Schwetz, "Global fit to three neutrino mixing: critical look at present precision," *JHEP*, vol. 12, p. 123, 2012.

[181] S. Goswami and A. Watanabe, "Minimal Seesaw Textures with Two Heavy Neutrinos," *Phys. Rev.*, vol. D79, p. 033004, 2009.

[182] M. S. Berger and S. Santana, "Combined flavor symmetry violation and lepton number violation in neutrino physics," *Phys. Rev.*, vol. D74, p. 113007, 2006.

[183] W. Grimus, A. S. Joshipura, L. Lavoura, and M. Tanimoto, "Symmetry realization of texture zeros," *Eur. Phys. J.*, vol. C36, pp. 227–232, 2004.

[184] K. Ieki, *Observation of $\nu_\mu \to \nu_e$ oscillation in the T2K experiment.* PhD thesis, Kyoto U. (main), 2014.

[185] P. A. R. Ade *et al.*, "Planck 2013 results. XVI. Cosmological parameters," *Astron. Astrophys.*, vol. 571, p. A16, 2014.

[186] J. Lesgourgues and S. Pastor, "Neutrino cosmology and Planck," *New J. Phys.*, vol. 16, p. 065002, 2014.

[187] E. Ma, N. Pollard, R. Srivastava, and M. Zakeri, "Gauge $B - L$ Model with Residual Z_3 Symmetry," *Phys. Lett.*, vol. B750, pp. 135–138, 2015.

[188] Y. Muramatsu, T. Nomura, and Y. Shimizu, "Mass limit for light flavon with residual Z_3 symmetry," *JHEP*, vol. 03, p. 192, 2016.

[189] Y. Koide, "Quark and lepton mass matrices with a cyclic permutation invariant form," 2000.

[190] E. Ma and R. Srivastava, "Dirac or inverse seesaw neutrino masses with $B - L$ gauge symmetry and S_3 flavor symmetry," *Phys. Lett.*, vol. B741, pp. 217–222, 2015.

[191] F. P. An *et al.*, "New Measurement of Antineutrino Oscillation with the Full Detector Configuration at Daya Bay," *Phys. Rev. Lett.*, vol. 115, no. 11, p. 111802, 2015.

[192] J. Iizuka, Y. Kaneko, T. Kitabayashi, N. Koizumi, and M. Yasue, "CP violation in modified bipair neutrino mixing and leptogenesis," *Phys. Lett.*, vol. B732, pp. 191–195, 2014.

[193] T. Kitabayashi and M. Yasue, "CP violation in bipair neutrino mixing," *Phys. Lett.*, vol. B726, pp. 356–363, 2013.

[194] C. Duarah, A. Das, and N. N. Singh, "Charged lepton contributions to bimaximal and tri-bimaximal mixings for generating $\sin\theta_{13} \neq 0$ and $\tan^2\theta_{23} < 1$," *Phys. Lett.*, vol. B718, pp. 147–152, 2012.

[195] B. Adhikary and A. Ghosal, "Nonzero U(e3), CP violation and leptogenesis in a see-saw type softly broken A(4) symmetric model," *Phys. Rev.*, vol. D78, p. 073007, 2008.

[196] G. Altarelli, F. Feruglio, and I. Masina, "Can neutrino mixings arise from the charged lepton sector?," *Nucl. Phys.*, vol. B689, pp. 157–171, 2004.

[197] S. Verma, "Theoretical and Phenomenological Status of Neutrino Physics: A Brief Review," *Adv. High Energy Phys.*, vol. 2015, p. 385968, 2015.

[198] C. Hagedorn and E. Molinaro, "Flavor and CP symmetries for leptogenesis and 0 Î¡ÎšÎš decay," *Nucl. Phys.*, vol. B919, pp. 404–469, 2017.

[199] J. Bian, "First Results of ν_e Appearance Analysis and Electron Neutrino Identification at NOvA," in *Proceedings, Meeting of the APS Division of Particles and Fields (DPF 2015): Ann Arbor, Michigan, USA, 4-8 Aug 2015*, 2015.

[200] S. Dell'Oro, S. Marcocci, and F. Vissani, "Status of the search for neutrinoless double beta decay, circa 2015," *PoS*, vol. NEUTEL2015, p. 069, 2015.

[201] K. A. Olive *et al.*, “Review of Particle Physics,” *Chin. Phys.*, vol. C38, p. 090001, 2014.

[202] P. Chen, G.-J. Ding, F. Gonzalez-Canales, and J. W. F. Valle, “Generalized $\mu - \tau$ reflection symmetry and leptonic CP violation,” *Phys. Lett.*, vol. B753, pp. 644–652, 2016.

[203] W. Grimus, A. S. Joshipura, S. Kaneko, L. Lavoura, H. Sawanaka, and M. Tanimoto, “Non-vanishing U(e3) and cos 2 theta(23) from a broken Z(2) symmetry,” *Nucl. Phys.*, vol. B713, pp. 151–172, 2005.

[204] D. A. Dicus, S.-F. Ge, and W. W. Repko, “Generalized Hidden $\mathcal{Z}_2$ Symmetry of Neutrino Mixing,” *Phys. Rev.*, vol. D83, p. 093007, 2011.

[205] S.-F. Ge, D. A. Dicus, and W. W. Repko, “ Z_2 Symmetry Prediction for the Leptonic Dirac CP Phase,” *Phys. Lett.*, vol. B702, pp. 220–223, 2011.

[206] S.-F. Ge, D. A. Dicus, and W. W. Repko, “Residual Symmetries for Neutrino Mixing with a Large θ_{13} and Nearly Maximal δ_D,” *Phys. Rev. Lett.*, vol. 108, p. 041801, 2012.

[207] G. Ecker, W. Grimus, and H. Neufeld, “A Standard Form for Generalized CP Transformations,” *J. Phys.*, vol. A20, p. L807, 1987.

[208] C. Hagedorn, A. Meroni, and E. Molinaro, “Lepton mixing from ÎŤ$(3n^2)$ and ÎŤ$(6n^2)$ and CP,” *Nucl. Phys.*, vol. B891, pp. 499–557, 2015.

[209] P. Chen, G.-J. Ding, and S. F. King, “Leptogenesis and residual CP symmetry,” *JHEP*, vol. 03, p. 206, 2016.

[210] A. S. Joshipura and W. Rodejohann, “Scaling in the Neutrino Mass Matrix, mu-tau Symmetry and the See-Saw Mechanism,” *Phys. Lett.*, vol. B678, pp. 276–282, 2009.

[211] P. S. Bhupal Dev, S. Goswami, M. Mitra, and W. Rodejohann, "Constraining Neutrino Mass from Neutrinoless Double Beta Decay," *Phys. Rev.*, vol. D88, p. 091301, 2013.

[212] N. Abgrall *et al.*, "The Majorana Demonstrator Neutrinoless Double-Beta Decay Experiment," *Adv. High Energy Phys.*, vol. 2014, p. 365432, 2014.

[213] H. Nunokawa, S. J. Parke, and J. W. F. Valle, "CP Violation and Neutrino Oscillations," *Prog. Part. Nucl. Phys.*, vol. 60, pp. 338–402, 2008.

[214] A. Riotto and M. Trodden, "Recent progress in baryogenesis," *Ann. Rev. Nucl. Part. Sci.*, vol. 49, pp. 35–75, 1999.

[215] E. Bertuzzo, P. Di Bari, F. Feruglio, and E. Nardi, "Flavor symmetries, leptogenesis and the absolute neutrino mass scale," *JHEP*, vol. 11, p. 036, 2009.

[216] S. Antusch, S. F. King, and A. Riotto, "Flavour-Dependent Leptogenesis with Sequential Dominance," *JCAP*, vol. 0611, p. 011, 2006.

[217] P. Minkowski, "$\mu \to e\gamma$ at a Rate of One Out of 10^9 Muon Decays?," *Phys. Lett.*, vol. B67, pp. 421–428, 1977.

[218] M. Gell-Mann, P. Ramond, and R. Slansky, "Complex Spinors and Unified Theories," *Conf. Proc.*, vol. C790927, pp. 315–321, 1979.

[219] T. Yanagida, "Horizontal Symmetry and Masses of Neutrinos," *Prog. Theor. Phys.*, vol. 64, p. 1103, 1980.

[220] A. D. Sakharov, "Violation of CP Invariance, c Asymmetry, and Baryon Asymmetry of the Universe," *Pisma Zh. Eksp. Teor. Fiz.*, vol. 5, pp. 32–35, 1967. [Usp. Fiz. Nauk161,61(1991)].

[221] W. Buchmuller, P. Di Bari, and M. Plumacher, "Leptogenesis for pedestrians," *Annals Phys.*, vol. 315, pp. 305–351, 2005.

[222] B. Adhikary, "Soft breaking of L(mu) - L(tau) symmetry: Light neutrino spectrum and Leptogenesis," *Phys. Rev.*, vol. D74, p. 033002, 2006.

[223] C. Hagedorn, E. Molinaro, and S. T. Petcov, "Majorana Phases and Leptogenesis in See-Saw Models with A(4) Symmetry," *JHEP*, vol. 09, p. 115, 2009.

[224] S. Blanchet, D. Marfatia, and A. Mustafayev, "Examining leptogenesis with lepton flavor violation and the dark matter abundance," *JHEP*, vol. 11, p. 038, 2010.

[225] M. Borah, D. Borah, and M. K. Das, "Discriminating Majorana neutrino textures in light of the baryon asymmetry," *Phys. Rev.*, vol. D91, p. 113008, 2015.

[226] J. Gehrlein, S. T. Petcov, M. Spinrath, and X. Zhang, "Leptogenesis in an SU(5) x A5 Golden Ratio Flavour Model: Addendum," *Nucl. Phys.*, vol. B899, pp. 617–630, 2015.

[227] W. Buchmuller, P. Di Bari, and M. Plumacher, "The Neutrino mass window for baryogenesis," *Nucl. Phys.*, vol. B665, pp. 445–468, 2003.

[228] G. Engelhard, Y. Grossman, E. Nardi, and Y. Nir, "The Importance of N2 leptogenesis," *Phys. Rev. Lett.*, vol. 99, p. 081802, 2007.